Natural product chemistry and biosynthetic studies of secondary metabolites from the marine-derived fungus *Stachylidium* sp.

Dissertation

zur

Erlangung des Doktorgrades (Dr. rer. nat.)

der

Mathematisch-Naturwissenschaftlichen Fakultät

der

Rheinischen Friedrich-Wilhelms-Universität Bonn

vorgelegt von

Fayrouz El Maddah

aus

Kairo, Ägypten

Bonn 2015

Angefertigt mit Genehmigung der Mathematisch-Naturwissenschaftlichen Fakultät der

Rheinischen Friedrich-Wilhelms-Universität Bonn

1. Gutachterin : Prof. Dr. G. M. König

2. Gutachterin : Prof. Dr. T. Schneider

Tag der Promotion: 03.03.2016

Erscheinungsjahr: 2016

Vorveröffentlichungen der Dissertation/In Advance Publications of the Dissertation

Teilergebnisse aus dieser Arbeit wurden mit Genehmigung der Mathematisch-Naturwissenschaftlichen Fakultät, vertreten durch die Mentorin/Betreuerin der Arbeit, in folgenden Beiträgen vorab veröffentlicht:

Parts of this study have been published in advance by permission of the Mathematisch-Naturwissenschaftlichen Fakultät, represented by the supervisor of this study:

Publikationen/Research Papers

El Maddah F., Nazir M., Kehraus S., König G. M., Biosynthetic origin of N-methyl-3-(3-furyl)-alanine in cyclic peptides produced by *Stachylidium* sp.. *Planta Med*, 2014, 80 - P1N10.

El Maddah F., Nazir M., Almeida C., Kehraus S., König G. M., Cyclic tetrapeptides from the marine-derived fungus *Stachylidium* sp. and insights into their biosynthesis. (*in preparation*)

Tagungsbeiträge/Research Presentations

El Maddah F., Nazir M., Kehraus S., König G. M., Biosynthetic labeling studies of cyclic peptides from the marine fungus *Stachylidium* sp.. Poster presented at the International PhD students meeting of the German Pharmaceutical Society (DPhG), March 10th–12th, 2014, Wuppertal, Germany.

El Maddah F., Nazir M., Kehraus S., König G. M., Insights into the biosynthesis of N-methyl-3-(3-furyl)-alanine in cyclic peptides from *Stachylidium* sp.. Poster presented at the 4th International Student Conference on Microbial Communication, March 31st– April 3rd, 2014, Jena, Germany.

El Maddah F., Nazir M., Kehraus S., König G. M., Biosynthetic origin of N-methyl-3-(3-furyl)-alanine in cyclic peptides produced by *Stachylidium* sp.. Poster presented at the 62nd International Congress and Annual Meeting of the Society for Medicinal Plant and Natural Product Research – GA 2014, August 31st- September 4th, 2014, Guimaraes, Portugal.

König G. M., El Maddah F., Nazir M., Hufendiek P., Schrör J., Almeida C., Kehraus S., Marine-derived fungal metabolites-focusing on structural diversity, biosynthesis and bioactivity. Inaugural lecture held by König G. M. at the 1st International Conference of the Marine Fungal Natural Products Consortium, July 22nd-24th, 2015, Nantes, France.

El Maddah F., Nazir M., Kehraus S., König G. M., Biosynthetic studies of secondary metabolites produced by the sponge-derived fungus *Stachylidium* sp.. Oral presentation at the 9th European Conference on Marine Natural Products (ECMNP 2015), August 30th-September 3rd, 2015, Glasgow, Scotland.

“When you have eliminated the impossible, whatever remains, however improbable,

must be the truth.”

Sir Arthur Conan Doyle

(1859-1930)

Acknowledgments

With this thesis I come to the end of the road of my PhD studies, which I could not have accomplished without the help and support of several people, to whom I am highly indebted.

First and foremost I would like to express my sincere gratitude to my supervisor Prof. Dr. G. M. König for giving me the opportunity to join her working group and for helping me until I got here to Germany. I thank her for entrusting me with this project, which had been a real challenge for me, and which without her continuous support and encouragement would not have been possible to conclude.

Special thanks go to Prof. Dr. T. Schneider for officiating as a second referee, and to Prof. Dr. W. Knöss and Prof. Dr. U. Deppenmeier for their kind participation in the examination committee.

I am highly grateful to Dr. Stefan Kehraus, our structural elucidation guru, for his time, patience and immense NMR knowledge.

Thanks are also due to our collaborator, working group Kostenis, Dr. Harald Dargatz (Institute for Pharmaceutical Biology, Univeristy of Bonn, Germany), for performing galanin receptor assays. I would like to cordially thank Dr. Christel Drewke for clarifying methods and results.

My sincere thanks goes out to the technical support staff of the Institute for Pharmaceutical Biology, University of Bonn, including Ekaterina Eguereva for introducing me to fungi and for LC-MS measurements, Edith Neu for agar diffusion assays, Thomas Kögler for responding to technical emergencies always with a receptive smile and Emilie Gorlaski for friendly talks.

I must also acknowledge Prof. Dr. Heinz G. Floss (University of Washington) and Prof. Dr. Taifo Mahmud (Oregon State University) for instantaneously providing me with labeled shikimic acid for feeding experiments.

To everyone past and present in the working group König, a big thank you. It was a real pleasure getting to know all of you, you made daily lab work less tedious and more pleasant. Special thanks go to Mamona Nazir for discussions regarding biosynthetic feeding experiments, and for good times especially during conferences. I am also grateful to Dr. Sarah Bouhired for being a good friend and someone to turn to in difficult times.

I would like to thank my small family for teaching me strength and patience, especially my dear son who took his first steps here in Germany and bore with me the good and bad times throughout my post-graduate studies.

This research would not have been possible without financial assistance of the Ministry of Higher Education of the Government of Egypt, the University of Bonn and the DAAD.

Finally, I would never have been able to complete this without the warm prayers of all my family, friends, and colleagues back home. I am really grateful to my parents for their continuous love, support and encouragements throughout the years. Special thanks go to Prof. Dr. Mona El Mahdy and Dr. Ghada Farouk in the National Organization for Drug Control and Research, Cairo, Egypt.

Abbreviations

°C	degrees Celsius
1D	one dimensional
2D	two dimensional
3-DHQ	3-dehydroquinic acid
3-DHS	3-dehydroshikimic acid
$[\alpha]_D^T$	specific rotator power, sodium D-line (589 nm); T: temperature
α	optical rotation
δ	NMR chemical shifts [ppm]
λ	wavelength [nm]
ε	molar absorption coefficient
µ	micro (10^{-6})
µg	10^{-6} gram
µl	10^{-6} liter
µM	10^{-6} molar, micromolar (=10^{-6} mol L^{-1})
ν	wave number [cm^{-1}]
AAA	aromatic amino acid
Ac	acetone
ACV	δ-(L-α-aminoadipyl)-L-cysteine-D-valine
AHBA	3-amino-5-hydroxybenzoic acid
AIDS	acquired immune deficiency syndrome
AMP	antimicrobial peptide
Aoe	2-amino-8-oxo-9,10-epoxydecanoic acid
APIs	active pharmaceutical ingredients
ASW	artificial sea water
BBr_3	boron tribromide
BDA	bisdethiobis(methylthio)-acetylaranotin
BDAA	bisdethiobis(methylthio)-acetylapoaranotin
BMS	biomalt salt

br	broad (in connection with NMR data)
c	concentration
C_{18}	C-18 modified silica gel
Ca^{+2}	calcium ion
$CaCl_2$	calcium chloride
calcd	calculated
cDNA	complementary deoxyribonucleic acid
cf.	confer [lat.], compared to
CHAP	cyclic hydroxamic acid containing peptides
CO_2	carbon dioxide
CoA	coenzyme A
conc.	concentration
COSY	correlated spectroscopy
cm	10^{-2} meter
d	doublet (in connection with NMR data)
dd	doublet of doublet (in connection with NMR data)
Da	Dalton
DAD	diode array detector
DAHP	3-deoxy-D-*arabino*-heptulosonic acid-7-phosphate
DCM	dichloromethane
DEPT	distortionless enhancement by polarization transfer
DHAP	dihydroxyacetone phosphate
DKP	diketopiperazine
dm	10^{-1} meter
DMAPP	dimethylallyl diphosphate
DMEM	Dulbecco’s modified Eagle's medium
DMR	dynamic mass redistribution
DMSO	dimethylsulfoxide
E-4-P	erythrose-4-phosphate

EA	ethylacetate
e.g.	exempli gratia [lat.] or example given (for example)
EI	electron ionization
ES	enniatin synthase
ESI	electron spray ionization
et al.	et alli [lat.]; and others
EtOAc	ethylacetate
EtOH	ethanol
ETP	epipolythiodioxopiperazine
FCS	fetal calf serum
FDA	food and drug administration
FDAA	1-fluoro-2-4-dinitrophenyl-5-L-alanine amide
Fr	fraction
FurAla	furylalanine
g	gram
G418	Geneticin
GalR	galanin receptor
GI	growth inhibition
GPCR	G protein-coupled receptor
GPP	geranyl diphosphate
h	hour
H_3BO_4	boric acid
HCl	hydrochloric acid
HDAC	histone deacetylase
HDP	host defence peptide
HEK	human embryonic kidney
HIF-1α	hypoxia inducible factor-1 alpha
HMBC	heteronuclear multiple-bond correlation
HMG-CoA	3-hydoxy-3-methylglutaryl-CoA

HPLC	high performance liquid chromatography
HR	high resolution
HSQC	heteronuclear single quantum correlation
H_2O	water
IBS	irritable bowel syndrome
i.e.	id est [lat.]; that is
IL-2	interleukin 2
IPP	Isopentenyl diphosphate
IR	infrared
J	spin-spin coupling constant [Hz]
KBr	potassium bromide
KCl	potassium chloride
l	cell length
L	liter
LC	liquid chromatography
Leu	leucine
LPS	lysergylpeptidyl synthase
m	meter
m	multiplet (in connection with NMR)
m/z	mass-to-charge ratio (in connection with mass spectrometry)
Me	methyl
MeOH	methanol
MEP	methylerythritol phosphate
mg	10^{-3} gram
$MgCl_2$	magnesium chloride
MHz	megahertz
min	minute
mL	10^{-3} liters
mm	10^{-3} meters

mM	10^{-3} molar, millimolar (=10^{-3} mol L^{-1})
MRSA	methicillin resistant *Staphylococcus aureus*
MS	mass spectrometry
MVA	mevalonic acid
N	normality
NaCl	sodium chloride
$NaHCO_3$	sodium bicarbonate
Na_2SO_4	sodium sulfate
n.d.	not detectable
n.e.	not enriched
NFAT	nuclear factor of activated T-cells
ng	10^{-9} gram
NH_4Ac	ammonium acetate
nm	10^{-9} meter
N-Me	N-methyl
NMR	nuclear magnetic resonance spectroscopy
no	number
NOE	nuclear Overhauser effect
NOESY	nuclear Overhauser effect spectroscopy
NP	normal phase (in connection to chromatography)
NRPS	non-ribosomal peptide synthase
NSCLC	non-small cell lung cancer
OSMAC	one strain many compounds
p-	para
PBP	penicillin binding protein
PDA	photodiode array
PE	petroleum ether
PEP	phosphoenolpyruvate
PGPR	plant growth promoting rhizobacteria

pH	potentia hydrogenii
Phe	phenylalanine
PKS	polyketide synthase
PLP	pyridoxal phosphate
ppm	part per million
PPP	pentose phosphate pathway
PTX	pertussis toxin
qC	quaternary carbon
ROESY	rotating frame Overhauser effect spectroscopy
RP	reversed phase (in connection with chromatography)
RPP	reductive pentose phosphate
rpm	revolutions per minute
RT	room temperature
s	singlet (in connection with NMR data)
SAR	structure activity relationship
sec	second
Si	silica gel
sp.	species
spp.	species (plural)
$SrCl_2$	strontium chloride
t	triplet (in connection with NMR data)
t_R	retention time
TE	thioestrase
TLC	thin layer chromatography
U-	uniformely
USD	United States dollar
UV	ultraviolet
Val	valine
VIS	visible

VLC	vacuum liquid chromatography
v/v	volume for volume
WG	working group
w/v	mass for volume

Table of contents Page

1. Introduction

1.1 The role of peptides in therapy

A thorough inspection of pharmacy shelves could one let perceive that commonly marketed drugs are either 'small-molecule' chemicals or high molecular weight biologics, the latter mostly being proteins. There is however a third group with a molecular weight in the medium range (500 – 5000 Da), i.e. peptide-based drugs, which are gradually moving to the front stage.[1] Peptides are set apart from proteins in that they are composed of less than 50 amino acids.[2] Peptides that occur in nature as secondary metabolites, such as daptomycin and cyclosporine, are furthermore characterized by the unusual amino acid building blocks like D-amino acids and N-methylated amino acids. Physiological peptides are known to be involved in many processes, e.g. acting as signals as in the case of cytokines, neurotransmitters as for example galanin or hormones like somatotropin.[3] Since most biological targets, referred to as drug targets in pharmacy, are proteins, e.g. enzymes, ion-channels and receptors, peptidic natural products may be envisaged as prospective ligands. Additionally, they may exhibit target specificity and hence minimal toxicity, the latter is also credited to there sound metabolism to the constituent amino acids which are readily cleared from the body with minimal tissue build-up.[4]

Peptide chemists, inspired by the structure and function of peptides isolated from natural sources, were successful in synthesizing peptide analogues through chemical or biological synthesis.[5] However there is still the need for new peptide scaffolds, able to serve as drug leads that may have arisen from natures biosynthetic machineries. This calls for the dedicated work of natural product chemists in isolating and characterizing such peptides, further exploring them deeper to understand their biosynthesis and biological activities and later on to be implemented in the drug-design process.

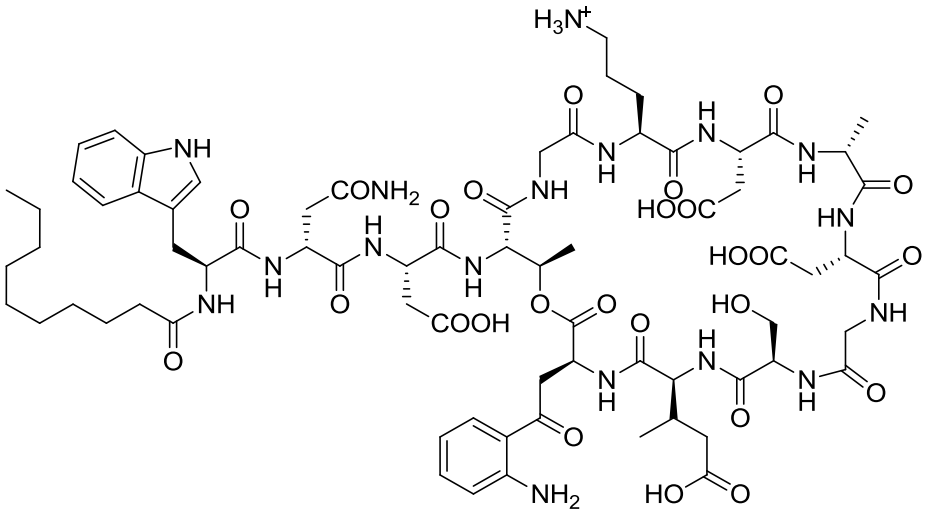

Daptomycin

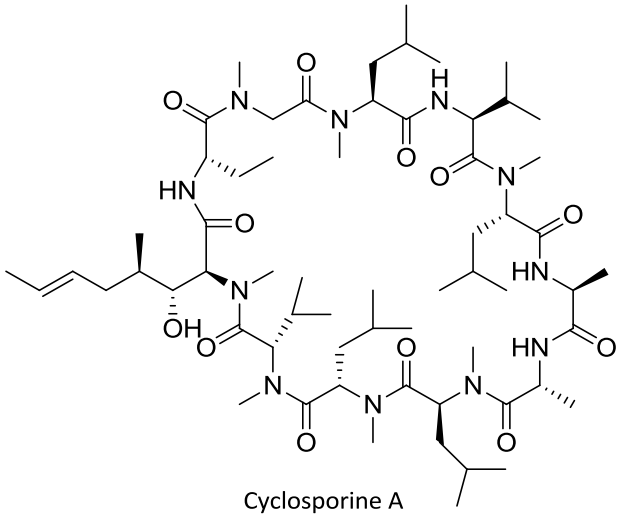

Cyclosporine A

Fig 1-1. Peptide secondary metabolites.

1.2 Peptides from fungi

Peptides are produced by prokaryotes and eukaryotes alike.[6] The fungal kingdom is regarded as a rich source to be investigated further for the production of secondary metabolites including peptides. Their structures were refined through years of evolution, since these compounds are important for the survival and growth of the producers in their rivalry natural habitat. Such compounds may act as siderophores, toxins or signaling molecules for communication.[7] From a human point of view, fungi are double-faced organisms, their dark-side being associated with their disease-causing or putrescent properties, some of these properties being attributed to their metabolite production, e.g.

mycotoxins. However, fungal metabolites provide us already today with important drugs, e.g. lovastatins, and are of importance for our future drugs.[8]

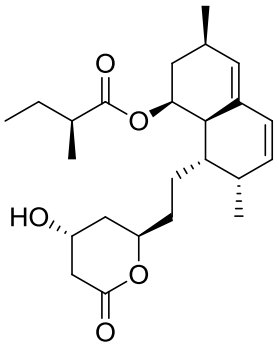

Lovastatin

Fig 1-2. Fungal metabolite used as drug.

1.2.1 Fungal peptides assembly lines

Fungal peptides are assembled either through the ribosomal machinery, i.e. through direct gene translation, including the amatoxins and phalloidin,[9] or by multi-modular non-ribosomal peptide synthetases (NRPS), the later accounting for most of the isolated fungal peptides.[10] These are megaenzymes divided into modules termed initiation and elongation modules where each module is responsible for integrating an amino acid into the growing peptide chain. This is done with the help of catalytic domains, a subdivision of each module. Fundamental domains are indispensable for the selection and activation of the building blocks (adenylation, A-domain), the tethering of the product to the enzyme (peptidyl carrier protein, PCP-domain) and peptide bond formation (condensation, C-domain). Structural diversity arises due to the presence of auxillary domains imparting unique structural features to the non-ribosomal peptides. These include epimerization (E) domains for incorporating D-amino acids, N-methylation (N-Mt) and C-methylation (C-Mt) domains for introducing methyl groups, formylation (F) domain for introducing formyl groups and oxidation (Ox) and reduction (R) domains for formation of thiazoles, oxazoles and thiazolidines, oxazolidines, respectively.[11] While bacterial NRPS feature a thioesterase (TE) domain at the end of the NRPS template to catalyze peptide release and cyclization, fungal NRPS employ an alternative enzymatic cyclization strategy with the help of a condensation like C_T-domain.[12] Based on the type of cyclization linkage, fungal cyclic peptides are classified into homodetic cyclic peptides,

whose ring is solely composed of normal peptide bonds arising from head-to-tail cyclization, heterodetic cyclic peptides featuring other covalent bonds during cyclization, e.g. depsipeptides, and complex cyclic peptides combining both types of linkage, e.g. bicyclic peptides.[13]

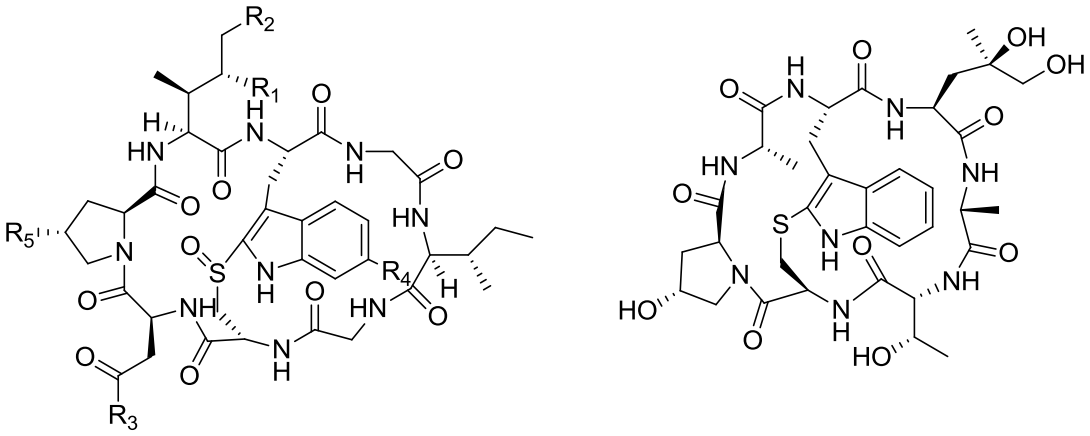

Fig 1-3. Ribosomally synthesized fungal peptides.

Fungal NRPS are classified into 3 major classes based on genetic studies of the domain architecture and the end peptide produced.[14] Type A with a linear NRPS template, as seen for the δ-(L-α-aminoadipyl)-L-cysteine-D-valine (ACV) synthetase and cyclosporine synthetase which are responsible for the production of the penicillin core structure and cyclosporine, respectively. Here the sequence of the end peptide is easily forecasted from the module architecture, as each module is responsible for incorporating a single amino acid building block. The second class is type B with an iterative NRPS template, where the modules are repetitively being used during peptide assembly, e.g. enniatin synthetase (ES). Lastly type C with a non-linear NRPS template, featuring an irregular domain architecture, from which the end peptide could not be inferred. So far, most studied fungal NRPS belong to the first 2 classes, whereas products of the last class have not been isolated so far. This is imminent to change, as fungal genes are increasingly being sequenced with the aim to explain fungal NRPS enzymology and probably isolate more secondary metabolites.

1.2.2 Fungal non-ribosomal peptides

Fungal non-ribosomal peptides share common structural features making them interesting drug scaffolds:

1. A cyclic architecture, bestowing several attractive attributes such as structural rigor eliciting better target binding and thus specific and enhanced biological activity. Stitching the loose ends, normally targeted by proteolytic enzymes, gives them added stability against enzymatic degradation. Moreover, masking of the charged termini, infers better membrane permeability.[15]
2. N-methylation of the peptide skeleton imposes steric hindrance about the N-methylated peptide bond which effects the whole peptide conformation. This plays an additional role in receptor affinity and selectivity. Replacing a hydrogen with a methyl group effects the hydrogen-bonding capabilities of the peptide, i.e. intra and intermolecular bonding. This is speculated to play a role in improving intestinal permeability and thus enhancing oral bioavailability, although the exact mechanism is still not clear.[16]
3. Presence of atypical building units, aside from the known L-configured 20 amino acids, such as D-amino acids, non-proteinogenic amino acids and carboxy acids, further improves their proteolytic stability.[17]

Due to these advantages, peptide-based drugs from fungal origin are employed since some time as extremely valuable drugs.

1.2.3 Fungal peptides as drugs

The β-lactams, 'a story that never grows old'

The antibiotic era was shaped by the fortunate discovery of penicillin, a non-ribosomal cyclic tripeptide isolated from *Penicillium* sp. in 1928, which played a pivotal role in saving the life's of hundreds from infection.[10] Since then, the search for antibiotics from microorganisms is commonplace, due to the development of resistance. The cephalosporins, a ring expanded form of the penicillins, were later isolated from *Cephalosporioum acremonium* obtained from a water sample off the coast of Sardinia in

1949, which is the first metabolite to be isolated from a water source.[18] Both penicillins and cephalosporins follow a similar biosynthetic route from the tripeptide δ-(L-α-aminoadipyl)-L-cysteine-D-valine (ACV) assembled by ACV synthetase. With the help of isopenicillin-*N*-synthase (IpnA), cyclization of the linear tripeptide gives the famous β-lactam nucleus, isopenicillin-N. Isopenicillin-N, a common intermediate for both antibiotics, acts as a branching point from which the complete biosynthesis of penicillin and cephalosporin is further realized using several more synthases.[19] β-lactams exert their anti-bacterial activity through irreversibly inhibiting the penicillin binding protein (PBP), responsible for cross-linking of the growing peptidoglycan layer of bacterial cell wall.[20]

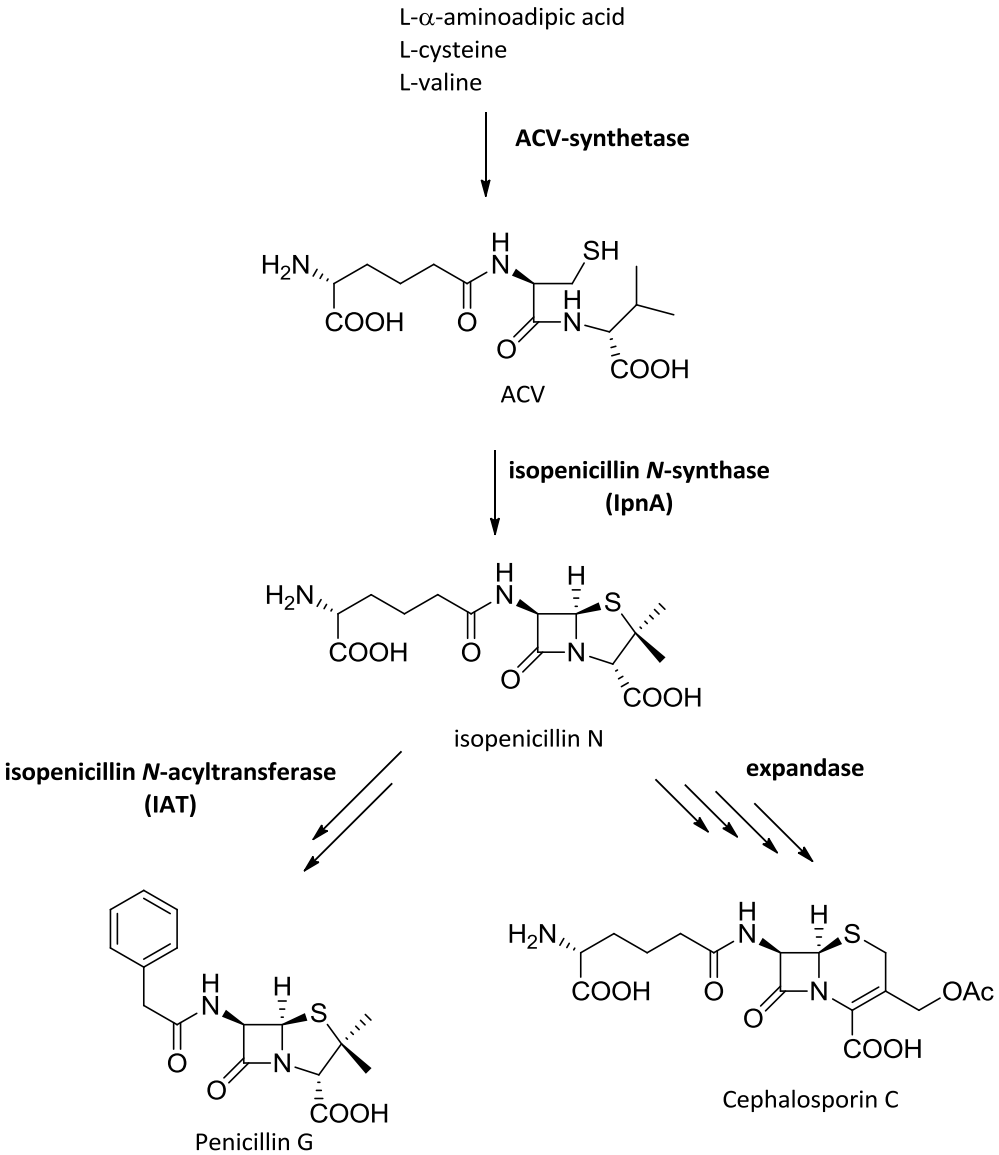

Fig 1-4. Biosynthetic route for β-lactam antibiotics, penicillin G and cephalosporin C (adopted from literature).[19]

To this day, both antibiotic peptide classes have been modified in several ways, through synthetic and semi-synthetic approaches, to provide us with more potent and superior analogues in terms of improved pharmacokinetics and antibiotic activity. The latest 5th generation cephalosporin antibiotic ceftaroline fosamil (Zinforo®), active against MRSA, was recently approved in the European Union in 2012 and many more are in the pipeline, indicating that a lot could still be derived from the β-lactam nucleus. [21,22]

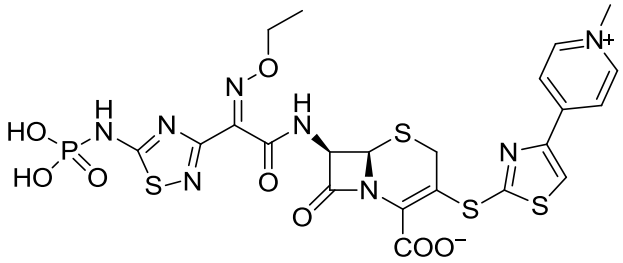

Ceftaroline fosamil (Zinforo®)

Fig 1-5. Ceftaroline fosamil a fifth generation cephalosporin antibiotic.

Cyclosporine peptides more than just immunosuppressants

Customary organ transplantation success is credited to cyclosporine A (Fig 1-1), a cyclic non-ribosomal undecapeptide, originally isolated in 1972 from *Tolypocladium inflatum*. It consists of several N-methylated amino acids, D-amino acid, i.e. D-alanine, as well as unusual amino acids such as L-α-aminobutyric acid and butenylmethyl-threonine. Its immunosuppressive property is due to its high affinity binding to cyclophilins in T-cells, inhibiting calcinuerin, a protein phosphatase, responsible for activation of NFAT (Nuclear factor of activated T-cells), a transcription factor that stimulates the expression of IL-2 (Interleukin 2), a cytokine signaling molecule, hence repressing the activity of the T-cells, an integral part of the immune system.[23] It is originally marketed as oral and intravenous formulations for use in organ transplantation, rheumatoid arthritis and psoriasis (Neoral®), with total net sales in 2013 exceeding 750 million USD.[24] A new formulation, ophthalmic emulsion (Restasis®), was launched in 2002 for the treatment of dry eyes.[25] Voclosporin, a cyclosporine A analogue with a single modified amino acid, was granted orphan designation for treatment of non-infectious uveitis, and is now in phase 2b clinical

trials for treatment of lupus nephritis.[26] Alisporivir, a second-generation cyclophilin inhibitor, synthetically modified from cyclosporine A but lacking immunosuppressive activity,[27] is currently in phase 3 clinical trials for AIDS treatment and is in phase 2 clinical trials for treatment of hepatitis C.[24]

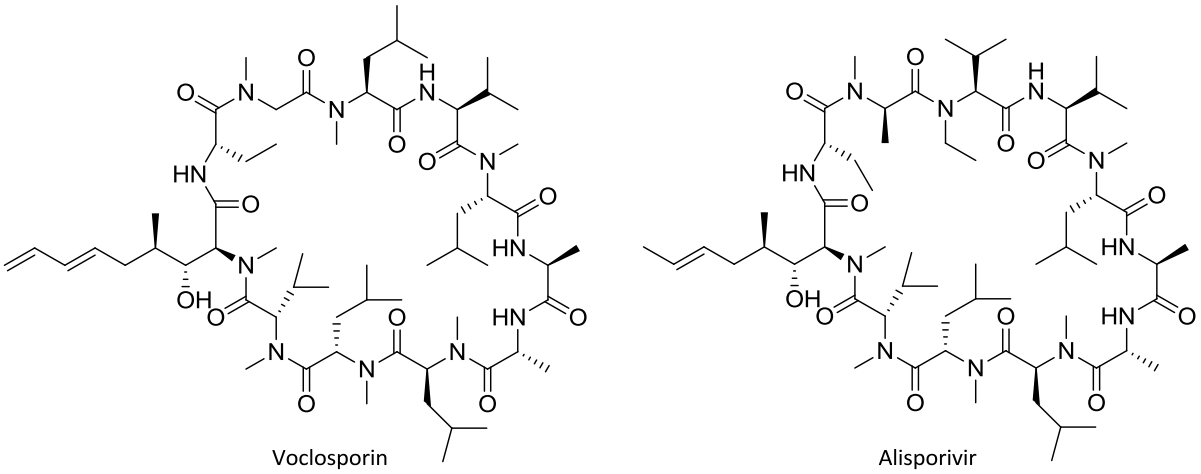

Fig 1-6. Cyclosporine peptide analogues in clinical trials.

The 'Penicillin of anti-fungals'

Echinocandins are the most recent clinically approved antifungal drug class, comprising the caspofungin, micafungin and anidulafungin. All are semi-synthetic analogues of the natural echinocandin B, isolated from *Aspergillus nidulans* in 1974, not clinically applicable due to its hemolytic activity. Echinocandins are cyclic lipo-hexapeptides with an N-linked fatty acyl side chain, along with several hydroxylated non-proteinogenic amino acids.[28]

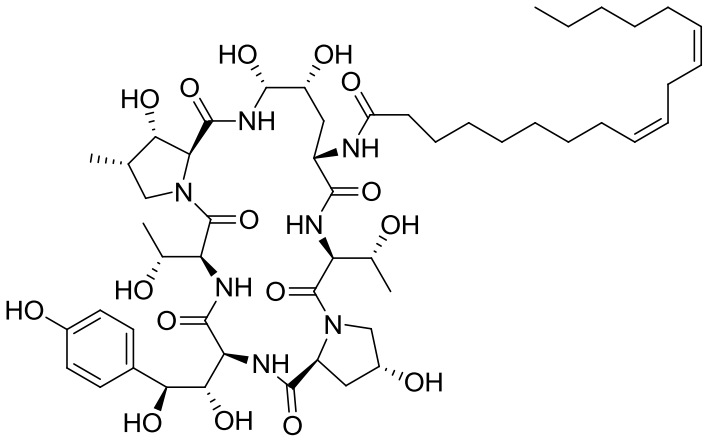

Echinocandin B

Fig 1-7. One of the first naturally isolated echinocandins.

Echinocandin biosynthesis is achieved by a six-module non-ribosomal peptide synthetase EcdA, along with several additional synthetases, such as EcdI for incorporating fatty acids.[29] They are considered the 'penicillin of antifungals` due to their exclusive mode of action targeting fungal cell wall, not the case for older antifungals. They non-competitively inhibit the β-1,3-D-glucan synthase, responsible for the biosynthesis of an integral part of fungal cell wall. Their mode of action makes them selective to fungal cell wall with no effect on mammalian host cells, in view of their different cell wall construction. They thus exhibit good safety and tolerability profiles with minimal toxicities and drug interactions. They are fungicidal against *Candida* sp., including azole-resistant strains, and fungistatic against *Aspergillus* sp..[30] Unfortunately, echinocandins are not orally bioavailable and have to be administered intravenously; this incites organic chemists in finding newer analogues that can overcome this formulation shortcoming. Aminocandin a new member of this class in clinical trials has a longer half-life, and hence may partially avoid the common drawback of a daily intravenous administration, allowing an extended dosing interval.[31]

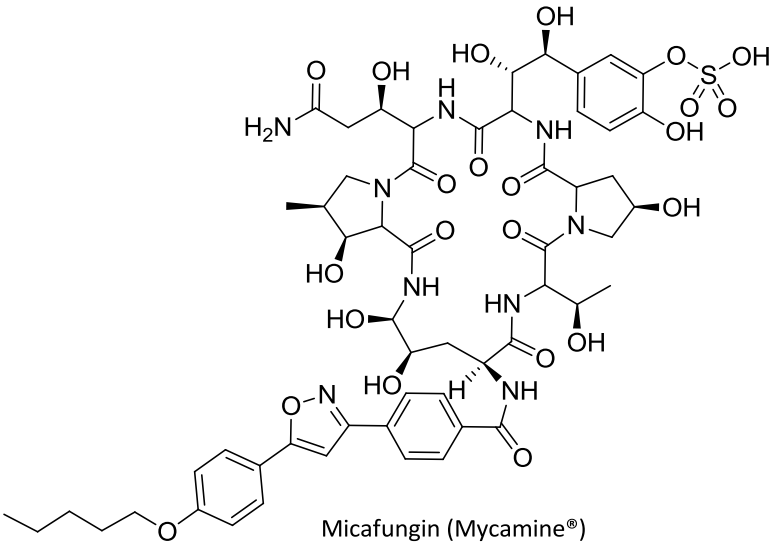

Micafungin (Mycamine®)

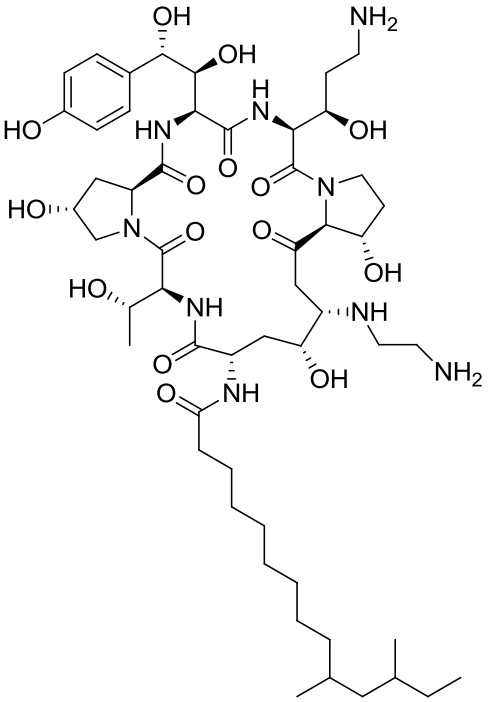

Caspofungin (Cancidas®)

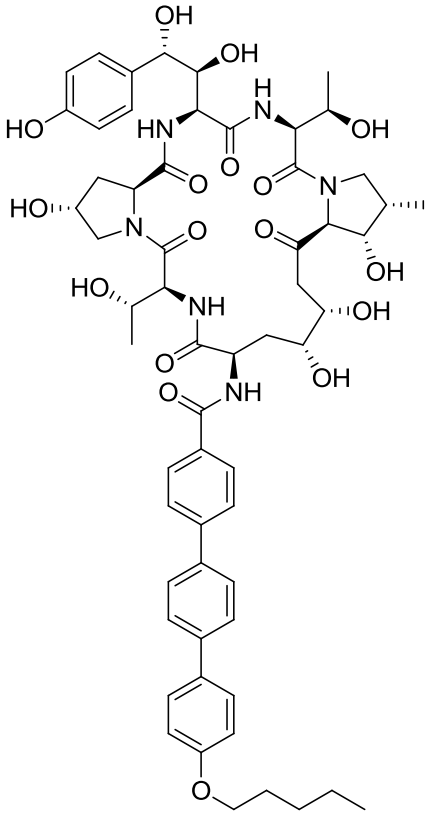

Anidulafungin (Ecalta®)

Fig 1-8. Approved semi-synthetic echinocandin antifungal drugs on the market.

The emerging increase in fatal invasive fungal infections, and the limited antifungal drug classes clinically at hand, calls upon the urgent intervention to introduce newer antifungals.[32] Echinocandins being the first antifungal drug class to target cell wall biosynthesis, prompted the interest in searching for newer antifungal drugs with a similar

mode of action, favorably orally administered. Recently, a semi-synthetic enfumafungin derivative MK-3118, a fungal triterpenoid glycoside, is in clinical trials as an orally active antifungal, similarly targeting the β-1,3-D-glucan synthase.[33]

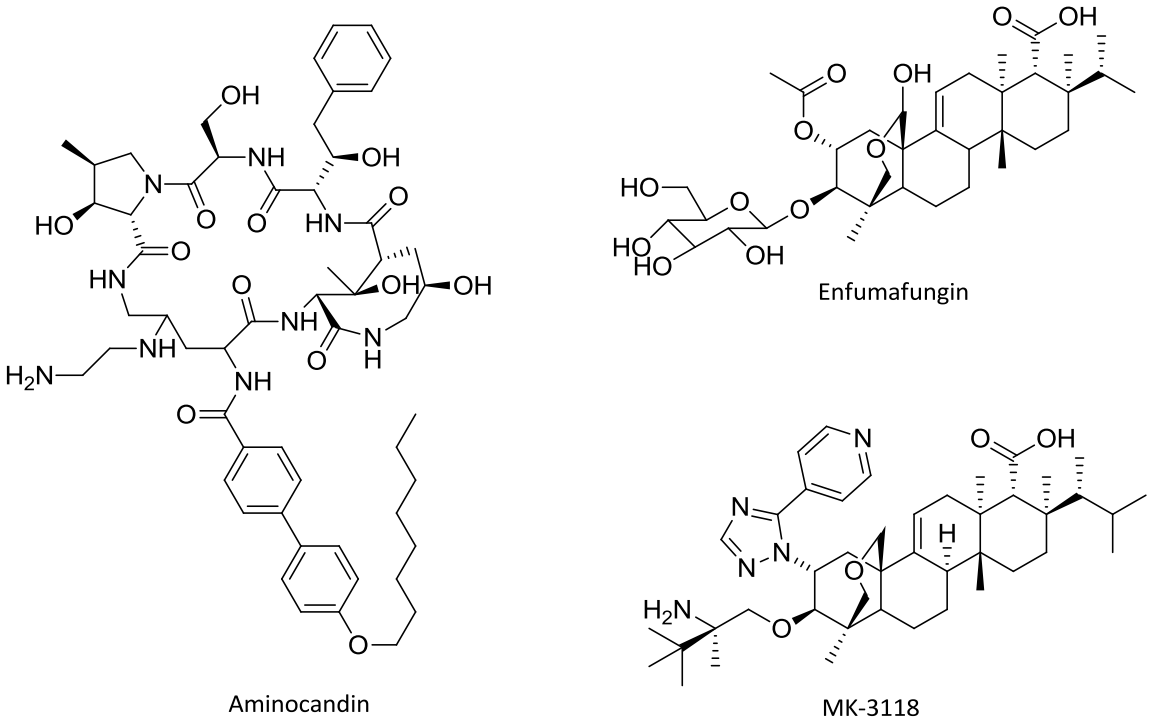

Fig 1-9. Newer antifungal drugs in clinical trials targeting the β-1,3-D-glucan synthase.

Fungal cyclic hexadepsipeptides

The enniatins are a family of cyclohexadepsipeptides initially isolated from *Fusarium* sp., but also produced by other fungal genera. So far 29 enniatins have been isolated, all featuring three N-methyl-L-amino acids, such as valine, leucine and isoleucine, and three D-hydroxyacids, with alternating ester and amide bonds forming a ring structure.[34] They are biosynthesized in an iterative manner with the help of the enniatin synthetase (ES), a two-module multienzyme, showing flexible substrate selectivity incorporating variable amino acids, which explains the structural diversity of the enniatins.[35] Beauvericin and destruxin are other fungal cyclohexadepsipeptides, structurally related to the enniatins, which were originally isolated from the entomopathogenic fungi *Beauveria bassiana* and *Metarhizium anisopliae* respectively.[36,37]

A characteristic feature of these fungal cyclohexadepsipeptides is their ionophoric activity. They form cation selective pores or channels, which disturbs the cell's normal ion balance and thus disrupt the cell membrane integrity leading to cell death. This mechanism is suggested to account for their wide range of interesting biological activities, including insecticidal, anti-microbial, cytotoxic and anti-viral activity, nominating them as prospective drug leads.[34,36,37] Currently fusafungine, an enniatin mixture, is marketed for topical use in upper respiratory tract infection for its antibiotic and anti-inflammatory properties.[38]

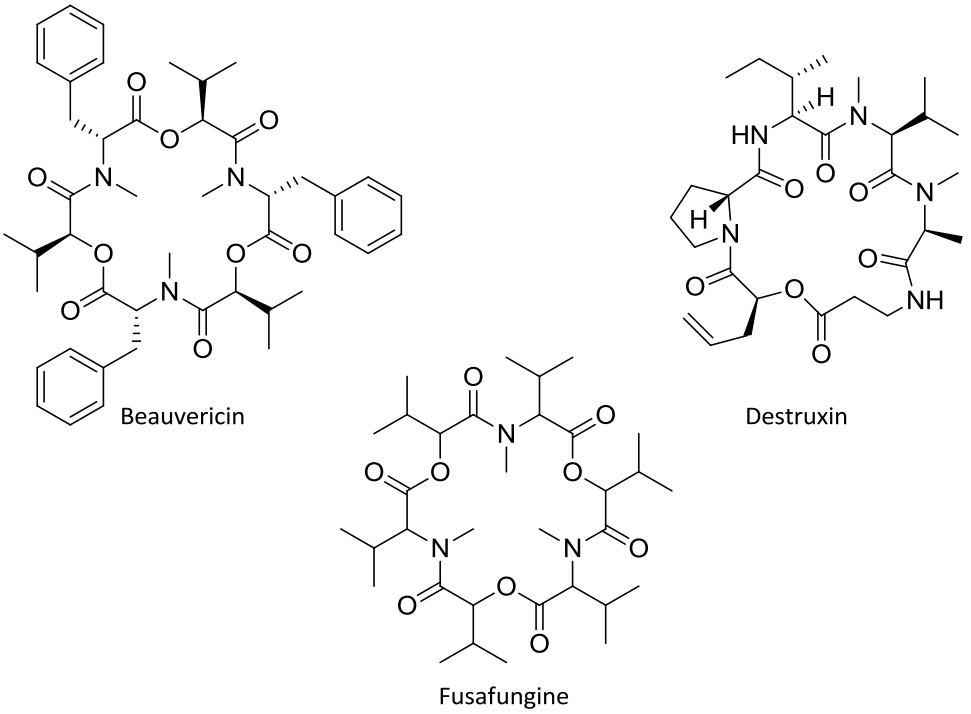

Fig 1-10. The enniatins, fungal cyclohexadepsipeptides.

Fungal cyclo-dipeptides in cancer chemotherapy

Cyclo-dipeptides, referred to as diketopiperazines, are the smallest peptides composed of two amino acids joined in a head-to-tail fashion to form a characteristic heterocyclic ring. Their simple, rigid and chiral structure endows them with interesting biological activities, such as cytotoxic, anti-microbial and anti-inflammatory activities.[39]

Since the concomitant isolation of phenylahistin (halimide) from cultures of a terrestrial and marine *Aspergillus* sp., by two independent work groups from opposite sides of the world, and the frantic quest for newer better anti-cancer analogues, employing the

natural scaffold of phenylahistin is ongoing.[40,41] Phenylahistin features a phenylalanine and an isoprenylated dehydrohistidine moieties. With most of the anticancer drugs available to date being derived from natural products, nature's contribution in treating and providing a better understanding of the cancer black box is highly appreciated.[42] Phenylahistin inhibited cell proliferation through a colchicine-like tubulin depolymerizing activity and showed cytotoxic activity towards several cancer cell lines.[43] Plinabulin (NPI-2358), a chemically modified analogue still retaining important structural features required for anticancer activity, i.e. a pseudo-tricyclic structure, an L-phenylalanine and a gem-dimethyl at position 5 of the imidazole,[44] has completed phase 2 clinical studies as a vascular disrupting agent (VDA) in combination with docetaxel in patients with non-small cell lung cancer (NSCLC). VDA's are a new class of anti-angiogenic agents targeting the present tumor vasculature, necessary for the growth and proliferation of solid tumors.[45] Plinabulin displayed notable antitumor activity with satisfactory safety and toxicity profiles and is to be moved to phase 3 testing.[46] Profiting from emerging drug delivery technologies, an antibody drug conjugate of plinabulin is being developed for selective targeting of cancer cells.[47]

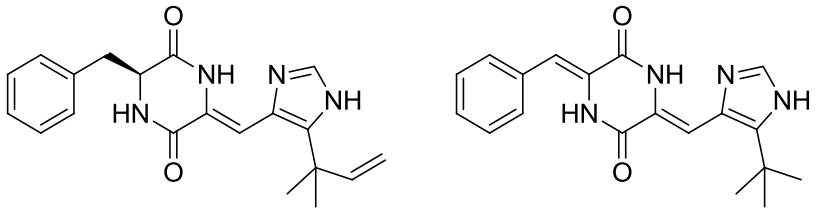

Fig 1-11. Fungal diketopiperazines as anticancer drug leads.

Another fungal diketopiperazine overarched by a disulfide bridge, which is gaining much attention, is the mycotoxin gliotoxin. It's the prototype of the compound class epipolythiodioxopiperazine (ETP). Its biosynthesis from 2 amino acid building blocks, i.e. L-serine and L-phenylalanine has been extensively studied.[48] Its toxicity is dependent on the sulfide bridge, which on the other hand is responsible for its potential therapeutic value. Gliotoxin targets hypoxia inducible factor-1 alpha (HIF-1α), which plays an important role in tumor progression and angiogenesis, and hence makes a promising anticancer drug scaffold.[49]

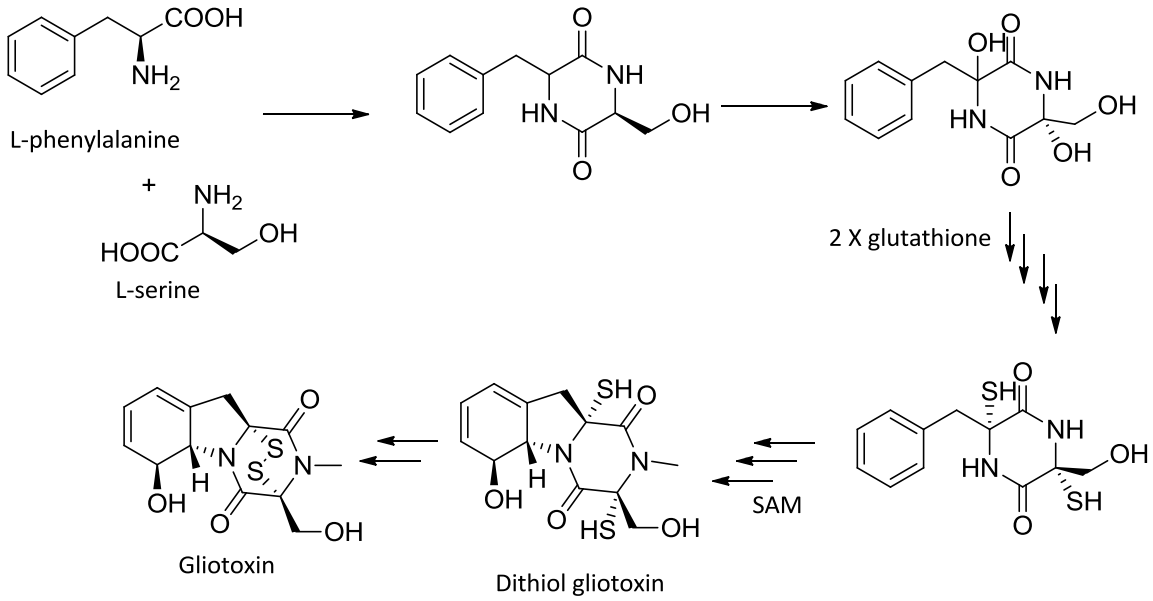

Fig 1-12. Gliotoxin biosynthesis, involving a series of enzyme-catalyzed steps converting phenylalanine and serine to gliotoxin (adopted from literature).[48]

Fungal cyclic tetrapeptides as histone deacetylase (HDAC) inhibitors

With the guidance of a trapoxin-based affinity compound, purification of histone deacetylase, an enzyme ubiquitously distributed and involved in several cellular mechanisms such as cell growth and development, was possible for the first time.[50] Epigenetic changes in the level of expression of histone deacetylase, results in several life threatening disorders, such as cardiovascular and neurological diseases, metabolic disorders and cancers. Histone deacetylase is regarded as the molecular target of histone deacetylase inhibitors and are thus recognized as a potential therapeutic domain for a wide range of prevalent diseases.[51] Furthermore, cyclic peptides are an important class of HDAC inhibitors.

Trapoxin, a hydrophobic cyclic tetrapeptide isolated from the fungus *Helicoma ambiens,* features a unique amino acid, 2-amino-8-oxo-9,10-epoxydecanoic acid (Aoe), which is responsible for its irreversible HDAC inhibitory activity. Other previously isolated fungal cyclic tetrapeptides with an epoxy-ketone group, such as HC toxin, chlamydocin, WF-3161 and Cyl-2, similarly exhibited isoform selective inhibition of HDAC. A synthetic hybrid between the epoxy-ketone containing cyclic tetrapeptides and the hydroxamate class of HDAC inhibitors, resulted in a new class termed cyclic hydroxamic acid containing peptides (CHAP) with improved inhibitory activity and selectivity towards HDAC isoform classes.[52] Apicidin isolated from *Fusarium* sp., although lacking a terminal α-keto epoxide, posses HDAC inhibitory activity. Thus Aoe is not essential for biological activity apart from exerting an irreversible inhibitory mechanism.[50] The combined use of apicidin and docetaxol, a cytotoxic agent, was found to exhibit a synergistic anticancer effect with a reduction in adverse effects, thus discerning the beneficial effect of novel combination regimes for cancer treatment.[53] Moreover, these non-ribosomally assembled cyclic tetrapeptides are used as conformational rigid scaffolds for the preparation of new HDAC inhibitors and simultaneously attain a deeper understanding of the pharmacophore elements essential for HDAC inhibitory activity.[54]

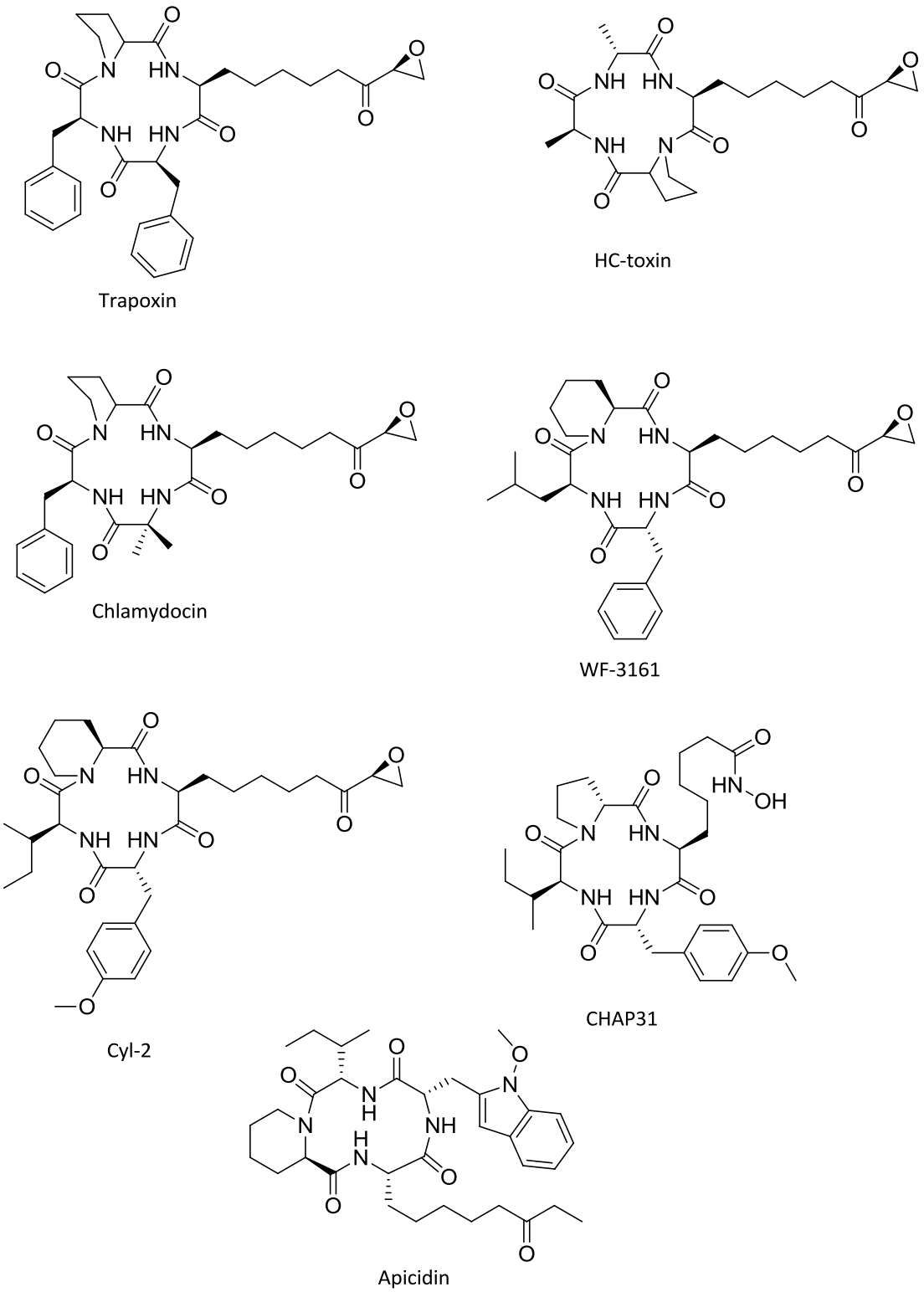

Fig 1-13. Fungal HDAC inhibitor peptides.

Ergopeptines/ Ergopeptides

Ergopeptides are considered one of the oldest fungal metabolites. These are peptidic alkaloids isolated from the ergot fungus belonging to the genus *Claviceps*. They are composed of a tripeptide, modified into a bicyclic cyclo-lactam structure, linked to a tetracyclic ergoline ring. They have been used in folk medicine by midwives as an abortifacient, to induce labor and in treatment of post-partum hemorrhage. Their mode of action is generally realized from their agonist activity to several receptors as a result of their structural analogy to several neurotransmitters, e.g. serotonin, dopamine and epinephrine.[55] Ergotamine, the major alkaloid produced by ergot, is still prescribed for acute migraines usually in combination with caffeine (Cafergot®). Bromocriptine (Parlodel®), a semi-synthetic derivative of the ergopeptide ergocriptine, is used in the treatment of hyperprolactinaemia and parkinson disease.[56] In 2009, bromocriptine mesylate (Cycloset®) was approved by the FDA for treatment of type 2 diabetes.[57]

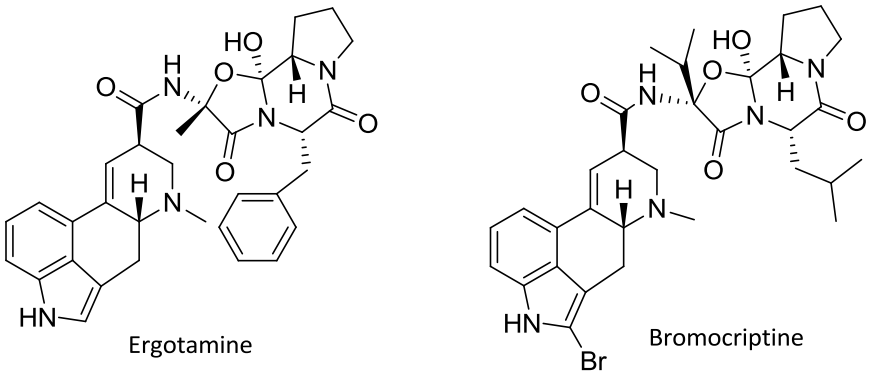

Fig 1-14. Ergopeptides used as drugs.

A unique feature of ergopeptine biosynthesis is their assembly by two NRPS subunits, a trimodular lysergylpeptidyl synthetase 1 (LPS1) and a monomodular lysergylpeptidyl synthetase 2 (LPS2). LPS2 is responsible for activation of D-lysergic acid, a modified tryptophan, which is sequentially elongated by LPS1 to form D-lysergyltripeptide. This is released as D-lysergyltripeptide lactam (L-ergopeptam), which then undergoes heterocyclization to give the ergopeptines.[58]

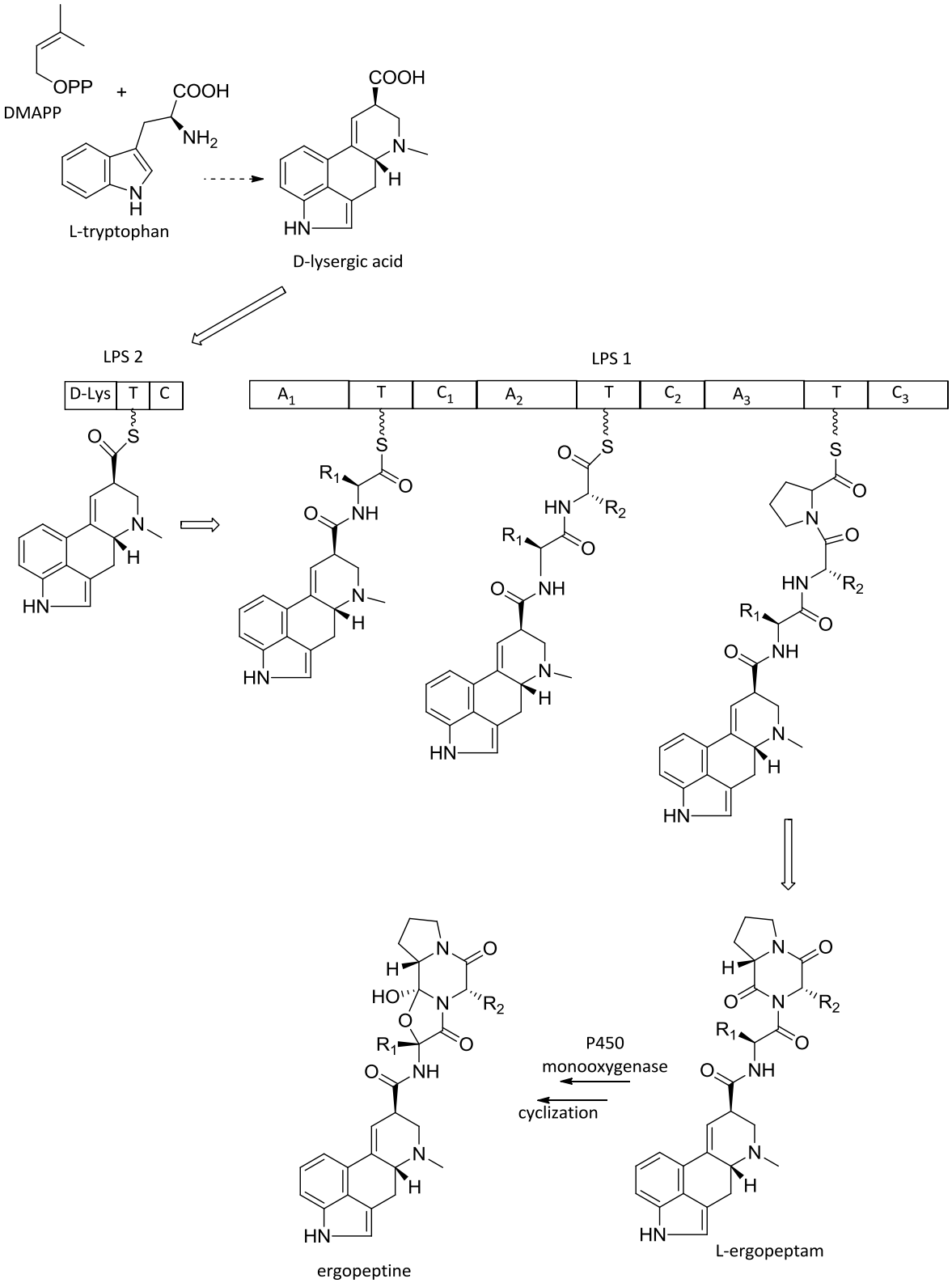

DMAPP: dimethylallyl diphosphate
A: adenylation domain
C: condensation domain
LPS: lysergylpeptidyl synthetase
T: thiolation domain

Fig 1-15. Ergopeptines biosynthesis. (adopted from literature).[58]

Fungal Antimicrobial Peptides (AMP)

With the upsurge of antibiotic resistant pathogens and its impact on the global public health, the relentless search for new antibiotics classes, that don't readily develop resistance, is becoming no longer an extravagance.[59,60] Antimicrobial peptides (AMP) preferably named host defense peptides (HDP), as their activities includes more than being antimicrobial, is an archaic part of the innate immune system of most multi-cellular organisms. Recently they have been the focus of research, initially for their novel anti-infective potential, but also for a wide range of other clinical applications, such as anti-inflammatory, anticancer, wound healing, vaccine adjuvants etc.[61]

Defensins, the largest family of HDP, are gene-encoded cationic amphipathic cysteine-rich peptides stabilized through disulfide bridges.[62] Plectasin, the first fungal defensin, was isolated from a black saprophytic ascomycete *Pseudoplectania nigrella.*[63] It displayed potent antibacterial activity against Gram *+ve* bacteria, by inhibiting cell wall biosynthesis through complexing with bacterial cell wall precursor Lipid II.[64] NZ-2114 a plectasin derivative with three mutational amino acids, showed superior activity against streptococci and staphylococci, including methicillin resistant *Staphylococcus aureus* (MRSA). Additionally, it demonstrated minimal cell toxicity with prolonged serum stability and *in-vivo* half-life, credited to its protease resistant disulfide-stabilized scaffold.[65,66] NZ-2114 is currently undergoing preclinical development and may soon join other HDP entering clinical trials as a promising new generation of antibiotics.[67]

a) GFGCNGPWDEDDMQCHNHCKSIKGYKGGYCAKGGF--VCKCY

b)

© *Nature* 2005

Fig 1-16. a) Plectasin amino acid sequence, b) A single representative structure of plectasin in cartoon mode showing the proximity of disulphide bridges. Cystine bridges are highlighted in orange (adopted from literature).[63]

1.3 Peptides incorporating 3-(3-furyl)-alanine and their bioactivities

Almost three decades ago, rhizonin A a heptapeptide mycotoxin, was isolated from *Rhizopus microsporus*, a fungus used to prepare fermented food such as tempeh, a popular vegetarian meat substitute.[68] Two decades later, it was found to be originally produced by the bacterial endosymbiont *Burkholderia* sp.[69] Rhizonin A is considered the major metabolite produced by the plant growth promoting rhizobacteria (PGPR) strain *Burkholderia* sp., enhancing seed germination and growth, and is to be explored for sustainable agriculture production.[70] Interestingly, rhizonin A is the first naturally isolated peptide that contains 3-(3-furyl)-alanine, a non-proteinogenic amino acid rarely encountered in nature. Rhizonin A showed *in-vitro* hepatotoxicity, as well as *in-vitro* fat-accumulation inhibitory activity against 3T3-L1 murine adipocytes.[71] Synthetic replacement of 3-(3-furyl)-alanine with phenylalanine gave analogues with increased fat-accumulation inhibitory activity and reduced cytotoxicity when compared to rhizonin A. Accordingly, cytotoxicity of rhizonin A could be ascribed to its 3-(3-furyl)-alanine content, which appears to be non-essential for the observed biological activity.[72] This is in agreement with earlier studies focusing on synthetic heterocyclic analogues of phenylalanine, i.e. 3-(3-furyl)-alanine, exhibiting growth inhibitory activity in both bacteria and fungi, which was reversed by the addition of phenylalanine.[73]

A cyclic pentapeptide bingchamide B, isolated from the soil-dwelling bacterial strain *Streptomyces bingchenggensis*, was also seen to incorporate this rare amino acid moiety. Bingchamide B showed *in-vitro* cytotoxic activity towards a human colon cancer cell line with an IC_{50} value of 18 μg ml^{-1}. This makes it an interesting scaffold for the development of antitumor agents.[74]

Chemically synthesized L-3-(3-furyl) and L-3-(2-furyl)-alanine are used as an agrochemical fungicide, industrial microbiocide and wood preservative.[75] So far, 3-(3-furyl)-alanine was never independently isolated from natural sources, apart from a carboxy derivative isolated from the fruiting bodies of the gilled mushrooms *Phyllotopsis nidulans* and *Tricholomopsis rutilans*.[76,77]

Little is known about the biosynthesis of this unusual amino acid, apart from being considered as a potential substrate of the NRPS machinery, known to incorporate such atypical building blocks.

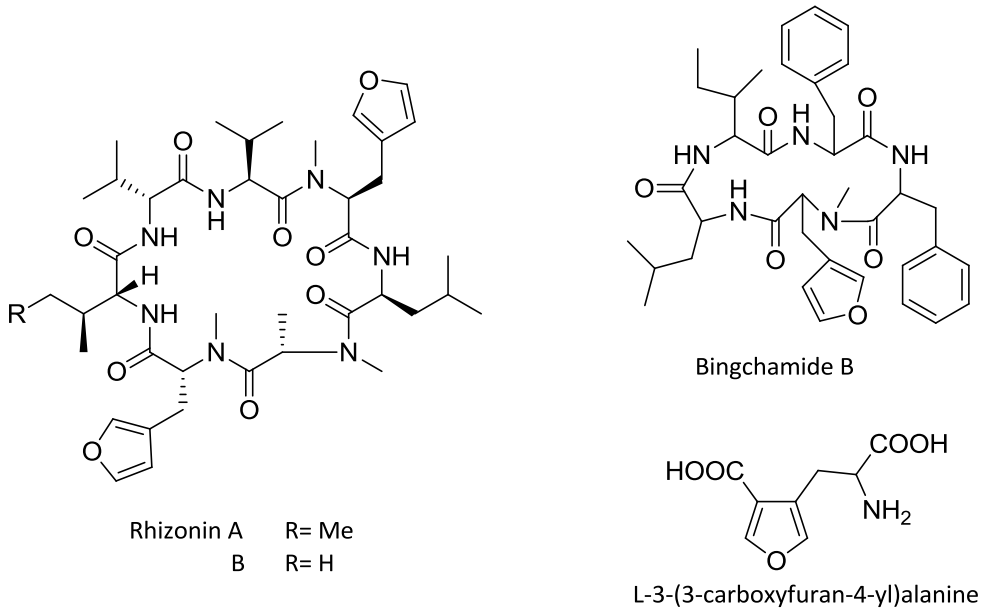

Fig 1-17. Peptides incorporating 3-(3-furyl)-alanine and a carboxy derivative of 3-(3-furyl)-alanine.

2. Scope of the present study

With the current trend towards peptide-based drugs, as observed in the increasing number of such compounds entering clinical trials annually,[6] the search for new peptide scaffolds is ongoing. They are used for their diverse disease curing properties, as a platform for selective drug delivery or as a diagnostic tool to study biological process.[78] The design of peptides by fungal metabolism is unprecedented, which is notable from the growing number of publications focusing on fungal peptides. Fungi from diverse habitats, both terrestrial and marine, are investigated and yielded fascinating structural diversity and a wide spectrum of biological activity.[18,79,80,81,82]

The scantly explored marine fungal strain *Stachylidium* sp. is elected in the present study for an in-depth investigation. Previous studies in our group demonstrated the metabolic capabilities of this strain in terms of unique metabolites. These belong to different compound classes (including peptides), with both interesting chemistry and biological activity.[83,84,85] Furthermore, the *Stachylidium* sp. belongs to the phylum Ascomycota, the largest fungal phylum, whose members include the well known *Penicillum* and *Aspergillus* spp. extensively studied for their medicinal and disease causing properties. They are the most frequent producers of natural products, including the penicillin antibiotics and the cholesterol lower drug lovastatin. It is believed that the full biosynthetic potential of the *Stachylidium* sp. has not been totally brought to light. Much could be earned from studying this strain, in terms of unique chemistry, biosynthetic mechanisms employed and most important promising biological activity.

Course of study

The first part of the study has the aim to isolate and elucidate novel peptide scaffolds. With the help of chromatographic (VLC, HPLC) and spectroscopic (NMR, MS, UV, IR) techniques successful isolation and chemical characterization of novel metabolites is anticipated.

The focus of the second part of the study is the intensive investigation of the biosynthetic origin of the isolated metabolites. Thus, classical isotope feeding experiments are planned, preceded by preliminary experiments to assist in setting up a successful feeding

protocol that would ensure maximal incorporation of fed precursors into the target metabolites.

The third and last part is to evaluate the biological activity of the isolated metabolites with focus on their potential activity on the G protein-coupled galanin receptors.

3. Materials and Methods (General procedures)

3.1 Fungal material

The marine-derived fungus *Stachylidium* sp. was isolated in our lab from the sponge *Callyspongia* sp. cf. *C. flammea*, collected from the coral reef in Bare Island, New South Wales, Australia. The fungal strain was identified through the Belgian coordinated collections of microorganisms of the Catholic University of Louvain (BCCM/MUCL) by Dr. P. Massart and Dr. C. Decock. A fungal specimen is deposited at the Institute for Pharmaceutical Biology, University of Bonn, isolation number "293K04", running number "220".

3.2 Cultivation and extraction

Culture media

Biomalt salt medium (BMS): 20 g L^{-1} biomalt extract, 15 g L^{-1} agar (for solid medium) and 1 L ASW (artificial sea water): 0.10 g L^{-1} KBr, 23.48 g L^{-1} NaCl, 10.61 g L^{-1} $MgClx6H_2O$, 1.47 g L^{-1} $CaCl_2x2H_2O$, 0.66 g L^{-1} KCl, 0.04 g L^{-1} $SrCl_2x6H_2O$, 3.92 g L^{-1} Na_2SO_4, 0.19 g L^{-1} $NaHCO_3$ and 0.03 g L^{-1} H_3BO_3.

Pre-cultures

First pre-culture (solid): fungal strain was inoculated on BMS agar petri-dishes and incubated at 25°C for 4 weeks.

Second pre-culture (liquid): from the first pre-culture, a seed inoculum was used to inoculate 1 L Erlenmeyer flasks (3 flasks) each containing 300 ml of liquid BMS media. Liquid pre-cultures were shaken at 121 rpm at 25°C for 10 days.

Main culture

From the previous liquid pre-culture, liquid seed inoculums were aseptically transferred to Fernbach flasks (5 ml for each flask) containing 250 ml BMS agar media and incubated at room temperature for 30 days.

Extraction

At the end of the cultivation period (30 or 60 days), the homogenized fungal biomass and cultivation media were exhaustively extracted with ethyl acetate and concentrated under vacuum (using vacuum rotatory evaporator, 40°C) to yield the crude extract.

3.3 Chromatography

3.3.1 Thin Layer Chromatography (TLC)

Standard chromatograms of extracts and fractions were developed on either TLC aluminum sheets silica gel 60 F_{254} (Merck) as stationary phase using a petroleum ether/acetone mixture in different concentrations or TLC aluminum sheets RP-18 F_{254} (Merck) as stationary phase using a methanol/water mixture in different concentrations, both at room temperature under saturated conditions. Chromatogram detection was accomplished under UV light (λ 254 nm and 366 nm) and using vanillin-sulphuric acid spraying reagent (0.5 g vanillin dissolved in a mixture of 85 ml methanol, 10 ml acetic acid and 5 ml sulphuric acid, TLC plates heated at 100°C after spraying).

3.3.2 Vacuum Liquid Chromatography (VLC)

VLC was used for crude extract fractionation using Merck silica gel 60M (0.040-0.063 mm, 230-400 mesh size) as sorbent. Standard glass columns (dimensions 10 x 2 cm) were wet packed and equilibrated under vacuum using petroleum ether. Two gradient solvent systems of increasing polarity were used for sample elution, either starting with 100% petroleum ether to 100% dichloromethane to 100% ethyl acetate to 100% acetone to 100% methanol yielding 9 fractions or starting with 100% petroleum ether to 100% acetone to 100% methanol yielding 8 fractions. Fractions were collected and concentrated under vacuum (using vacuum rotatory evaporator, 40°C).

3.3.3 High Performance Liquid Chromatography (HPLC)

Preparative HPLC was performed on either (a) HPLC system composed of a Waters 515 pump with a Knauer K-2300 differential refractometer, using a Knauer column (250 x 8 mm, 5µm, Eurospher II-100 Si, flow rate 2 ml min^{-1}) or (b) a Merck-Hitachi system

equipped with an L-6200A pump, an L-4500A photodiode array detector and a D-6000 interface, using Macherey-Nagel columns (Nucleodur C_{18} EC Isis and Nucleodur C_{18} Sphinx RP each with 250 x 4.6 mm, 5µm, flow rate 1 ml min^{-1}).

3.4 Structure elucidation

The chemical structures of the isolated compounds were established using one dimensional and two dimensional NMR techniques along with MS methods. Additional structural information was provided from optical rotation measurements, UV and IR spectroscopy. Database and literature search using MarinLit database®, AntiBase database® and Scifinder database® was performed to determine the novelty of the isolated compounds.

3.4.1 NMR spectroscopy

All NMR spectra were recorded in acetone-d_6 or methanol-d_4 referenced to residual solvent signals with resonances at $\delta_{H/C}$ 2.04/29.8 and $\delta_{H/C}$ 3.35/49.0 respectively, using either a Bruker Avance 300 DPX spectrometer operating at 300 MHz (^{1}H) and 75 MHz (^{13}C) or a Bruker Avance 500 DRX spectrometer operating at 500 MHz (^{1}H) and 125 MHz (^{13}C). Spectra were processed using Bruker 1D WIN-NMR, 2D WIN-NMR or XWIN-NMR version 2.6, 3.1 and 3.5 software. The following NMR experiments: ^{1}H, ^{13}C, DEPT 135, ^{1}H-^{1}H COSY, ^{1}H-^{13}C direct correlation (HSQC), ^{1}H-^{13}C long range correlation (HMBC) and ^{1}H-^{1}H ROESY, were performed for structural assignment. From DEPT experiments, multiplicity of carbons could be deduced. Incorporation of ^{13}C-labeled precursors was evaluated using both ^{1}H decoupled ^{13}C NMR spectroscopy and inverse gated ^{1}H decoupled ^{13}C NMR spectroscopy.

3.4.2 Mass Spectrometry (MS)

HPLC-MS measurements were conducted by Ekaterina Eguereva (Institute for Pharmaceutical Biology, University of Bonn, Germany), employing an Agilent 1100 Series HPLC including DAD, with RP C_{18} column (Macherey Nagel Nucleodur 100, 125 x 2 mm, 5µm) and a 2 mmol NH_4Ac buffered methanol/water gradient elution system (flow rate 0.25 ml min^{-1}), starting from 10% to 100% MeOH over a 20 min period, then isocratic for

10 min. The HPLC system was coupled with an API 2000, Triple Quadrupole LC/MS/MS, Applied Biosystems/MDS Sciex and an ESI source. Samples were dissolved in MeOH (1 mg ml^{-1}) prior to injection.

HRESIMS measurements were conducted by C. Sondag (Department of Chemistry, University of Bonn, Germany) using a Bruker Daltonik micrOTOF-Q mass spectrometer with an ESI source.

3.4.3 Optical rotation

Optical rotations were measured on a Jasco DIP 140 polarimeter (1 dm, 1 cm^3 cell) operating at wavelength λ=589 nm corresponding to the sodium D line at room temperature. Specific optical rotation $[\alpha]_D^T$ was calculated pursuant to:

$$[\alpha]_D^T = \frac{100 \times \alpha}{c \times l}$$

T: temperature [°C]

D: sodium D line at λ=589 nm

c: concentration [g/100 ml]

l: cell length [dm]

α: optical rotation

Compounds were dissolved in methanol and the average optical rotation α was based on at least 10 measurements.

3.4.4 UV measurements

UV spectra were obtained using a Perkin Elmer Lambda 40 UV/Vis spectrometer with UV WinLab Version 2.80.03 software, using 1.0 cm quartz cell. The molar absorption coefficient ε was determined in accordance with the Lambert-Beer-Law:

$$A = \varepsilon \times c \times b \iff \varepsilon = A/(c \times b)$$

ε: molar absorption coefficient [L/mol×cm]

A: absorption at peak maximum

c: concentration [mol L^{-1}]

b: layer thickness of solution [cm]

3.4.5 IR spectroscopy

IR spectra were recorded as film using Perkin Elmer FT-IR Spectrum BX spectrometer, with Spectrum v3.01 software.

3.4.6 Advanced Marfey's method

Peptide hydrolysis: Peptides (0.5 mg of each) were separately dissolved in 6 N HCl (0.5 ml) and heated at 110°C for 16 hours in closed glass vials. After cooling, the solvent was removed using a nitrogen stream and redissolved in 50µl H_2O.

Derivatization: The peptide hydrolysate and 1 mg of each respective standard L- and D-amino acid were resuspended in 50 µl H_2O, and 100 µl of 1% (*w/v*) L-FDAA (in acetone) and 40 µl of 1 M $NaHCO_3$ were added. The mixture was heated at 70°C for 40 minutes. After cooling to room temperature, the reaction was quenched by adding 20 µl of 2 N HCl, and solvents evaporated to dryness.

Analysis: Samples were resuspended in MeOH (1 mg ml^{-1}) for HPLC-MS analyses. Comparison of the retention times observed for the derivatized hydrolysates and the derivatized standards revealed the absolute configuration of the peptide residues.

3.5 Biosynthetic studies

3.5.1 Time-scale cultures

The fungus was cultivated on BMS agar petri-dishes (incubated at room temperature) and liquid BMS Erlenmeyer flasks (shaken at 121 rpm and 25°C). Unlabeled compounds

(glycerol, phenylalanine and sodium acetate) were added as filter sterile aqueous solutions to some of the cultures (final concentration 1 mg ml^{-1}). After defined time intervals (days 5, 9, 14, 20, 30 and 55), representative cultures were extracted with ethyl acetate and analyzed using HPLC-MS. Metabolites of interest were monitored at specific retention times.

3.5.2 Precursor directed biosynthesis

The fungus was cultivated on liquid (with shaking) and solid BMS media to which several precursors, including amino acids and halogenated precursors, were added as filter sterilized aqueous solutions (final conc. 1 mg ml^{-1}) and cultivated for 15 and 30 days respectively, followed by extraction with ethyl acetate and analysis.

3.5.3 Feeding experiment with [1-^{13}C]phenylalanine

The fungus was cultivated in four Fernbach flasks each containing 250 ml BMS agar media using a liquid seed inoculum from the second liquid fungal pre-culture (5 ml for each Fernbach flask). [1-^{13}C]phenylalanine was added as filter sterilized aqueous solution twice on day 5 and day 10 (final conc. 1 mg ml^{-1}). The flasks were incubated at room temperature for 30 days, followed by extraction with ethyl acetate and analysis.

3.5.4 Feeding experiment with [U-^{13}C]glycerol

The fungus was cultivated in two Fernbach flasks each containing 250 ml BMS agar media using a liquid seed inoculum from the second liquid fungal pre-culture (5 ml for each Fernbach flask). [U-^{13}C]glycerol was added as filter sterilized aqueous solution twice on day 5 and day 10 (final conc. 2 mg ml^{-1}). The flasks were incubated at room temperature for 30 days, followed by extraction with ethyl acetate and analysis.

3.5.5 Feeding experiment with [1-^{13}C]glucose

The fungus was cultivated in two Fernbach flasks each containing 250 ml BMS agar media using a liquid seed inoculum from the second liquid fungal pre-culture (5 ml for each Fernbach flask). [1-^{13}C]glucose was added as filter sterilized aqueous solution twice on

day 5 and day 10 (final conc. 2 mg ml^{-1}). The flasks were incubated at room temperature for 30 days, followed by extraction with ethyl acetate and analysis.

3.5.6 Feeding experiment with [1-^{13}C]sodium acetate

The fungus was cultivated in six Fernbach flasks each containing 250 ml BMS agar media using a liquid seed inoculum from the second liquid fungal pre-culture (5 ml for each Fernbach flask). [1-^{13}C]sodium acetate was added as an autoclaved aqueous solution thrice on day 10, day 20 and day 30 (final conc. 2.5 mg ml^{-1}). The flasks were incubated at room temperature for 60 days, followed by extraction with ethyl acetate and analysis.

3.5.7 Feeding experiment with [*Me*-^{13}C]methionine

The fungus was cultivated in six Fernbach flasks each containing 250 ml BMS agar media using a liquid seed inoculum from the second liquid fungal pre-culture (5 ml for each Fernbach flask). [*Me*-^{13}C]methionine was added as filter sterilized aqueous solution thrice on day 10, day 20 and day 30 (final conc. 1.3 mg ml^{-1}). The flasks were incubated at room temperature for 60 days, followed by extraction with ethyl acetate and analysis.

3.5.8 Feeding experiment with [1,7-^{13}C]shikimic acid

The fungus was cultivated in a petri-dish containing 10 ml BMS agar media using a liquid seed inoculum (0.5 ml) from the second liquid fungal pre-culture. [1,7-^{13}C]shikimic acid was added as filter sterilized aqueous solution twice on day 5 and day 10 (final conc. 1 mg ml^{-1}). The petri-dish was incubated at room temperature for 30 days, followed by extraction with ethyl acetate and analysis.

3.6 Biological testing

3.6.1 Agar diffusion assays

Antimicrobial tests of isolated compounds were performed by Edith Neu (Institute for Pharmaceutical Biology, University of Bonn) following the method described by Schulz *et al*.[86,87] The bacteria *Bacillus megaterium* and *Escherichia coli* were used as representatives for *gram positive* and *gram negative* bacteria. *Microbotryum violaceum* (Ustomycetes),

Eurotium rubrum (formerly *E. repens*) (Ascomycetes), and *Mycotypha microspora* (Zygomycetes) were used as fungal test organisms.

Pure compounds were dissolved in acetone or methanol to give a concentration of 1 mg ml^{-1} per test sample. 50 µl (equivalent to 50 µg) of each solution were pipetted onto sterile filter disks (diameter: 9 mm, Schleicher & Schuell 2668), which was then placed onto the appropriate agar medium and sprayed with a suspension of the test organism. Growth media, preparation of spraying suspensions and conditions of incubation were carried out according to Schulz *et al*.[87] For tested samples, a growth inhibition zone ≥ 3 mm and/or a complete inhibition ≥ 1 mm, measured from the edge of the filter disk, were regarded as a positive result. Growth inhibition was defined as follows: growth of the appropriate test organism was significantly inhibited compared to a negative control; total inhibition: no growth at all in the appropriate zone. Benzyl penicillin (1 mg ml^{-1} MeOH), streptomycin (1 mg ml^{-1} MeOH) and miconazole (0.5 mg ml^{-1} DCM) were used as positive controls.

3.6.2 Label-free dynamic mass redistribution (DMR) assay for galanin receptors - HEK293 cell lines

Label-free dynamic mass redistribution assays were performed by working group Kostenis (Institute for Pharmaceutical Biology, University of Bonn), as described previously in detail, recorded on the EnSpire® multimode plate reader (Perkin Elmer, Hamburg, Germany) at 37°C.[88,89]

Native and recombinant human embryonic kidney (HEK293) cell lines were cultured in Dulbecco's modified Eagle's medium (DMEM) supplemented with 10% (*v/v*) fetal calf serum (FCS), penicillin (100 U ml^{-1}) and streptomycin (100 µg ml^{-1}). For recombinant HEK293 cell lines harboring human galanin receptor type1 (GalR1), the medium was supplemented with G418 (450 µg ml^{-1}) (InvivoGen). cDNA coding for this receptor cloned into pcDNA3.1+ (Invitrogen) at EcoRI (5') and XhoI (3') was purchased from UMR cDNA Resource center, University of Missouri-Rolla, Rolla, USA. Stable single cell clone-derived cell lines were generated by Ca^{2+} phosphate co-precipitation in conjunction with clonal selection using G418 as described previously.[90] All cells were cultivated with 5% CO_2 at

37°C in a humidified atmosphere. For signal pathway inhibition, cells were incubated for 16 h with 200 ng ml^{-1} of pertussis toxin (PTX).

3.7 Chemicals and other materials

Chemicals were supplied by Merck (Germany), Fluka (Switzerland), Roth (Germany) and Sigma-Aldrich (Germany). Stable isotope labeled compounds [1-^{13}C]phenylalanine, [U-^{13}C]glycerol, [1-^{13}C]glucose, [1-^{13}C]sodium acetate and [*Me*-^{13}C]methionine were obtained from Cambridge Isotope Laboratories. [1,7-^{13}C]shikimic acid was kindly provided by Prof. Dr. Taifo Mahmud from the Oregon State University, USA. All precursors were filter sterilized using Millipore filters (pore size 0.20 µm) or autoclaved (for [1-^{13}C]sodium acetate). Deuterated NMR solvents were supplied from Deutero GmbH (Germany).

Solvents used where either distilled before use, of HPLC grade or LC/MS grade.

Deionized water used was obtained from a Milli-Q-system.

3.7.1 Materials and reagents for cell culture and molecular biology

Tissue culture media and reagents were purchased from Invitrogen. Pertussis toxin (PTX) was from BIOTREND Chemikalien GmbH, restriction endonucleases and modifying enzymes were from New England Biolabs. All other laboratory reagents for cell culture, molecular biology and DMR assays were obtained from Sigma-Aldrich unless otherwise specified.

3.7.2 Synthesis of 2-chloro-protocatechuic acid

Demethylation of commercially available 2-chloro-3,4-dimethoxybenzoic acid to give 2-chloro-protocatechuic acid was conducted under supervision of Dr. Nader Boshta, Pharmaceutical Chemistry I, University of Bonn. Demethylation was carried out using boron tribromide in dichloromethane (molar ratio of 2-chloro-3,4-dimethoxybenzoic acid to BBr_3 1:2) for 24 h. The reaction mixture was then neutralized with $NaHCO_3$ until evolution of CO_2 stopped (pH 7.0). The mixture was then extracted three times with dichloromethane, washed with water and dried over $MgSO_4$.[91]

4. Results

4.1 Isolation of novel cyclic peptides from *Stachylidium* sp.

A 3 liter culture of *Stachylidium* sp. on biomalt agar medium supplemented with sea salt was cultivated for 30 days at room temperature (see 3.2). Fungal biomass and media were homogenized with an Ultra-Turrax followed by exhaustive extraction with ethyl acetate to yield 600 mg of crude extract. This was further subjected to VLC fractionation on silica open columns using a gradient solvent system of increasing polarity (see 3.3.2), starting with 100% petroleum ether to 100% dichloromethane to 100% ethyl acetate to 100% acetone to 100% methanol, yielding 9 fractions. Cyclic tetrapeptides (peptides 1-7) were isolated from VLC fraction 4, by NP-HPLC fractionation using petroleum ether/acetone (3:1) and RP-HPLC using methanol/water systems. Diketopiperazines (peptides 8 and 9) were isolated from VLC fractions 6 and 7, by NP-HPLC fractionation using petroleum ether/acetone (2:3) and RP-HPLC using a methanol/water system (Fig 4-1).

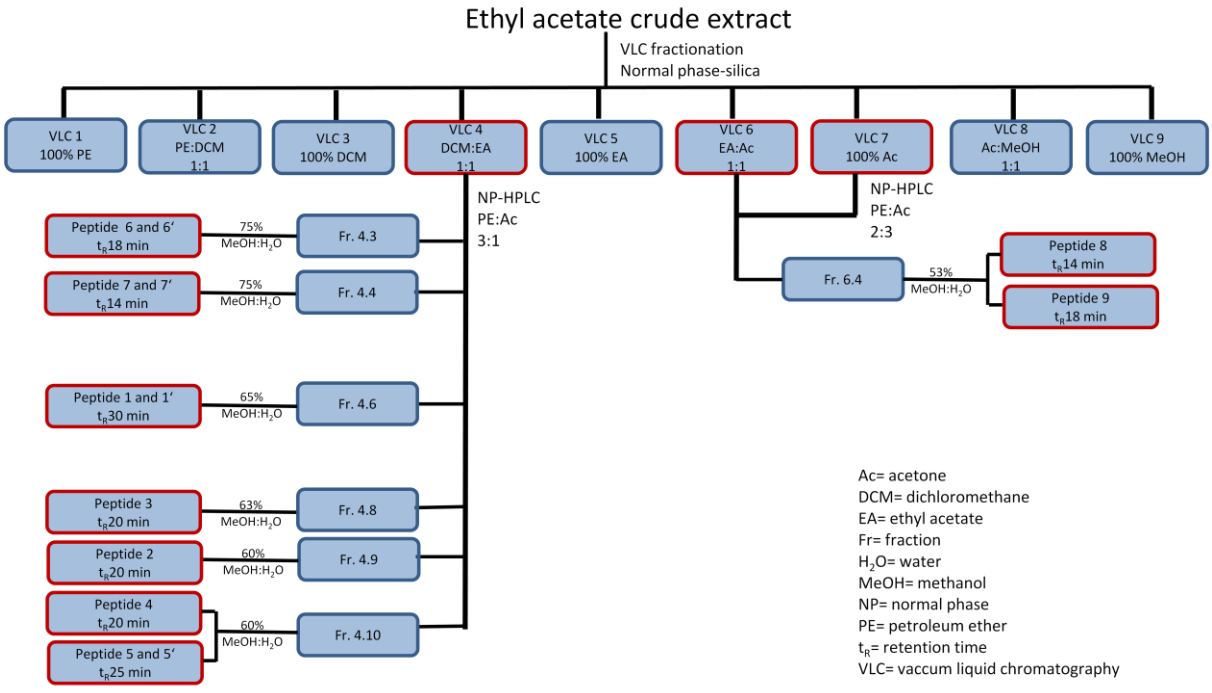

Fig 4-1. Isolation scheme for cyclic peptides (1-9) from a 30 day *Stachylidium* sp. culture on biomalt salt agar medium. Experimental details are described in section 3.3.

4.2 Structure elucidation of isolated novel cyclic peptides

^{1}H and ^{13}C NMR spectra of the isolated compounds 1-7 exhibited typical signals indicative of a tetrapeptide molecule. The ^{1}H NMR spectra showed four signals between δ 4 - 5 characteristic for the α protons of four amino acid residues, two methyl singlets at around δ 2.8, indicative of N-methyl protons, and two broad doublets at around δ 7.9 characteristic for amide protons. Diastereotopic β proton resonances were observed between δ 2.5 - 3.7. The region between δ 7.0 - 7.5 showed overlapping resonances due to aromatic ring protons pointing to the inclusion of aromatic amino acid residues. In addition, the ^{13}C NMR spectra displayed four down-field signals between δ 170 and δ 173, attributable to amide carbonyls, as well as signals between δ 50 - 70, where peptidic α-carbons normally appear. Presence of 2 amide protons and N-methyl singlets in the spectra implied a cyclic structure for the tetrapeptides.

Four of the isolated peptides, i.e. peptides 1, 5, 6 and 7, displayed doubling of the signals in both ^{1}H and ^{13}C NMR spectra. A first hint pointed to the likely-hood of the presence of conformational isomers, frequently seen in peptides and justified by the conformational flexibility of the constituent amino acid residues.[92] NMR measurements at elevated temperatures or using different solvents did not result in improvements of NMR resolution as normally expected with peptide conformers.[93] From the detailed investigation of the 2D-NMR spectroscopic data we could conclude that these peptides are isolated as a mixture of co-eluting positional isomers with similar chromatographic properties and differing only in the connectivities of the constituent amino acid residues. Trials to purify them further using different HPLC stationary phases and mobile phase systems were unsuccessful, especially due to the small amounts isolated, and in several instances separation of peptide isomers using liquid chromatography was most challenging.[94]

HRESIMS of **peptide 1 and 1'** showed an ion peak at *m/z* 547.2902 $[M+Na]^{+}$ and was assigned a molecular formula of $C_{29}H_{39}N_4O_5$ indicating 12 degrees of unsaturation. The ^{1}H NMR and ^{13}C NMR spectra revealed doubling of signals suggesting the presence of inseparable isomers (Fig S3 and S4). The ^{1}H NMR spectrum displayed eight α proton signals between δ 4 – 5, two splitted singlets at δ 2.7 and δ 2.8, indicated the presence of

N-methyl protons, and two doublets at δ 7.84 and δ 7.92, characteristic for amide protons. The ^{13}C NMR spectrum displayed six carbonyl signals, four resonances at δ 171.8, δ 172.2, δ 172.5 and δ 172.9, and two signals at δ 170.5, and δ 170.9 with double the intensity, along with four splitted α carbon signals at δ 49.0, δ 56.0, δ 62.0 and δ 63.0. This pointed to the preliminary assignment of a mixture of two closely related cyclic tetrapeptide isomers. Proton and carbon resonances in the aromatic region were suggestive of two distinct aromatic moieties, of which one incorporates an oxygen atom (as indicated from the molecular formula), anticipated to be a furyl moiety, while the remaining resonances in the aromatic region where indicative of a phenyl moiety. The structure of the remaining amino acid residues were assigned as valine and leucine. Comprehensive analysis of the 2D NMR spectroscopic data revealed the structures and sequence of four heterogeneous amino acid residues: N-MeFurAla, Leu, N-MePhe and Val (Table 4-1).

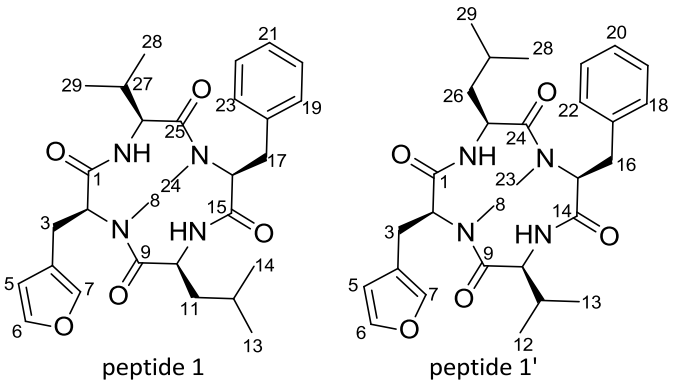

An L-configuration is implied at C-2

For **peptide 1**, spin systems in COSY and HMBC were assigned to valine, as correlations ranging from CH_3-28 and CH_3-29 to βCH-27 and αCH-26, and correlations of βCH-27 and αCH-26 with qC-25 were observed. The valine unit was not methylated as COSY correlations were observed between αH-26 (δ_H 4.26) and NH-26 (δ_H 7.84). Another subunit was allocated as leucine determined from the COSY spin system linking the two methyl groups, CH_3-13 and CH_3-14, to NH-10 (δ_H 7.92) through γH-12, βH_2-11 and αH-10. Further HMBC correlations of βCH_2-11 and αCH-10 to the qC-9 finalized the assignment of a non-methylated leucine. Characteristic carbon resonances at δ 144.5, δ 141.1, δ 110.9 and δ 122.0 along with their relevant proton resonances at δ 7.55, δ 7.46 and δ 6.41 established a furyl moiety. Two of the three *sp*^{2} methine protons of the furyl moiety, i.e

H-6 (δ_H 7.55) and H-7 (δ_H 7.46), were shifted downfield due to the deshielding effect of a common adjacent oxygen. CH-5 and CH-7 are both connected to the quaternary carbon, qC-4 (δ_c 122.0), deduced from the HMBC correlations of H-5 and H-7 to qC-4, hence closing the furyl ring. Supplementary COSY and HMBC correlations of CH-5 and CH-7 to βCH_2-3, and between βCH_2-3 and αCH-2, along with that between the carbonyl qC-1 (δ_C 170.9) and the NCH_3-8 (δ_H 2.80) ascribed this residue as N-methyl-3-(3-furyl)-alanine. Residual resonances were assigned to the second aromatic and last residue. The COSY spectrum revealed correlations of five aromatic methine protons, which were assigned a spin system H-19, H-20, H-21, H-22 and H-23. HMBC correlations between H-19 and H-23 to CH_2-17 (δ_c 34.7), H-20 and H-22 to qC-18 (δ_c 139.0), of H_2-17 and H-16 to the carbonyl qC-15 (δ_C 170.5), and of αCH-16 to NCH_3-24 (δ_H 2.75) concluded the last residue as an N-methyl-phenylalanine. The sequential relationship of the four amino acid residues was deduced from HMBC correlations of the α-protons of the amino acid residues and the carbonyl carbon of the adjacent amino acid, thus αCH-2 (NMeFurAla) to qC-9 (Leu), αCH-10 (Leu) to qC-15 (NMePhe), αCH-16 (NMePhe) to qC-25 (Val) and αCH-26 (Val) to qC-1 (NMeFurAla). This was fortified with HMBC correlations of the N-methyl substituents with the adjacent carbonyl carbons and α protons, that is NCH_3-8 (δ_H 2.80) to qC-9 (δ_c 172.9) and αCH-2 (δ_H 4.42), NCH_3-24 (δ_H 2.75) to qC-25 (δ_c 171.8) and αCH-16 (δ_H 4.51). Thus the final peptide sequence was assigned as cyclo-[N-methyl-3-(3-furyl)-alanyl, leucyl, N-methyl-phenylalanyl, valinyl].

For **peptide 1'**, the same amino acid residues were confirmed, differing only in their connectivity. This was deduced from HMBC correlations between amide protons to carbonyl carbons of the adjacent amino acids, i.e. NH-10 (Val) to qC-14 (NMePhe) and from NH-25 (Leu) to qC-1 (NMeFurAla), as well as HMBC correlations between the N-methyl and the adjacent carbonyl carbons and α-protons, i.e. from NCH_3-8 (NMeFurAla) to qC-9 (Val) and αCH-2 (NMeFurAla), and from NCH_3-23 (NMePhe) to qC-24 (Leu) and αCH-15 (NMePhe). Thus the final peptide sequence was assigned as cyclo-[N-methyl-3-(3-furyl)-alanyl, valinyl, N-methyl-phenylalanyl, leucyl].

Table 4-1. 1D NMR spectroscopic data for peptide 1 and 1'.
Peptide 1: (-)-Cyclo-[(N-methyl-(L)-3-(3-furyl)-alanyl), (L)-leucyl, N-methyl-(L)-phenylalanyl, (L)-valinyl]
Peptide 1': (-)-Cyclo-[(N-methyl-(L)-3-(3-furyl)-alanyl), (L)-valinyl, N-methyl-(L)-phenylalanyl, (L)-leucyl]

Peptide 1				Peptide 1'			
Amino acid	Position	δ_C, mult.[a, b, c]	δ_H[a, b] (*J* in Hz)	Amino acid	Position	δ_C, mult.[a, b, c]	δ_H[a, b] (*J* in Hz)
N-Me-L-FurAla	1	170.90, qC	-	N-Me-L-FurAla	1	170.50, qC	-
	2	62.80, CH	4.42, dd (3.3,11.7)		2	62.70, CH	4.34, dd (3.3, 11.7)
	3	24.50, CH_2	a: 2.97, dd (11.0, 15.0)		3	24.50, CH_2	a: 2.96, dd (11.0, 15.0)
			b: 3.42, dd (3.3, 15.0)				b: 3.41, dd (3.3, 15.0)
	4	122.00, qC	-		4	122.00, qC	-
	5	110.90, CH	6.41, br s		5	110.90, CH	6.41, br s
	6	144.50, CH	7.55, br s		6	144.50, CH	7.55, br s
	7	141.10, CH	7.46, br s		7	141.10, CH	7.46, br s
	8	30.70, CH_3	2.80, s		8	30.40, CH_3	2.76, s
	N				N		
L-Leu	9	172.90, qC	-	L-Val	9	172.20, qC	-
	10	49.30, CH	4.71, m		10	56.30, CH	4.39, t (8.8)
	11	42.00, CH_2	a:1.33, m		11	30.20, CH	2.15, m
			b:1.67, m		12	20.80, CH_3	0.87, d (6.6)
	12	25.00, CH	1.45, m		13	18.40, CH_3	0.90, d (6.6)
	13	22.50, CH_3	0.83, d (6.6)		NH-10	-	7.84, d (9.5)
	14	23.20, CH_3	0.78, d (6.6)	N-Me-L-Phe	14	170.90, qC	-
	NH-10	-	7.92, d (9.5)		15	63.80, CH	4.59, br d (11.7)
N-Me-L-Phe	15	170.50, qC	-		16	34.70, CH_2	a: 3.01, m
	16	63.50, CH	4.51, br d (11.7)				b: 3.69, m
	17	34.70, CH_2	a: 3.00, m		17	139.00, qC	-
			b: 3.67, m		18	129.20, CH	7.31, m
	18	139.00, qC	-		19	129.50, CH	7.31, m
	19	129.20, CH	7.31, m		20	127.50, CH	7.24, m

Peptide 1				Peptide 1‘			
Amino acid	Position	δ_C, mult.[a, b, c]	δ_H[a, b] (*J* in Hz)	Amino acid	Position	δ_C, mult.[a, b, c]	δ_H[a, b] (*J* in Hz)
	20	129.50, CH	7.31, m		21	129.50, CH	7.31, m
	21	127.50, CH	7.24, m		22	129.20, CH	7.31, m
	22	129.50, CH	7.31, m		23	30.70, CH_3	2.81, s
	23	129.20, CH	7.31, m		N		
	24	30.40, CH_3	2.75, s	L-Leu	24	172.50, qC	-
	N				25	49.10, CH	4.60, m
L-Val	25	171.80, qC	-		26	41.90, CH_2	a:1.23, m
	26	56.20, CH	4.26, t (8.8)				b:1.60, m
	27	30.00, CH	2.03, m		27	25.00, CH	1.58, m
	28	20.70, CH_3	0.72, d (6.6)		28	22.50, CH_3	0.91, d (6.6)
	29	18.40, CH_3	0.83, d (6.6)		29	23.30, CH_3	0.87, d (6.6)
	NH-26	-	7.84, d (9.5)		NH-25	-	7.92, d (9.5)

[a] CD_3COCD_3, 300/75.5 MHz. [b] Assignments are based on extensive 1D and 2D NMR experiments (HMBC, HSQC, COSY). [c] Implied multiplicities determined by DEPT.

Peptide 2 was assigned a molecular formula of $C_{32}H_{37}N_4O_5$ using HRESIMS, indicating 16 degrees of unsaturation. The ^{13}C NMR and DEPT135 spectra revealed 32 resonances, resulting from four methyls, three methylenes, five *sp*^{3} methines, 13 *sp*^{2} methines and seven quaternary carbons. The ^1H NMR spectrum (Fig S5) displayed four α proton signals at δ 4.26, δ 4.50, δ 4.55 and δ 4.78. Two singlets at δ 2.72 and δ 2.79 indicated the presence of two N-methyl protons and two doublets at δ 7.79 and δ 7.93 are characteristic for amide protons. The ^{13}C NMR spectrum (Fig S6) displayed four carbonyl signals at δ 170.4, δ 171.0, δ 171.8 and δ 172.2, along with four α carbon signals at δ 51.4, δ 56.2, δ 63.5 and δ 63.6, all resulting in the preliminary assignment of a peptide-like molecule, composed of four amino acid residues, two of which are N-methylated. Comprehensive analysis of the 2D NMR spectroscopic data revealed the sequence and structures of the four amino acid residues of peptide 2 as NMePhe, FurAla, NMePhe and Val (Table 4-2). COSY revealed correlations of two closely related spin systems, each consisting of five aromatic methine protons, one reaching from H-5 through to H-9, and a second from H-22 through to H-26. HMBC correlations assigned quaternary carbons qC-4 (δ_C 138.93) to the first and qC-21 (δ_C 138.90) to the second aromatic ring respectively. The first aromatic ring displayed HMBC correlations between H-5 (δ_H 7.27), and H-9 (δ_H 7.27), to CH_2-3 (δ_c 35.0), which showed a strong correlation in both COSY and HMBC to αCH-2 (δ_H/δ_C 4.55/63.6). Both CH_2-3 and αCH-2 displayed HMBC correlations to the quaternary carbonyl qC-1 (δ_C 171.0), hence concluding the first aromatic amino acid as phenylalanine (Phe A). The second aromatic ring showed similar correlations and hence concluded the second aromatic amino acid also to be phenylalanine (Phe B). HMBC correlations from CH_3-31 and CH_3-32 to βCH-30 and αCH-29, and from H-30 (δ_H 2.04) and H-29 (δ_c 4.26), to the quaternary carbonyl carbon qC-28 (δ_c 171.8), along with COSY correlations of H-29 and NH-29 (δ_H 7.79), lead to the identification of a valine amino acid unit which was not N-methylated. The last residue displayed carbon resonances characteristic for a 3-substituted furyl moiety, i.e. δ 143.2, δ 141.1, δ 121.8 and δ 112.7. This is confirmed with HMBC correlations from *sp*^{2} methines H-15 (δ_H 6.20), and H-17 (δ_H 7.14), to the quaternary furyl carbon qC-14 (δ_C 121.8). COSY evidenced a spin system from αH-12 (δ_H 4.78), to NH-12 (δ 7.93). The αCH-

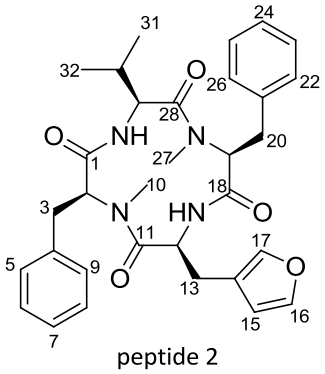

peptide 2
An L-configuration is implied at C-12

12 (δ_C 51.35) carbon resonance was shifted upfield indicating that this unit was not N-methylated. HMBC correlations of αCH-12 and βCH-13 with the carbonyl carbon qC-11 (δ_C 172.2), finalized the assignment of the last residue as 3-(3-furyl)-alanine. The sequential relationship of the four amino acid residues was deduced from HMBC correlations of the α-protons of the amino acid residues and the carbonyl carbon of the adjacent amino acid, i.e. αCH-2 (Phe A) to qC-11 (FurAla), αCH-12 (FurAla) to qC-18 (Phe B), αCH-19 (PheB) to qC-28 (Val) and αCH-29 (Val) to qC-1 (Phe A). The N-methyl substituents were positioned on the relevant amino acid residues Phe A and Phe B, based on HMBC correlations with their adjacent carbonyl carbons and α protons, that is NCH_3-10 to qC-11 and αCH-2, NCH_3-27 to qC-28 and αCH-19. This supplemented the peptide sequence, as cyclo-(N-methyl-phenylalanyl, furylalanyl, N-methyl-phenylalanyl, valinyl).

Table 4-2. 1D and 2D NMR spectroscopic data for peptide 2, (-)-Cyclo-[N-methyl-(L)-phenylalanyl, (L)-furylalanyl, N-methyl-(L)-phenylalanyl, (L)-valinyl].

Amino acid	position	δ_C, mult.[a, b, e]	δ_H[a, b] (*J* in Hz)	COSY[a, c]	HMBC[a, d]
N-Me-L-Phe	1	171.00, qC	-		
	2	63.64, CH	4.55, dd (3.3, 11.7)	3a, 3b	1, 3, 4, 10, 11
	3	35.00, CH_2	a: 3.67, dd (3.3, 15.0)	2, 3b	2, 4, 5, 9
			b: 3.02, dd (11.7, 15.0)	2, 3a	1, 2, 4, 5, 10
	4	138.93, qC	-		
	5	129.10, CH	7.27, m	6	3, 4, 6, 7
	6	129.50, CH	7.30, m	5, 7	5, 7, 8
	7	127.50, CH	7.23, m	6, 8	5, 6, 8, 9
	8	129.50, CH	7.30, m	7, 9	6, 7, 9
	9	129.10, CH	7.27, m	8	3, 4, 7, 8
	10	30.90, CH_3	2.79, s		2, 11
	N				
L-FurAla	11	172.20, qC	-		
	12	51.35, CH	4.78, dt (9.5, 6.6)	13a, 13b, NH-12	11, 13, 14, 18
	13	28.00, CH_2	a: 2.52, dd (6.6, 15.0)	12, 13b, 17	11, 12, 14, 15, 17
			b: 2.90, dd (6.6, 15.0)	12, 13a, 17	
	14	121.80, qC	-		
	15	112.70, CH	6.20, br s	16, 17	13, 14, 16, 17
	16	143.20, CH	7.38, t (1.8)	15, 17	15, 17
	17	141.10, CH	7.14, br s	13, 15, 16	13, 14, 15, 16
	NH-12	-	7.93, d (9.5)	12	
N-Me-L-Phe	18	170.40, qC	-		
	19	63.50, CH	4.50, dd (3.3, 11.7)	20a, 20b	18, 20, 21, 27, 28
	20	34.70, CH_2	a: 3.61, dd (3.3, 15.0)	19, 20b	18, 21
			b: 2.92, dd (11.7, 15.0)	19, 20a	
	21	138.90, qC	-		
	22	129.20, CH	7.27, m	23	20, 21, 23, 24
	23	129.50, CH	7.30, m	22, 24	21, 22, 24, 25
	24	127.50, CH	7.23, m	23, 25	22, 23, 25, 26
	25	129.50, CH	7.30, m	24, 26	20, 21, 23, 24, 26
	26	129.20, CH	7.27, m	25	19, 20, 21, 22, 25
	27	30.50, CH_3	2.72, s		19, 28
	N				
L-Val	28	171.80, qC	-		
	29	56.20, CH	4.26, dd (7.7, 9.2)	30, NH-29	1, 28, 30, 31, 32
	30	30.40, CH	2.04, m	29, 31, 32	28, 29, 31, 32
	31	20.70, CH_3	0.68, d (6.6)	30	29, 30, 32
	32	18.40, CH_3	0.82, d (7.0)	30	29, 30, 31
	NH-29	-	7.79, d (9.2)	29	

[a] CD_3COCD_3, 300/75.5 MHz. [b] Assignments are based on extensive 1D and 2D NMR experiments (HMBC, HSQC, COSY). [c] Numbers refer to proton resonances. [d] Numbers refer to carbon resonances. [e] Implied multiplicities determined by DEPT.

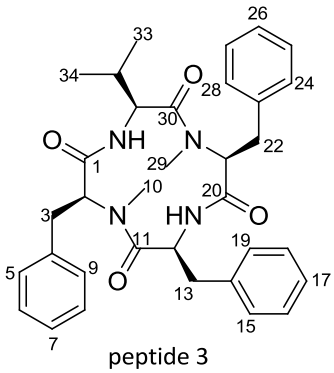

peptide 3

Peptide 3 was assigned a molecular formula of $C_{34}H_{40}N_4O_4$ using HRESIMS, indicating 17 degrees of unsaturation. The ^{13}C NMR and DEPT135 spectra revealed 34 resonances, resulting from four methyls, three methylenes, five *sp*^{3} methines, 15 *sp*^{2} methines and seven quaternary carbons. The molecular formula of peptide 3 had one oxygen atom less than peptide 2, suggesting a closely related structure in which the furylalanine moiety is replaced by a more hydrophobic residue as deduced from NP-HPLC. Signals similar to those of peptide 2 were observed in the ^1H and ^{13}C NMR spectra (Fig S7 and S8), due to the presence of a valine and two N-methyl-phenylalanine moieties. Characteristic signals for the furylalanine moiety were not observed, instead overlapping resonances were observed in the aromatic region and these were assigned to the aromatic spin systems H-15, H-16, H-17, H-18 and H-19. They displayed HMBC correlations between H-15 (δ_H 7.07), and H-19 (δ_H 7.07), to βCH_2-13 (δ_C 38.4), which showed a strong correlation to αCH-12 (δ_H/δ_C 4.91/52.1). Both αCH-12 and βCH_2-13 displayed HMBC correlations to the quaternary qC-14 (δ_C 139.0) and carbonyl qC-11 (δ_C 172.1), thus concluding an additional phenylalanine residue. This is consistent with our earlier speculations concerning the replacement of the furylalanine residue with an aromatic and probably more hydrophobic residue in this case phenylalanine. The HRESIMS spectrum showed an ion peak at *m/z* 569.3119 $[M+H]^+$, which through comparison of spectroscopic data with literature values revealed this peptide as cyclo-(N-methyl-phenylalanyl, phenylalanyl, N-methyl-phenylalanyl, valinyl) (Table 4-3). This peptide was reported from an entomopathogenic fungus *Hirsutella* sp. and was named hirsutide sequent to the producing organism.[95]

Table 4-3. 1D and 2D NMR spectroscopic data for peptide 3, (-)-Cyclo-[N-methyl-(L)-phenylalanyl, (L)-phenylalanyl, N-methyl-(L)-phenylalanyl, (L)-valinyl].

Amino acid	Position	δ_C, mult.[a, b, e]	δ_H[a, b] (*J* in Hz)	COSY[a, c]	HMBC[a, d]
N-Me-L-Phe	1	171.00, qC	-		
	2	63.58, CH	4.56, dd (3.3, 11.7)	3	1, 3, 4, 10
	3	34.98, CH_2	a: 3.66, dd (3.3, 15.0) b: 3.01, dd (11.7, 15.0)	2	2, 4, 5, 9
	4	139.00, qC	-		
	5	129.00, CH	7.24, m	6, 7	3, 4, 7, 9
	6	129.50, CH	7.30, m	5, 7	5, 7, 8, 9
	7	127.50, CH	7.24, m	6, 8	5, 6, 8, 9
	8	129.50, CH	7.30, m	7, 9	4, 7, 9
	9	129.00, CH	7.24, m	8	3, 4, 7, 8
	10	31.25, CH_3	2.77, s	2, 3	2, 11
	N				
L-Phe	11	172.10,qC	-		
	12	52.10,CH	4.91, dt (9.5, 7.0)	13, NH-12	11, 13, 14
	13	38.40, CH_2	a: 2.66, dd (7.0, 13.9) b:3.11, dd (7.0, 13.9)	12	11, 12, 14, 15, 19
	14	139.00, qC	-		
	15	130.20, CH	7.07, d (7.0)	16	13, 14, 16, 17
	16	128.80, CH	7.22, m	15, 17	14, 15, 18
	17	126.80, CH	7.16, m	16, 18	14, 15, 16, 18, 19
	18	128.80, CH	7.22, m	17, 19	14, 16, 17, 19
	19	130.20, CH	7.07, d (7.0)	18	13, 14, 17, 18
	NH-12	-	7.97, d (9.5)	12	
N-Me-L-Phe	20	170.10, qC	-		
	21	63.40, CH	4.46, dd (3.3, 11.7)	22	20, 22, 23, 29
	22	34.68, CH_2	a: 3.52, br d (15.0) b: 2.80, dd (11.7, 15.0)	21	21, 23, 24, 28, 29
	23	139.00, qC	-		21, 22, 24, 25
	24	129.00, CH	7.24, m	22a, 25	22, 23, 25, 26
	25	129.50, CH	7.30, m	24, 26	23, 24, 26, 27
	26	127.47, CH	7.24, m	25, 27	24, 25, 27, 28
	27	129.50, CH	7.30, m	26, 28	23, 25, 26, 28
	28	129.00, CH	7.24, m	22a, 27	21, 22, 26, 27
	29	31.07, CH_3	2.72, s		21, 30
	N				
L-Val	30	171.80, qC	-		
	31	56.20, CH	4.25, br t (8.05)	32, NH-31	30, 32, 33, 34
	32	30.50, CH	2.04, m	31, 33, 34	31, 33, 34
	33	20.70, CH_3	0.70, d (6.6)	32, 34	31, 32, 34
	34	18.50, CH_3	0.82, d (6.6)	32, 34	31, 32, 33
	NH-31	-	7.8, d (9.5)	31	

[a] CD_3COCD_3, 300/75.5 MHz. [b] Assignments are based on extensive 1D and 2D NMR experiments (HMBC, HSQC, COSY). [c] Numbers refer to proton resonances. [d] Numbers refer to carbon resonances. [e] Implied multiplicities determined by DEPT.

Peptides 4 and peptide 5 and 5' were isolated from the same NP-HPLC fraction, showed very close HPLC retention times and an ion peak at *m/z* of 571.2532 $[M+Na]^+$ and 571.2526 $[M+Na]^+$ using HRESIMS for peptide 4 and peptide 5 and 5', respectively. They were assigned a molecular formula of $C_{30}H_{35}N_4O_6$, indicating 15 degrees of unsaturation. They displayed differing ^1H and ^{13}C NMR spectra which suggested two closely related compounds with probably the same amino acid composition but differing in their connectivity.

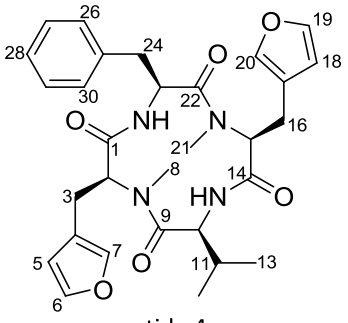

peptide 4
An L-configuration is implied at C-2 & C-15

The ^{13}C NMR and DEPT135 spectra of **peptide 4** revealed 30 resonances, resulting from four methyls, three methylenes, five *sp*^{3} methines, 11 *sp*^{2} methines and seven quaternary carbons. ^1H and ^{13}C NMR spectra (Fig S9 and S10) displayed characteristic proton and carbon resonances for two magnetically equivalent 3-(3-furyl)-alanine moieties, which were N-methylated. The remaining proton and carbon resonances in the aromatic region where indicative of a phenylalanine residue. COSY correlations between NH-23 (δ_H 7.93) and αH-23 (δ_H 4.96) indicated that the phenylalanine residue was not N-methylated. The last residue was ascribed as valine based on COSY and HMBC correlations. COSY correlations between NH-10 (δ_H 7.77) and αH-10 (δ_H 4.36) indicated that the valine residue was not N-methylated. The sequential relationship of the four amino acid residues was deduced from HMBC correlations of the α-protons of the amino acid residues and the carbonyl carbon of the adjacent amino acid, i.e. αCH-2 (FurAla A) to qC-9 (Val), αCH-10 (Val) to qC-14 (FurAla B), αCH-15 (FurAla B) to qC-22 (Phe) and αCH-23 (Phe) to qC-1 (FurAla A) and was supplemented with HMBC correlations of the N-methyl substituents. Thus peptide 4 was assigned as cyclo-[N-methyl-3-(3-furyl)-alanyl, valinyl, N-methyl-3-(3-furyl)-alanyl, phenylalanyl] (Table 4-4).

Table 4-4. 1D and 2D NMR spectroscopic data for peptide 4, (-)-Cyclo-[(N-methyl-(L)-3-(3-furyl)-alanyl), (L)-valinyl, (N-methyl-(L)-3-(3-furyl)-alanyl), (L)-phenylalanyl].

Amino acid	Position	δ_C, mult.[a, b, e]	δ_H[a, b] (*J* in Hz)	COSY[a, c]	HMBC[a, d]
N-Me-	1	169.80, qC	-		
L-FurAla	2	62.50, CH	4.25, dd (3.3, 11.7)	3a, 3b	1, 3, 4, 8, 9
	3	24.30, CH_2	a: 2.73, m	2, 3b	1, 2, 4, 5, 7
			b: 3.22, dd (3.3, 15.6)	2, 3a, 7	
	4	122.00, qC	-		
	5	110.95, CH	6.30, dd (0.9, 1.7)	6, 7	3a, 4, 6, 7
	6	144.40, CH	7.50, t (1.7)	5	4, 5, 7
	7	140.90, CH	7.37, br s	5, 3b	3a, 4, 5, 6
	8	30.50, CH_3	2.71, s		2, 9
	N				
L-Val	9	172.10, qC	-		
	10	56.20, CH	4.36, m	11, NH	12, 13
	11	30.40, CH	2.11, m	10, 12, 13	12, 13
	12	20.80, CH_3	0.82, d (6.6)	11, 13	10, 11, 13
	13	18.40, CH_3	0.84, d (6.6)	11, 12	10, 11, 12
	NH-14	-	7.77, d (9.5)	10	
N-Me-	14	170.70, qC	-		
L-FurAla	15	62.70, CH	4.34, m	20a, 20b	18, 20, 21, 25
	16	24.68, CH_2	a: 2.95, dd (11.3, 15.6)	19, 20b	18, 19, 21, 22, 24
			b: 3.36, dd (3.3, 15.6)	19, 20a, 24	18, 19, 21, 22, 24
	17	121.90, qC	-		
	18	110.80, CH	6.31, dd (0.9, 1.7)	23, 24	20a, 20b, 24
	19	144.40, CH	7.44, t (1.7)	22	21, 22, 24
	20	141.00, CH	7.38, br s	20b, 22	21, 22, 23
	21	30.64, CH_3	2.78, s		19, 26
	N				
L-Phe	22	172.50, qC	-		
	23	52.20, CH	4.96, m	24a, 24b, NH	24a, 24b
	24	38.50, CH_2	a: 3.20, dd (6.8, 13.9)	23, 24b	22, 23, 25, 26, 30
			b: 2.72, m	23, 24a	22, 23, 25, 26, 30
	25	139.00, qC	-		
	26	130.40, CH	7.18, m	24a, 27	24a
	27	128.70, CH	7.24, m	26, 28	25, 26, 28
	28	126.90, CH	7.17, m	27, 29	26, 27, 29, 30
	29	128.70, CH	7.24, m	28, 30	25
	30	130.40, CH	7.18, m	29	24a
	NH-10	-	7.93, d (9.5)	23	

[a] CD_3COCD_3, 500/125 MHz. [b] Assignments are based on extensive 1D and 2D NMR experiments (HMBC, HSQC, COSY). [c] Numbers refer to proton resonances. [d] Numbers refer to carbon resonances. [e] Implied multiplicities determined by DEPT.

Proton and carbon signals for **peptide 5 and 5'** were doubled suggesting the presence of two isomers. The presence of 3-(3-furyl)-alanine and phenylalanine units was undoubted from primal examination of the ^{1}H and ^{13}C NMR spectra (Fig S11 and S12) and was verified after detailed analysis of the 2D NMR data. COSY and HMBC correlations revealed the presence of two distinct 3-(3-furyl)-alanine residues, one of which showed downfield shifted furyl protons, i.e. H-5, H-6 and H-7, and α carbon resonances, i.e C-2, and was assigned as N-methyl-3-(3-furyl)-alanine. The other 3-(3-furyl)-alanine was not N-methylated, as implied from COSY correlations of the α protons, i.e H-10 (δ_H 4.86) for peptide 5 and H-25 (δ_H 4.76) for peptide 5', to the corresponding amide protons, i.e. NH-10 (δ_H 7.93) for peptide 5 and NH-25 (δ_H 7.97) for peptide 5'. Residual resonances in the aromatic region were assigned to N-methyl-phenylalanine. The last residue was assigned as valine and COSY correlations between α proton and amide proton indicated that it was not N-methylated.

This shows that peptide 4 and peptide 5 and 5' have similar amino acid composition but differ in the positioning of the N-methyl substituent. Lastly, sequential relationship of the four amino acid residues was deduced from HMBC correlations of the α-protons of the amino acid residues and the carbonyl carbon of the adjacent amino acid with HMBC correlations of the N-methyl substituents confirming the sequence. Thus, peptide 5 was assigned as cyclo-[N-methyl-3-(3-furyl)-alanyl, furylalanyl, N-methyl-phenylalanyl, valinyl] and peptide 5' as cyclo-[N-methyl-3-(3-furyl)-alanyl, valinyl, N-methyl-phenylalanyl, 3-(3-furyl)-alanyl] (Table 4-5).

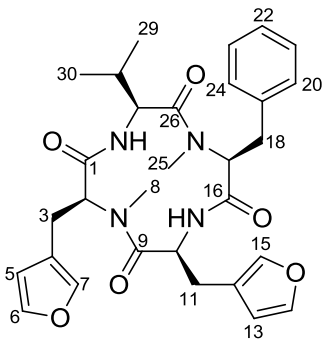

peptide 5

An L-configuration is implied at C-2, C-10, C-17 & C-27

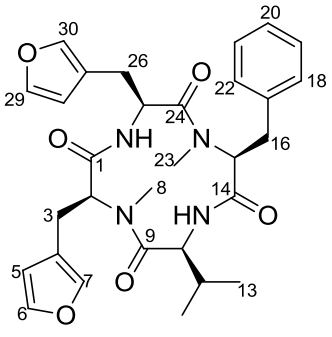

peptide 5'

An L-configuration is implied at C-2, C-10, C-15 & C-25

Table 4-5. 1D NMR spectroscopic data for peptide 5 and 5'.

Peptide 5: (-)-Cyclo-[(N-methyl-(L)-3-(3-furyl)-alanyl), (L)-3-(3-furyl)-alanyl, (N-methyl-(L)-phenylalanyl), (L)-valinyl]

Peptide 5': (-)-Cyclo-[(N-methyl-(L)-3-(3-furyl)-alanyl), (L)-valinyl, (N-methyl-(L)-phenylalanyl), (L)-3-(3-furyl)-alanyl]

Peptide 5				Peptide 5'			
Amino acid	Position	δ_C, mult.[a, b, c]	δ_H[a, b] (*J* in Hz)	Amino acid	Position	δ_C, mult.[a, b, c]	δ_H[a, b] (*J* in Hz)
N-Me-L-FurAla	1	170.87, qC	-	N-Me-L-FurAla	1	170.25, qC	-
	2	62.77, CH	4.37, m		2	62.57, CH	4.32, m
	3	24.73, CH_2	a: 2.96, dd (8.0, 11.7)		3	24.44, CH_2	a: 2.85, dd (8.0, 11.7)
			b: 3.40, dd (3.3, 8.0)				b: 3.33, dd (3.3, 8.0)
	4	121.90, qC	-		4	121.90, qC	-
	5	110.90, CH	6.36, br s		5	110.90, CH	6.37, br s
	6	144.40, CH	7.47, t (1.5)		6	144.40, CH	7.52, t (1.5)
	7	141.10, CH	7.43, br s		7	141.10, CH	7.43, br s
	8	30.87, CH_3	2.79, s		8	30.55, CH_3	2.72, s
	N				N		
L-FurAla	9	172.5, qC	-	L-Val	9	172.11, qC	-
	10	51.39, CH	4.86, dt (9.2, 6.9)		10	56.30, CH	4.37, t (8.4)
	11	27.97, CH_2	a: 2.61, m		11	30.28, CH	2.13, m
			b: 2.97, m		12	20.78, CH_3	0.84, d (6.5)
	12	121.7, qC	-		13	18.43, CH_3	0.86, d (6.5)
	13	112.7, CH	6.19, br s		NH-10	-	7.81, d (9.3)
	14	143.1, CH	7.38, t (1.5)	N-Me-L-Phe	14	170.87, q C	-
	15	141.0, CH	7.13, br s		15	63.59, CH	4.54, dd (3.3, 11.7)
	NH-10	-	7.93, d (9.8)		16	34.96, CH_2	a:3.01, dd (11.7, 15.3)
N-Me-L-Phe	16	170.25, qC	-				b: 3.65, dd (3.3, 15.3)
	17	63.46, CH	4.46, dd (3.3, 11.7)		17	138.9, qC	-
	18	34.63, CH_2	a: 2.89, dd (11.7, 15.3)		18	129.10, CH	7.26, m
			b: 3.58, dd (3.3, 15.3)		19	129.40, CH	7.26, m

Peptide 5				Peptide 5’			
Amino acid	Position	δ_C, mult.[a, b, c]	δ_H[a, b] (*J* in Hz)	Amino acid	Position	δ_C, mult.[a, b, c]	δ_H[a, b] (*J* in Hz)
	19	138.90, qC	-		20	127.50, CH	7.26, m
	20	129.20, CH	7.26, m		21	129.40, CH	7.26, m
	21	129.50, CH	7.26, m		22	129.10, CH	7.26, m
	22	127.50, CH	7.26, m		23	30.87, CH_3	2.80, s
	23	129.50, CH	7.26, m		N		
	24	129.20, CH	7.26, m	L-FurAla	24	172.11, qC	-
	25	30.55 , CH_3	2.71, s		25	51.23, CH	4.76, dt (9.2, 6.9)
	N				26	27.97, CH_2	a: 2.50, m
L-Val	26	171.72, qC	-				b: 2.87, m
	27	56.30, CH	4.23, t (8.4)		27	121.90, qC	-
	28	30.08, CH	2.00, m		28	112.90, CH	6.30, br s
	29	20.67, CH_3	0.69, d (6.5)		29	143.10, CH	7.41, t (1.5)
	30	18.43, CH_3	0.80, d (6.6)		30	141.10, CH	7.27, br s
	NH-27	-	7.81, d (9.3)		NH-25	-	7.97, d (9.8)

[a] CD_3COCD_3, 300/75.5 MHz. [b] Assignments are based on extensive 1D and 2D NMR experiments (HMBC, HSQC, COSY). [c] Implied multiplicities determined by DEPT.

Peptides 6 and 6' and 7 and 7' showed quite similar ^{1}H and ^{13}C NMR spectra, differing only in the resonances observed in the aromatic region. On the basis of HRESIMS data the molecular formulae $C_{28}H_{44}N_4O_4$ and $C_{26}H_{42}N_4O_5$ were assigned for peptides 6 and 6' and peptide 7 and 7', respectively. Detailed analysis of the NMR data established the presence of the branched amino acids valine and two leucines in each peptide. NMR spectra of peptide 6 and 6' (Fig S13 and S14) featured characteristic signals for a phenylalanine residue, while those of peptide 7 and 7' featured signals characteristic for a furyl moiety (Fig S15 and S16). Thus the structural difference between both peptides was found to lie in the substitution of a phenylalanine moiety in peptide 6 and 6' with a 3-(3-furyl)-alanine in peptide 7 and 7'. This is consistent with a higher hydrophobicity observed in NP-HPLC for peptide 6 and 6' as compared to peptide 7 and 7'. Based on HMBC correlations, the N-methyl substituents were positioned on the amino acid residues, leucine and the aromatic amino acids, i.e. phenylalanine in peptide 6 and 6' and 3-(3-furyl)-alanine in peptide 7 and 7'.

Detailed interpretation of 2D-NMR spectra revealed that both peptide 6 and 6' and peptide 7 and 7', consist of inseparable positional isomers, accounting for the proton and carbon signals observed in pairs. Thus, peptide 6 was assigned as cyclo-[N-methyl-phenylalanyl, leucyl, N-methyl-leucyl, valinyl] and peptide 6' as cyclo-[N-methyl-phenylalanyl, valinyl, N-methyl-leucyl, leucyl] (Table 4-6). Similarliy, peptide 7 was assigned as cyclo-[N-methyl-3-(3-furyl)-alanyl, leucyl, N-methyl-leucyl, valinyl] and peptide 7' as cyclo-[N-methyl-3-(3-furyl)-alanyl, valinyl, N-methyl-leucyl, leucyl] (Table 4-7).

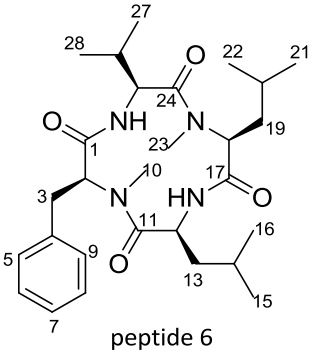

peptide 6

An L-configuration is implied at C-2, C-12, C-18 & C-25

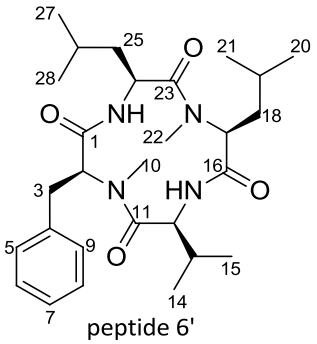

peptide 6'

An L-configuration is implied at C-2, C-12, C-17 & C-24

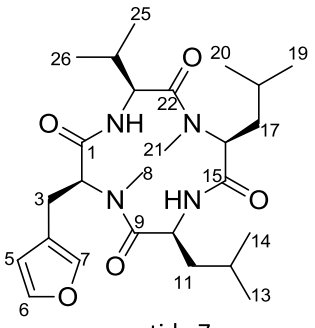

peptide 7

An L-configuration is implied at C-2, C-10, C-16 & C-23

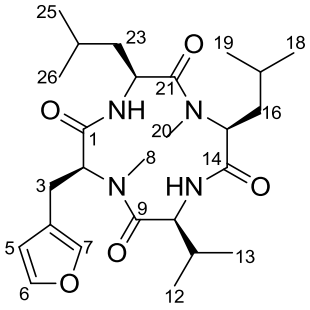

peptide 7'

An L-configuration is implied at C-2, C-10, C-15 & C-22

Table 4-6. 1D NMR spectroscopic data for peptide 6 and 6'.

Peptide 6: (-)-Cyclo-[N-methyl-L-phenylalanyl, (L)-leucyl, (N-methyl-(L)-leucyl), (L)-valinyl]

Peptide 6': (-)-Cyclo-[N-methyl-L-phenylalanyl), (L)-valinyl, (N-methyl-(L)-leucyl), (L)-leucyl]

Peptide 6				Peptide 6'			
Amino acid	Position	δ_C, mult.[a, b, c]	δ_H[a, b] (*J* in Hz)	Amino acid	Position	δ_C, mult.[a, b, c]	δ_H[a, b] (*J* in Hz)
N-Me-L-Phe	1	170.40, qC	-	N-Me-L-Phe	1	170.50, qC	-
	2	63.40, CH	4.51, dd (3.7, 11.5)		2	63.70, CH	4.60, dd (3.5, 11.5)
	3	34.70, CH_2	a: 2.96, dd (11.5, 15.0)		3	34.80, CH_2	a: 2.98, dd (11.5, 15.0)
			b: 3.62, dd (3.5, 15.0)				b: 3.67, dd (3.5, 15.0)
	4	139.10, qC	-		4	139.50, qC	-
	5	129.10, CH	7.25, m		5	129.10, CH	7.25, m
	6	129.40, CH	7.30, t (7.5)		6	129.40, CH	7.30, t (7.5)
	7	127.40, CH	7.20, t (7.3)		7	127.50, CH	7.20, t (7.3)
	8	129.40, CH	7.30, t (7.5)		8	129.40, CH	7.30, t (7.5)
	9	129.10, CH	7.25, m		9	129.10, CH	7.25, m
	10	30.50, CH_3	2.73, s		10	30.50, CH_3	2.79, s
	N				N		
L-Leu	11	172.00, qC	-	L-Val	11	172.60, qC	-
	12	48.80, CH	4.60, m		12	55.93, CH	4.26, m
	13	42.00, CH_2	a: 1.19, m		13	30.50, CH	2.00, m
			b: 1.54, m		14	20.80, CH_3	0.68, d (6.7)
	14	25.00, CH	1.66, m		15	18.40, CH_3	0.76, d (6.7)
	15	23.20, CH_3	0.92, d (6.7)		NH-12		7.70, d (8.8)
	16	22.47, CH_3	0.97, d (6.7)	N-Me-L-Leu	16	172.00, qC	-
	NH-12	-	7.79, d (8.8)		17	60.00, CH	4.26, dd (3.7, 11.4)
N-Me-L-Leu	17	171.49, qC	-		18	38.10, CH_2	a: 1.77, m
	18	60.00, CH	4.18, dd (3.7, 11.4)				b:1.95, m
	19	37.95, CH_2	a: 1.74, m		19	25.64, CH	1.43, m

Peptide 6				Peptide 6’			
Amino acid	Position	δ_C, mult.[a, b, c]	δ_H[a, b] (*J* in Hz)	Amino acid	Position	δ_C, mult.[a, b, c]	δ_H[a, b] (*J* in Hz)
			b: 1.93, m		20	23.60, CH_3	0.95, d (6.7)
	20	25.55, CH	1.41, m		21	22.50, CH_3	0.97, d (6.7)
	21	23.20, CH_3	0.76, d (6.7)		22	30.80, CH_3	2.74, s
	22	22.50, CH_3	0.80, d (6.7)		N		
	23	30.40, CH_3	2.71, s	L-Leu	23	173.10, qC	-
	N				24	49.40, CH	4.90, m
L-Val	24	172.40, qC	-		25	42.25, CH_2	a: 1.41, m
	25	56.40, CH	4.58, m				b: 1.79, m
	26	31.40, CH	2.25, m		26	25.07, CH	1.66, m
	27	20.90, CH_3	0.92, d (6.7)		27	23.27, CH_3	0.92, d (6.7)
	28	18.50, CH_3	0.96, d (6.7)		28	22.47, CH_3	0.97, d (6.7)
	NH-25	-	7.81, d (8.8)		NH-24	-	7.88, d (8.8)

[a] CD_3COCD_3, 300/75.5 MHz. [b] Assignments are based on extensive 1D and 2D NMR experiments (HMBC, HSQC, COSY). [c] Implied multiplicities determined by DEPT.

Table 4-7. 1D NMR spectroscopic data for peptide 7 and 7'.

Peptide 7: (-)-Cyclo-[(N-methyl-(L)-3-(3-furyl)-alanyl), (L)-leucyl, (N-methyl-(L)-leucyl), (L)-valinyl]

Peptide 7': (-)-Cyclo-[(N-methyl-(L)-3-(3-furyl)-alanyl), (L)-valinyl, (N-methyl-(L)-leucyl), (L)-leucyl]

		Peptide 7				Peptide 7'	
Amino acid	Position	δ_C, mult.[a, b, c]	δ_H[a, b] (*J* in Hz)	Amino acid	Position	δ_C, mult.[a, b, c]	δ_H[a, b] (*J* in Hz)
N-Me-L-FurAla	1	170.60, qC	-	N-Me-L-FurAla	1	170.33, qC	-
	2	62.70, CH	4.40, dd (3.3, 11.7)		2	62.50, CH	4.37, dd (3.3, 11.7)
	3	24.20, CH_2	a: 2.94, m		3	24.40, CH_2	a: 2.92, m
			b: 3.38, m				b: 3.36, m
	4	122.10, qC	-		4	122.20, qC	-
	5	110.90, CH	6.35, br s		5	111.00, CH	6.36, br s
	6	144.40, CH	7.50, t (1.65)		6	144.50, CH	7.50, t (1.65)
	7	141.00, CH	7.41, br s		7	141.10, CH	7.42, br s
	8	30.50, CH_3	2.78, s		8	30.60, CH_3	2.78, s
	N				N		
L-Leu	9	173.09, qC	-	L-Val	9	172.29, qC	-
	10	49.40, CH	4.88, m		10	55.90, CH	4.37, t (9.0)
	11	42.00, CH_2	a: 1.39, m		11	30.50, CH	2.11, m
			b: 1.77, m		12	20.76, CH_3	0.81, d (6.7)
	12	25.08, CH	1.64, m		13	18.40, CH_3	0.82, d (6.7)
	13	23.50, CH_3	0.92, d (6.7)		NH-10		7.70, d (9.5)
	14	22.50, CH_3	0.95, d (6.7)	N-Me-L-Leu	14	171.80, qC	-
	NH-10	-	7.90, d (9.5)		15	60.00, CH	4.26, dd (3.7, 11.4)
N-Me-L-Leu	15	171.40, qC	-		16	38.00, CH_2	a: 1.77, m
	16	60.00, CH	4.18, dd (3.7, 11.4)				b:1.95, m
	17	38.10, CH_2	a: 1.74, m		17	25.70, CH	1.40, m
			b: 1.93, m		18	23.50, CH_3	0.96, d (6.7)
	18	25.60, CH	1.40, m		19	21.40, CH_3	0.97, d (6.7)

Peptide 7				Peptide 7'			
Amino acid	Position	δ_C, mult.[a, b, c]	δ_H[a, b] (*J* in Hz)	Amino acid	Position	δ_C, mult.[a, b, c]	δ_H[a, b] (*J* in Hz)
	19	23.30, CH_3	0.81, d (6.7)		20	30.80, CH_3	2.74, s
	20	22.50, CH_3	0.84, d (6.7)		N		
	21	30.40, CH_3	2.71, s	L-Leu	21	173.00, qC	-
	N				22	49.00, CH	4.70, m
L-Val	22	172.30, qC	-		23	42.20, CH_2	a: 1.27, m
	23	56.40, CH	4.56, t (9.0)				b: 1.63, m
	24	30.50, CH	2.25, m		24	25.11, CH	1.64, m
	25	20.90, CH_3	0.90, d (6.7)		25	23.30, CH_3	0.92, d (6.7)
	26	18.45, CH_3	0.94, d (6.7)		26	22.50, CH_3	0.95, d (6.7)
	NH-23	-	7.81, d (9.5)		NH-22	-	7.80, d (9.5)

[a] CD_3COCD_3, 500/125 MHz. [b] Assignments are based on extensive 1D and 2D NMR experiments (HMBC, HSQC, COSY). [c] Implied multiplicities determined by DEPT.

^{1}H and ^{13}C NMR spectra of **peptide 8** (Fig S17 and S18) **and peptide 9** (Fig S19 and S20) displayed various resemblances, including two amide carbonyl carbon resonances (between δ_C 165 - 168), two α proton signals (between δ_H 3.6 - 4.3) and a down-field shifted methyl singlet (around δ_H 3.0 / δ_C 33.0), together with proton and carbon resonances in the aromatic region, all concluding the presumption of an N-methylated dipeptide molecule incorporating an aromatic moiety. Additionally, both compounds showed an ion peak at *m/z* of 297.1568 $[M+Na]^+$ and 297.1555 $[M+Na]^+$, for peptide 8 and peptide 9, respectively, using HRESIMS, suggesting they share the same elemental composition. They have a molecular formula of $C_{16}H_{22}N_2O_2$, indicating seven degrees of unsaturation. ^{13}C NMR and DEPT135 spectra revealed 16 resonances, resulting from three methyls, two methylenes, three sp^3 methines, five sp^2 methines and three quaternary carbons. Comprehensive analysis of the 1D and 2D NMR spectroscopic data uncovered the identity of the two amino acid residues, as leucine and phenylalanine. Placement of the methyl functionality was based on COSY and HMBC correlations of the N-methyl substituent with their adjacent carbonyl carbons and α-protons, i.e. for peptide 8, NCH_3-16 to qC-1 and αCH-8, and for peptide 9, NCH_3-7 to qC-8 and αCH-2. This accounts for the shifted resonances observed for the α-carbons of the leucine and phenylalanine residues. For peptide 8, the αCH-8 carbon resonance (δ_C 64.3) of the phenylalanine residue was shifted downfield indicating that this unit was N-methylated. In turn the αCH-2 carbon resonance (δ_C 60.5) of the leucine residue of peptide 9 was shifted downfield indicating that leucine was N-methylated. Their cyclic structure was deduced from HMBC correlations of αCH-2 (δ_H/δ_C 3.64/54.1) to qC-7 (δ_C 166.8), αCH-8 (δ_H/δ_C 4.21/64.3) to qC-1 (δ_C 167.2) and NCH_3-16 (δ_H/δ_C 3.03/32.9) to qC-1 for peptide 8 and of αCH-2 (δ_H/δ_C 3.61/60.5) to qC-8 (δ_C 165.8), αCH-9 (δ_H/δ_C 4.26/57.6) to qC-1 (δ_C 167.60) and NCH_3-7 (δ_H/δ_C 2.85/32.6) to qC-8 for peptide 9. Thus, peptide 8 was assigned as cyclo-(leucyl, N-methyl-phenylalanyl) (Table 4-8) and peptide 9 as cyclo-(N-methyl-leucyl, phenylalanyl) (Table 4-9), diketopiperazines varying in the positioning of the N-methyl substituent.

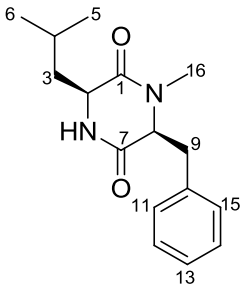

peptide 8

An L-configuration is implied at C-2 & C-8

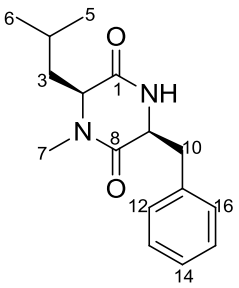

peptide 9

An L-configuration is implied at C-2 & C-9

Table 4-8. 1D and 2D NMR spectroscopic data for peptide 8, (-)-Cyclo-[(L)-leucyl, N-methyl-(L)-phenylalanyl].

Amino acid	Position	δ_C, mult.[a, b, e]	δ_H[a, b] (*J* in Hz)	COSY[a, c]	HMBC[a, d]
L-Leu	1	167.20, qC	-		
	2	54.10, CH	3.64, ddd (3.7, 4.8, 9.8)	3a,3b, NH-2	1, 3, 4
	3	45.60, CH_2	a: -0.11, ddd (4.8, 9.9, 13.9)	2, 3b, 4	1, 2, 4, 5, 6
			b: 0.75, ddd (4.4, 9.5, 13.9)	2, 3a, 4	1, 2, 4, 5, 6
	4	24.50, CH	1.48, m	3a, 3b, 5, 6	3
	5	21.80, CH_3	0.70, d (6.6)	3a, 4, 6	3, 4, 6
	6	23.70, CH_3	0.65, d (6.6)	4, 5	3, 4, 5
	NH				
N-Me-	7	166.80, qC	-		
L-Phe	8	64.30, CH	4.21, t (4.4)	9a, 9b, 16	7, 9, 10, 16
	9	37.60, CH_2	a: 3.24, dd (4.4, 13.9)	8, 9b	7, 8, 10, 11, 15,16
			b: 3.18, dd (4.4, 13.9)	8, 9a,11, 15	7, 8, 10, 11, 15, 16
	10	137.50, qC	-		
	11	131.40, CH	7.13, dd (2.2, 7.7)	12	9, 10, 12, 13, 15
	12	129.60, CH	7.29, t (7.7)	11, 13	10, 11, 13, 14
	13	128.30, CH	7.25, t (7.7)	12, 14	11, 12, 14, 15
	14	129.60, CH	7.29, t (7.7)	13, 15	10, 12, 13, 15
	15	131.40, CH	7.13, dd (2.2, 7.7)	14	9
	16	32.90, CH_3	3.03, s	8	1, 8, 9
	N				

[a] CD_3COCD_3, 300/75.5 MHz. [b] Assignments are based on extensive 1D and 2D NMR experiments (HMBC, HSQC, COSY). [c] Numbers refer to proton resonances. [d] Numbers refer to carbon resonances. [e] Implied multiplicities determined by DEPT.

Table 4-9. 1D and 2D NMR spectroscopic data for peptide 9, (-)-Cyclo-[N-methyl-(L)-leucyl, (L)-phenylalanyl].

Amino acid	Position	δ_C, mult.[a, b, e]	δ_H[a, b] (*J* in Hz)	COSY[a, c]	HMBC[a, d]
N-Me-L-Leu	1	167.60, qC	-		
	2	60.50, CH	3.61, dd (3.7, 9.2)	3b	3a, 3b, 7
	3	42.70, CH_2	a: 0.96, ddd (4.0, 9.3, 13.8)	3b, 4	2, 5, 6
			b: 0.47, ddd (4.6, 9.5, 13.8)	2, 3a	2, 5, 6
	4	25.50, CH	1.70, m	3a, 5, 6	2, 3a, 3b
	5	23.30, CH_3	0.69, d (6.5)	4, 6	3a, 3b, 6
	6	21.80, CH_3	0.81, d (6.5)	4, 5	3a, 3b, 5
	7	32.60, CH_3	2.85, s		2
	N				
L-Phe	8	165.80, qC	-		
	9	57.60, CH	4.26, m	10a, 10b	10a, 10b
	10	40.40, CH_2	a: 3.18, dd (5.5, 13.4)	9, 10b	9, 11, 12, 16
			b: 3.00, dd (4.7, 13.4)	9, 10a	9, 11, 12, 16
	11	137.50, qC	-		10a, 10b, 12, 16
	12	131.10, CH	7.18, d (7.7)	13, 14	11, 13
	13	129.20, CH	7.29, t (7.7)	12, 14	14
	14	127.80, CH	7.23, m	13, 15	13, 15
	15	129.20, CH	7.29, t (7.7)	14, 16	14, 16
	16	131.10, CH	7.18, d (7.7)	14, 15	11, 15
	NH				

[a] CD_3COCD_3, 500/125 MHz. [b] Assignments are based on extensive 1D and 2D NMR experiments (HMBC, HSQC, COSY). [c] Numbers refer to proton resonances. [d] Numbers refer to carbon resonances. [e] Implied multiplicities determined by DEPT.

The absolute configuration of the amino acids in the isolated peptides, i.e. peptide 1 and 1', peptide 2, peptide 3 and peptide 4, were assigned after acidic hydrolysis followed by derivatization of the amino acids with Marfey's reagent and HPLC analysis (see 3.4.6). Based on comparison of retention times to standard amino acids we could assign the L-configuration to the amino acids valine, leucine and phenylalanine (Fig S42-S45). As for the 3-(3-furyl)-alanine moiety for which no standard was available, an L-configuration was suggested as determined earlier from X-ray crystallography of endolide A (Fig 4-2), a cyclic tetrapeptide formerly isolated from the same fungal strain.[96] For those peptides isolated in lower quantities, i.e. peptide 5 and 5', peptide 6 and 6', peptide 7 and 7', peptide 8 and peptide 9, it was not possible to establish the absolute configuration of the amino acid residues, however based on biogenetic origin an L-configuration is implied for them.

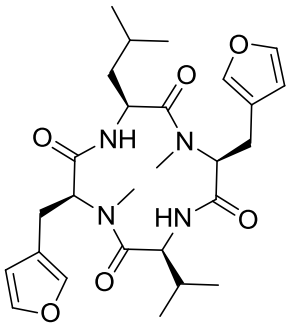

endolide A

Fig 4-2. Endolide A, cyclo-[(N-methyl-(L)-3-(3-furyl)-alanyl), L-valinyl, (N-methyl-(L)-3-(3-furyl)-alanyl), L-leucyl], cyclic tetrapeptide formely isolated from the *Stachylidium* sp.[96]

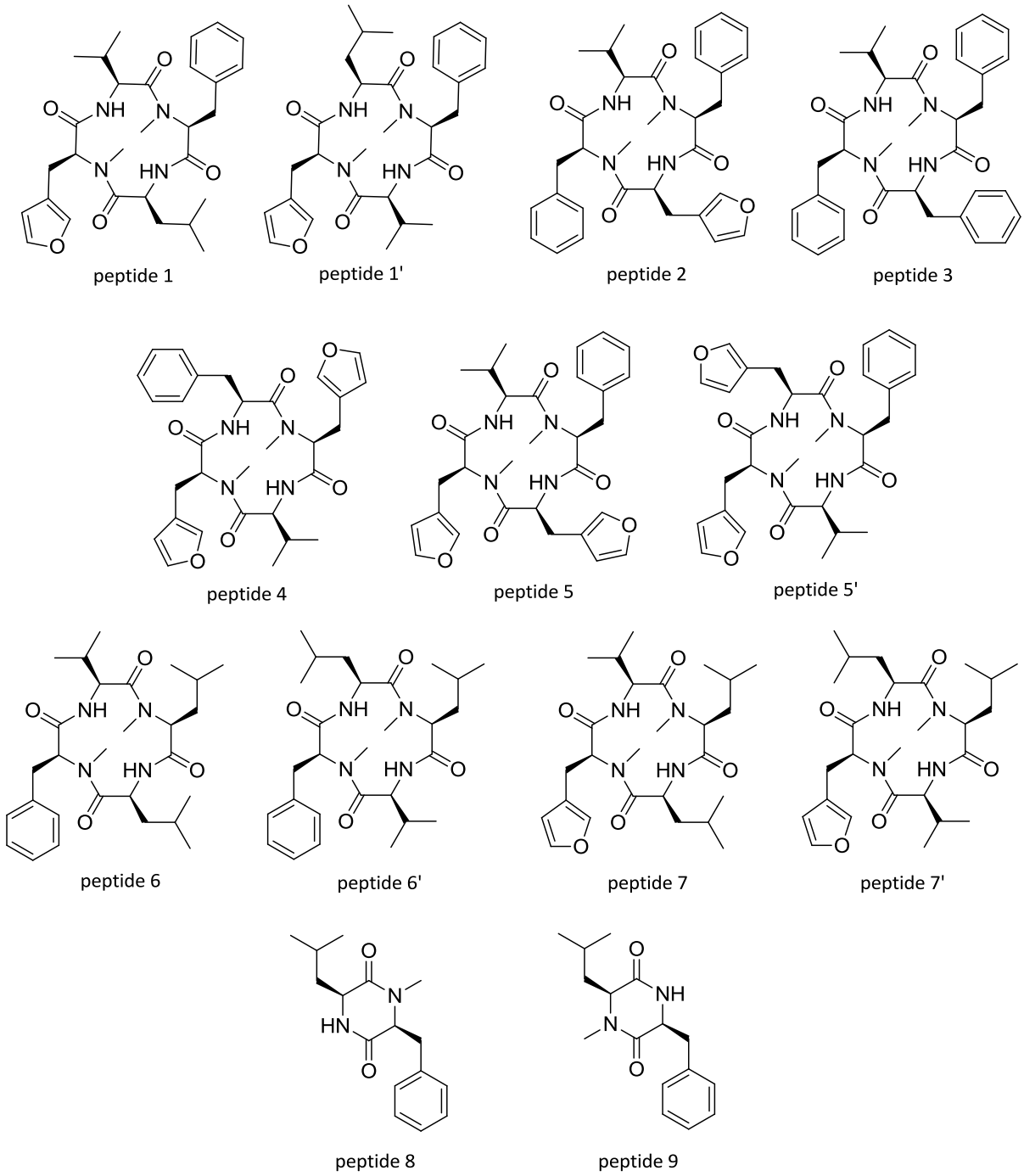

Fig 4-3. Structures of the isolated cyclic peptides.

Peptides isolated

Peptide 1 and 1', cyclic tetrapeptide, peptide 1 (-)-Cyclo-[(N-methyl-(L)-3-(3-furyl)-alanyl), (L)-leucyl, (N-methyl-(L)-phenylalanyl), (L)-valinyl] and peptide 1' (-)-Cyclo-[(N-methyl-(L)-3-(3-furyl)-alanyl), (L)-valinyl, (N-methyl-(L)-phenylalanyl), (L)-leucyl]: white solid (2.5 mg L^{-1}), $[\alpha]_D^{23}$ -133 (*c* 0.44, MeOH); UV (MeOH) λ_{max} 204 nm (log ϵ 4.69); IR (ATR) ν_{max} 3345 (br), 2958, 2871, 1704, 1660, 1511, 1364, 1089 cm^{-1}; ^1H NMR and ^{13}C NMR (Table 4-1); LRESIMS *m/z* 525.5 $[M+H]^+$, *m/z* 523.9 $[M-H]^-$; HRESIMS *m/z* 547.2902 $[M+Na]^+$ (calcd. for $C_{29}H_{40}N_4NaO_5$, 547.2896).

Peptide 2, cyclic tetrapeptide, (-)-Cyclo-[N-methyl-(L)-phenylalanyl, (L)-furylalanyl, N-methyl-(L)-phenylalanyl, (L)-valinyl]: white solid (1.5 mg L^{-1}), $[\alpha]_D^{23}$ -129 (*c* 0.2, MeOH); UV (MeOH) λ_{max} 204 nm (log ϵ 3.45); IR (ATR) ν_{max} 3330 (br), 2961, 2360, 1704, 1660, 1514, 1362, 1091 cm^{-1}; ^1H NMR and ^{13}C NMR (Table 4-2); LRESIMS *m/z* 559.4 $[M+H]^+$, *m/z* 557.6 $[M-H]^-$; HRESIMS *m/z* 581.2731 $[M+Na]^+$ (calcd. for $C_{32}H_{38}N_4NaO_5$, 581.2740).

Peptide 3, cyclic tetrapeptide, (-)-Cyclo-[N-methyl-(L)-phenylalanyl, (L)-phenylalanyl, N-methyl-(L)-phenylalanyl, (L)-valinyl]: white solid (1 mg L^{-1}), $[\alpha]_D^{23}$ -153 (*c* 0.125, MeOH); UV (MeOH) λ_{max} 207 nm (log ϵ 3.06); IR (ATR) ν_{max} 3329 (br), 2961, 1703, 1659, 1512, 1362, 1090 cm^{-1}; ^1H NMR and ^{13}C NMR (Table 4-3); LRESIMS *m/z* 569.7 $[M+H]^+$, *m/z* 567.7 $[M-H]^-$; HRESIMS *m/z* 569.3119 $[M+H]^+$ (calcd. for $C_{34}H_{41}N_4O_4$, 569.3128). Data are in accordance with those in literature.[95]

Peptide 4, cyclic tetrapeptide, (-)-Cyclo-[(N-methyl-(L)-3-(3-furyl)-alanyl), (L)-valinyl, (N-methyl-(L)-3-(3-furyl)-alanyl), (L)-phenylalanyl]: white solid (1.4 mg L^{-1}), $[\alpha]_D^{23}$ -76 (*c* 0.058, MeOH); UV (MeOH) λ_{max} 204 nm (log ϵ 3.62); IR (ATR) ν_{max} 3331 (br), 2926, 2359, 1660, 1505, 1386, 1090 cm^{-1}; ^1H NMR and ^{13}C NMR (Table 4-4); LRESIMS *m/z* 549.4 $[M+H]^+$, *m/z* 547.5 $[M-H]^-$; HRESIMS *m/z* 571.2532 $[M+Na]^+$ (calcd. for $C_{30}H_{36}N_4NaO_6$, 571.2533).

Peptide 5 and 5', cyclic tetrapeptide, peptide 5 (-)-Cyclo-[(N-methyl-(L)-3-(3-furyl)-alanyl), (L)-3-(3-furyl)-alanyl, (N-methyl-(L)-phenylalanyl), (L)-valinyl] and peptide 5' (-)-Cyclo-[(N-methyl-(L)-3-(3-furyl)-alanyl), (L)-valinyl, (N-methyl-(L)-phenylalanyl), (L)-3-(3-furyl)-alanyl]: white solid (0.6 mg L^{-1}), $[\alpha]_D^{23}$ -110 (*c* 0.166, MeOH); UV (MeOH) λ_{max} 204 nm (log

ϵ 3.41); IR (ATR) ν_{max} 3331 (br), 2925, 2358, 1663, 1515, 1401, 1088 cm^{-1}; ^{1}H NMR and ^{13}C NMR (Table 4-5); LRESIMS *m/z* 549.4 $[M+H]^+$, *m/z* 547.5 $[M-H]^-$; HRESIMS *m/z* 571.2526 $[M+Na]^+$ (calcd. for $C_{30}H_{36}N_4NaO_6$, 571.2533).

Peptide 6 and 6', cyclic tetrapeptide, peptide 6 (-)-Cyclo-[N-methyl-(L)-phenylalanyl, (L)-leucyl, N-methyl-(L)-leucyl, (L)-valinyl] and peptide 6' (-)-Cyclo-[N-methyl-(L)-phenylalanyl, (L)-valinyl, N-methyl-(L)-leucyl, (L)-leucyl]: white solid (0.6 mg L^{-1}), $[\alpha]_D^{23}$ -105 (*c* 0.108, MeOH); UV (MeOH) λ_{max} 206 nm (log ϵ 3.03); IR (ATR) ν_{max} 3332 (br), 2957, 2358, 1667, 1507, 1456 cm^{-1}; ^{1}H NMR and ^{13}C NMR (Table 4-6); LRESIMS *m/z* 501.4 $[M+H]^+$, *m/z* 499.4 $[M-H]^-$; HRESIMS *m/z* 501.3438 $[M+H]^+$ (calcd. for $C_{28}H_{45}N_4O_4$, 501.3441).

Peptide 7 and 7', cyclic tetrapeptide, peptide 7 (-)-Cyclo-[N-methyl-(L)-3-(3-furyl)-alanyl, (L)-leucyl, N-methyl-(L)-leucyl, (L)-valinyl] and peptide 7' (-)-Cyclo-[N-methyl-(L)-3-(3-furyl)-alanyl, (L)-valinyl, N-methyl-(L)-leucyl, (L)-leucyl]: white solid (0.6 mg L^{-1}), $[\alpha]_D^{23}$ -67 (*c* 0.083, MeOH); UV (MeOH) λ_{max} 204 nm (log ϵ 3.12); IR (ATR) ν_{max} 3342 (br), 2924, 2359, 1714, 1652, 1520, 1365 cm^{-1}; ^{1}H NMR and ^{13}C NMR (Table 4-7); LRESIMS *m/z* 491.9 $[M+H]^+$, *m/z* 489.8 $[M-H]^-$; HRESIMS *m/z* 513.3045 $[M+Na]^+$ (calcd. for $C_{26}H_{42}N_4NaO_5$, 513.3053).

Peptide 8, diketopiperazine, (-)-Cyclo-[(L)-leucyl, N-methyl-(L)-phenylalanyl]: white solid (0.35 mg L^{-1}), $[\alpha]_D^{23}$ -14 (*c* 0.083, MeOH); UV (MeOH) λ_{max} 203 nm (log ϵ 3.12); IR (ATR) ν_{max} 3198 (br), 2954, 2924, 2359, 1678, 1455, 1326 cm^{-1}; ^{1}H NMR and ^{13}C NMR (Table 4-8); LRESIMS *m/z* 275.6 $[M+H]^+$, *m/z* 273.4 $[M-H]^-$; HRESIMS *m/z* 297.1568 $[M+Na]^+$ (calcd. for $C_{16}H_{22}N_2NaO_2$, 297.1579).

Peptide 9, diketopiperazine, (-)-Cyclo-[N-methyl-(L)-leucyl, (L)-phenylalanyl]: white solid (0.15 mg L^{-1}), $[\alpha]_D^{23}$ -241 (*c* 0.066, MeOH); UV (MeOH) λ_{max} 203 nm (log ϵ 2.85); IR (ATR) ν_{max} 3248 (br), 2925, 2359, 1681, 1455, 1340 cm^{-1}; ^{1}H NMR and ^{13}C NMR (Table 4-9); LRESIMS *m/z* 275.6 $[M+H]^+$, *m/z* 273.4 $[M-H]^-$; HRESIMS *m/z* 297.1555 $[M+Na]^+$ (calcd. for $C_{15}H_{20}N_2NaO_2$, 297.1573).

4.3 Biosynthetic studies of secondary metabolites from *Stachylidium* sp.

Cyclic peptides

For studying the biosynthesis of the cyclic peptides, peptide 1 and 1' (Fig 4-4) was chosen as a prototype, on the grounds that it incorporates all the four amino acid building blocks. A closer look into the structural architecture of the isolated peptides proposed a non-ribosomal biosynthetic origin, implied from the incorporated modified amino acid residues, i.e. N-methylated, and the unusual non-proteinogenic amino acid, i.e. 3-(3-furyl)-alanine. Three of the four amino acids, i.e. valine, leucine and phenylalanine, are discernibly derived from proteinogenic amino acids modified by methylation as seen in phenylalanine. Of special interest was the remaining amino acid, 3-(3-furyl)-alanine, a rare building block reported before in heptapeptides from the fungus *Rhizopus microsporus*[68] and more recently in the pentapeptide bingchamide B from *Streptomyces bingchenggensis.*[74] We thus set up to determine the biosynthetic origin of the 3-(3-furyl)-alanine, and propose a biosynthetic scheme for its biosynthesis, not investigated before, employing classical isotope tracer experiments.

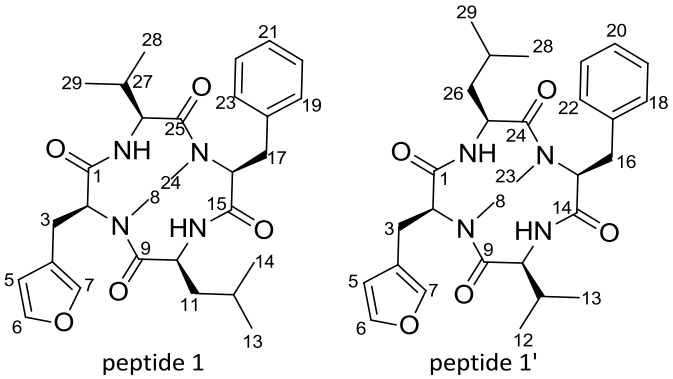

Fig 4-4. Structures of the positional isomers peptide 1 and 1'.

Polyketides

The marilones and marilines are polyketide compounds with a phthalide and phthalimidine skeleton, respectively (Fig 4-5).[83,84] This type of compound class is known to be produced by polyketide synthase (PKS) biosynthetic machineries, using acetate as basic building blocks in a Claisen-type condensation reaction to expand the growing ketide chain.[97] Precedent biosynthetic studies for the phthalide skeleton, such as in

mycophenolic acid,[98] nidulol and silvaticol,[99] proved the tetraketide nature of the phthalide skeleton, while no biosynthetic studies were conducted for phthalimidine metabolites, which probably follows a similar biosynthetic route. An unusual structural feature in both the marilones and marilines is the methyl substituent at C-8. This could be postulated to be introduced either from a propionate starter unit, by methylation of an acetate starter unit, or by loss of a carbon unit from a pentaketide intermediate, generally not known in fungal polyketide biosynthesis. Thus, biosynthetic studies would help to resolve this ambiguity.

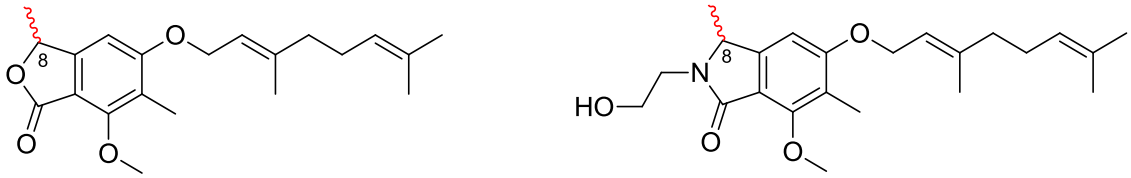

marilone A mariline B

Fig 4-5. Structures of isolated polyketides, marilone A and mariline B.

4.3.1 Preliminary feeding experiments

Biosynthetic feeding studies in marine organisms are generally known to be faced with major difficulties.[100,101] These are related to the producing microorganisms, which are usually slow growing under laboratory conditions with low amounts of metabolites being produced. Another facet is related to the used feeding protocol, which includes the choice of growth media, and the concentration and the time of feeding the precursors. Liquid media have generally been regarded as the media of choice in biosynthetic studies, as they ensure adequate distribution of the fed precursors. The amount of fed precursor should be sufficient for being incorporated and analytically detected in the final metabolite, and at the same time not too high as to hamper biosynthesis or to be toxic for the growing microorganism. Lastly, the time course of feeding the precursor should be adjusted, as biosynthesis of secondary metabolites usually follows primary metabolism after the microorganism has fully developed.[10] Therefore, a too early feeding of a single precursor dose may be used up in primary metabolism, and thus multiple feeding after sufficient microorganism growth could likely overcome this hurdle.

To address these difficulties, preliminary experiments were initiated in both solid and liquid biomalt salt culture media, with and without the putative precursors of interest (see 3.5.1 for experimental details). The aim was to determine the onset of metabolite production and to investigate possible changes in the level of metabolite production before proceeding further with biosynthetic experiments. Information gained from these preliminary experiments was essential in setting up a successful feeding protocol that would ensure maximal incorporation of the labeled precursors into the metabolites of interest.

From the time-scale experiment, we tracked the production of secondary metabolites, where solid biomalt salt cultures were harvested at different time points and analyzed using LC-MS. The peptides were starting to be detected at around day 9, with the amounts increasing with fungal growth, becoming highly distinct at around day 30, and still being clearly detected throughout the 55 days cultivation period. As for the polyketides, i.e. marilones and marilines, they were starting to be produced at a fairly later stage, around day 20, in clearly lower amounts compared to the peptides (Table 4-10).

Table 4-10. Production of secondary metabolites on solid biomalt salt medium as implied from LC-MS results of time-scale experiment.

Day	Peptides[1]	Polyketides[2]
5	-	-
9	+	-
14	++	-
20	++	+
30	+++	+
55	+++	++

[1] for structures see Fig 4-3, [2] for structures see Fig 4-5

Liquid culture medium was found unsuitable for further biosynthetic studies as preliminary experiments in liquid biomalt salt culture medium showed the absence of some of the major metabolites of interest, i.e. peptides with a 3-(3-furyl)-alanine amino acid.

Addition of general precursors normally employed in biosynthetic studies such as glucose, glycerol, shikimic acid or sodium acetate, did not exhibit any deleterious effect on the growing fungus, or noticeably affect the amount of metabolite produced. On the other hand, addition of phenylalanine clearly led to an increased production of those peptides incorporating a phenylalanine residue.

From a liquid biomalt salt culture medium supplemented with phenylalanine two compounds, hitherto not encountered in this fungus, were isolated (see 3.5.2). Through the interpretation of the NMR data (Fig S21-S24 and Table S1) and literature search, they were assigned as bisdethiobis(methylthio)-acetylaranotin (BDA) and bisdethiobis(methylthio)-acetylapoaranotin (BDAA), thiodiketopiperazines previously reported from the fungi *Arachniotus aureus* and *Aspergillus terreus* (Fig 4-6).[102] Their biosynthesis involves a phenylalanine intermediate, thus supplementing the culture media with phenylalanine, probably stimulated their production.[103] They belong to the group of epipolythiodioxopiperazines, a class of fungal toxins, featuring a seven membered 4,5-dihydrooxepine ring, with absence of a disulfide bridge. They were tested for antimicrobial activity against *Escherichia coli*, *Bacillus megaterium*, *Microbotryum violaceum*, *Eurotium rubrum* and *Mycotypha microspora* and were found to be inactive (see 3.6.1 for experimental details).

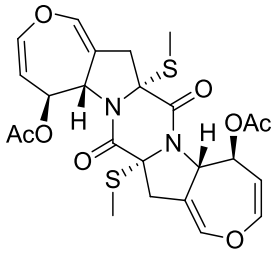

Bisdethiobis(methylthio)-acetylaranotin (BDA)

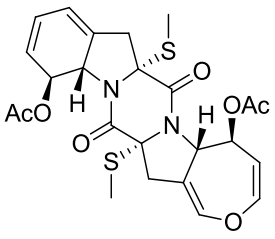

Bisdethiobis(methylthio)-acetylapoaranotin (BDAA)

Fig 4-6. Isolated epipolythiodioxopiperazines from liquid biomalt medium fed with phenylalanine.

Based on observations from the preliminary experiments, a biosynthetic feeding protocol on solid biomalt salt culture media was established (Table 4-11). For the peptides a twice feeding starting on day 5, supplemented with a second feeding on day 10 and harvesting after a 30 day period would be optimal, to avoid dilution of the labeled peptides with unlabeled peptides. For the polyketides, a longer cultivation period of around 60 days

would be necessary and a thrice feeding starting on day 10, as to avoid consumption of the labeled precursor in primary metabolism, and on days 20 and 30 would ensure a stable supply of the labeled precursors during polyketide biosynthesis.

Table 4-11. Established feeding protocol for labeled precursors based on observations from preliminary experiments.

Day	Peptides[1]	Polyketides[2]
1	Fungal Inoculation	
5	1st feeding	
10	2nd feeding	1st feeding
20		2nd feeding
30	Harvesting & Extraction	3rd feeding
60		Harvesting & Extraction

[1] for structures see Fig 4-3, [2] for structures see Fig 4-5

4.3.2 Biosynthetic/Metabolic origin of building blocks in peptide 1 and 1'

For the experimental investigation of any biosynthetic pathway, it is necessary to establish a hypothetical biosynthetic scheme for the conversion of fed precursors into the target metabolite. Our first hypothesis was based on the structural relationship between the 3-(3-furyl)-alanine and the phenylalanine skeleton and points to the possibility of 3-(3-furyl)-alanine being derived by ring cleavage of a phenylalanine intermediate, notably that both amino acid moieties are incorporated into the isolated peptides. As little was known about the biosynthetic origin of 3-(3-furyl)-alanine, a general carbon source precursor involved in several biosynthetic pathways, such as glucose or glycerol, could help in delineating the involved biosynthetic pathway. This approach was supported by earlier biosynthetic studies on the reductiomycin antibiotic produced by *Streptomyces xanthochromogenus*, in which they fed labeled glycerol to study the biosynthetic origin of the dihydrofuranacrylic acid moiety of reductiomycin,[104] which shares the basic skeleton with 3-(3-furyl)-alanine. Their results point to the shikimate pathway as the origin for the dihydrofuranacrylic acid moiety. To test our hypotheses, stable isotope precursors labeled at one or more positions were fed to the growing fungal culture (see 3.5 for experimental details), followed by extraction and isolation of the metabolites of interest using VLC fractionation and HPLC techniques (see 3.3 for chromatographic isolation details and Fig 4-1 for isolation scheme). The labeling pattern was then established using NMR and mass spectroscopic techniques (see 3.4). With mass spectrometry we could detect the mass difference between natural abundance isotopic distribution and isotopically enriched molecules, although the exact site of incorporation cannot be deduced.[105] While with ^{13}C-NMR spectroscopy, incorporation of a precursor containing ^{13}C at more than natural abundance, i.e. more than 1.1%, in a specific position gives rise to an enhanced signal in the ^{13}C-NMR spectra as compared to those carbons of natural abundance. The labeling pattern can thus be deduced by comparing the ^{13}C-NMR spectrum of the labeled metabolite with the spectrum of the unlabeled metabolite.[106]

4.3.2.1 Labeling studies with [1-^{13}C]phenylalanine

By feeding [1-^{13}C]phenylalanine, we tested whether phenylalanine, an aromatic amino acid of shikimate biosynthetic origin, could be a plausible intermediate in the biosynthesis

of 3-(3-furyl)-alanine (see 3.5.3 for experimental details). Incorporation of fed [1-^{13}C]phenylalanine in peptide 1 and 1' was monitored using LC-MS. A signal was observed at *m/z* 526.1 $[M+H+1]^+$, with a 1 Da mass shift compared to the unlabeled control, i.e. *m/z* 525.2 $[M+H]^+$ (Fig S36). This was further verified after isolation of peptide 1 and 1' and ^{13}C-NMR spectroscopic analysis, where we observed a prominent signal for the carbonyl carbon, i.e. C-15 (δ_c 170.5) and C-14 (δ_c 170.9), of the phenylalanine residue of peptide 1 and 1' (Fig S26). However, no incorporation of the labeled phenylalanine was observed in the 3-(3-furyl)-alanine residue (Fig 4-7).

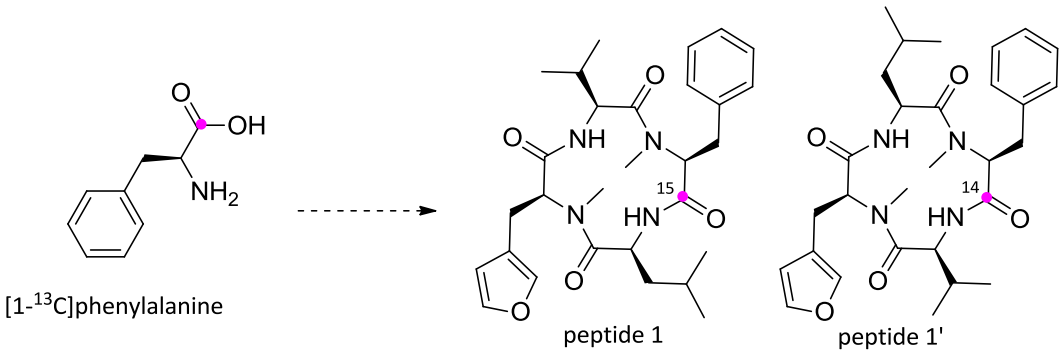

Fig 4-7. Observed ^{13}C enrichment in peptide 1 and 1' after feeding [1-^{13}C]phenylalanine. Pink dots indicate ^{13}C enriched atoms.

Validity of this experiment was confirmed with the simultaneous isolation of peptide 3 (Fig 4-3), which was found to incorporate three [1-^{13}C]phenylalanine units identified as three enhanced signals for the carbonyl carbons, i.e. C-1 (δ_c 171.0), C-11 (δ_c 172.1), C-20 (δ_c 170.1), of the phenylalanine residues in the ^{13}C-NMR spectrum (Fig S27). Along with that, a 3 Da mass shift was observed for peptide 3 in the LC-MS spectrum of the crude extract of the *Stachylidium* sp. culture supplemented with [1-^{13}C]phenylalanine. Labeled peptide 3 showed a signal at *m/z* 572.4 $[M+H+3]^+$ compared to the unlabeled control, i.e. *m/z* 569.2 $[M+H]^+$ (Fig S37).

4.3.2.2 Labeling studies with [U-^{13}C] glycerol

Feeding fully labeled [U-^{13}C]glycerol gave a complex ^{13}C-NMR spectrum (Fig S28) for the isolated peptide 1 and 1' (see 3.5.4 for experimental details). Detailed analysis of the signal pattern and ^{13}C-^{13}C coupling constants in the inverse gated proton decoupled ^{13}C-NMR spectrum of the 3-(3-furyl)-alanine moiety of peptide 1 and 1' showed the presence

of two doubly coupled spin systems, i.e. C-1/C-2/C-3 and C-5/C-4/C-7, and a single enriched non-coupled signal for C-6 (Fig 4-8). For detailed chemical shifts and coupling constants see Table S2 and S3 for [U-^{13}C]glycerol-derived peptide 1 and 1', respectively.

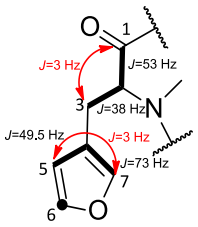

Fig 4-8. Observed ^{13}C-labeling pattern for the 3-(3-furyl)-alanine moiety of peptide 1 and 1' from the experiment with [U-^{13}C]glycerol: bold lines indicate ^{13}C labeled isotopomers with directly adjacent ^{13}C atoms, arrows indicate ^{13}C atoms connected by long-range coupling and their corresponding coupling constants (*J* values) in Hz. Dots indicate ^{13}C enriched atoms.

From the established metabolic fate of glycerol, glycolysis gives rise to an intact three-carbon unit in the form of phosphoenolpyruvate.[104] Concurrently, glycerol is converted in the reductive pentose phosphate (RPP) cycle, via dihydroxyacetone phosphate and phosphoglyceraldehyde into fructose-6-phosphate, which contains two coupled three-carbon units, which with the help of a transketolase gives erythrose-4-phosphate with one intact three-carbon units and a single non-coupled carbon (Fig 4-9).[107]

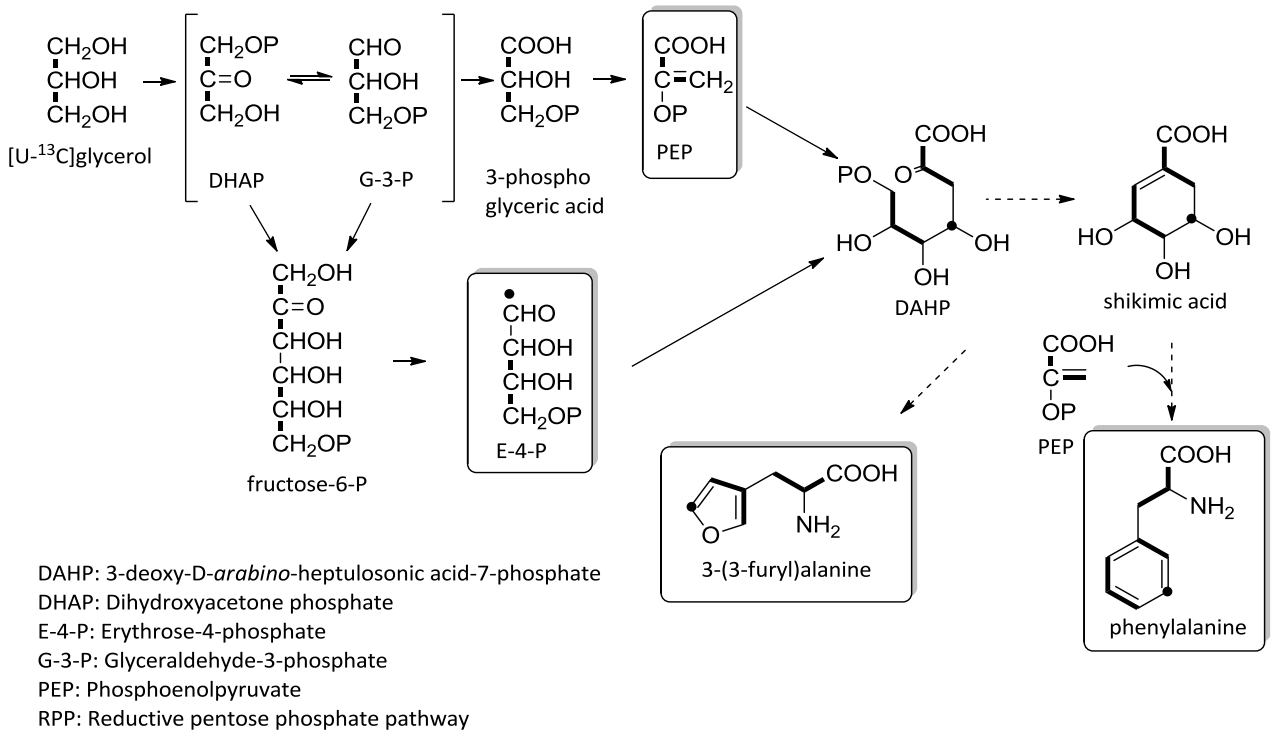

Fig 4-9. Formation of PEP and E-4-P from [U-^{13}C]glycerol via the glycolytic and RPP pathway and their incorporation into 3-(3-furyl)-alanine and phenylalanine of peptide 1 and 1'. Bold lines indicate ^{13}C labeled isotopomers with directly adjacent ^{13}C atoms. Dots indicate ^{13}C enriched atoms.

4.3.2.3 Labeling studies with [1-^{13}C]glucose

The observed labeling pattern in the [U-^{13}C]glycerol experiment was further supported by feeding studies using [1-^{13}C]glucose (see 3.5.5 for experimental details). We observed enriched signals for C-3 (δ_c 24.5) and C-5 (δ_c 110.9) of the 3-(3-furyl)-alanine moiety of peptide 1 and 1' (Fig S29). These originate from [3-^{13}C]phosphoenolpyruvate via glycolysis and [4-^{13}C]erythrose-4-phosphate via the pentose phosphate pathway, following conversion of [1-^{13}C]glucose to [6-^{13}C]glucose-6-phosphate or [1,6-^{13}C]glucose-6-phosphate via glycolysis and gluconeogenesis (Fig 4-10).[108]

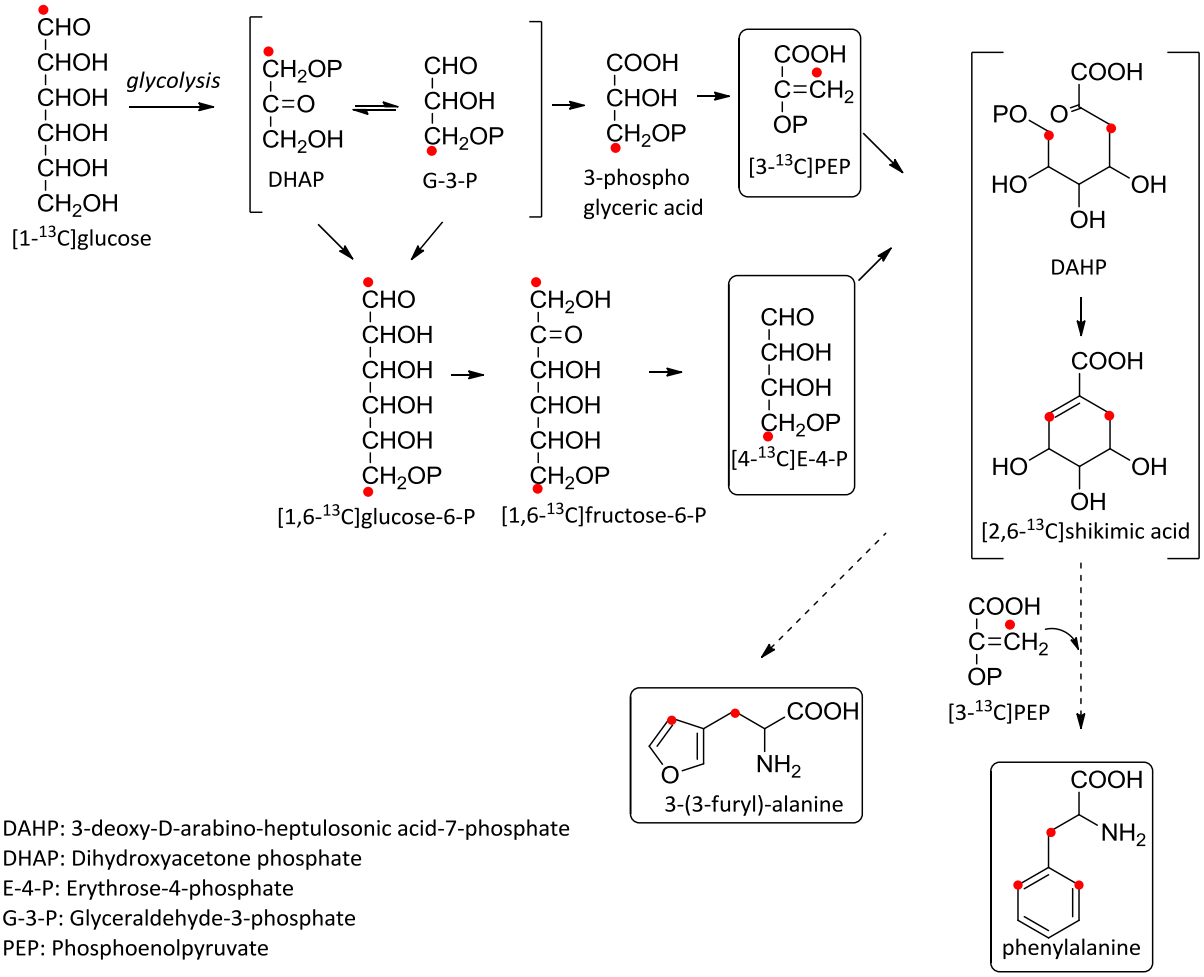

Fig 4-10. Formation of PEP and E-4-P from [1-^{13}C]glucose via the glycolytic and pentose phosphate pathway and their incorporation into 3-(3-furyl)-alanine and phenylalanine of peptide 1 and 1'. Dots indicate ^{13}C enriched atoms originating from [1-^{13}C]glucose.

Thus, the observed labeling pattern after feeding [U-^{13}C]glycerol and [1-^{13}C]glucose points to a shikimate-related pathway for the biosynthesis of 3-(3-furyl)-alanine, from condensation of phosphoenolpyruvate and erythrose-4-phosphate with 3-deoxy-D-*arabino*-heptulosonic acid-7-phosphate as an intermediate (Fig 4-11).

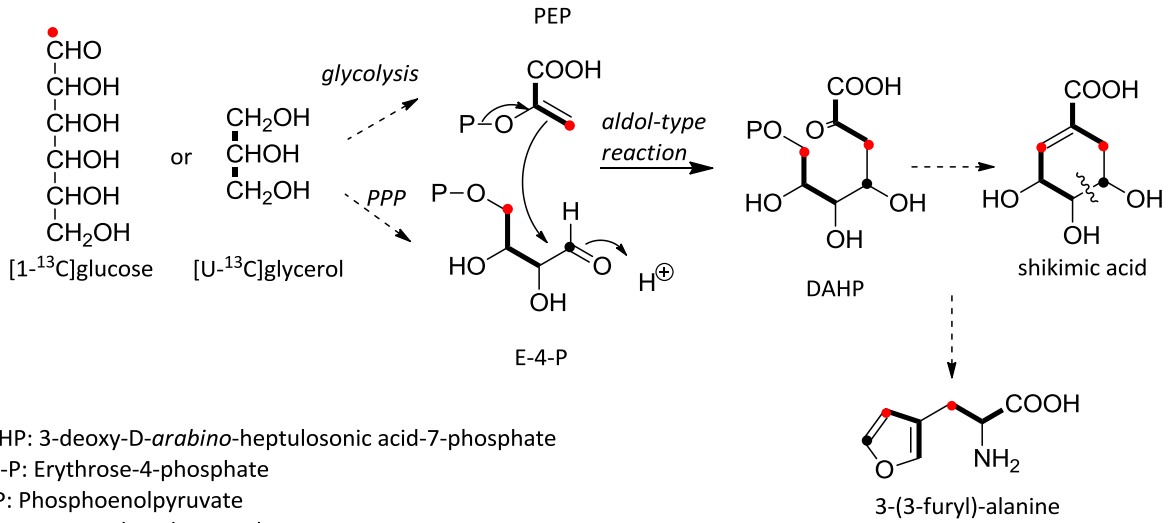

Fig 4-11. Summary of ^{13}C enrichment pattern in the 3-(3-furyl)-alanine moiety of peptide 1 and 1' from a biomalt salt agar culture of *Stachylidium* sp. labeled with both [1-^{13}C]glucose and [U-^{13}C]glycerol in separate experiments. Bold lines indicate ^{13}C-labeled isotopomers with directly adjacent ^{13}C atoms. Dots indicate ^{13}C enriched atoms.

4.3.2.4 Labeling studies with [1,7-^{13}C]shikimic acid

For the verification of the shikimate origin of 3-(3-furyl)-alanine, [1,7-^{13}C]shikimic acid was chosen to be fed (see 3.5.8 for experimental details). However, no labeled 3-(3-furyl)-alanine and phenylalanine could be observed in LC-MS (Fig S38(B)). Failure of this experiment can be attributed to several reasons. The applied feeding protocol, i.e. a too low concentration, or the impermeability of fungal cells to labeled shikimic acid are plausible explanations. The latter was previously reported from several biosynthetic studies[109] and was thought more likely as the added labeled shikimic acid was detected intact in the fungal crude extract. Thus results of this experiment were not predictive (Fig 4-12).

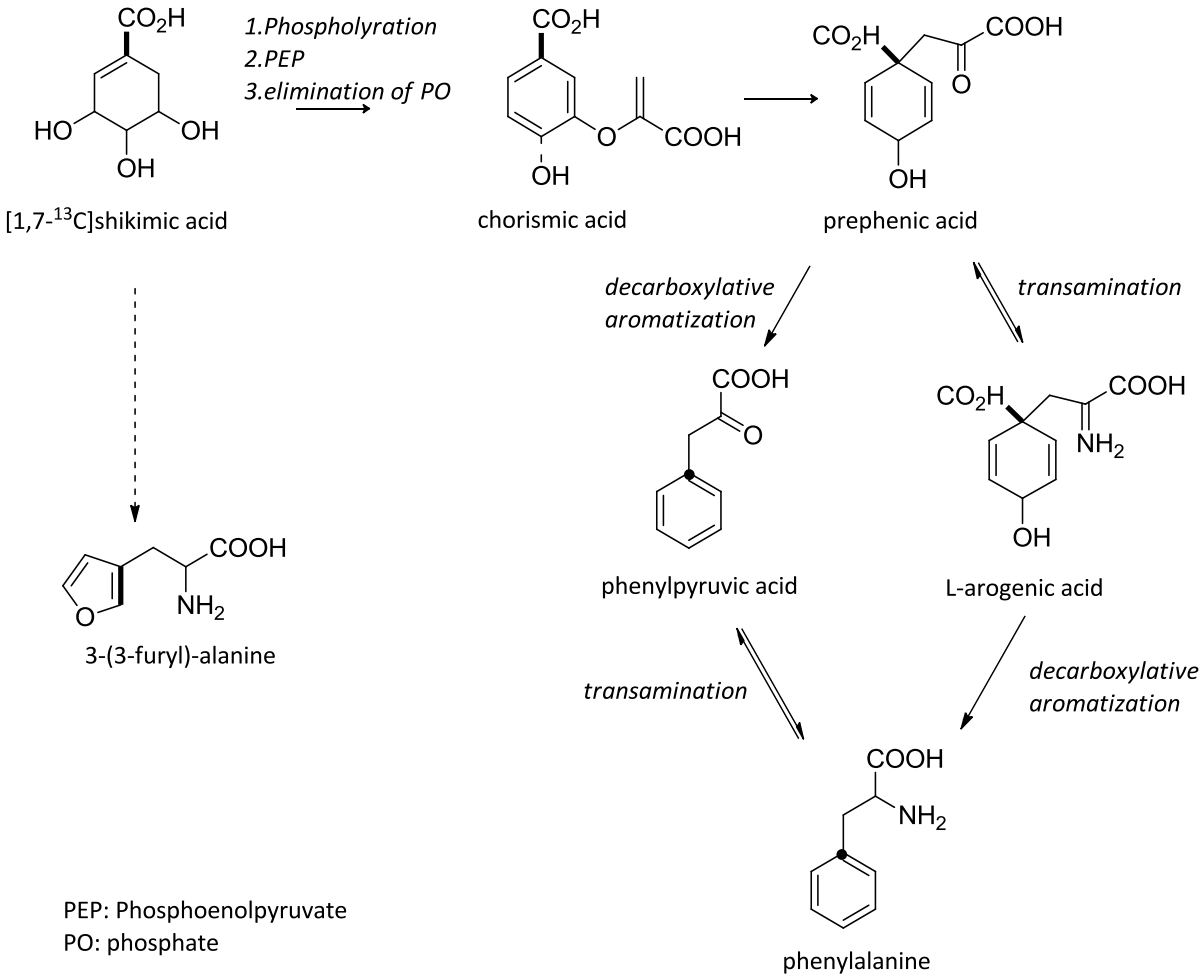

Fig 4-12. Predicted labeling patterns for the 3-(3-furyl)alanine and phenylalanine moieties of peptide 1 and 1' from the experiment with [1,7-^{13}C]shikimic acid. Bold lines indicate ^{13}C-labeled isotopomers with directly adjacent ^{13}C atoms. Dots indicate ^{13}C enriched atoms. Unfortunately, the conducted labeling experiment did not result in any incorporation

4.3.2.5 Feeding studies with halogenated precursors and proteinogenic amino acids

Earlier studies have investigated the use of halogenated precursors as a biosynthetic label benefiting from their low cost in comparison to ^{13}C labeled precursors.[110] Additionally, the incorporation of the halogenated precursors and the isolation of novel metabolite analogues with superior and selective biological activity is exploited (precursor directed biosynthesis).[111] In our continuous search for a plausible intermediate involved in the biosynthesis of 3-(3-furyl)-alanine, we fed 2-chloro-protocatechuic acid, with protocatechuic acid being a known intermediate in the shikimate pathway. 2-chloro-protocatechuic acid was synthesized from 2-chloro-3,4-dimethoxybenzoic acid after

successful demethylation using BBr_3 in dichloromethane (see 3.7.2 for experimental details). Added 2-chloro-protocatechuic acid was not seen to be incorporated into peptide 1 and 1', by LC-MS analysis (Fig S38(C)). This indicates failure of incorporation, due to its irrelevance to the 3-(3-furyl)-alanine biosynthesis, or because the biosynthetic enzymes do not accept chlorinated substrates, or as in the labeled shikimic acid experiment due to fungal cell impermeability. Again, results of this experiment were not conclusive (see 3.5.2 for experimental details).

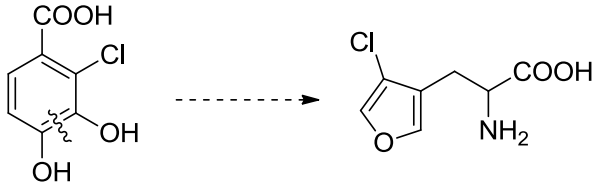

2-chloro-protocatechuic acid 4-chloro-3-(3-furyl)-alanine

Fig 4-13. Proposed incorporation of 2-chloro-protocatechuic acid in the 3-(3-furyl)-alanine moiety. Unfortunately, the conducted experiment did not result in any incorporation.

The involvement of yet another phenolic acid such as 4-hydroxybenzoic acid, a symmetric intermediate frequently encountered in the biosynthesis of several metabolites[108,112] including reductiomycin,[104] was tested through feeding 2-fluoro-4-hydroxybenzoic acid (see 3.5.2 for experimental details), but did not result in any incorporation into peptide 1 and 1' as observed in LC-MS (Fig S38(D)).

However, feeding halogenated ring-substituted phenylalanine such as 2-fluoro-phenylalanine and 3-fluoro-phenylalanine, resulted in the production of new peptide analogues as revealed in LC-MS with a new mass peak at *m/z* 543.6 $[M+19]^+$, representing incorporation of a single fluoro-phenylalanine into peptide 1 and 1' scaffold. In contrast, 4-fluoro-phenylalanine and tyrosine (a *p*-hydroxylated phenylalanine) were not seen to be incorporated into the peptides (Fig S39) (see 3.5.2 for experimental details).

Additionally, the incorporation of alternative amino acids in the peptides was tested by feeding several proteinogenic amino acids, such as alanine, glycine, proline, tryptophan, tyrosine and serine, to the growing fungus media, but did not result in the detection of any further new analogues as seen in LC-MS (see 3.5.2 for experimental details).

4.3.2.6 Labeling studies with [1-^{13}C]sodium acetate

Although some carbon atoms of the 3-(3-furyl)-alanine moiety of peptide 1 and 1' displayed some ^{13}C enrichment in the ^{13}C-NMR spectrum after feeding [1-^{13}C]sodium acetate, this is not indicative of any known metabolic mechanism (Fig S31). This could be attributed to metabolic turnover of [1-^{13}C]sodium acetate during fungal growth. Thus, the possibility of a polyketide pathway, which utilizes acetate as a basic building block, being involved in the biosynthesis of the 3-(3-furyl)-alanine was deemed implausible (see 3.5.6 for experimental details).

4.3.2.7 Labeling studies with [*Me*-^{13}C]methionine

[*Me*-^{13}C]methionine, a universal methylating agent used frequently in biosynthetic studies, was supplemented to *Stachylidium* sp. biomalt salt agar cultures and gave high enrichments for N-methyl carbons (δ_c 30.4 and δ_c 30.7) of peptide 1 and 1' as observed in the ^{13}C-NMR spectrum (Fig S30), indicating that the N-methyl groups are derived from *S*-adenosyl-L-methionine (see 3.5.7 for experimental details).

4.3.2.8 Proposed biosynthetic scheme for N-methyl-3-(3-furyl)-alanine

Based on the results of the feeding experiments, a scheme for the biosynthesis of N-methyl-3-(3-furyl)-alanine is proposed for the first time, clearly following the shikimate pathway (Fig 4-14). Concerning the sequence of steps and intermediate precursors involved, many questions remain open. Ring cleavage of a shikimate intermediate resulting in ring opening with subsequent cyclisation would lead to the formation of the furan moiety, as disclosed from biosynthetic studies for the dihyrdofuranacrylic acid moiety of reductiomycin.[104] Introduction of the amino group, probably from glutamic acid catalyzed by a transaminase, would lead to the basic carbon skeleton of 3-(3-furyl)-alanine.[97] A methyl group is then transferred from *S*-adenosyl-L-methionine to the nitrogen, with the help of a methyltransferase, releasing *S*-adenosyl-L-homocysteine in the process.[16]

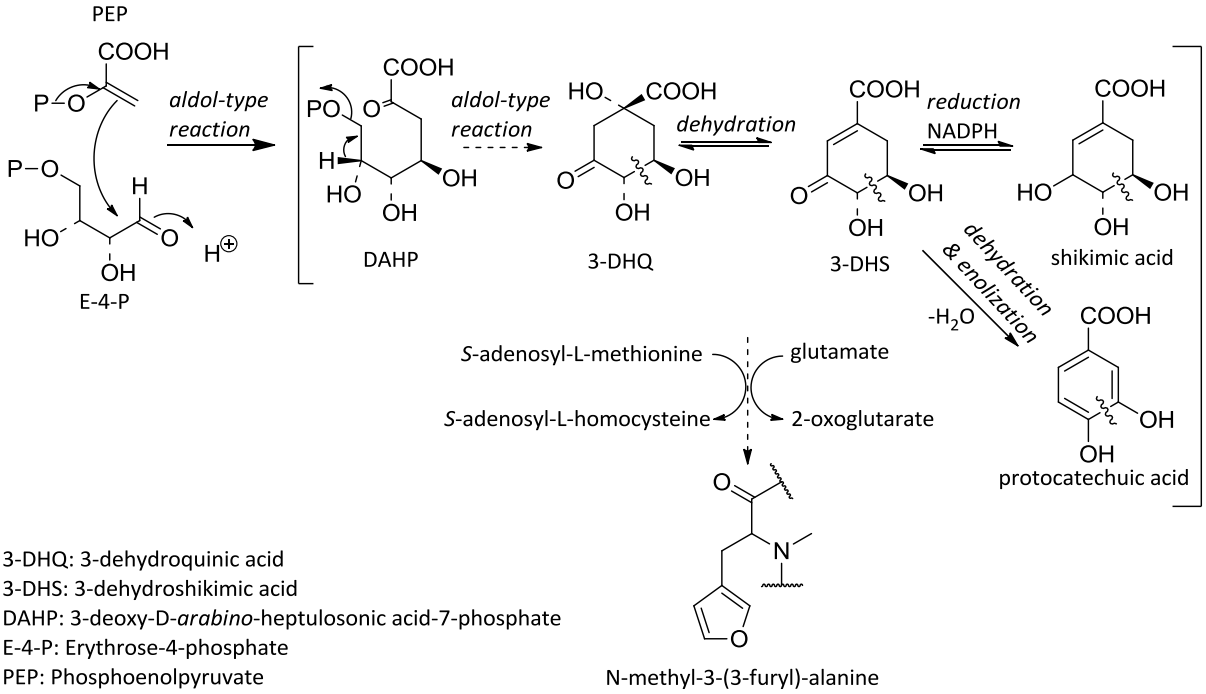

Fig 4-14. Postulated biosynthesis of N-methyl-3-(3-furyl)-alanine of peptide 1 and 1'.

Biosynthetic/Metabolic origin of valine and leucine in peptide 1 and 1'

Both branched-chain amino acids, leucine and valine follow a similar biosynthesis from two pyruvate starter units with α-ketoisovalerate as an intermediate. The additional carbon for leucine is provided through an aldol condensation of α-ketoisovalerate with acetyl-CoA, followed by decarboxylation of the intermediate β-keto acid to give α-ketoisocaproate. Lastly a pyridoxal phosphate (PLP)-dependent transamination with glutamate introduces the amino group to give valine and leucine.[113]

The labeling patterns observed for valine and leucine after feeding [U-^{13}C]glycerol, [1-^{13}C]glucose and [1-^{13}C]sodium acetate is biosynthetically trivial, but validates the applied feeding protocols. Metabolic turnover of fed [U-^{13}C]glycerol and [1-^{13}C]glucose through the glycolytic pathway, provides [U-^{13}C]pyruvate, [1,2-^{13}C]acetyl-CoA, and [3-^{13}C]pyruvate and [2-^{13}C]acetyl-CoA, respectively. This is reflected in the observed labeling pattern for [U-^{13}C]glycerol incorporation, where carbons of valine and leucine occurred as either enriched doublets, i.e. C-9/C-10, C-12/C-14 of leucine and C-25/C-26, C-27/C-28 of valine for peptide 1 and C-9/C-10, C-11/C-12 of valine and C-24/C-25 and C-27/C-29 of leucine for peptide 1', due to the contribution of intact two-carbon units, or as enriched singlets,

i.e. C-11 and C-13 of leucine and C-29 of valine for peptide 1 and C-13 of valine and C-26 and C-28 of leucine for peptide 1', as a result of carbon rearrangements (Fig S28). For detailed chemical shifts and coupling constants see Table S2 and S3 for [U-^{13}C]glycerol-derived peptide 1 and 1' respectively. This is in agreement with the labeling of C-10 (δ_c 49.3), C-13 (δ_c 22.5) and C-14 (δ_c 23.2) of leucine and C-28 (δ_c 20.7) and C-29 (δ_c 18.4) of valine for peptide 1 and C-12 (δ_c 20.8) and C-13 (δ_c 18.4) of valine and C-25 (δ_c 49.1), C-28 (δ_c 22.5) and C-29 (δ_c 23.3) of leucine for peptide 1', after feeding [1-^{13}C]glucose (Fig S29). Furthermore, feeding [1-^{13}C]sodium acetate resulted in enrichments at carbonyl carbon (Fig S31), i.e. C-9 (δ_c 172.9) of leucine for peptide 1 and C-24 (δ_c 172.5) of leucine for peptide 1', from direct incorporation of fed [1-^{13}C]sodium acetate (Fig 4-15).

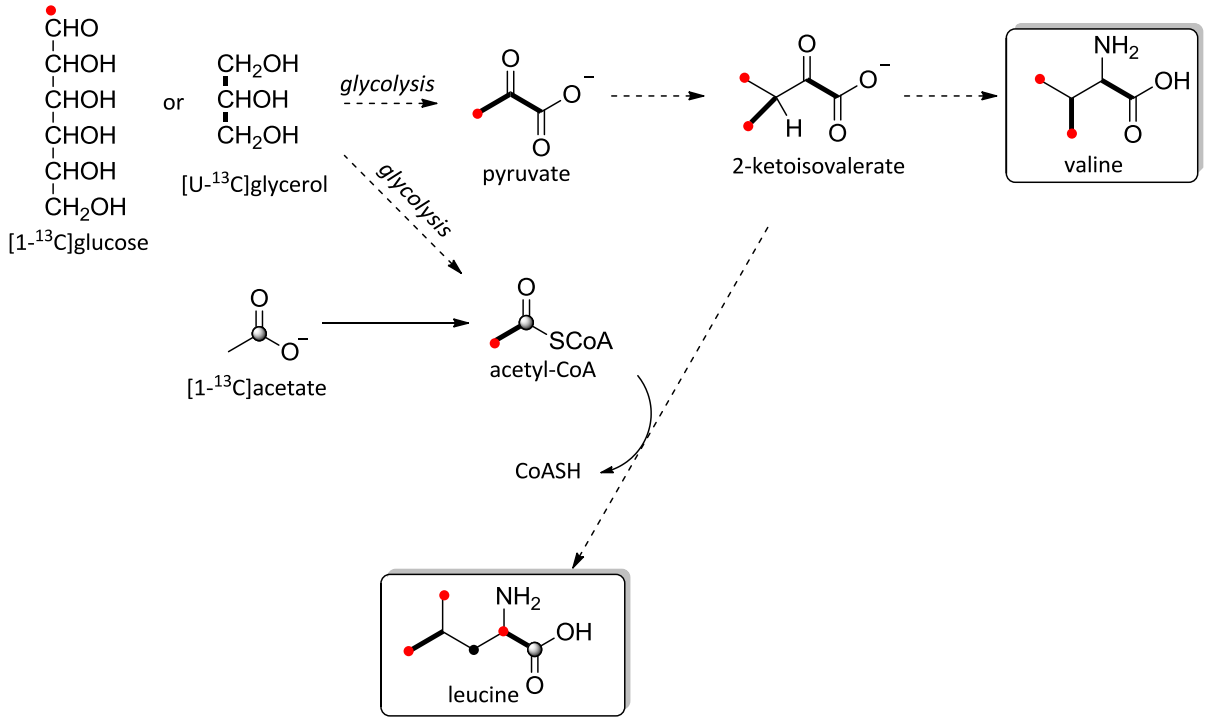

Fig 4-15. Observed labeling patterns for valine and leucine moieties of peptide 1 and 1' after feeding ^{13}C labeled precursors. Bold lines indicate ^{13}C labeled isotopomers with directly adjacent ^{13}C atoms. Dots indicate ^{13}C enriched atoms. Balls indicate ^{13}C labeled positions from [1-^{13}C]sodium acetate.

Table 4-12. Results of feeding experiments for peptide 1.

No.	Fed precursor	Enriched carbon atoms in peptide 1[1]			
		N-*Me*-FurAla	Leu	N-*Me*-Phe	Val
1	[1-^{13}C]phenylalanine	n.e.	n.e.	C-15	n.e.
2	[U-^{13}C]glycerol	C-1/C-2/C-3, C-5/C-4/C-7, C-6	C-9/C-10, C-12/C-14, C-11, C-13	n.d.	C-25/C-26, C-27/C-28, C-29
3	[1-^{13}C]glucose	C-3, C-5	C-10, C-13, C-14	C-17, C-19, C-23	C-28, C-29
4	[1-^{13}C]sodium acetate	n.e.	C-9	n.e	n.e
5	[*Me*-^{13}C]methionine	C-8	n.e.	C-24	n.e

n.e.: not enriched, n.d.: not detectable due to signal overlapping, [1] for structure see Fig 4-4

Table 4-13. Results of feeding experiments for peptide 1'.

No.	Fed precursor	Enriched carbon atoms in peptide 1'[1]			
		N-*Me*-FurAla	Val	N-*Me*-Phe	Leu
1	[1-^{13}C]phenylalanine	n.e.	n.e.	C-14	n.e.
2	[U-^{13}C]glycerol	C-1/C-2/C-3, C-5/C-4/C-7, C-6	C-9/C-10, C-11/C-12, C-13	n.d.	C-24/C-25, C-27/C-29, C-26, C-28
3	[1-^{13}C]glucose	C-3, C-5	C-12, C-13	C-16, C-18, C-22	C-25, C-28, C-29
4	[1-^{13}C]sodium acetate	n.e.	n.e	n.e	C-24
5	[*Me*-^{13}C]methionine	C-8	n.e.	C-23	n.e

n.e.: not enriched, n.d.: not detectable due to signal overlapping, [1] for structure see Fig 4-4

4.3.3 Biosynthetic/Metabolic origin of marilone A and mariline B

4.3.3.1 Labeling studies with [1-^{13}C]sodium acetate

Labeled marilone A and mariline B were isolated from a biomalt salt agar culture supplemented with [1-^{13}C]sodium acetate following the previously described isolation scheme (see 3.5.6 for experimental details and Fig S2).[83,84] Identity of the isolated marilone A and mariline B was confirmed using LC-MS, with molecular ion peaks at *m/z* 345.2 $[M+H]^+$ and *m/z* 388.5 $[M+H]^+$ for marilone A and mariline B, respectively (Fig S40 and S41).[83,84] Additionally, the isotope pattern observed in the MS spectra indicated the incorporation of [1-^{13}C]sodium acetate into the isolated metabolites. ^{13}C-NMR spectra were analyzed by comparison with ^{13}C-NMR spectra of previously reported unlabeled marilone A (Fig S32 and S33) and mariline B (Fig S34 and S35) from *Stachylidium* sp.[83,84] Chemical shift assignments were consistent with those previously reported (Table S4). Marilone A and mariline B showed enrichments for C-1, C-3, C-5 and C-7 of the basic skeleton, and C-1', C-3', C-5'and C-7' of the geranyl side chain. Thus, alternate carbon atoms of marilone A and mariline B were found to incorporate intact acetate units.

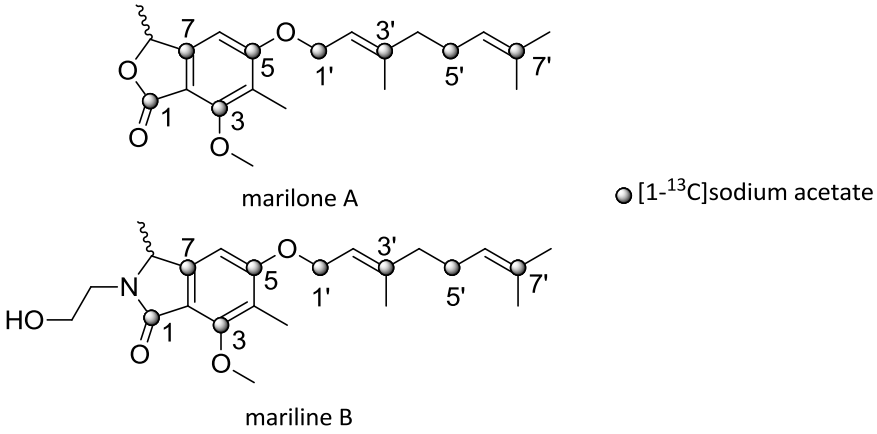

Fig 4-16. Observed labeling patterns for marilone A and mariline B after feeding [1-^{13}C]sodium acetate. Balls indicate ^{13}C enriched atoms.

4.3.3.2 Labeling studies with [*Me*-^{13}C]methionine

It was not possible to isolate marilone A and mariline B from a [*Me*-^{13}C]methionine fed biomalt salt agar culture and not much could be deduced from this experiment with respect to the polyketides biosynthesis (see 3.5.7 for experimental details).

4.3.3.3 Proposed biosynthetic scheme for marilone A and mariline B

The observed labeling pattern for marilone A and mariline B after feeding [1-^{13}C]sodium acetate suggests a total of four intact acetate units to be joined in a head-to-tail fashion forming a tetraketide chain to outline the biosynthesis of the marilone A and mariline B basic carbon skeleton. Subsequently, cyclisation and methylation of this chain would afford an intermediate 3-methyl orsellinic acid derivative. Ring closure and formation of the lactone or lactam ring takes place to form the phthalide and phthalimidine skeleton, respectively. The nitrogen atom for the lactam ring of mariline B is probably derived from ethanolamine. Recently, the biomimetic synthesis of the phthalimidine core structure was carried out using *ortho*-formyl-arylketone which smoothly condenses with ethanolamine under mild conditions to yield the mariline B core structure, supporting this presumption.[114] *O*-prenylation and *O*-methylation further decorates the basic carbon skeleton, with the help of a prenyltransferase and methyltransferase, respectively.

The observed labeling pattern for the geranyl side chain of marilone A and mariline B after feeding [1-^{13}C]sodium acetate, confirms it's mevalonate origin. Through condensation of three units of acetyl CoA, 3-hydroxy-3-methylglutaryl-CoA (HMG-CoA) is formed, which is further reduced to mevalonic acid. Mevalonic acid is then transformed into a phosphorylated isoprene unit (isopentenyl diphosphate), the basic building unit of terpenes. Isopentenyl diphosphate (IPP) is isomerized to give dimethylallyl diphosphate (DMAPP). Combination of DMAPP and IPP would give the geranyl diphosphate (GPP) side chain (Fig 4-17).[97]

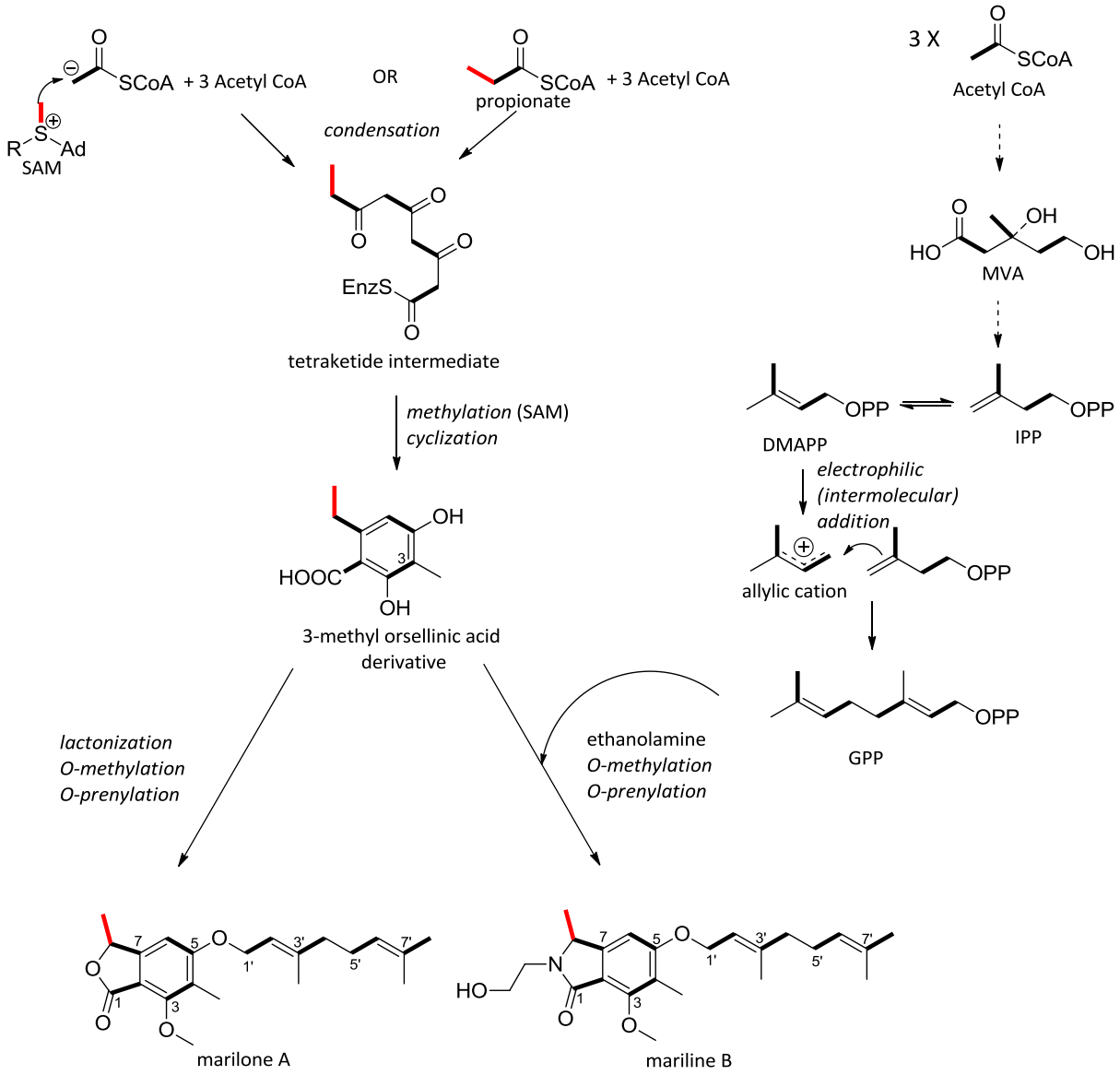

MVA: mevalonic acid
IPP: isopentenyl diphosphate
DMAPP: dimethylallyl diphosphate
GPP: geranyl diphosphate

Fig 4-17. Proposed biosynthetic scheme for marilone A and mariline B.

4.3.4 Discussion

Peptide 1 and 1'

Feeding experiments with [U-^{13}C]glycerol, [1-^{13}C]glucose, [1-^{13}C]phenylalanine, [1-^{13}C]sodium acetate and [*Me*-^{13}C]methionine in *Stachylidium* sp. ascertained the biosynthetic origin of the peptide building blocks, i.e. valine, leucine, phenylalanine and 3-(3-furyl)-alanine (Fig 4-18). Labeling patterns observed after feeding both [U-^{13}C]glycerol and [1-^{13}C]glucose were in accordance with previously reported labeling patterns for shikimate-derived metabolites.[108,112,115] The involvement of shikimic acid as a biosynthetic intermediate could not be verified unambiguously, nonetheless the incorporation patterns for both [U-^{13}C]glycerol and [1-^{13}C]glucose into peptide 1 and 1' give clear evidence for the involvement of a shikimate-related pathway in the biosynthesis of 3-(3-furyl)-alanine. The shikimate pathway is thus believed to account for all the carbon atoms of the N-methyl-3-(3-furyl)-alanine, apart from the N-methyl group, which is provided by the methyl group of methionine. The remaining amino acids are derived from standard building blocks as described in literature.[97,113]

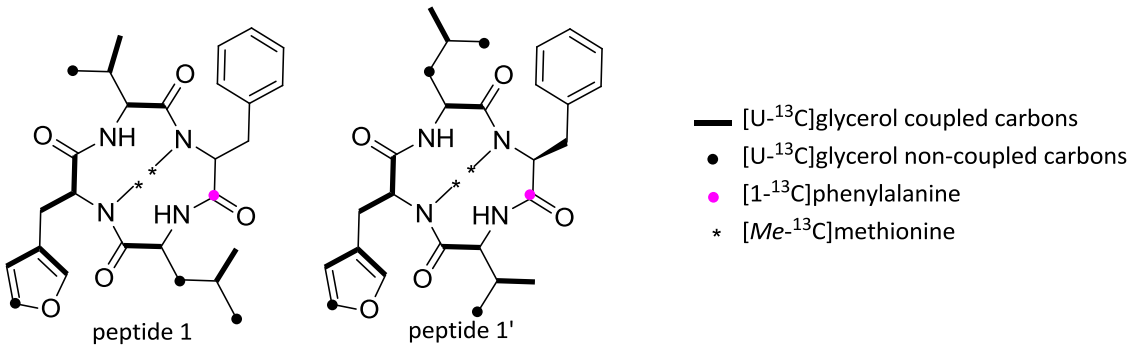

Fig 4-18. Biosynthetic origin of the carbons in peptide 1 and 1'. ^{13}C labeling patterns from the incorporation of [U-^{13}C]glycerol, [1-^{13}C]phenylalanine and [*Me*-^{13}C]methionine.

Exogenous supply of phenylalanine, both labeled and unlabeled, resulted in an increase in the amount of isolated peptides showing a phenylalanine residue, attributed to an increased supply of the precursor amino acid. This is normally encountered in precursor-directed biosynthetic studies, a strategy frequently exploited to boost the production of a target metabolite.[116,117] At the same time, this resulted in a decrease in the amounts of isolated peptides featuring a 3-(3-furyl)-alanine, presumably as a result of feedback

inhibition (Fig S36). This indicates the biosynthetic relationship between both phenylalanine and 3-(3-furyl)-alanine. At the same time, failure of incorporation of labeled phenylalanine into 3-(3-furyl)-alanine indicated that phenylalanine is not an intermediate in the biosynthesis of 3-(3-furyl)-alanine as hypothesized earlier, but rather an earlier intermediate in the shikimate pathway must provide the carbon units for the biosynthesis of 3-(3-furyl)-alanine.

Unlike biosynthetic results reported for the reductiomycin, two distinct labeling patterns for the dihydrofuranacrylic acid moiety of reductiomycin were observed after feeding [U-^{13}C]glycerol (Fig 4-19). In our experiments a single labeling pattern was observed for 3-(3-furyl)-alanine after feeding [U-^{13}C]glycerol. Presence of two labeling patterns for the dihydrofuranacrylic acid moiety of reductiomycin was justified by the involvement of a symmetric intermediate, in this case 4-hydroxybenzoic acid, undergoing two plausible ring cleavage reactions leading to the dihydrofuranacrylic acid moiety. This was confirmed with feeding studies using labeled 4-hydroxybenzoic acid.[104] The involvement of 4-hydroxybenzoic acid as a putative intermediate in the biosynthesis of 3-(3-furyl)-alanine was thus not plausible and was ruled out. This is also mirrored in the failure to detect incorporation of a fluoro-substituted-4-hydroxybenzoic acid in peptide 1 and 1’ (Fig S38(D)).

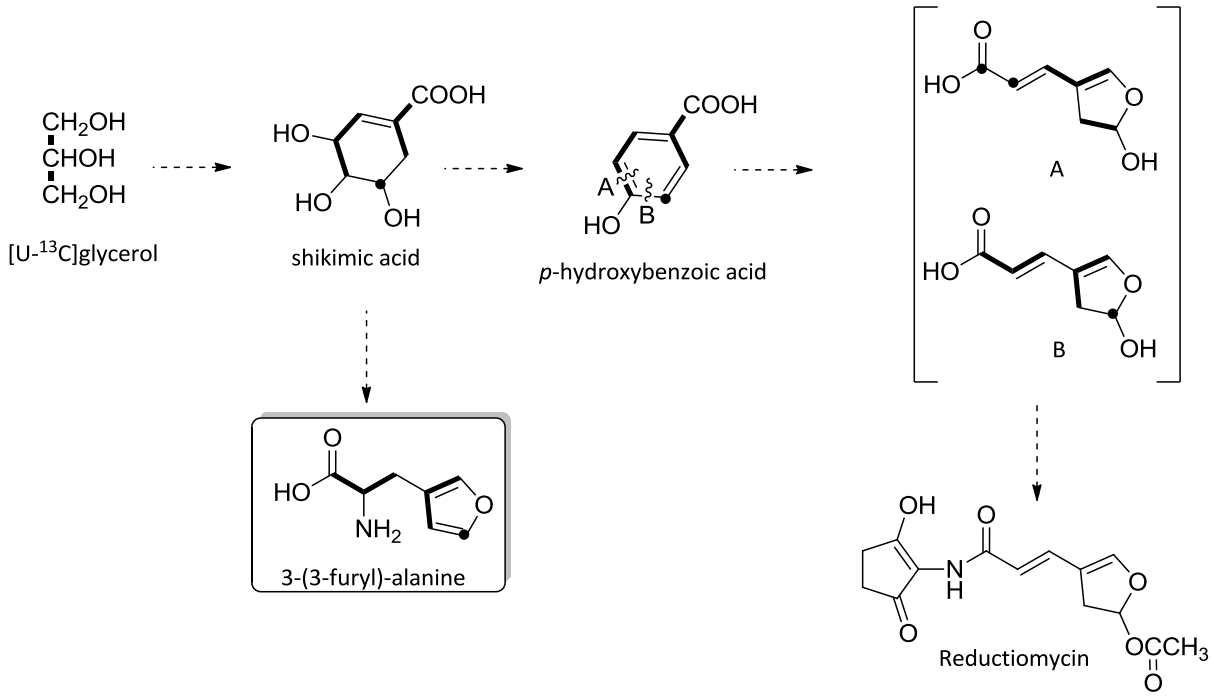

Fig 4-19. Labeling and ^{13}C-^{13}C coupling pattern in the dihydrofuranacrylic acid moiety of reductiomycin derived from [U-^{13}C]glycerol according to literature.[104] Observed labeling pattern for 3-(3-furyl)-alanine after feeding [U-^{13}C]glycerol. Bold lines indicate ^{13}C labeled isotopomers with directly adjacent ^{13}C atoms. Dots indicate ^{13}C enriched atoms.

Biosynthesis of a furan moiety is generally believed to proceed through a mixed acetate-glycerol pathway, through condensation of dihydroxyacetone and a β-ketothioester as seen in methylenomycin furans and (propenyl-3-furanyl)carbonyl α-L-rhamnopyranoside.[118,119,120] This could not be seen as the case here, as fed [U-^{13}C]glycerol was not observed to label C-3/C-4/C-7 of 3-(3-furyl)-alanine, and feeding [1-^{13}C]sodium acetate resulted in high background, non-specific labeling of 3-(3-furyl)-alanine explained by metabolic turnover of [1-^{13}C]sodium acetate during primary metabolism. Accordingly, a mixed acetate-glycerol biosynthetic pathway being involved in the biosynthesis of 3-(3-furyl)-alanine is ruled out (Fig 4-20).

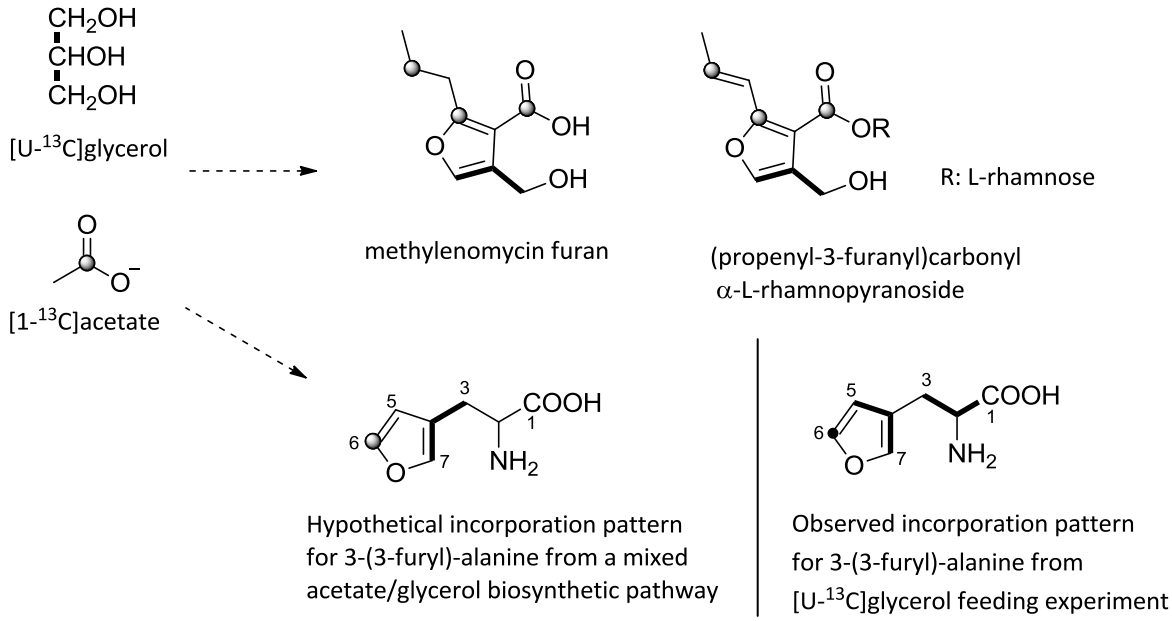

Fig 4-20. Observed incorporation patterns for compounds of mixed acetate-glycerol biosynthesis, i.e methylenomycin furan and acyl α-L-rhamnopyranoside, adopted from literature.[119,120] Hypothetical and observed incorporation patterns for 3-(3-furyl)-alanine with glycerol and sodium acetate as precursors, excluding the involvement of a mixed acetate-glycerol pathway in the biosynthesis. Bold lines indicate ^{13}C-labeled isotopomers with directly adjacent ^{13}C atoms and dots indicate ^{13}C enriched atoms arising from [U-^{13}C]glycerol. Balls indicate ^{13}C labeled positions from [1-^{13}C]sodium acetate.

After feeding [U-^{13}C]glycerol all carbons of 3-(3-furyl)-alanine occurred either as doublet of doublets, i.e. C-1/C-2/C-3 and C-5/C-4/C-7, or as a singlet, i.e. C-6, eliminating the contribution of two-carbon units, recognized as coupled doublets in ^{13}C-NMR, from acetyl-CoA arising from metabolism of glycerol through glycolysis. This was further confirmed through feeding studies with [1-^{13}C]sodium acetate, that ruled out the involvement of the polyketide pathway. Thus, the contribution of the mevalonate pathway, incorporating three acetyl-CoA building blocks, in the biosynthesis of 3-(3-furyl)-alanine is excluded.[97] Moreover, the observed labeling pattern after feeding [1-^{13}C]glucose does not imply the contribution of isopentenyl diphosphate (IPP), neither through the mevalonate (MVA) nor the methylerythritol phosphate pathway (MEP), in the formation of the furan ring of the 3-(3-furyl)-alanine (Fig 4-21).[121]

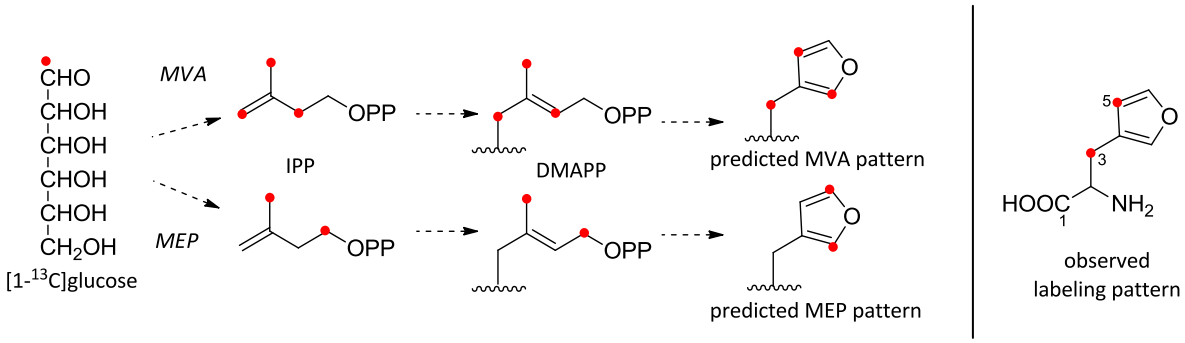

MVA: Mevalonic acid pathway
MEP: Methylerythritol phosphate pathway
IPP: Isopentenyl diphosphate
DMAPP: Dimethylallyl diphosphate

Fig 4-21. Exclusion of the involvement of a terpenoid biosynthetic pathway for 3-(3-furyl)-alanine. Hypothetical formation of a furan moiety using isopentenyl diphosphate (IPP) and dimethylallyl diphosphate (DMAPP) via the mevalonic acid (MVA) and methylerythritol phosphate (MEP) pathways and observed labeling pattern for 3-(3-furyl)-alanine from [1-^{13}C]glucose feeding experiment. Dots indicate ^{13}C enriched positions arising from [1-^{13}C]glucose. Adopted from literature.[121]

Cyclisation of sedoheptulose-7-phosphate, an intermediate of the pentose phosphate pathway, is not considered relevant to the biosynthesis of the carbon skeleton of 3-(3-furyl)-alanine. A sedoheptulose biosynthetic pathway, involved in the biosynthesis of the C_7N moiety of the carba sugar acarbose and the antibiotic validamycin, gives a unique C_2-C_2-C_3 labeling pattern, as opposed to the C_3-C_4, i.e. phosphoenolpyruvate-erythrose-4-phosphate, pattern for a shikimate pathway (Fig 4-22).[122]

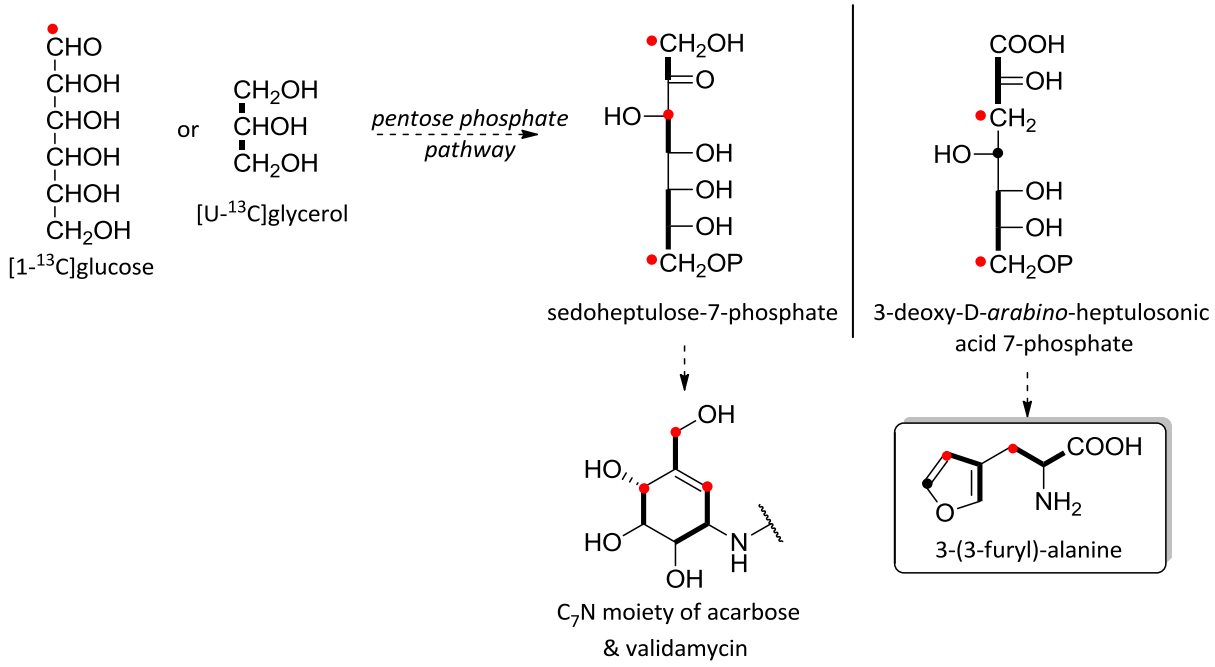

Fig 4-22. Biosynthetic origin of the C_7N unit of acarbose and validamycin A from sedoheptulose-7-phosphate based on incorporation patterns after feeding [1-^{13}C]glucose and [U-^{13}C]glycerol.[122] Observed labeling pattern for 3-(3-furyl)-alanine from [1-^{13}C]glucose and [U-^{13}C]glycerol feeding experiments excluding the involvement of sedoheptulose-7-phosphate in the biosynthesis. Bold lines indicate ^{13}C labeled isotopomers with directly adjacent ^{13}C atoms and black dots indicate ^{13}C enriched atoms arising from [U-^{13}C]glycerol. Red dots indicate ^{13}C enriched atoms arising from [1-^{13}C]glucose.

Polyketides

Due to the small culture size of 1.5 L biomalt salt agar medium, and the low amounts of polyketides, i.e. 0.26 – 0.5 mg L^{-1}, produced by the *Stachylidium* sp., as previously noted from the preliminary experiments, it was infeasible to isolate the whole array of marilones and marilines previously reported.[83,84] Nevertheless, we succeeded in isolating labeled marilone A and mariline B, a representative of each compound class, i.e. phthalide and phthalimidine, respectively. Both showed very similar enriched ^{13}C-NMR spectra, indicating their analogous biosynthetic origin. For the basic nucleus of marilone A and mariline B, four intact acetate units were incorporated, joined in a head-to-tail fashion, to form a tetraketide chain that undergoes subsequent cyclisation to form the aromatic ring, as encountered in other phthalide metabolites, i.e. mycophenolic acid,[98] nidulol and silvaticol.[99] The folding of the tetraketide chain probably follows the mode F,

which is typical for fungal producers of fused-ring aromatic structures.[123] The labeling pattern observed for the geranyl side chain, evidenced its origin through the mevalonate pathway as seen in mycophenolic acid.[98] It is known that fungi and animals exclusively use the mevalonate pathway for the synthesis of their terpenoid units.[124] Marilone A and mariline B are thus considered to be of mixed biosynthetic origin, featuring both a polyketide and terpenoid part. For the starter unit involved in the biosynthesis, accounting for the unusual methyl substituent at C-8, this could not be unequivocally deduced from the feeding study with [1-^{13}C]sodium acetate. Yet, the efficient incorporation of an acetate unit at C-7 as seen for both marilone A and mariline B, favors a methylated acetate starter unit over a propionate unit. If enrichment of C-7 was due to metabolic turnover of [1-^{13}C]acetate to [1-^{13}C]propionate (Fig 4-23), we would have expected a less intense signal for C-7 as compared to other carbons, i.e. C-1, C-3 and C-5, of the basic carbon skeleton. Definite proof for this speculation could only be confirmed by further feeding studies employing labeled precursors, such as propionate or methionine, or through genetic investigations.

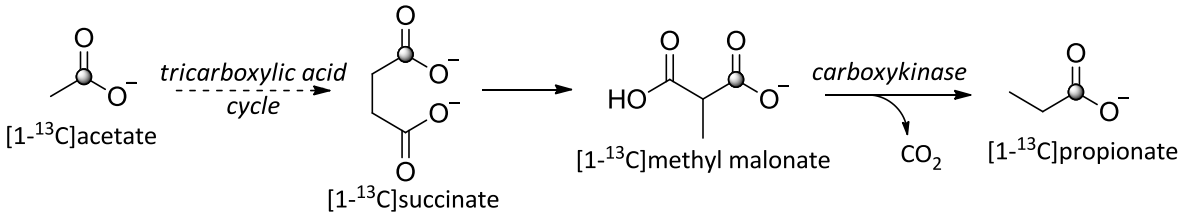

Fig 4-23. Metabolism of [1-^{13}C]acetate into [1-^{13}C]propionate.[125]

4.4 Biological activity of peptide 1 and 1' on galanin receptors (GalR)

Peptide 1 and 1' (Fig 4-4) displayed selective *in-vitro* agonist activity to galanin receptor subtype 1 (GalR1), in a pilot label-free dynamic mass redistribution (DMR) assay, using recombinant human embryonic kidney (HEK) cells stably expressing GalR1 (see 3.6.2 for experimental details).[88,89] When applied in a micromolar range (10-100 µM), peptide 1 and 1' showed a concentration-dependant increase of DMR recordings as compared to native HEK cells, lacking GalR1 receptors. Preincubation of the cells with pertussis toxin (PTX), a specific inhibitor of the GalR1-coupled G protein α_i subunit, followed by addition of a mixture of peptide 1 and 1', resulted in a reduction of the DMR recordings nearly to the niveau of native HEK cells (Fig 4-24). These results clearly reveal the association of an increased DMR with an activation of the GalR1 by peptide 1 and 1', and are in accordance with the *in-vivo* anti-convulsive activity data of endolide A (Fig 4-2), a cyclic tetrapeptide formerly isolated from the same fungal strain.[96]

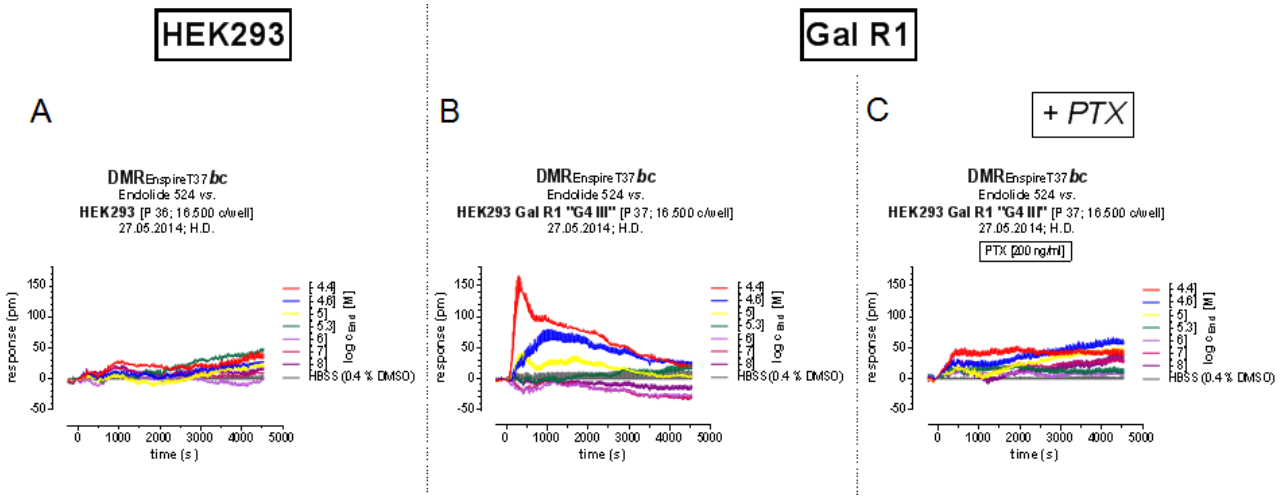

Fig 4-24. DMR-profiles of non-recombinant (A) and GalR1 stably expressing (B,C) HEK293 cells. Stimulation of the cells with different concentrations of peptide 1 and 1' results in a concentration-dependent increase in wavelength shift for the recombinant cell line (B), which is absent in native HEK cells (A). Pre-incubation of the recombinant cells with pertussis toxin (PTX, 200 ng ml^{-1}) causes a significant blunting of the DMR signals (C) in comparison to PTX-untreated cells (B), resembling the DMR profile of the control cells lacking the receptor (A). Assays were performed by Dr. Harald Dargatz, WG Kostenis, Institute for Pharmaceutical Biology, University of Bonn.

5. General Discussion

5.1 Chemical diversity of *Stachylidium* sp. secondary metabolites

Although the *Stachylidium* sp. strain has been chemically investigated before in our group, new metabolites could be still isolated during the current study. This delineates the impressive biosynthetic capabilities of this fungal strain as illustrated in the plethora of secondary metabolite classes reported so far. Compound classes isolated range from polyketides,[83,84] to *O*-prenylated tyrosine-derived compounds,[85] to furyl derivatives,[126] and of special interest the novel peptides characterized in the current study. These peptides are constructed from a varying combination of four basic building blocks, two branched chain amino acids, i.e. L-valine, L-leucine, and two aromatic amino acids, i.e. L-phenylalanine and L-3-(3-furyl)-alanine. Structural similarities between the isolated peptides are quite remarkable. They only exhibit slight differences in terms of the constituent amino acids. The individual peptides differ also in terms of N-methyl substituents and amino acid sequence. Their very closely related structures made their isolation and subsequent characterization most challenging. The novel peptides and diketopiperazines isolated in this study (Fig 4-3) further expand the range of compound classes metabolically produced by the here targeted *Stachylidium* sp. strain. Two previously reported thiodiketopiperazines (Fig 4-5), i.e. bisdethiobis(methylthio)-acetylaranotin (BDA) and bisdethiobis(methylthio)-acetylapoaranotin (BDAA),[102,155] were also isolated from a phenylalanine supplemented liquid biomalt culture medium.

5.2 Novel cyclic peptides and the putative non-ribosomal peptide assembly line

The novel isolated peptides are proposed to be synthesized by the non-ribosomal peptide biosynthetic machinery (NRPS). This is supported by the structural architecture of the peptides, incorporating unusual amino acid motifs with additional N-methylation and cyclization. These features are all privileged attributes frequently encountered in non-ribosomal peptides. Contradictory to the wide array of produced cyclic peptides in the *Stachylidium* sp., a single NRPS is believed to be involved in the biosynthesis of these structures. This was previously observed for structurally related peptides from fungal species, e.g. 25 naturally occuring cyclosporins[97] and as much as 29 isolated enniatins.[34] This is credited to the flexibility of NRPS systems being able to incorporate varying

building blocks. Rationalized by the microheterogenicity of the involved adenylation domains accepting different building blocks, e.g. surfactin synthetase adenylation domain is capable of activating L-leucine, L-valine and L-isoleucine.[127] Promiscuity of fungal NRPS to alternative amino acid residues is generally encountered, and has been exploited with the aim to obtain new analogues of naturally produced peptides luckily with better activity and/or selectivity.[128,129,130] At the same time this could provide additional information for biosynthetic studies.[110] Feeding experiments using other amino acids, such as alanine, glycine, proline, tryptophan and serine, did not result in the production of newer analogues. Therefore, it is believed that enzymes involved in the biosynthesis of those peptides are specific for their amino acid residues, i.e. valine, leucine, phenylalanine and 3-(3-furyl)-alanine. Here the *Stachylidium* sp. NRPS machinery generated a natural combinatorial/chemical library of cyclopeptides. Using only a small number of basic building blocks and applying the LEGO principle a wide array of metabolites were formed.[131] Shuffling of those four amino acids in four different positions, we could imagine a total of 256 different peptides to be produced, of which only a small fraction had been isolated in this study. In fact some of the peptides were predominately produced over other peptides, pointing towards the preferred activation of certain amino acids by the adenylation domains.

5.3 Biosynthetic considerations

5.3.1 General considerations of feeding protocols

The contribution of classical isotope tracer experiments in the study of mechanisms involved in the assembly of secondary metabolites cannot be underestimated.[105,106,110] In spite of the growing trend to apply molecular genetic techniques for biosynthetic studies on secondary metabolites, classical isotope tracer experiments are still regarded as an indispensable tool in exploring the biogenesis of secondary metabolites basic framework and revealing convergent pathways in different species.[123,132,133] Information gained from the incorporation of isotopically labeled precursors could provide the starting point for further biosynthetic studies and frequently both approaches are applied synchronously.[112,108,134,135,136]

Regardless of the general hurdles encountered in biosynthetic feeding studies in marine organisms, as outlined earlier (see 4.3.1), and the non-reproducibility of biosynthetic experiments with different precursors, we established here a successful feeding protocol for the precursors of interest on solid biomalt salt media. Biosynthetic feeding approaches should generally be customized with regard to the nature of the microorganism, the prospective metabolite of interest and the fed precursor. The here implemented feeding protocol was carefully planned according to the valuable input collected from the preliminary experiments. We were confined to the use of solid media, not regarded as the medium of choice for biosynthetic feeding studies, since only there the metabolites of interest are efficiently produced. Few biosynthetic feeding studies use solid media,[137,138,139,140,141] compared to the use of liquid shake media.[98,99,104,112,115,118,136] The amount of precursor fed depends on its nature and the target metabolite incorporating it. A general carbon source precursor such as glucose or glycerol has to be added in higher quantities compared to a more specific precursor such as phenylalanine, shikimic acid or methionine. This is largely due to the universality of the former, being involved in several biosynthetic pathways. At the same time this of course helps in defining the involved biosynthetic pathway, from the resulting ^{13}C-labeled positions in the target metabolite. High costs of labeled precursors also dictated the volume of culture media used, limited to 0.5 to 1.5 liter media, which made isolation of the target metabolites most challenging. A multiple feeding protocol as applied in this study ensured a steady supply of precursors during metabolite biosynthesis, but care had to be taken in maintaining aseptic conditions throughout the cultivation period. The long cultivation period of 30 and 60 days, due to the slow-growing nature of the *Stachylidium* sp. strain, meant unavoidable lengthy waiting periods.

In the end, it was possible to isolate the compounds of interest in ^{13}C-labeled form, whose detailed analysis using NMR and mass spectrometric techniques unveiled the biosynthetic origin of those target metabolites, i.e. the peptides and polyketides (see 4.3).

5.3.2 Biosynthesis of the cyclic peptides: The shikimate pathway as a source of secondary metabolites

Our results confirm the origin of the amino acid building blocks of the cyclic peptides from the *Stachylidium* sp.. Information gained from this study, concluded the involvement of the shikimate pathway in the biosynthesis of the non-proteinogenic amino acid N-methyl-3-(3-furyl)-alanine, not frequently encountered in nature, and whose biosynthetic origin was never revealed before. The opening line in the shikimate pathway involves the condensation of phosphoenolpyruvate, from glycolysis, and erythrose-4-phosphate, from the pentose phosphate pathway, to give 3-deoxy-D-*arabino*-heptulosonate-7-phosphate (DAHP), catalysed by DAHP synthase. Elimination of phosphoric acid followed by an intramolecular aldol reaction gives the first carbocycle intermediate 3-dehydroquinic acid, which further undergoes dehydration and reduction to give shikimic acid, the first significant intermediate from which the shikimate pathway got its name. This is then followed by several metabolic steps that end with the synthesis of another key intermediate, chorismic acid, which has incorporated an additional phosphoenolpyruvate. Chorismic acid then serves as the starting point for the synthesis of the aromatic amino acids (AAA), i.e. phenylalanine, tyrosine and tryptophan.[97]

The shikimate pathway is one of the important biosynthetic pathways in microorganisms and plants, extensively studied to reveal the pathway reactions and involved enzymology.[142,143] In addition to its significance in the biosynthesis of the aromatic amino acids, as part of the primary metabolism, it is involved in the biosynthesis of a variety of secondary metabolites. It is generally accepted that secondary metabolites are not biosynthesized *de novo* and are dependent on the input of primary metabolism to provide the biosynthetic machinery with building blocks. These primary metabolites are thus modified in secondary metabolism. This way microorganisms and plants produce a wide variety of specialized compounds essential for their inherent needs, exemplified in the mycotoxins, pigments and antibiotics.[144] Some of these secondary metabolites are being directly derived from modification of the final end products of the shikimate pathway, e.g. ephedra alkaloids originally isolated from *Ephedra* sp. have their biosynthetic origin from phenylalanine[145] and ergot alkaloids whose basic ergoline skeleton is derived from tryptophan (Fig 5-1).[58] Others are derived from branching points

alongside the shikimate biosynthetic route, e.g. the antibiotic chloramphenicol (Fig 5-1), originally isolated from the bacterium *Streptomyces venezuelae*, originates in the shikimate pathway via 4-amino-4-deoxy-chorismic acid,[146] and the aromatic *m*-C_7N unit of the mitomycin and ansamycin antibiotics, e.g. rifamycin, is derived from the starter unit 3-amino-5-hydroxybenzoic acid (AHBA) originating from the shikimate pathway (Fig 5-2).[147] These shikimate derived secondary metabolites are already important active pharmaceutical ingredients (APIs) used as drugs nowadays. Shikimic acid itself is used as the starting material for the industrial synthesis of oseltamivir (Tamiflu®), an antiviral drug used against influenza (Fig 5-3).[97]

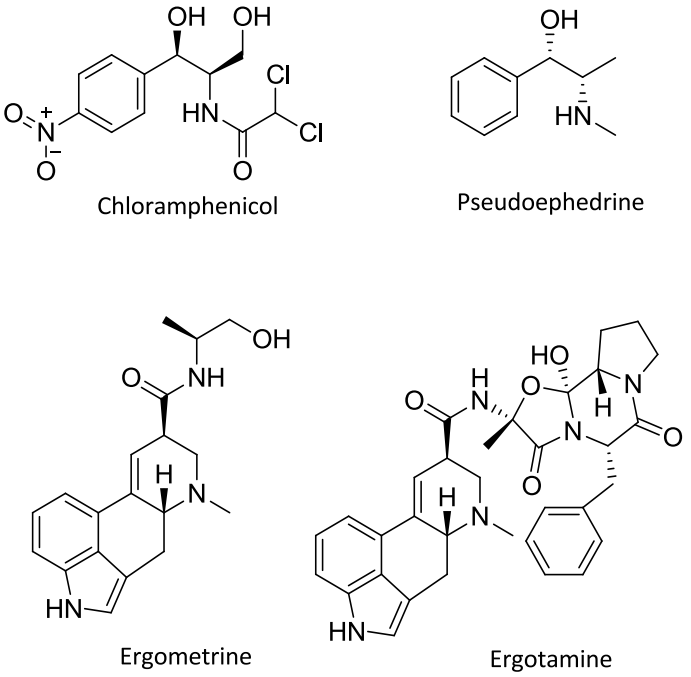

Fig 5-1. Secondary metabolites of shikimate origin.

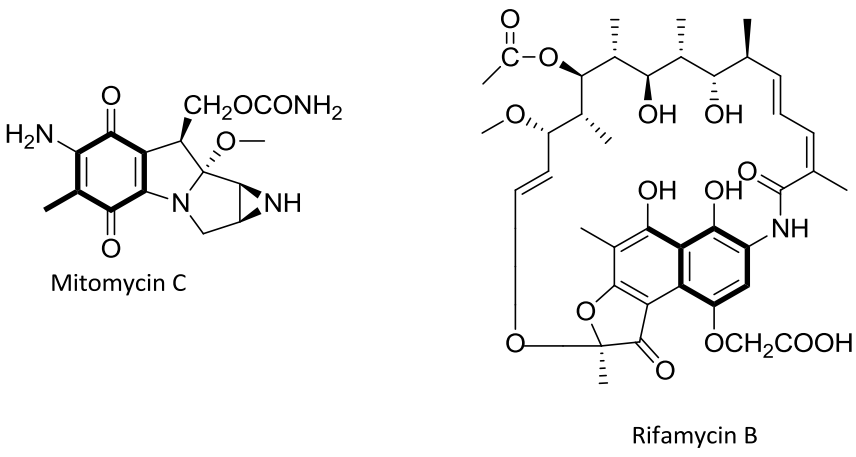

Fig 5-2. Structures of *m*-C_7N unit containing natural antibiotics derived from the shikimate pathway.

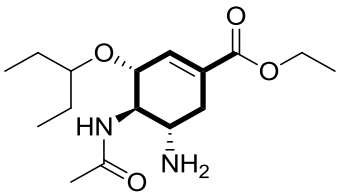

Oseltamivir (Tamiflu®)

Fig 5-3. Synthetic drug derived from shikimic acid.

Additionally, the shikimate pathway accounts for the unique chemistry realized in several non-aromatic metabolites such as the fused bicyclic β-lactone in vibralactone isolated from the basidomycete fungus *Boreostereum vibrans*,[108] the tricyclic acetal-lactone structure of echinosporin isolated from *Streptomyces erythraceus*,[115] or the dihydrofuranacrylic acid moiety of reductiomycin (Fig 5-4).[104] It thus comes as no surprise that the shikimate pathway is responsible for the biosynthesis of the unprecedented heterocyclic aromatic amino acid 3-(3-furyl)-alanine.

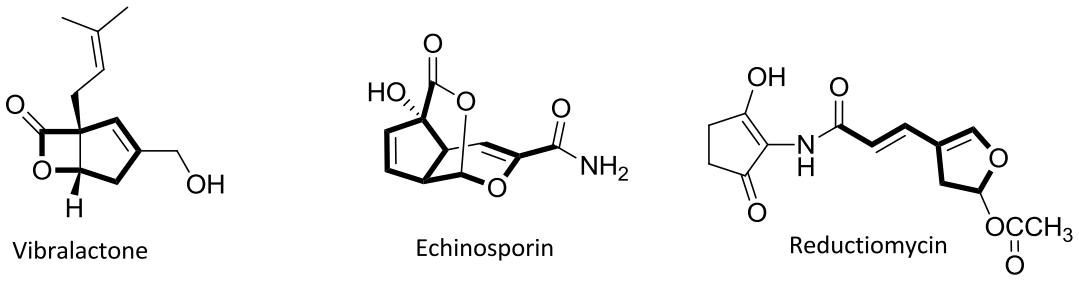

Vibralactone Echinosporin Reductiomycin

Fig 5-4. Secondary metabolites with unique chemistry derived from the microbial shikimate pathway.

5.3.3 Phthalides and phthalimidines biosynthesis

A second focus of this study yielded fruitful insights concerning the biosynthesis of the polyketide metabolites of the *Stachylidium* sp.. The educated guess that the phthalide and phthalimidine basic skeletons are biosynthetically related was confirmed based on the similar incorporation patterns observed after feeding [1-^{13}C]sodium acetate. We could not yet fully ascertain the starter unit accountable for the unique methyl substituent at C-8 (Fig 4-5). Nevertheless, our results propose a methylated acetate starter unit. Yet we cannot exclude that both starter units, i.e. methylated acetate or alternatively propionate, could be involved as seen in the biosynthesis of the mycotoxin

aurovertin B.[148] The phthalide and phthalimidine aromatic nucleus is proposed to be biosynthesized from a tetraketide chain with a 3-methyl orsellinic acid derivative as an intermediate. Biosynthetic modifications of derivatives of the archetypical tetraketide orsellinic acid are seen in the production of several known fungal metabolites. These include the toluquinonoid nucleus of fumigatin and spinulosin, the 7-membered aromatic tropolone ring in puberulic and stipitatic acid, and the phthalide skeleton of gladiolic acid and mycophenolic acid (Fig 5-5).[10]

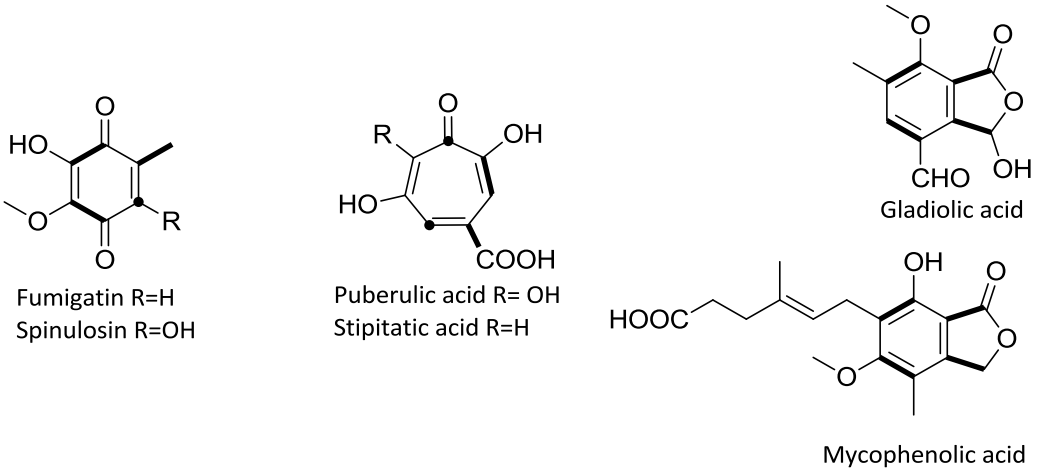

Fig 5-5. Fungal tetraketide metabolites. Bold lines indicate intact acetate units incorporated. Dots indicate enriched carbons after cleavage or rearrangement of acetate units.

5.4 Pharmacological relevance of isolated peptides

One of the major goals of natural product research, including this study, is the characterization of secondary metabolites that could be used as drug leads. The interest in peptide drug scaffolds is currently on the rise, and peptides inherent characteristics nominates them as interaction partners for biological targets, e.g. pasireotide (Signifor®) a somatostatin receptor agonist indicated for Cushing's disease, carfilzomib (Kyprolis®) a chymotrypsin-like protease inhibitor for treatment of multiple myeloma, linaclotide (Constella®) a guanylate cyclase receptor agonist indicated for chronic idiopathic constipation and irritable bowel syndrome (IBS) and monomethyl auristatin E (vedotin) a neoplastic agent linked to a monoclonal antibody, are to name just a few peptide-based drugs approved in the last 5 years (Fig 5-6).[2,149]

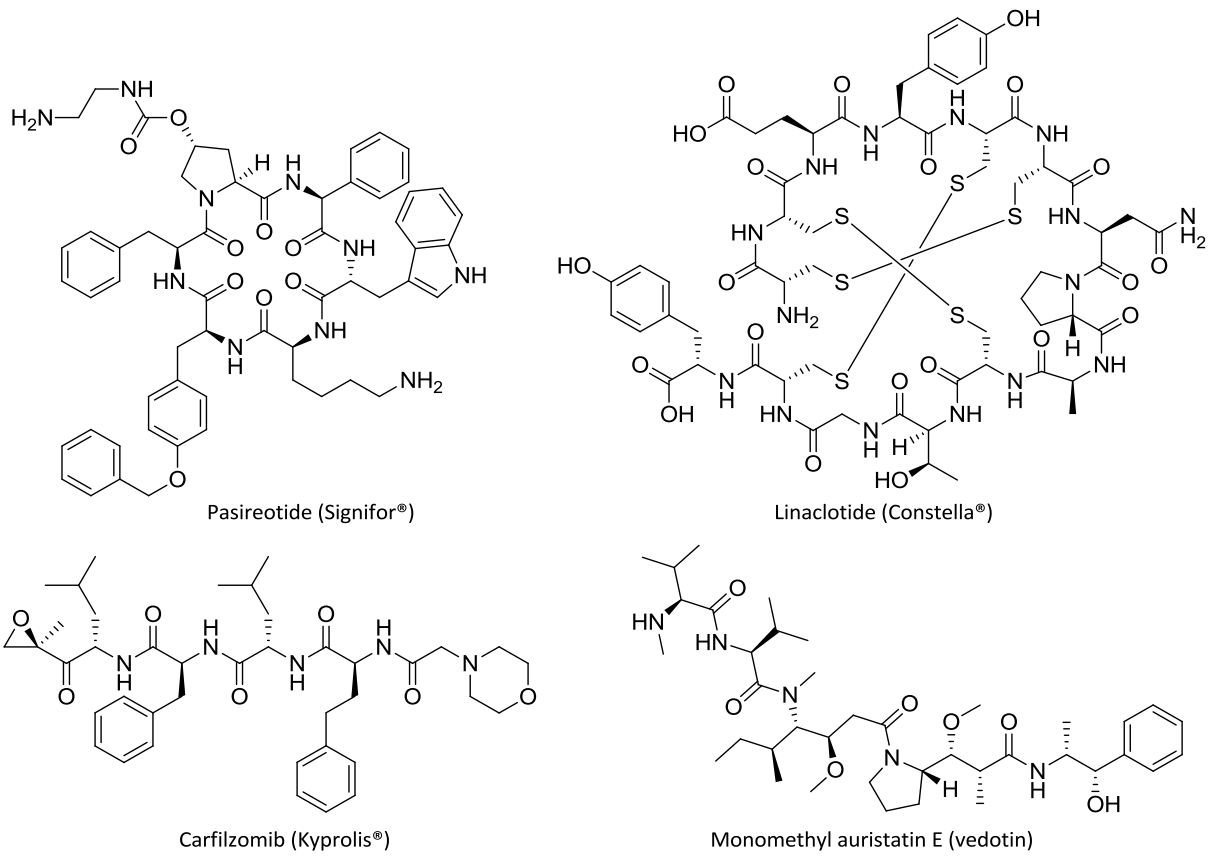

Fig 5-6. Peptide-based drugs approved in the last 5 years.

The small amounts of novel peptides isolated in this study impeded the possibility of performing comprehensive bioactivity studies for the full spectrum of peptides. The promising results obtained for peptide 1 and 1' on the galanin receptor subtype-1 (GalR1) stimulate further studies using the full array of isolated peptides. Galanin receptors are members of the G protein-coupled receptors (GPCR), a large group of peptide drug targets with around 39% of peptides in clinical trials targeting GPCRs.[2] Up to now three galanin receptor subtypes have been recognized, i.e. GalR1 - 3, differentially expressed throughout the peripheral and central nervous systems, as well as the endocrine system.[150] The ubiquitous distribution and association of the galanin receptor subtypes in various physiological and pathological states makes them interesting drug targets, being addressed by either agonists or antagonists.[151] GalR1 and GalR2 seem to play a role in seizures, with GalR1 being responsible for seizure induction and GalR2 in maintaining and controlling the strength of the seizure. GalR3 showed a more limited distribution with less defined roles.[152] Observing that galanin, an endogenous 29/30 amino acid neuropeptide,

was extensively up-regulated during epileptic seizures as well as in Alzehimer's disease, proposed targeting the galanin system for the treatment of neuronal damage. Galanin analogues have been synthesized to overcome the poor pharmacokinetic properties, i.e. poor bioavailability and poor blood brain barrier penetration of endogenous galanin. They include chimeric peptidic ligands such as M15 and M35 (Table 5-1), and other ligands, like galnon and galmic acid (Fig 5-7), acting as either agonists or antagonists to one or more of the galanin receptor subtypes.[152]

Table 5-1. Amino acid sequence of human galanin and peptide ligands, i.e. M15 and M35 (adopted from literature).[150]

	Sequence
Human galanin	GWTLNSAGYLLGPHAVGNHRSFSDKNGLTS
M15 (antagonist)	GWTLNSAGYLLGPQQFFGLM-amide
M35 (antagonist)	GWTLNSAGYLLGPPPGFSPFR-amide

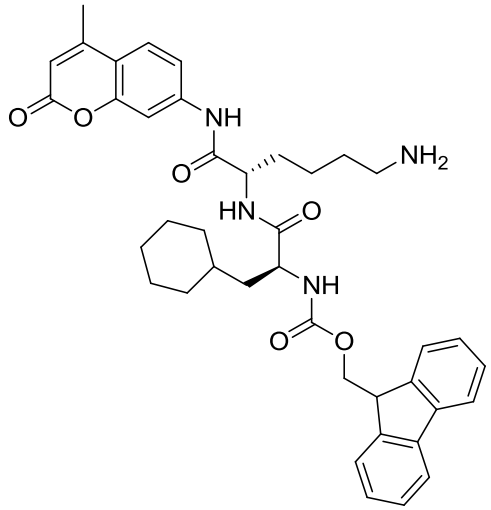

galnon (GalR1-3 agonist)

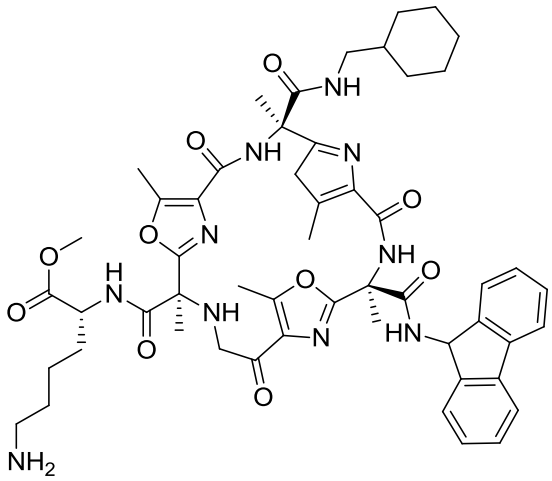

galmic acid (GalR1 agonist)

Fig 5-7. Galanin receptor ligands.

Despite the number of available galanin receptor ligands,[150] the demand for receptor sub-type selective ligands is on-going, whether as possible therapeutics or as a tool for gaining a deeper understanding of the galanin receptor system. The current study shows that the marine environment, in particular the scantly explored marine fungus *Stachylidium* sp.,

could be a source for such ligands on galanin receptors (Fig 4-24). And the natural combinatorial/chemical library of microheterogeneous peptides isolated so far could be employed for further biological testing to obtain more selective and potent ligands to the galanin receptors and subsequently the identification of the chemically simplest scaffold that maintains the desired biological activity. At the same time, a deeper understanding of structure activity relationships has to be sought.

5.5 Future directions and concluding remarks

The current study highlighted the biosynthetic potential of this fungal strain, although focusing on a single culture medium, i.e. biomalt salt agar medium. The use of other solid and liquid culture media, i.e. the OSMAC approach (One Strain Many Compounds), could probably lead to the production of more metabolites with intriguing structural features and promising biological activity.[153]

The inclusion of fluoro-containing amino acids, i.e. 2-fluoro-phenylalanine and 3-fluoro-phenylalanine (see 4.3.2.5), into the peptide architecture opens up possibilities for the production of a variety of peptide analogues. These could expand the peptide assortment used for biological testing. Halogenated natural product derivatives, particularly fluorinated ones, are of special interest. Several drugs available on the market contain a fluorine substitution, the earliest being fluorouracil, an antineoplastic drug, as well as the antidepressant drug fluoxetine, and the macrolide antibiotic fluorithromycin.[154] A fluorine substitution generally improves the pharmacological properties of a compound, in terms of improved metabolic stability, bioavailability and receptor binding.[111] It is thus anticipated that the new fluorinated peptide analogues would show superior biological activity. Moreover, further precursors should be tested. Additionally, the accumulation of peptides incorporating phenylalanine after supplementing the cultivation medium with this amino acid as observed in our feeding studies is a practical strategy that could be employed to stimulate the production of metabolites of interest.[116,117] After feeding the relevant precursors, the metabolites of interest could be isolated in bigger amounts, and then be used for exhaustive biological testing.

It could not be ascertained whether the isolated epipolythiodioxopiperazines, i.e. BDA and BDAA, from a liquid biomalt salt culture medium supplemented with phenylalanine,

are normally produced by the fungus but went unnoticed from our initial isolation or are strictly produced after addition of phenylalanine, a known precursor of this class of compounds.[103] It could still be concluded that the required gene for biosynthesis exists in the fungus and addition of the precursor probably provoked the fungal biosynthetic machinery to produce them. This speculation requires further studies and the prospect of obtaining other compounds belonging to this class is plausible. BDA and BDAA did not exhibit any biological activity when tested for antimicrobial activity in agar-diffusion assays (see 4.3.1). This coincides with previous studies that reported their minimal biological activity,[155] apart from a growth inhibitory activity towards *Mycobacterium tuberculosis,*[156] when compared to their disulfide bridge containing counterparts, i.e. acetylaranotin and acetylapoaranotin. The disulfide bridge is thus hypothesized to mediate biological activity and molecular toxicity of fungal epipolythiodioxopiperazines.[103]

Our continuous trials to purify peptides featuring positional isomers, i.e peptide 1 and 1', peptide 5 and 5', peptide 6 and 6', peptide 7 and 7', where unavailing. This necessitates the ongoing development in HPLC stationary phase properties and modified mobile phase systems for the selective separation of peptides, a compound class gaining increasing attention lately.[157,158]

Overall, the *Stachylidium* sp. is believed to be a talented fungal strain, whose biosynthetic capabilities have not yet been given its full due. This study is a sequel to the ongoing efforts undertaken to unravel its biosynthetic potential, with special emphasis on the biogenesis of the novel isolated peptides and polyketides. With regards to the isolated peptides, still there is an information gap on the underlying biosynthetic mechanisms involved in converting the shikimate intermediate into the 3-(3-furyl)-alanine. Further study of this process is merited as it should contribute to the full elucidation of this rare amino acid biosynthesis in *Stachylidium* sp. and probably in other microorganisms incorporating the same amino acid.[68,74]

Much progress has been made to study fungal genomes.[159] A single fungal genome encoding several biosynthetic enzymes is capable of providing us with a plethora of secondary metabolite classes. Several web-based software tools, such as SMURF

customized for fungal genomes, have been built for easy mapping of fungal genome clusters.[160] With the help of genomic approaches, exploring the *Stachylidium* sp. secondary metabolome will reveal details of the assembly of the amino acid building blocks in the peptides and the starter unit involved in the polyketide metabolites. Furthermore, genetic manipulation of these assembly lines could maximize the chemical diversity of the produced metabolites.[116]

It is hoped that the results presented here will elicit further studies in exploring this unique fungal strain more extensively, on both the chemical and genetic level.

6. Summary

The fungal kingdom has made considerable contributions to the production of peptide secondary metabolites, many of them with therapeutic potential, e.g. the immunosuppressant cyclosporine and the antifungal echinocandins.

The detailed investigation of the marine-derived fungus *Stachylidium* sp. was the main purpose of this research, which focused on the isolation, structural elucidation and biosynthesis of novel cyclic peptides. From a fungal culture on biomalt agar medium supplemented with sea salt, we succeeded in isolating and characterizing a family of novel structurally related peptides (Fig 6-1). Structural elucidation of the isolated peptides was achieved using 1D and 2D NMR spectroscopic analysis along with high-resolution mass spectrometry. The absolute configuration of the amino acid building blocks was assigned as L-configuration using advanced Marfey's method and X-ray crystallography. The four amino acids, i.e. L-valine, L-leucine, L-phenylalanine and L-3-(3-furyl)-alanine form the basis of the isolated peptides. Structural similarities between the isolated peptides are quite remarkable. They only exhibit slight differences in terms of the constituent amino acids. The individual peptides differ also in terms of N-methyl substituents and amino acid sequence. Their very closely related structures made their isolation and subsequent characterization most challenging.

The cyclic nature and N-methylation of the isolated peptides, as shared with other fungal peptides, implied their inherent potential as interesting drug scaffolds. The positional isomers peptide 1 and 1' were tested on galanin receptors, in a concentration range 10-100 µM, and displayed a concentration-dependant selective agonist activity towards the galanin 1 receptor subtype (GalR1). This nominates them as potential ligands for therapeutic applications or as a tool for studying the galanin receptor system.

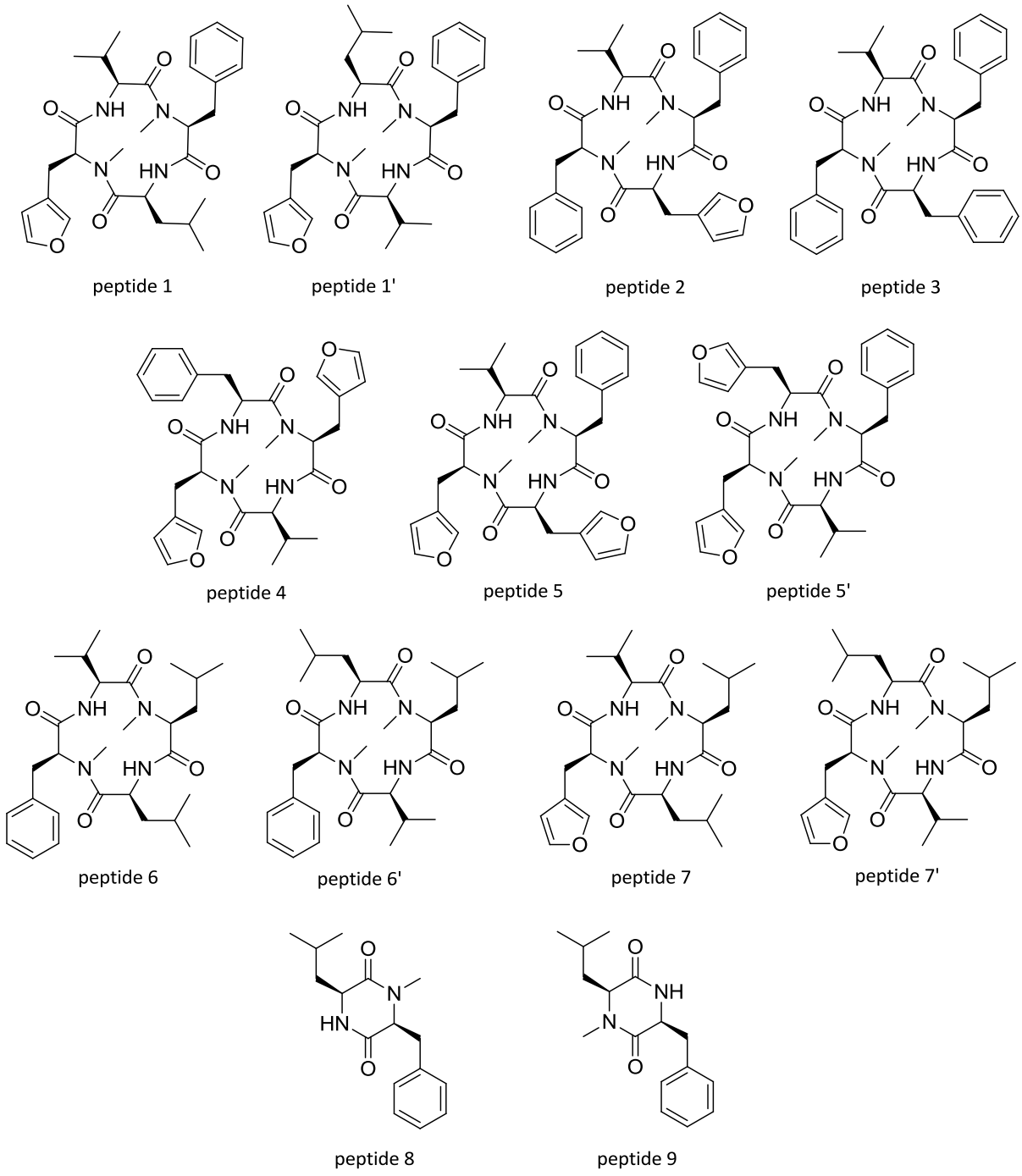

Fig 6-1. Structures of the isolated cyclic peptides.

A most intriguing feature of some of the isolated peptides was the incorporation of the rarely encountered amino acid 3-(3-furyl)-alanine, to date only reported in the heptapeptides rhizonin A and B and the pentapeptide bingchamide B. Due to the novel nature of this building block, the current study set out to study its metabolic origin. Biosynthetic studies employing classical isotope tracer experiments revealed the

shikimate origin of this rare amino acid, along with confirming the metabolic origin of the other proteinogenic amino acids, with the N-methyl group being derived from methionine (Fig 6-2, Fig 6-3).

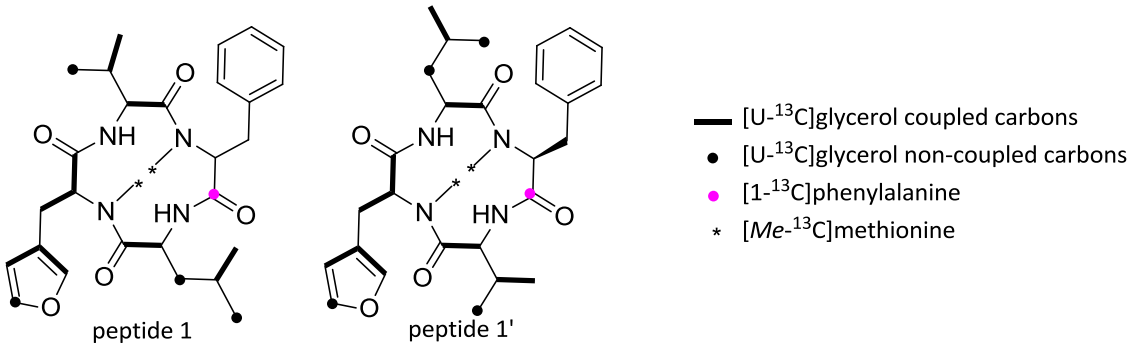

Fig 6-2. Origin of the carbon atoms of peptide 1 and 1' as implied from results of feeding experiments.

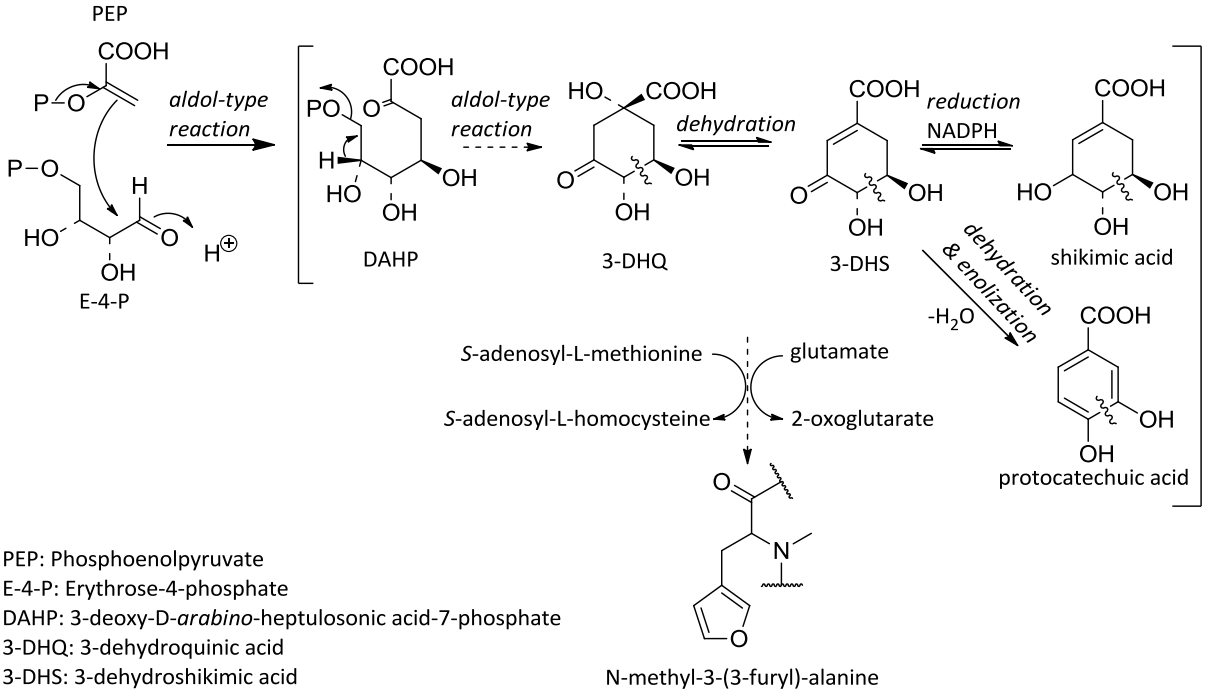

Fig 6-3. Postulated biosynthesis of N-methyl-3-(3-furyl)alanine as proposed from the analysis of peptide 1 and 1' after classical isotope experiments using labeled precursors including [1-^{13}C]phenylalanine, [U-^{13}C]glycerol, [1-^{13}C]glucose and [*Me*-^{13}C]methionine.

Concerning the biosynthesis of the marilone A and mariline B, phthalide and phthalimidine metabolites previously reported from this fungal strain, labeling studies

with [1-^{13}C]sodium acetate were undertaken. Their biosynthesis involves a polyketide and mevalonate mixed pathway (Fig 6-4).

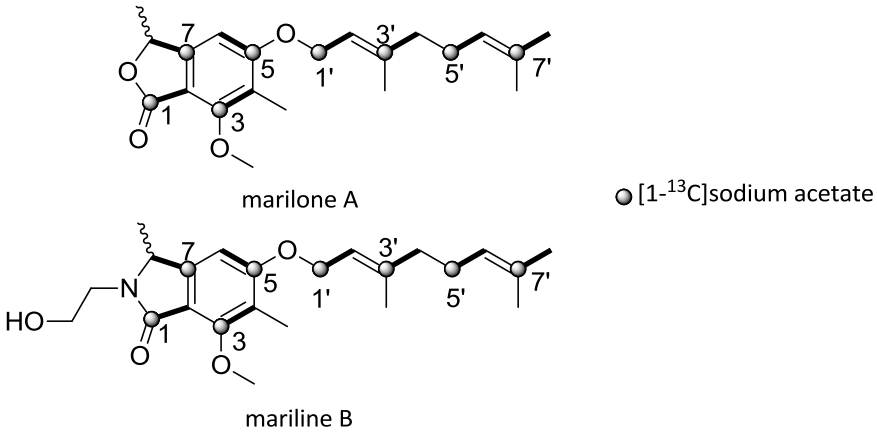

Fig 6-4. Origin of the carbon atoms of marilone A and mariline B as implied from results of the feeding experiment using [1-^{13}C]sodium acetate.

Overall, these results emphasize the outstanding biosynthetic potential of the here investigated *Stachylidium* sp.. It displays exceptional competence in employing various metabolic pathways, through which a diverse array of secondary metabolites are produced. Consequently, the novel isolated metabolites characterized in this study could serve as lead structures for drug discovery. Furthermore, insights gained from the here applied classical isotopic tracer experiments will serve as the basis for future investigations employing genetic and enzymatic approaches. Sequencing of the *Stachylidium* sp. genome and identifying the biosynthetic gene cluster associated with the production of those unique fungal metabolites would lead to a conclusion concerning still unresolved ambiguity.

7. References

(1) Craik D. J., Fairlie D. P., Liras S. and Price D. The future of peptide-based drugs. *Chem Biol Drug Des*, **2013**, *81*, 136–147.

(2) Kaspar A. A. and Reichert J. M. Future directions for peptide therapeutics development. *Drug Discov Today*, **2013**, *17-18*, 807-817.

(3) Sun L. Peptide-based drug development. *Mod Chem Appl,* **2013**, *1*, 1.

(4) Olmez E. O. and Akbulut B. S. Protein-peptide interactions revolutionize drug development, binding protein. PhD. Kotb Abdelmohsen **2012** (Ed.), ISBN: 978-953-51-0758-3, InTech, DOI: 10.5772/48418. Available from: http://www.intechopen.com/books/binding-protein/protein-peptide-interactions-revolutionize-drug-development.

(5) Goodwin D., Simerska P. and Toth I. Peptides as therapeutics with enhanced bioactivity. *Curr Med Chem*, **2012**, *19*, 4451-4461.

(6) Uhlig T., Kyprianou T., Martinelli F. G., Oppici C. A., Heiligers D., Hills D., Calvo X. R., Verhaert P. The emergence of peptides in the pharmaceutical business: From exploration to exploitation. *EuPA open proteomics*, **2014**, *4*, 58-69.

(7) Brakhage A. A. Regulation of fungal secondary metabolism. *Nature Rev Microbiol*, **2013**, *11*, 21-31.

(8) Kück U., Bloemendal S. and Teichert I. Putting fungi to work: Harvesting a cornucopia of drugs, toxins, and antibiotics. *PLOS*, **2014**, *10*, 3.

(9) Cascales L. and Craik D. J. Naturally occurring circular proteins: Distribution, biosynthesis and evolution. *Org Biomol Chem*, **2010**, *8*, 5035-5047.

(10) Hanson J. R. The chemistry of fungi **©2008**, RSC Publishing. PDF eISBN: 978-1-84755-832-9. DOI:10.1039/9781847558329.

(11) Marahiel M. A. Working outside the protein-synthesis rules: Insights into non-ribosomal peptide synthesis. *J Peptide Sci*, **2009**, *15*, 799–807.

(12) Gao X., Haynes S. W., Ames B. D., Wang P., Vien L. P., Walsh C. T. and Tang Y. Cyclization of fungal nonribosomal peptides by a terminal condensation-like domain. *Nat Chem Biol*, **2012**, *8(10)*, 823–830.

(13) Bockus A. T., McEwen C. M. and Lokey R. S. Form and function in cyclic peptide natural products: A pharmacokinetic perspective. *Curr Top Med Chem*, **2013**, *13*, 821-836.

(14) Eisfeld K. Non-ribosomal peptide synthetase of fungi. *Physiology and Genetics, The Mycota,* **2009**, *15*, 305-330.

(15) Passioura T., Katoh T., Goto Y., and Suga H. Selection-based discovery of drug like macrocyclic peptides. *Annu Rev Biochem,* **2014**, *83*, 727–52.

(16) Chatterjee J., Rechenmacher F. and Kessler H. *N*-Methylation of peptides and proteins: An important element for modulating biological functions. *Angew Chem Int Ed*, **2013**, *52*, 254–269.

(17) Gentilucci L., De Marco R. and Cerisoli L. Chemical modifications designed to improve peptide stability: Incorporation of non-natural amino acids, pseudo-peptide bonds, and cyclization. *Curr Pharm Des,* **2010**, *16(28),* 3185-3203.

(18) Rateb M. E. and Ebel R. Secondary metabolites of fungi from marine habitats. *Nat Prod Rep*, **2011**, *28*, 290-344.

(19) Hoffmeister D. and Keller P. N. Natural products of filamentous fungi: Enzymes, genes and their regulation. *Nat Prod Rep,* **2007**, *24*, 393-416.

(20) Kong K. F., Schneper L. and Mathee K. Beta-lactam antibiotics: From antibiosis to resistance and bacteriology. *APMIS*, **2010**, *118(1)*, 1–36.

(21) Laudano J. B. Ceftaroline fosamil: A new broad-spectrum cephalosporin. *J Antimicrob Chemother,* **2011**, *66 Suppl 3*, iii11 –iii18.

(22) Mendes C. and Antunes A. M. Pipeline of known chemical classes of antibiotics. *Antibiotics,* **2013**, *2*, 500-534.

(23) Thell K., Hellinger R., Schabbauer G. and Gruber C. W. Immunosuppressive peptides and their therapeutic applications. *Drug Discov Today*, **2014**, *19(5)*, 645-653.

(24) Novartis Annual Report **2013**. www.novartis.com/annualreport2013.

(25) Hessen M. and Akpek E. K. Dry eye: An inflammatory ocular disease. *J Ophthalmic Vis Res,* **2014**, *9(2),* 240-250.

(26) Schultz C. Voclosporin as a treatment for noninfectious uveitis. *Ophthalmol Eye Dis*, **2013**, *5*, 5-10.

(27) Gallay P. A. and Lin K. Profile of alisporivir and its potential in the treatment of hepatitis C. *Drug Des Devel Ther,* **2013**, *7*, 105-115.

(28) Perlin D. S. Current perspectives on echinocandin class drugs. *Future Microbiol*, **2011**, *6(4),* 441–457.

(29) Cacho R. A., Jiang W., Chooi Y. H., Walsh C. T. and Tang Y. Identification and characterization of the echinocandin B biosynthetic gene cluster from *Emericella rugulosa* NRRL 11440. *J Am Chem Soc,* **2012**, *134*, 16781−16790.

(30) Roemer T. and Krysan D. J. Antifungal drug development: Challenges, unmet clinical needs, and new approaches. *Cold Spring Harb Perspect Med,* **2014**, *4(5)*.

(31) Paiva J. A. and Pereira J. M. New antifungal antibiotics. *Curr Opin Infect Dis,* **2013**, *26*, 168–174.

(32) Brown G. D., Denning D. W. and Levitz S. M. Tackling human fungal infections. *Science*, **2012**, *336(6082),* 647.

(33) Jiménez-Ortigosa C., Paderu P., Motyl M. R., and Perlin D. S. Enfumafungin derivative MK-3118 shows increased in vitro potency against clinical echinocandin-resistant *Candida* species and *Aspergillus* species isolates. *Antimicrob Agents Chemother,* **2014**, *58(2)*, 1248-1251.

(34) Sy-Cordero A. A., Pearce C. J. and Oberlies N. H. Revisiting the enniatins: A review of their isolation, biosynthesis, structure determination, and biological activities. *J Antibiot (Tokyo),* **2012**, *65(11)*, 541–549.

(35) Hornbogen T., Glinski M. and Zocher R. Biosynthesis of depsipeptide mycotoxins in *Fusarium*. *Eur J Plant Pathol*, **2002**, *108*, 713–718.

(36) Wang Q. and Lijian X. Beauvericin, a bioactive compound produced by fungi: A short review. *Molecules,* **2012**, *17*, 2367-2377.

(37) Liu B. L. and Tzeng Y. M. Development and applications of destruxins: A review. *Biotech Adv*, **2012**, *30*, 1242–1254.

(38) German-Fattal M. and Ralph Mösges R. How to improve current therapeutic standards in upper respiratory infections: Value of fusafungine. *Curr Med Res Opin*, **2004**, *20(11)*, 1769-1776.

(39) Huang R. M., Yi X. X., Zhou Y., Su X., Peng Y. and Gao C. H. An update on 2,5-diketopiperazines from marine organisms. *Mar Drugs,* **2014**, *12*, 6213-6235.

(40) Cai S. X. Small molecule vascular disrupting agents: Potential new drugs for cancer treatment. *Recent Pat Anticancer Drug Discov,* **2007**, *2,* 79-101.

(41) Liao S., Qin X., Li D., Tu Z., Li J., Zhou X., Wang J., Yang B., Lin X., Liu J., Yang X. and Liu Y. Design and synthesis of novel soluble 2,5-diketopiperazine derivatives as potential anticancer agents. *Eur J Med Chem,* **2014**, *83*, 236-244.

(42) Kingston D. G. Tubulin-interactive natural products as anticancer agents. *J Nat Prod*, **2009**, *72(3)*, 507–515.

(43) Kanoh K., Kohno S., Katada J., Takahashi J. and Uno I. (-)-Phenylahistin arrests cells in mitosis by inhibiting tubulin polymerization. *J Antibiot (Tokyo)*, **1999**, *52(2)*, 134-141.

(44) Hayashi Y., Yamazaki-Nakamura Y. and Yakushiji F. Medicinal chemistry and chemical biology of diketopiperazine-type antimicrotubule and vascular-disrupting agents. *Chem Pharm Bull,* **2013**, *61(9)*, 889–901.

(45) Gridelli C., Rossi A., Maione P., Rossi E., Castaldo V., Sacco P. C. and Colantuoni G. Vascular disrupting agents: A novel mechanism of action in the battle against non-small cell lung cancer. *Oncologist*, **2009**, *14(6)*, 612-620.

(46) Heist R. S., Aren O. R., Mita A. C., Polikoff J., Bazhenova L., Lloyd G. K., Mikrut W., Reich S. D., Spear M. A. and Huang L. Randomized phase 2 trial of plinabulin (NPI-2358) plus docetaxel in patients with advanced non-small cell lung cancer (NSCLC), *J Clin Oncol*, 2014, *32:5s (suppl; abstr 8054).*

(47) Muguruma K., Kawamata R., Taguchi A., Takayama K., Yakushiji F., Ito Y. and Hayashi Y. Preparation of non-covalent antibody-drug conjugate for tumor targeting of vascular disrupting agent "Plinabulin". *J Pept Sci*, **2013**, *50*, 351-352.

(48) Dolan S. K., O'Keeffe G., Jones G. W., and Doyle S. Resistance is not futile: Gliotoxin biosynthesis, functionality and utility. *Trends Microbiol,* **2015**, *23(7)*, 419-428.

(49) Reece K. M., Richardson E. D., Cook K. M., Campbell T. J., Pisle S. T., Holly A. J., Venzon D. J., Liewehr D. J., Chau C. H., Price D. K. and Figg W. D. Epidithiodiketopiperazines (ETPs) exhibit *in vitro* antiangiogenic and *in vivo* antitumour activity by disrupting the HIF-1α/p300 complex in a preclinical model of prostate cancer. *Mol Cancer,* **2014**, *13*, 91.

(50) Mwakwari S. C., Patil V., Guerrant W. and Oyelere A. K. Macrocyclic histone deacetylase inhibitors. *Curr Top Med Chem,* **2010**, *10(14)*, 1423–1440.

(51) Heerboth S., Lapinska K., Synder N., Leary M., Rollinson S. and Sarkar S. Use of epigenetic drugs in disease: An overview. *Genet Epigenet*, **2014**, *6*, 9–19.

(52) Furumai R., Komatsu Y., Nishino N., Khochbin S., Yoshida M. and Horinouchi S. Potent histone deacetylase inhibitors built from trichostatin A and cyclic tetrapeptide antibiotics including trapoxin. *Proc Natl Acad Sci U S A*, **2001**, *98(1)*, 87-92.

(53) Buoncervello M., Borghi P., Romagnoli G., Spadaro F., Belardelli F., Toschi E. and Gabriele L. Apicidin and docetaxel combination treatment drives CTCFL expression and HMGB1 release acting as potential antitumor immune response inducers in metastatic breast cancer cells. *Neoplasia*, **2012**, *14(9)*, 855-867.

(54) Olsen C. A., Montero A., Leman L. J. and Ghadiri M. R. Macrocyclic peptoid–peptide hybrids as inhibitors of class I histone deacetylases. *ACS Med Chem Lett,* **2012**, *3(9)*, 749–753.

(55) Schardl C. L., Panaccione D. G. and Tudzynski P. Ergot alkaloids – biology and molecular biology. *Alkaloids Chem Biol*, **2006**, *63*, 45–86.

(56) Gerhards N., Neubauer L., Tudzynski P and Li S. M. Biosynthetic pathways of ergot alkaloids. *Toxins,* **2014**, *6*, 3281-3295.

(57) Weiland C. M. and Hilaire M. L. Bromocryptine mesylate (Cycloset) for type 2 diabetes mellitus. *Am Fam Physician*, **2013**, *87(10)*, 718-720.

(58) Wallwey C. and Li S. M. Ergot alkaloids: Structure diversity, biosynthetic gene clusters and functional proof of biosynthetic genes. *Nat Prod Rep*, **2011**, *28*, 496.

(59) Antimicrobial resistance: Global report on surveillance. ©World Health Organization **2014**.

(60) Ling L. L., Schneider T., Peoples A. J., Spoering A. L., Engels I., Conlon B. P., Mueller A., Schäberle T. E., Hughes D. E., Epstein S., Jones M., Lazarides L., Steadman V. A., Cohen D. R., Felix C. R., Fetterman K. A., Millet W. P., Nitti A. G., Zullo A. M., Chen C. and Lewis K. A new antibiotic kills pathogens without detectable resistance. *Nature,* **2015**, *517(7535)*, 455-459.

(61) Yeung A. T., Gellatly S. L. and Hancock R. E. Multifunctional cationic host defence peptides and their clinical applications. *Cell Mol Life Sci,* **2011**, *68(13)*, 2161–2176.

(62) Silva P. M., Goncalves S. and Santos N. C. Defensins: Antifungal lessons from eukaryotes. *Front Microbiol,* **2014**, *5,* 97.

(63) Mygind P. H., Fischer R. L., Schnorr K. M., Hansen M. T., Sönksen C. P., Ludvigsen S., Raventós D., Buskov S., Christensen B., De Maria L., Taboureau O., Yaver D., Elvig-Jørgensen S. G., Sørensen M. V., Christensen B. E., Kjærulff S., Frimodt-Moller N., Lehrer R. I., Zasloff M. and Kristensen H. H.. Plectasin is a peptide antibiotic with therapeutic potential from a saprophytic fungus. *Nature*, **2005**, *437*, 975-980.

(64) Schneider T., Kruse T., Wimmer R., Wiedemann I., Sass V., Pag U., Jansen A., Nielsen A. K., Myqind P. H., Raventós D. S., Neve S., Rayn B., Bonvin A. M., Demaria L., Andersen A. S., Gammelgaard L. K., Sahl H. G. and Kristensen H. H. Plectasin, a fungal defensin, targets the bacterial cell wall precursor lipid II. *Science*, **2010**, *328(5982),* 1168-1172.

(65) Xiong Y. Q., Hady W. A., Deslandes A., Rey A., Fraisse L., Kristensen H. H., Yeaman M. R. and Bayer A. S. Efficacy of NZ2114, a novel plectasin-derived cationic antimicrobial peptide antibiotic, in experimental endocarditis due to methicillin-resistant *Staphylococcus aureus*. *Antimicrob Agents Chemother*, **2011**, *55(11)*, 5325-5330.

(66) Zhang Y., Teng D., Mao R., Wang X., Xi D., Hu X. and Wang J. High expression of a plectasin-derived peptide NZ2114 in *Pichia pastoris* and its pharmacodynamics, postantibiotic and synergy against *Staphylococcus aureus*. *Appl Microbiol Biotechnol*, **2014**, *98(2)*, 681-694.

(67) Afacan N. J., Yeung A. T., Pena O. M. and Hancock R. E. Therapeutic potential of host defense peptides in antibiotic-resistant infections. *Curr Pharm Des,* **2012***, 18,* 807-819.

(68) Steyn P. S., Tuinman A. A., van Heerden F. R., van Rooyen P. H., Wessels P. L. and Rabie C. J. The isolation, structure, and absolute configuration of the mycotoxin, rhizonin A, a novel cyclic heptapeptide containing N-methyl-3-(3-furyl)alanine, produced by *Rhizopus microsporus*. *J Chem Soc, Chem Commun*, **1983**, 47-49.

(69) Partida-Martinez L. P., de Looss C. F., Ishida K., Ishida M., Roth M., Buder K. and Hertweck C. Rhizonin, the first mycotoxin isolated from the Zygomycota, is not a fungal metabolite but is produced by bacterial endosymbionts. *Appl Environ Microbiol,* **2007**, *73(3)*, 793–797.

(70) Kang S.-M., Khan A. L., Hussain J., Ali L., Kamran M., Waqas M. and Lee I. J. Rhizonin A from *Burkholderia* sp. KCTC11096 and its growth promoting role in lettuce seed germination. *Molecules*, **2012**, *17,* 7980-7988.

(71) Nakatsuka H., Shimokawa K., Miwa R., Yamada K. and Uemura D. First total synthesis and biological evaluation of the cyclic heptapeptide rhizonin A. *Tetrahedron Lett*, **2009**, *50*, 186-188.

(72) Shimokawa K., Yamada K. and Uemura D. Structure-based hybridization of the bioactive natural product rhizonin A and ternatin leading to a selective fat-accumulation inhibitor against 3T3-L1 adipocytes. *Bioorg Med Chem Lett*, **2009**, *19(3)*, 867-869.

(73) Lewis D. E. and Dunn F. W. β-3-furylalanine, a new analogue of phenylalanine. *Arch Biochem Biophys*, **1963**, *107*, 363-366.

(74) Xiang W. S., Wang J. D., Wang X. J. and Zhang J. Bingchamides A and B, two novel cyclic pentapeptides from the *Streptomyces bingchenggensis*: Fermentation, isolation, structural elucidation and biological properties. *J Antibiot (Tokyo)*, **2009,** *62(9),* 501- 505.

(75) Aleu J., Bustillo A. J., Hernández-Galán R. and Collado I. G. Biocatalysis applied to the synthesis of agrochemicals. *Curr Org Chem*, **2006**, *10*, 2037-2054.

(76) Doyle R. R. and Levenberg B. L-3-(3-carboxyfuran-4-yl)alanine, a new amino acid from the mushroom *Phyllotopsis nidulans*. *Phytochemistry*, **1974**, *13*, 2813-2814.

(77) Hatanaka S. and Niimura Y. L-3-(3-carboxy-4-furyl)alanine from *Tricholomopsis rutilans*. *Sci Pap Coll Gen Edu*, **1975**, *25(1)*, 35-37.

(78) Peptides as drugs, International pharmaceutical Industry, Spring **2012**, *4(2)*.

(79) Pomilio A. B., Battista M. E. and Vitale A. A. Naturally-occurring cyclopeptides: Structure and bioactivity. *Curr Org Chem*, **2006**, *10*, 2075-2121.

(80) Kang H. K., Seo C. H. and Park P. Marine peptides and their anti-infective activities. *Mar Drugs*, **2015**, *13*, 618-654.

(81) Abdalla M. A. and Matasyoh J. C. Endophytes as producers of peptides: An overview about recently discovered peptides from endophytic microbes. *Nat Prod Bioprospect,* **2014**, *4,* 257- 270.

(82) Süssmuth R., Müller J., von Döhren H. and Molnár I. Fungal cyclooligomer depsipeptides: From classical biochemistry to combinatorial biosynthesis. *Nat Prod Rep,* **2011**, *28*, 99-124.

(83) Almeida C., Kehraus S., Prudêncio M. and König G. M. Marilones A-C, phthalides from the sponge-derived fungus *Stachylidium* sp.. *Beilstein J Org Chem,* **2011**, *7*, 1636-1642.

(84) Almeida C., Hemberger Y., Schmitt S. M., Bouhired S., Natesan L., Kehraus S., Dimas K., Gütschow M., Bringmann G. and König G. M. Marilines A-C: Novel phthalimidines from the sponge-derived fungus *Stachylidium* sp.. *Chem Eur J,* **2012**, *18*, 8827-34.

(85) Almeida C. , Part N., Bouhired S., Kehraus S. and König G. M. Stachylines A−D from the sponge-derived fungus *Stachylidium* sp.. *J Nat Prod*, **2011**, *74(1)*, 21-25.

(86) Schulz B., Boyle C., Draeger S., Rommert A. K. and Krohn K. Endophytic fungi: A source of novel biologically active secondary metabolites. *Mycol Res,* **2002**, *106*, 996-1004.

(87) Schulz B., Sucker J., Aust H. J., Krohn K., Ludewig K., Jones P. G. and Döring D. Biologically active secondary metabolites of endopyhtc *Pezicula* species. *Mycol Res,* **1995**, *99*, 1007-1015.

(88) Schröder R., Janssen N., Schmidt J., Kebig A., Merten N., Hennen S., Müller A., Blättermann S., Mohr-Andrä M., Zahn S., Wenzel J., Smith N. J., Gomeza J., Drewke C., Milligan G., Mohr K. and Kostenis E. Deconvolution of complex G protein-coupled receptor signaling in live cells using dynamic mass redistribution measurements. *Nat Biotechnol,* **2010**, *28*, 943-949.

(89) Schröder R., Schmidt J., Blättermann S., Peters L., Janssen N., Grundmann M., Seemann W., Kaufel D., Merten N., Drewke C., Gomeza J., Milligan G., Mohr K. and Kostenis E. Applying label-free dynamic mass redistribution technology to frame signaling of G protein-coupled receptors noninvasively in living cells. *Nat Protoc,* **2011**, *6,* 1748-1760.

(90) Kostenis E., Martini L., Ellis J., Waldhoer M., Heydorn A., Rosenkilde M. M., Norregaard P. K., Jorgensen R., Whistler J. L. and Milligan G. A highly conserved glycine within linker I and the extreme C terminus of G protein alpha subunits interact cooperatively in switching G protein-coupled receptor-to-effector specificity. *J Pharmacol Exp Ther,* **2005**, *313*, 78-87.

(91) Mcomie J. F. W., Watts M. L. and West D. E. Demethylation of aryl methyl ethers by boron tribomide. *Tetrahedron*, **1968**, *24*, 2289-2292.

(92) Bierzyński A. Methods of peptide conformation studies. *Acta Biochim Pol*, **2001**, *48(4)*, 1091-1099.

(93) Craik D. J. and Jarvis J. A. Conformational studies of bioactive peptides by NMR. *Curr Med Chem*, **1994**, *1*, 115-144.

(94) Creese A. J., Smart J. and Cooper H. J. Large-scale analysis of peptide sequence variants: The case for high-field asymmetric waveform ion mobility spectrometry. *Anal Chem*, **2013**, *85(10)*, 4836-4843.

(95) Lang G., Blunt J. W., Cummings N. J., Cole A. L. and Munro M. H. Hirsutude, a cyclic tetrapeptide from a spider-derived entomopathogenic fungus, *Hirsutella* sp.. *J Nat Prod,* **2005**, *68*, 1303-1305.

(96) Almeida C., El Maddah F., Stables J., Kehraus S., Roth B. L., Schnakenburg G. and König G. M. Endolides A and B, N-methylated anticonvulsant peptides from the sponge-derived fungus *Stachylidium* sp. (in preparation).

(97) Dewick P. M. Medicinal natural products: A biosynthetic approach, 3rd edition, ©**2009** John Wiley & Sons Ltd. The Atrium, Southern Gate, Chichester, West Sussex, PO19 8SQ, United Kingdom.

(98) Bedford C. T., Knittel P., Money T., Phillips G. T. and Salisbury P. Biosynthesis of mycophenolic acid. *Can J Chem*, **1973**, *51*, 694–697.

(99) Ayer W. A. and Racok J. S. The metabolites of *Talaromyces flavus*. Part 2. Biological activity and biosynthetic studies. *Can J Chem*, **1990**, *68*, 2095–2101.

(100) Garson M. J. Biosynthetic studies on marine natural products. *Nat Prod Rep,* **1989**, *6*, 143.

(101) Bhakuni D. S. and Rawat D. S. Biosynthesis of bioactive metabolites of marine organisms. *Bioactive Marine Natural Products* ©**2005** Anamaya Publishers, New Delhi, India, 125-150.

(102) Neuss N., Boeck L. D., Brannon D. R., Cline J. C., DeLong D. C., Gorman M., Huckstep L. L., Lively D. H., Mabe J., Marsh M. M., Molloy B. B., Nagarajan R., Nelson J. D. and Stark W. M. Aranotin and related metabolites from *Arachniotus aureus* (Eidam) Schroeter. IV. Fermentation, isolation, structure elucidation, biosynthesis, and antiviral properties. *Antimicrob Agents Chemother (Bethesda)*, **1968**, *8*, 213-219.

(103) Guo C. J., Yeh H. H., Chiang Y. M., Sanchez J. F., Chang S. L., Bruno K. S. and Wang C. C. Biosynthetic pathway for the epipolythiodioxopiperazine acetylaranotin in *Aspergillus terreus* revealed by genome-based deletion analysis. *J Am Chem Soc,* **2013**, *135*, 7205-7213.

(104) Cho H., Beale J. M., Cynthia G., Mocek U., Nakagawa A., Omura S. and Floss H. G. Studies on the biosynthesis of the antibiotic reductiomycin in *Streptomyces xanthochromogenus. J Am Chem Soc,* **1993**, *115*, 12296-12304.

(105) Vederas J. C. The use of stable isotopes in biosynthetic studies. *Nat Prod Rep*, **1987**, 277-337.

(106) Schneider B. Nuclear magnetic resonance spectroscopy in biosynthetic studies. *Prog Nucl Magn Reson Spectrosc,* **2007**, *51*, 155-198.

(107) Hochuli M., Patzelt H., Oesterhelt D., Wüthrich K. and Szyperski T. Amino acid biosynthesis in the halophilic Archaeon *Haloarcula hispanica*. *J Bacteriol*, **1999**, *181(19)*, 3226-3237.

(108) Hansson D., Menkis A., Olson Å., Stenlid J., Broberg A. and Karlsson M. Biosynthesis of fomannoxin in the root rotting pathogen *Heterobasidion occidentale. Phytochemistry* **2012**, *84*, 31-39.

(109) Van't Land C. W., Mocek U. and Floss H. G. Biosynthesis of the phenazine antibiotics, the saphenamycins and esmeraldins, in *Streptomyces antibioticus. J Org Chem,* **1993**, *58*, 6576-6582.

(110) Simpson T. J. Application of isotopic methods to secondary metabolic pathways, Topics in current Chemistry, Vol. 195 ©Springer Verlag Berlin Heidelberg, **1998**.

(111) O'Connor N. K., Rai D. K., Clark B. R. and Murphy C. D. Production of the novel lipopeptide antibiotic trifluorosurfactin via precursor-directed biosynthesis. *J Fluorine Chem*, **2012**, *143*, 210-215.

(112) Zhao P. J., Yang Y. L., Du L., Liu J. K. and Zeng Y. Elucidating the biosynthetic pathway for vibralactone: A pancreatic lipase inhibitor with a fused bicyclic β-lactone. *Angew Chem Int Ed*, **2013**, *52*, 2298-2302.

(113) McMurry J. and Begley T. The organic chemistry of biological pathways, ©**2005** by Roberts and Company Publishers, 285-286.

(114) Augner D. and Schmalz H. G. Biomimetic synthesis of isoindolinones related to the marilines. *Synlett*, **2015**, *26*, 1395-1397.

(115) Dübeler A., Krastel P., Floss H. G. and Zeeck A. Biosynthesis of the antibiotic echinosporin by a novel branch of the shikimate pathway. *Eur J Org Chem,* **2002**, *6*, 983-987.

(116) Kennedy J. Mutasynthesis, chembiosynthesis, and back to semi-synthesis: Combining synthetic chemistry and biosynthetic engineering for diversifying natural products. *Nat Prod Rep,* **2008**, *25*, 25-34.

(117) Thiericke R. and Rohr J. Biological variation of microbial metabolites by precursor-directed biosynthesis. *Nat Prod Rep,* **1993**, *10(3)*, 265-289.

(118) Bender T., Schuhmann T., Magull J., Grond S. and Zezschwitz P. V. Total synthesis and biosynthesis of the novel spiroacetal okaspirodiol from *Streptomyces* sp.. *J Org Chem,* **2006**, *71*, 7125-7132.

(119) Corre C., Haynes S. W., Malet N., Song L. and Challis G. L. A butenolide intermediate in methylenomycin furan biosynthesis is implied by incorporation of stereospecifically ^{13}C-labelled glycerols. *Chem Commun,* **2010**, *46*, 4079-4081.

(120) Hoffmann L. and Grond S. Mixed acetate-glycerol biosynthesis and formation of benzoate directly from shikimate in *Streptomyces* sp.. *Eur J Org Chem*, **2004**, 4771-4777.

(121) Kutrzeba L., Dayan F. E., Howell J., Feng J., Giner J. L. and Zjawiony J. K. Biosynthesis of salvinorin A proceeds via the deoxyxylulose phosphate pathway. *Phytochemistry,* **2007**, *68(14)*, 1872-1881.

(122) Mahmud T. Isotope tracer investigations of natural products biosynthesis: The discovery of novel metabolic pathways*. J Label Compd radiopharm*, **2007**, *50*, 1039-1051.

(123) Bringmann G., Irmer A., Feineis D., Gulder T. A. M., and Fiedler H. P. Convergence in the biosynthesis of acetogenic natural products from plants, fungi and bacteria. *Phytochemistry*, **2009**, *70*, 1776-1786.

(124) Lombard J. and Moreira D. Origins and early evolution of the mevalonate pathway of isoprenoid biosynthesis in the three domains of Life. *Mol Biol Evol*, **2011**, *28(1)*, 87-99.

(125) Lee J. P., Tsao S. W., Chang C. J., He X. G. and Floss H. G. Biosynthesis of naphthomycin A in *Streptomyces collinus*. *Can J Chem*, **1994**, *(72)*, 182.

(126) Almeida C., Dissertation "Novel secondary metabolites from endophytic marine-derived fungi", Bonn **2011**.

(127) Challis G. L., Ravel J. and Townsend C. A. Predictive, structure-based model of amino acid recognition by nonribosomal peptide synthetase adenylation domains. *Chem Bio*, **2000,** *7(3)*, 211-24.

(128) Qiao K., Zhou H., Xu W., Zhang W., Garg N. and Tang Y. A fungal nonribosomal peptide synthetase module that can synthesize thiopyrazines. *Org Lett,* **2011**, *13*, 1758–1761.

(129) Krause M., Lindemann A., Glinski M., Hornbogen T., Bonse G., Jeschke P., Thielking G., Gau W., Kleinkauf H. and Zocher R. Directed biosynthesis of new enniatins. *J Antibiot (Tokyo),* **2001**, *54(10)*, 797–804.

(130) Xu Y., Zhan J., Wijeratne E. M. K., Burns A. M., Gunatilaka A. A. L., Molnár I. Cytotoxic and antihaptotactic beauvericin analogues from precursor-directed biosynthesis with the insect pathogen *Beauveria bassiana* ATCC 7159. *J Nat Prod,* **2007**, *70*, 1467– 1471.

(131) Fedorova N. D., Moktali V. and Medema M. H. Bioinformatic approaches and software for detection of secondary metabolic gene cluster. *Methods Mol Biol*, **2012**, *944*, 23-45.

(132) Dairi T., Kuzuyama T., Nishiyama M. and Fujii I. Convergent strategies in biosynthesis. *Nat Prod Rep,* **2011**, *28*, 1054-1086.

(133) Cutignano A., Villani G. and Fontana A. One metabolite, two pathways: Convergence of polypropionate biosynthesis in fungi and marine molluscs. *Org Lett*, **2012**, *14(4)*, 992-995.

(134) Weng J. K., Li Y., Mo H. and Chapple C. Assembly of an evolutionary new pathway for α-pyrone biosynthesis in *Arabidopsis*. *Science*, **2012**, *337*, 960-964.

(135) Höfer I., Crüsemann M., Radzom M., Geers B., Flachshaar D., Cai X., Zeeck A. and Piel J. Insights into the biosynthesis of hormaomycin, an exceptionally complex bacterial signaling metabolite. *Chem Biol*, **2011**, *18*, 381-391.

(136) Schultz A. W., Oh D. C., Carney J. R., Williamson R. T., Udwary D. W., Jensen P. R., Gould S. J., Fenical W. and Moore B. S. Biosynthesis and structures of cyclomarins and cyclomarazins, prenylated cyclic peptides of marine actinobacterial origin. *J Am Chem Soc*, **2008**, *130(13)*, 4507-4516.

(137) Needham J., Kelly M. T., Ishige M. and Anderson R. J. Andrimid and moiramides A-C, metabolites produced in culture by a marine isolate of the bacterium *Pseudomonas fluorescens*: Structure elucidation and biosynthesis. *J Org Chem*, **1994**, *59*, 2058-2063.

(138) Marfori E. C., Bamba T., Kajiyama S., Fukusaki E. and Kobayashi A. Biosynthetic studies of tetramic acid antibiotic trichosetin. *Tetrahedron*, **2002**, *58*, 6655-6658.

(139) Sasaki T., Takahashi S., Uchida K., Funayama S., Kainosho M. and Nakagawa A. Biosynthesis of quinolactacin A, a TNF production inhibitor. *J Antibiot*, **2006**, *59(7)*, 418-427.

(140) Takenaka Y., Hamada N. and Tanahashi T. Biosynthetic origin of graphenone in cultured lichen mycobionts of *Graphis handelii. Z Naturforsch C,* **2008**, *63(7-8)*, 565-568.

(141) Pathre S. V., Khadikar P. V. and Mirocha C. J. Biosynthesis of zearalenone: A simple and efficient method to incorporate [^{13}C]acetate label by using solid cultures. *Appl Environ Microbiol*, **1989**, *55(8)*, 1955–1956.

(142) Knaggs A. R. The biosynthesis of shikimate metabolites. *Nat Prod Rep,* **2003**, *20*, 119-136.

(143) Hawkins A. R., Lamb H. K., Moore J. D., Charles I. G. and Robers C. F. The pre-chorismate (shikimate) and quinate pathways in filamentous fungi: Theoretical and practical aspects. *J Gen Microbiol,* **1993**, *139(12)*, 2891-2899.

(144) Calvo A. M., Wilson R. A., Bok J. W. and Keller N. P. Relationship between secondary metabolism and fungal development. *Microbiol Mol Biol Rev*, **2002**, *66(3)*, 447–459.

(145) Krizevski R., Bar E., Shalit O., Sitrit Y., Ben-Shabat S. and Lewinsohn E., Composition and stereochemistry of ephedrine alkaloids accumulation in *Ephedra sinica* Stapf. *Phytochemistry* **2010**, *71(8-9)*, 895–903.

(146) Fernández-Martínez L. T., Borsetto C., Gomez-Escribano J. P., Bibb M. J., Al-Bassam M. M., Chandra G. and Bibb M. J. New insights into chloramphenicol biosynthesis in *Streptomyces venezuelae* ATCC 10712. *Antimicrob Agents Chemother*, **2014**, *58(12)*, 7441-7450.

(147) Floss H. G., Yu T. W. and Arakawa K. The biosynthesis of 3-amino-5-hydroxybenzoic acid (AHBA), the precursor of mC_7N units in ansamycin and mitomycin antibiotics: A review. *J Antibiot (Tokyo)*, **2011**, *64(1)*, 35-44.

(148) Steyn P. S., Vleggaar R. and Wessels P. L. Biosynthesis of the aurovertins B and D. The role of methionine and propionate in the simultaneous operation of two independent biosynthetic pathways. *J Chem Soc, Perkin Trans 1*, **1981**, 1298-1308.

(149) Fosgerau K. and Hoffmann T. Peptide therapeutics: Current status and future directions. *Drug Discov today,* **2015**, *20(1)*, 122-128.

(150) Webling K. E., Runesson J., Bartfai T. and Langel U. Galanin receptors and ligands. *Front Endocrinol*, **2012**, *3*, 1-14.

(151) Mitsukawa K., Lu X. and Bartfai T. Galanin, galanin receptors and drug targets. *Cell Mol Life Sci*, **2008**, *65(12)*, 1796-1805.

(152) Kovac S. and Walker M. C. Neuropeptides in epilepsy. *Neuropeptides*, **2013**, *47*, 467-475.

(153) Frisvad J. C. Media and growth conditions for induction of secondary metabolite production. *Methods Mol Biol*, **2012**, *944*, 47-58.

(154) Purser S., Moore P. R., Swallowb S. and Gouverneur V. Fluorine in medicinal chemistry. *Chem Soc Rev*, **2008**, *37*, 320–330.

(155) Kamata S., Sakai H. and Hirota A. Isolation of acetylaranotin, bisdethiodi(methylthio)acetylaranotin and terrein as plant growth inhibitors from a strain of *Aspergillus terreus. Agric Biol Chem*, **1983**, *11*, 2637-2638.

(156) Haritakun R., Rachtawee P., Chanthaket R., Boonyuen N. and Isaka M. Butyrolactones from the fungus *Aspergillus terreus* BCC 4651. *Chem Pharm Bull (Tokyo),* **2010**, *58(11)*, 1545-1548.

(157) Mant C. T., Cepeniene D. and Hodges R. S. Reversed-phase HPLC of peptides: Assessing column and solvent selectivity on standard, polar-embedded and polar endcapped columns. *J Sep Sci*, **2010**, *33*, 3005-3012.

(158) Issaq H. J., Chan K. C., Blonder J., Ye X. and Veenstra T. D. Seperation, detection and quantitation of peptides by liquid chromatography and capillary electrochromatography. *J Chromatogr A*, **2009**, *1216*, 1825-1837.

(159) Hoffmeister D. and Keller N. P. Natural products of filamentous fungi: Enzymes, genes and their regulation. *Nat Prod Rep,* **2007**, *24*, 393-416.

(160) Khaldi N., Seifuddin F. T., Turner G., Haft D., Nierman W. C., Wolfe K. H., and Fedorova N. D. SMURF: Genomic mapping of fungal secondary metabolite clusters. *Fungal Genet Biol,* **2010**, *47(9)*, 736–741.

8. Appendix

8.1 Metabolites isolated during this study

No.	
1	Peptide 1: (-)-Cyclo-[(N-methyl-(L)-3-(3-furyl)-alanyl), (L)-leucyl, (N-methyl-(L)-phenylalanyl), (L)-valinyl] Peptide 1': (-)-Cyclo-[(N-methyl-(L)-3-(3-furyl)-alanyl), (L)-valinyl, (N-methyl-(L)-phenylalanyl), (L)-leucyl]
2	Peptide 2 (-)-Cyclo-[N-methyl-(L)-phenylalanyl, (L)-furylalanyl, N-methyl-(L)-phenylalanyl, (L)-valinyl]
3	Peptide 3 (-)-Cyclo-[N-methyl-(L)-phenylalanyl, (L)-phenylalanyl, N-methyl-(L)-phenylalanyl, (L)-valinyl]
4	Peptide 4 (-)-Cyclo-[(N-methyl-(L)-3-(3-furyl)-alanyl), (L)- valinyl, (N-methyl-(L)-3-(3-furyl)-alanyl), (L)- phenylalanyl]
5	Peptide 5: (-)-Cyclo-[(N-methyl-(L)-3-(3-furyl)-alanyl), (L)-3-(3-furyl)-alanyl, (N-methyl-(L)-phenylalanyl), (L)-valinyl] Peptide 5': (-)-Cyclo-[(N-methyl-(L)-3-(3-furyl)-alanyl), (L)-valinyl, (N-methyl-(L)-phenylalanyl), (L)-3-(3-furyl)-alanyl]
6	Peptide 6: (-)-Cyclo-[N-methyl-(L)-phenylalanyl, (L)-leucyl, N-methyl-(L)-leucyl, (L)-valinyl] Peptide 6': (-)-Cyclo-[N-methyl-(L)-phenylalanyl, (L)-valinyl, N-methyl-(L)-leucyl, (L)-leucyl]
7	Peptide 7: (-)-Cyclo-[N-methyl-(L)-3-(3-furyl)-alanyl, (L)-leucyl, N-methyl-(L)-leucyl, (L)-valinyl] Peptide 7': (-)-Cyclo-[N-methyl-(L)-3-(3-furyl)-alanyl, (L)-valinyl, N-methyl-(L)-leucyl, (L)-leucyl]
8	Peptide 8 (-)-Cyclo-[(L)-leucyl, N-methyl-(L)-phenylalanyl]
9	Peptide 9 (-)-Cyclo-[N-methyl-(L)-leucyl, (L)-phenylalanyl]
10	Bisdethiobis(methylthio)-acetylaranotin (BDA)
11	Bisdethiobis(methylthio)-acetylapoaranotin (BDAA)
12	Marilone A
13	Mariline B

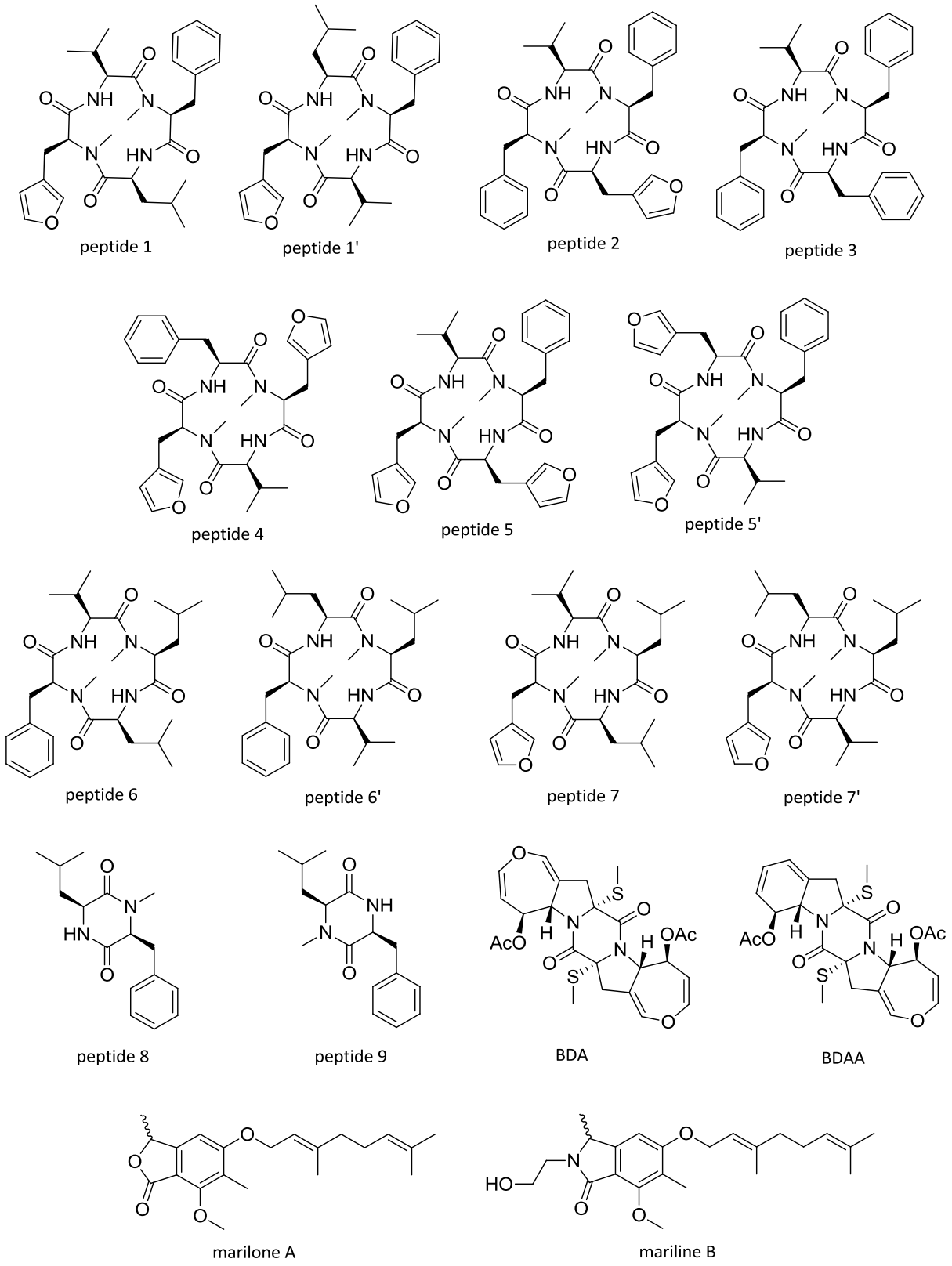

Fig S1. Structures of isolated metabolites.

Peptide 1 and 1', cyclic tetrapeptide, peptide 1 (-)-Cyclo-[(N-methyl-(L)-3-(3-furyl)-alanyl), (L)-leucyl, (N-methyl-(L)-phenylalanyl), (L)-valinyl] and peptide 1' (-)-Cyclo-[(N-methyl-(L)-3-(3-furyl)-alanyl), (L)-valinyl, (N-methyl-(L)-phenylalanyl), (L)-leucyl]: white solid (2.5 mg L^{-1}), $[\alpha]_D^{23}$ -133 (*c* 0.44, MeOH); UV (MeOH) λ_{max} 204 nm (log ϵ 4.69); IR (ATR) ν_{max} 3345 (br), 2958, 2871, 1704, 1660, 1511, 1364, 1089 cm^{-1}; ^1H NMR and ^{13}C NMR (table 4-1); LRESIMS *m/z* 525.5 $[M+H]^+$, *m/z* 523.9 $[M-H]^-$; HRESIMS *m/z* 547.2902 $[M+Na]^+$ (calcd. for $C_{29}H_{40}N_4NaO_5$, 547.2896).

Peptide 2, cyclic tetrapeptide, (-)-Cyclo-[N-methyl-(L)-phenylalanyl, (L)-furylalanyl, N-methyl-(L)-phenylalanyl, (L)-valinyl]: white solid (1.5 mg L^{-1}), $[\alpha]_D^{23}$ -129 (*c* 0.2, MeOH); UV (MeOH) λ_{max} 204 nm (log ϵ 3.45); IR (ATR) ν_{max} 3330 (br), 2961, 2360, 1704, 1660, 1514, 1362, 1091 cm^{-1}; ^1H NMR and ^{13}C NMR (table 4-2); LRESIMS *m/z* 559.4 $[M+H]^+$, *m/z* 557.6 $[M-H]^-$; HRESIMS *m/z* 581.2731 $[M+Na]^+$ (calcd. for $C_{32}H_{38}N_4NaO_5$, 581.2740).

Peptide 3, cyclic tetrapeptide, (-)-Cyclo-[N-methyl-(L)-phenylalanyl, (L)-phenylalanyl, N-methyl-(L)-phenylalanyl, (L)-valinyl]: white solid (1 mg L^{-1}), $[\alpha]_D^{23}$ -153 (*c* 0.125, MeOH); UV (MeOH) λ_{max} 207 nm (log ϵ 3.06); IR (ATR) ν_{max} 3329 (br), 2961, 1703, 1659, 1512, 1362, 1090 cm^{-1}; ^1H NMR and ^{13}C NMR (table 4-3); LRESIMS *m/z* 569.7 $[M+H]^+$, *m/z* 567.7 $[M-H]^-$; HRESIMS *m/z* 569.3119 $[M+H]^+$ (calcd. for $C_{34}H_{41}N_4O_4$, 569.3128).

Peptide 4, cyclic tetrapeptide, (-)-Cyclo-[(N-methyl-(L)-3-(3-furyl)-alanyl), (L)- valinyl, (N-methyl-(L)-3-(3-furyl)-alanyl), (L)- phenylalanyl]: white solid (1.4 mg L^{-1}), $[\alpha]_D^{23}$ -76 (*c* 0.058, MeOH); UV (MeOH) λ_{max} 204 nm (log ϵ 3.62); IR (ATR) ν_{max} 3331 (br), 2926, 2359, 1660, 1505, 1386, 1090 cm^{-1}; ^1H NMR and ^{13}C NMR (table 4-4); LRESIMS *m/z* 549.4 $[M+H]^+$, *m/z* 547.5 $[M-H]^-$; HRESIMS *m/z* 571.2532 $[M+Na]^+$ (calcd. for $C_{30}H_{36}N_4NaO_6$, 571.2533).

Peptide 5 and 5', cyclic tetrapeptide, peptide 5 (-)-Cyclo-[(N-methyl-(L)-3-(3-furyl)-alanyl), (L)-3-(3-furyl)-alanyl, (N-methyl-(L)-phenylalanyl), (L)-valinyl] and peptide 5' (-)-Cyclo-[(N-methyl-(L)-3-(3-furyl)-alanyl), (L)-valinyl, (N-methyl-(L)-phenylalanyl), (L)-3-(3-furyl)-alanyl]: white solid (0.6 mg L^{-1}), $[\alpha]_D^{23}$ -110 (*c* 0.166, MeOH); UV (MeOH) λ_{max} 204 nm (log ϵ 3.41); IR (ATR) ν_{max} 3331 (br), 2925, 2358, 1663, 1515, 1401, 1088 cm^{-1}; ^1H NMR and ^{13}C NMR (table 4-5); LRESIMS *m/z* 549.4 $[M+H]^+$, *m/z* 547.5 $[M-H]^-$; HRESIMS *m/z* 571.2526 $[M+Na]^+$ (calcd. for $C_{30}H_{36}N_4NaO_6$, 571.2533).

Peptide 6 and 6', cyclic tetrapeptide, peptide 6 (-)-Cyclo-[N-methyl-(L)-phenylalanyl, (L)-leucyl, N-methyl-(L)-leucyl, (L)-valinyl] and peptide 6' (-)-Cyclo-[N-methyl-(L)-phenylalanyl, (L)-valinyl, N-methyl-(L)-leucyl, (L)-leucyl]: white solid (0.6 mg L^{-1}), $[\alpha]_D^{23}$ -105 (*c* 0.108, MeOH); UV (MeOH) λ_{max} 206 nm (log ϵ 3.03); IR (ATR) ν_{max} 3332 (br), 2957, 2358, 1667, 1507, 1456 cm^{-1}; ^1H NMR and ^{13}C NMR (table 4-6); LRESIMS *m/z* 501.4 $[M+H]^+$, *m/z* 499.4 $[M-H]^-$; HRESIMS *m/z* 501.3438 $[M+H]^+$ (calcd. for $C_{28}H_{45}N_4O_4$, 501.3441).

Peptide 7 and 7', cyclic tetrapeptide, peptide 7 (-)-Cyclo-[N-methyl-(L)-3-(3-furyl)-alanyl, (L)-leucyl, N-methyl-(L)-leucyl, (L)-valinyl] and peptide 7' (-)-Cyclo-[N-methyl-(L)-3-(3-furyl)-alanyl, (L)-valinyl, N-methyl-(L)-leucyl, (L)-leucyl]: white solid (0.6 mg L^{-1}), $[\alpha]_D^{23}$ -67 (*c* 0.083, MeOH); UV (MeOH) λ_{max} 204 nm (log ϵ 3.12); IR (ATR) ν_{max} 3342 (br), 2924, 2359, 1714, 1652, 1520, 1365 cm^{-1}; ^1H NMR and ^{13}C NMR (table 4-7); LRESIMS *m/z* 491.9 $[M+H]^+$, *m/z* 489.8 $[M-H]^-$; HRESIMS *m/z* 513.3045 $[M+Na]^+$ (calcd. for $C_{26}H_{42}N_4NaO_5$, 513.3053).

Peptide 8, diketopiperazine, (-)-Cyclo-[(L)-leucyl, N-methyl-(L)-phenylalanyl]: white solid (0.35 mg L^{-1}), $[\alpha]_D^{23}$ -14 (*c* 0.083, MeOH); UV (MeOH) λ_{max} 203 nm (log ϵ 3.12); IR (ATR) ν_{max} 3198 (br), 2954, 2924, 2359, 1678, 1455, 1326 cm^{-1}; ^1H NMR and ^{13}C NMR (table 4-8); LRESIMS *m/z* 275.6 $[M+H]^+$, *m/z* 273.4 $[M-H]^-$; HRESIMS *m/z* 297.1568 $[M+Na]^+$ (calcd. for $C_{16}H_{22}N_2NaO_2$, 297.1579).

Peptide 9, diketopiperazine, (-)-Cyclo-[N-methyl-(L)-leucyl, (L)-phenylalanyl]: white solid (0.15 mg L^{-1}), $[\alpha]_D^{23}$ -241 (*c* 0.066, MeOH); UV (MeOH) λ_{max} 203 nm (log ϵ 2.85); IR (ATR) ν_{max} 3248 (br), 2925, 2359, 1681, 1455, 1340 cm^{-1}; ^1H NMR and ^{13}C NMR (table 4-9); LRESIMS *m/z* 275.6 $[M+H]^+$, *m/z* 273.4 $[M-H]^-$; HRESIMS *m/z* 297.1555 $[M+Na]^+$ (calcd. for $C_{15}H_{20}N_2NaO_2$, 297.1573).

Bisdethiobis(methylthio)-acetylaranotin (BDA): amorphous solid (0.5 mg L^{-1}), $[\alpha]_D^{23}$ -220 (*c* 0.092, MeOH)); UV (MeOH) λ_{max} 230 nm; IR (ATR) ν_{max} 1740, 1676, 1230 cm^{-1}; ^1H NMR and ^{13}C NMR (table S1); LREIMS *m/z* 552.3 $[M+H+18]^+$, molecular formula $C_{24}H_{26}O_8N_2S_2$. Spectral data are in accordance with published data.[102,103]

Bisdethiobis(methylthio)-acetylpoaranotin (BDAA): amorphous solid (1.2 mg L^{-1}), $[\alpha]_D^{23}$ -275 (*c* 0.1, MeOH)); UV (MeOH) λ_{max} 228 and 266 nm; IR (ATR) ν_{max} 1740, 1672, 1241, 750

cm^{-1}; ^{1}H NMR and ^{13}C NMR (table S1); LREIMS *m/z* 536.2 $[M+H+18]^{+}$, molecular formula $C_{24}H_{26}O_7N_2S_2$. Spectral data are in accordance with published data.[102,103]

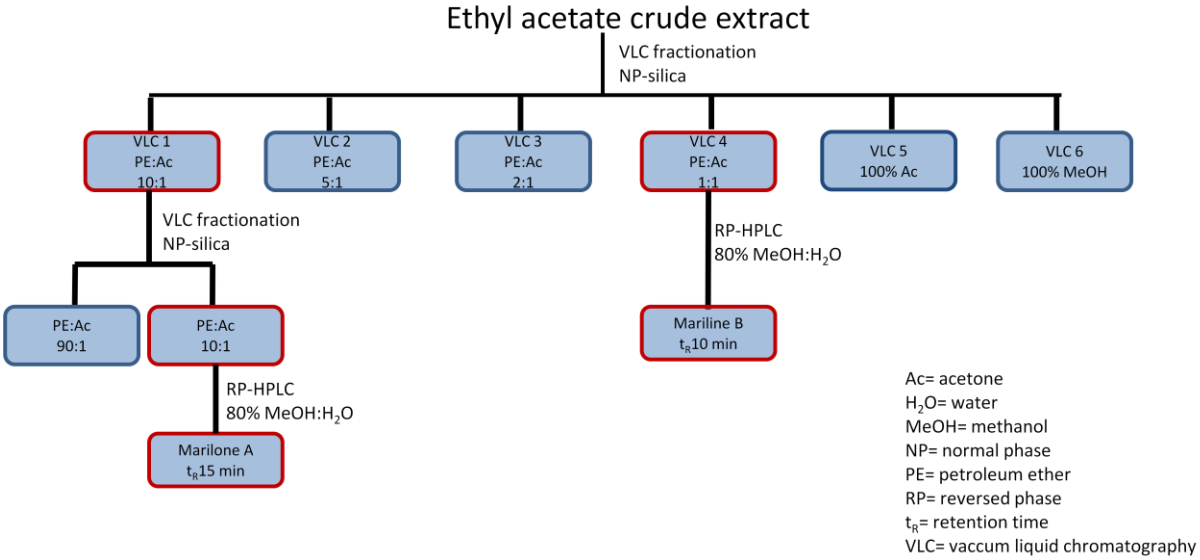

Fig S2. Isolation scheme for isolated polyketides (marilone A and mariline B) from a 60 day *Stachylidium* sp. culture on biomalt salt agar medium supplemented with [1-^{13}C]sodium acetate.

8.2 ^{1}H and ^{13}C NMR data of isolated metabolites

Fig S3. ^{1}H NMR (300 MHz, CD_3COCD_3) spectrum of peptide 1 and 1'.

Peptide 1: (-)-Cyclo-[(N-methyl-(L)-3-(3-furyl)-alanyl), (L)-leucyl, N-methyl-(L)-phenylalanyl, (L)-valinyl]

Peptide 1': (-)-Cyclo-[(N-methyl-(L)-3-(3-furyl)-alanyl), (L)-valinyl, N-methyl-(L)-phenylalanyl, (L)-leucyl]

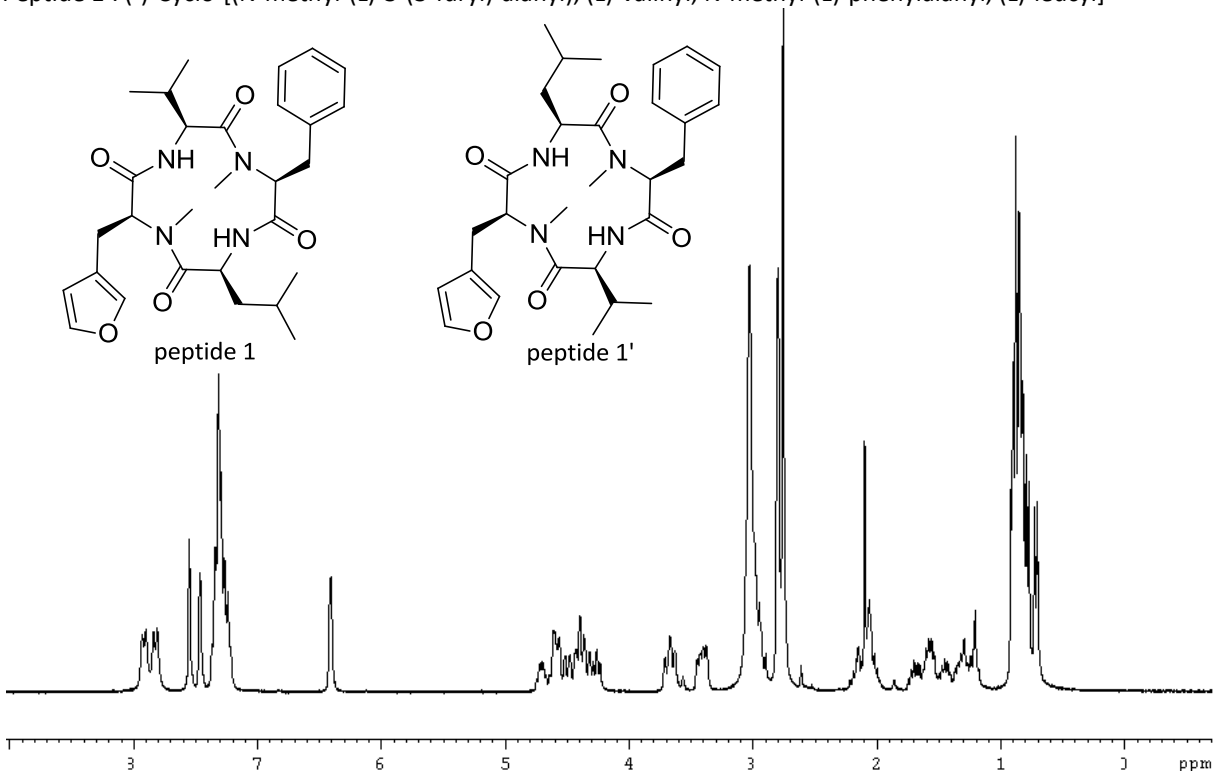

Fig S4. ^{13}C NMR (75 MHz, CD_3COCD_3) spectrum of peptide 1 and 1'.

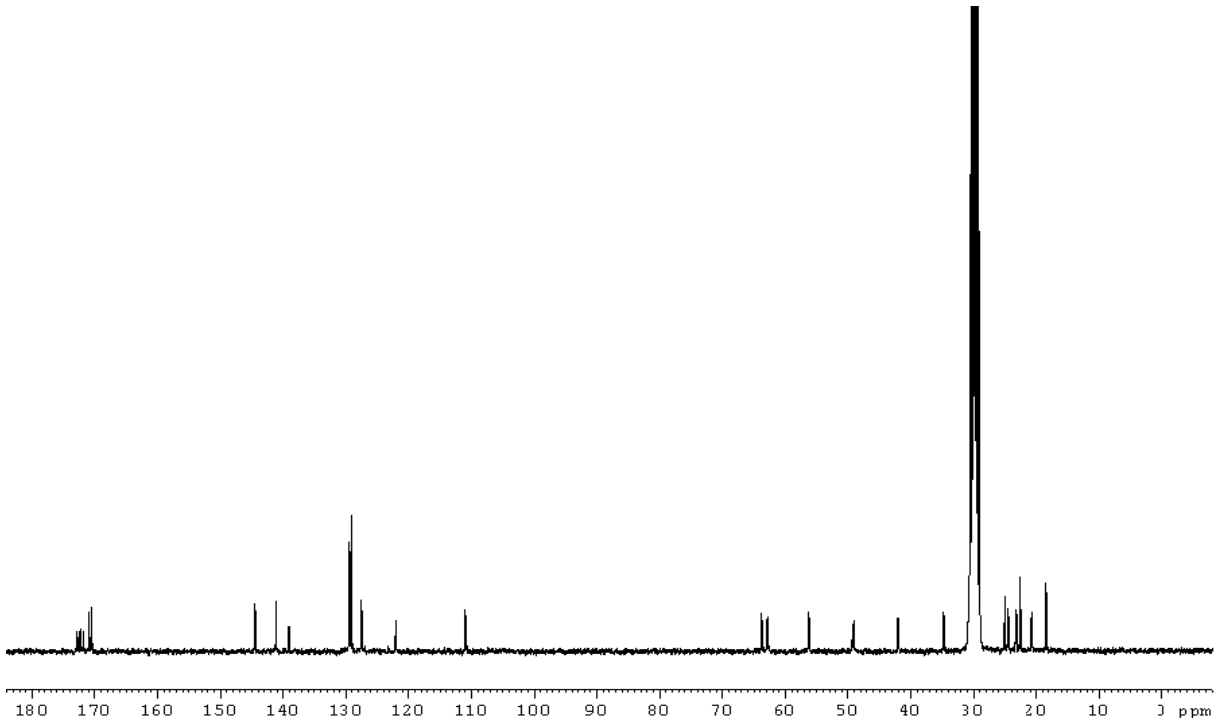

Fig S5. ^{1}H NMR (300 MHz, CD_3COCD_3) spectrum of peptide 2.

(-)-Cyclo-[N-methyl-(L)-phenylalanyl, (L)-3-(3-furyl-alanyl), N-methyl-(L)-phenylalanyl, (L)-valinyl]

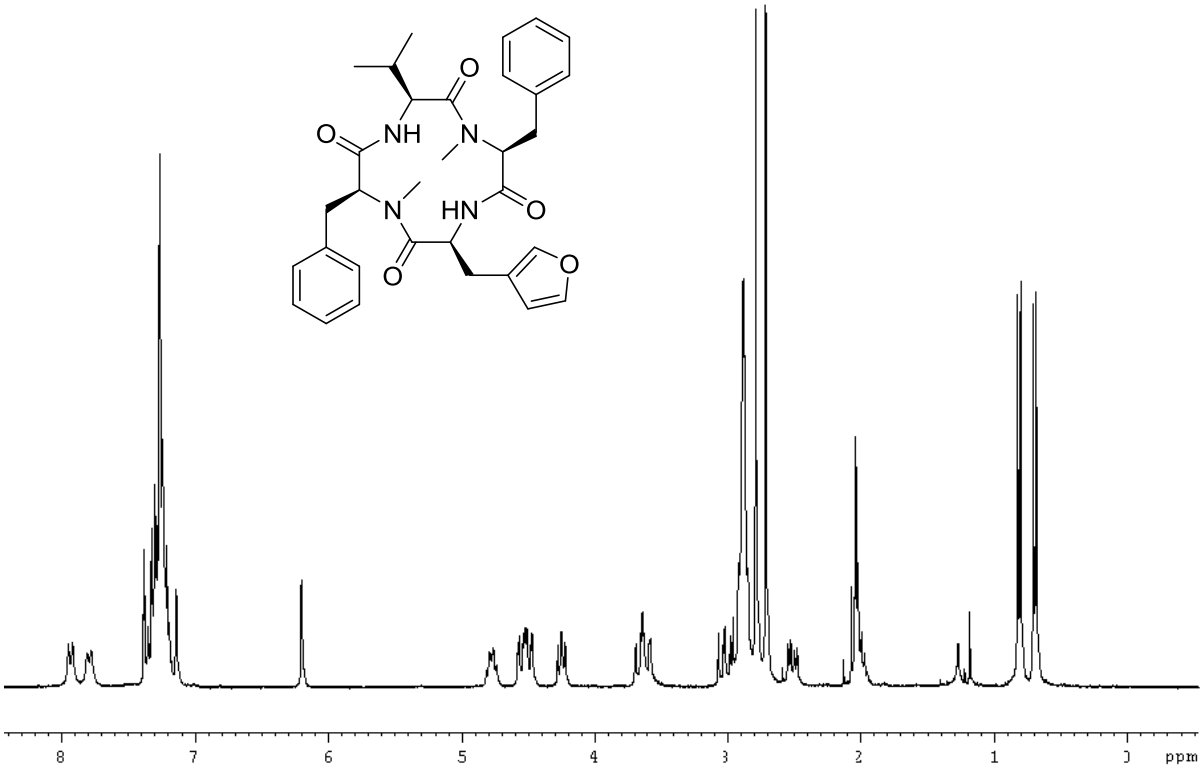

Fig S6. ^{13}C NMR (75 MHz, CD_3COCD_3) spectrum of peptide 2.

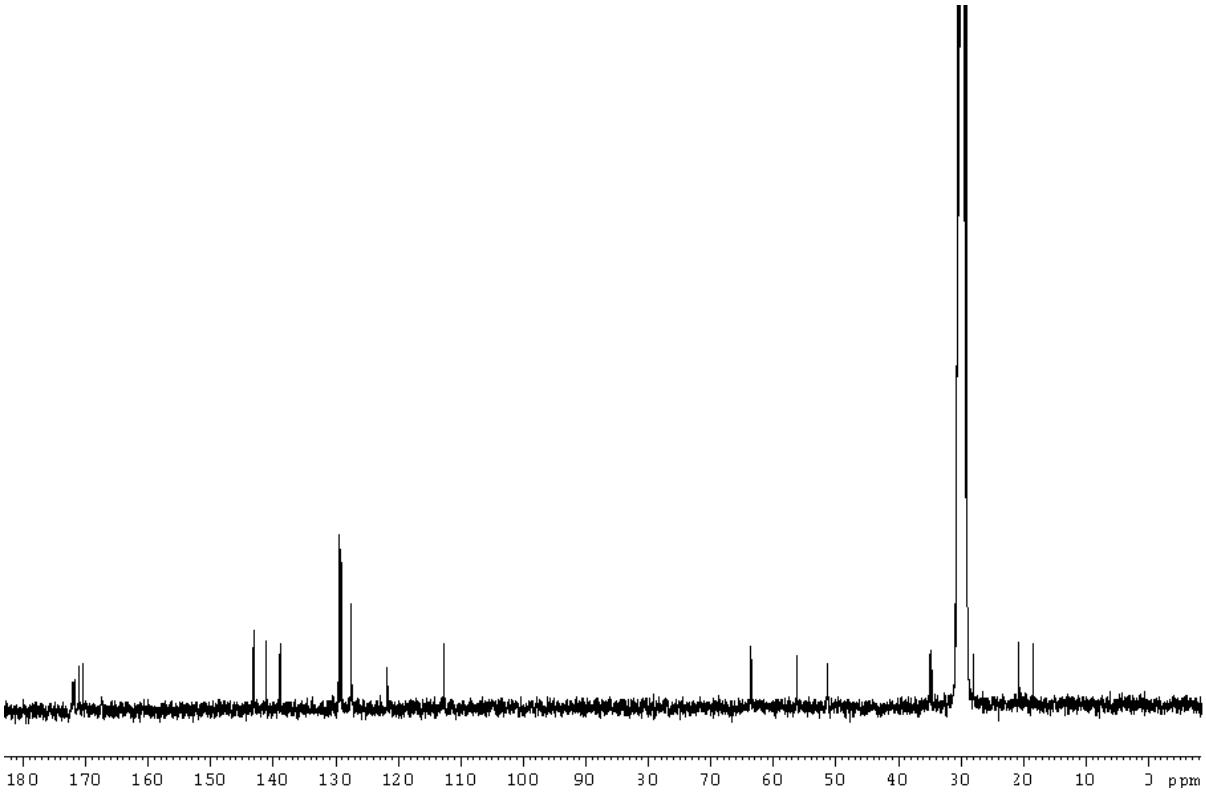

Fig S7. ^{1}H NMR (300 MHz, CD_3COCD_3) spectrum of peptide 3.

(-)-Cyclo-[N-methyl-(L)-phenylalanyl, (L)-phenylalanyl, N-methyl-(L)-phenylalanyl, (L)-valinyl]

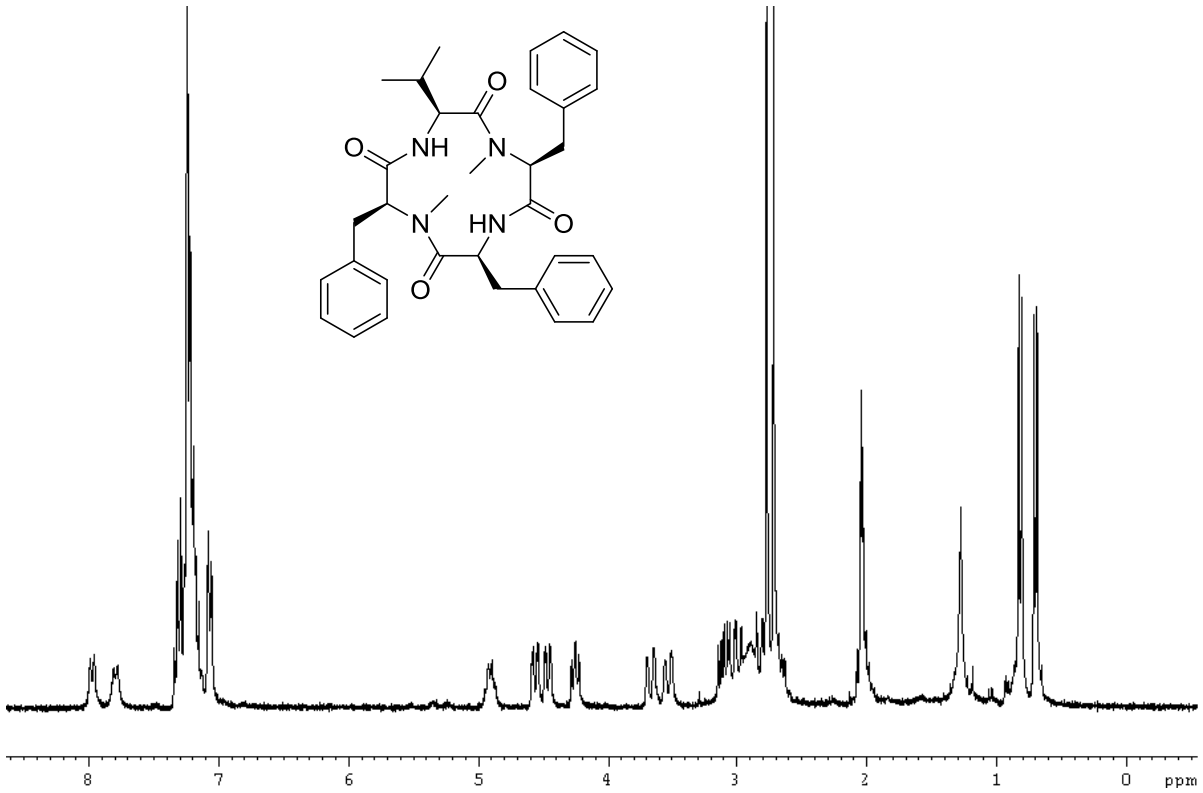

Fig S8. ^{13}C NMR (75 MHz, CD_3COCD_3) spectrum of peptide 3.

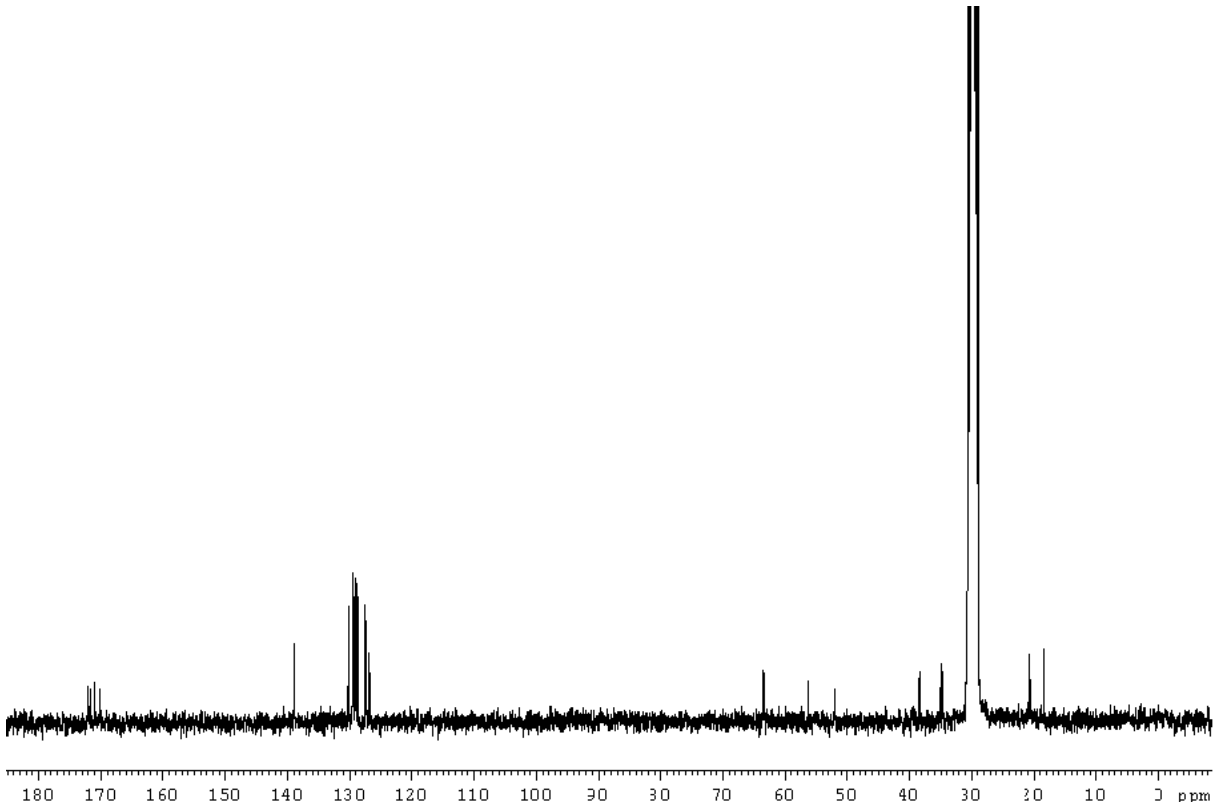

Fig S9. ^{1}H NMR (500 MHz, CD_3COCD_3) spectrum of peptide 4.

(-)-Cyclo-[(N-methyl-(L)-3-(3-furyl)-alanyl), (L)- valinyl, (N-methyl-(L)-3-(3-furyl)-alanyl), (L)- phenylalanyl]

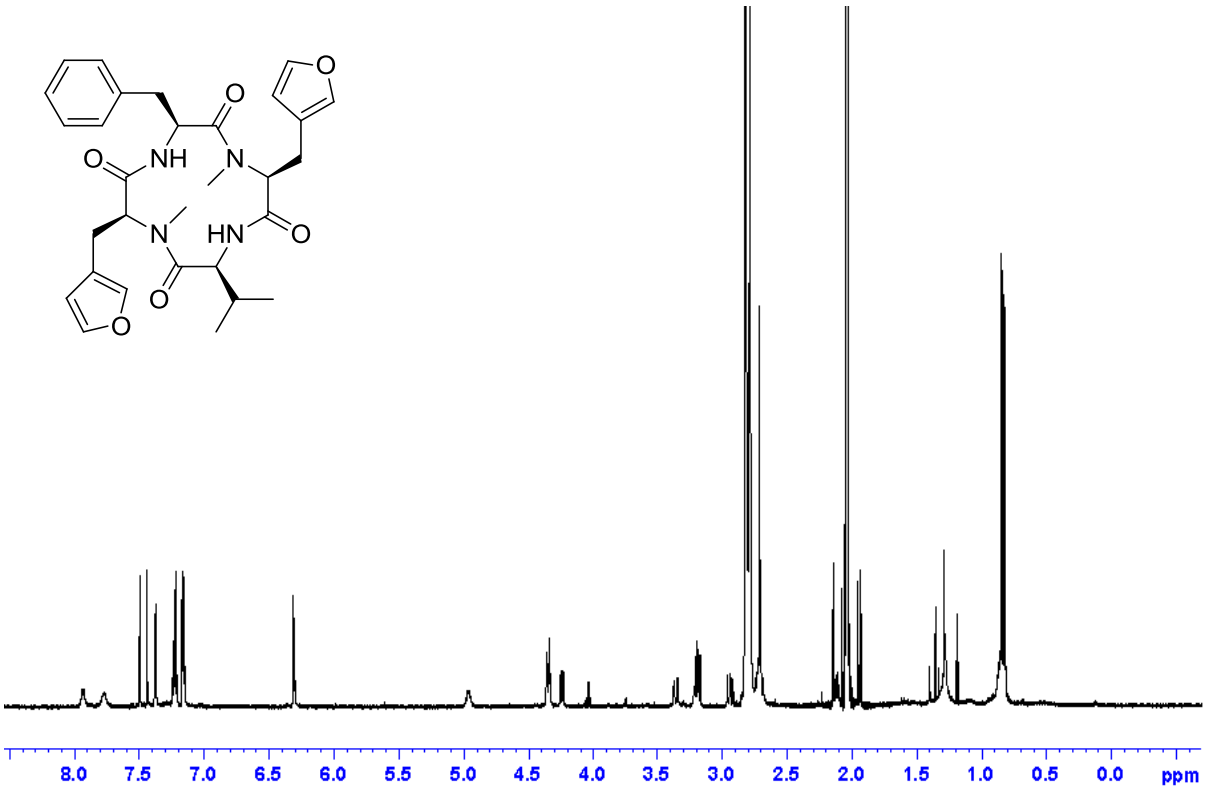

Fig S10. ^{13}C NMR (125 MHz, CD_3COCD_3) spectrum of peptide 4.

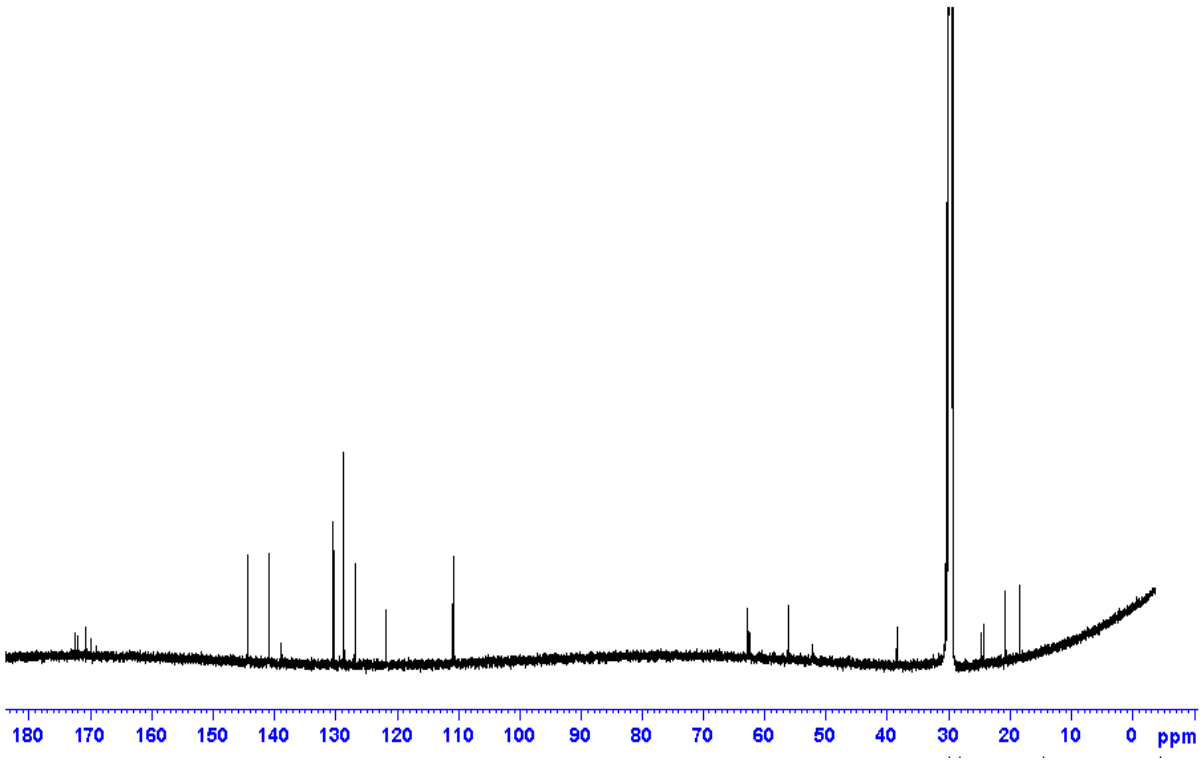

Fig S11. ^{1}H NMR (300 MHz, CD_3COCD_3) spectrum of peptide 5 and 5'.

Peptide 5: (-)-Cyclo-[(N-methyl-(L)-3-(3-furyl)-alanyl), (L)-3-(3-furyl)-alanyl, (N-methyl-(L)-phenylalanyl), (L)-valinyl]

Peptide 5': (-)-Cyclo-[(N-methyl-(L)-3-(3-furyl)-alanyl), (L)-valinyl, (N-methyl-(L)-phenylalanyl), (L)-3-(3-furyl)-alanyl]

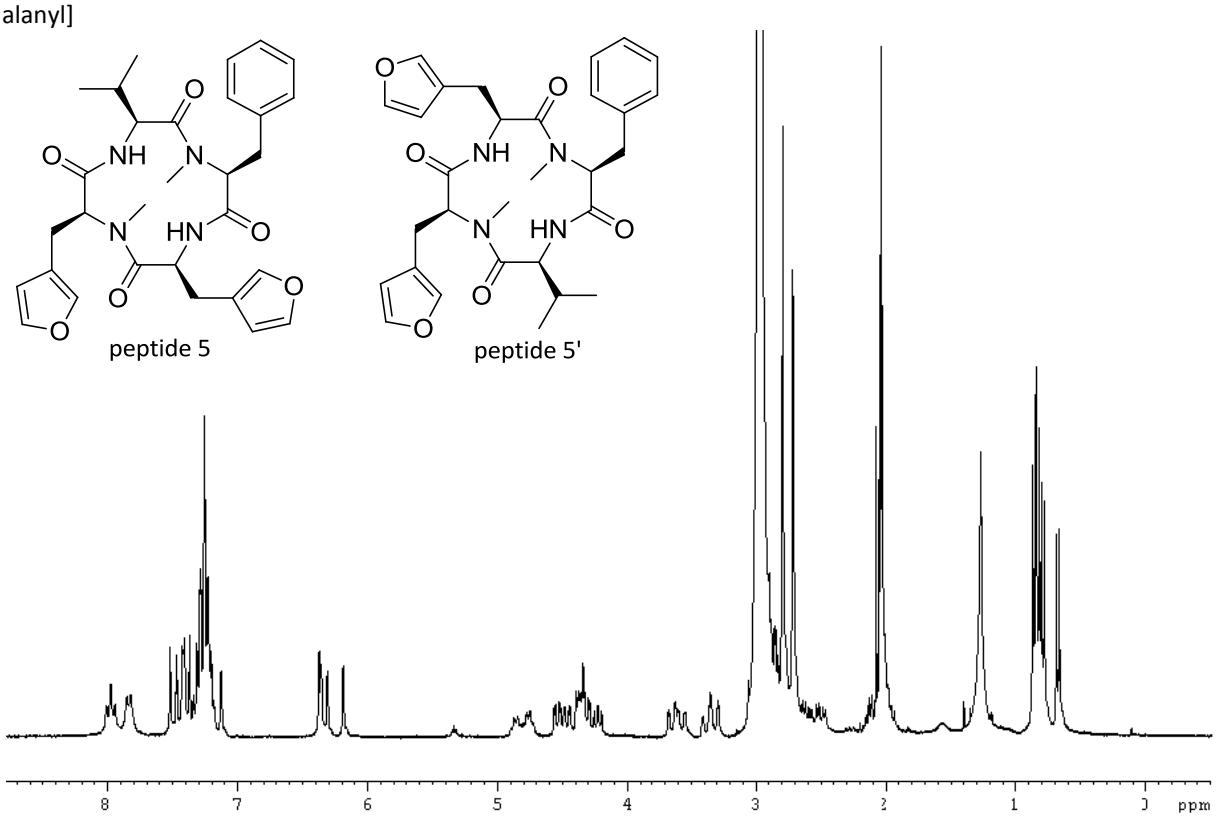

Fig S12. ^{13}C NMR (75 MHz, CD_3COCD_3) spectrum of peptide 5 and 5'.

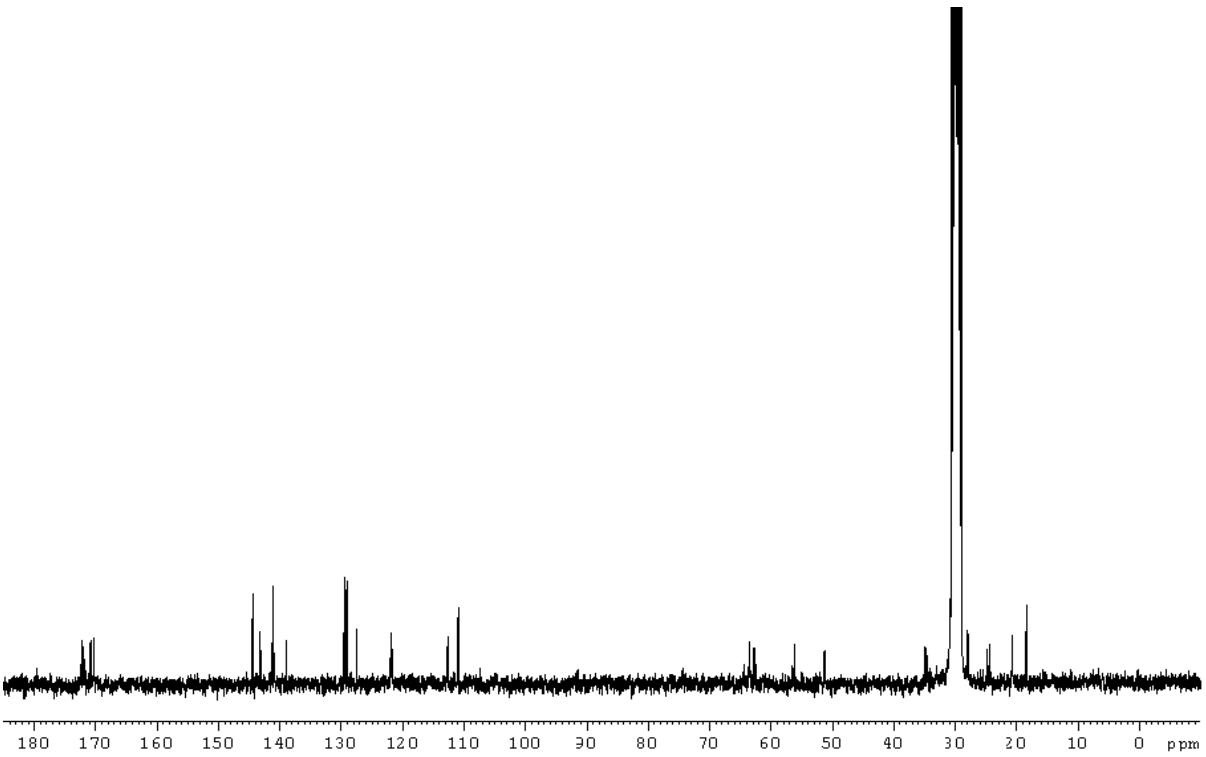

Fig S13. ^{1}H NMR (300 MHz, CD_3COCD_3) spectrum of peptide 6 and 6'.

Peptide 6: (-)-Cyclo-[N-methyl-(L)-phenylalanyl, (L)-leucyl, N-methyl-(L)-leucyl, (L)-valinyl]

Peptide 6': (-)-Cyclo-[N-methyl-(L)-phenylalanyl, (L)-valinyl, N-methyl-(L)-leucyl, (L)-leucyl]

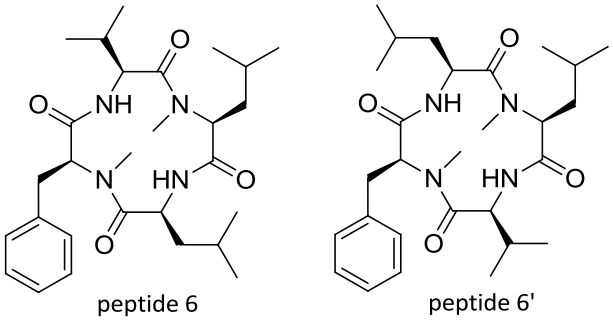

peptide 6

peptide 6'

Fig S14. ^{13}C NMR (75 MHz, CD_3COCD_3) spectrum of peptide 6 and 6'.

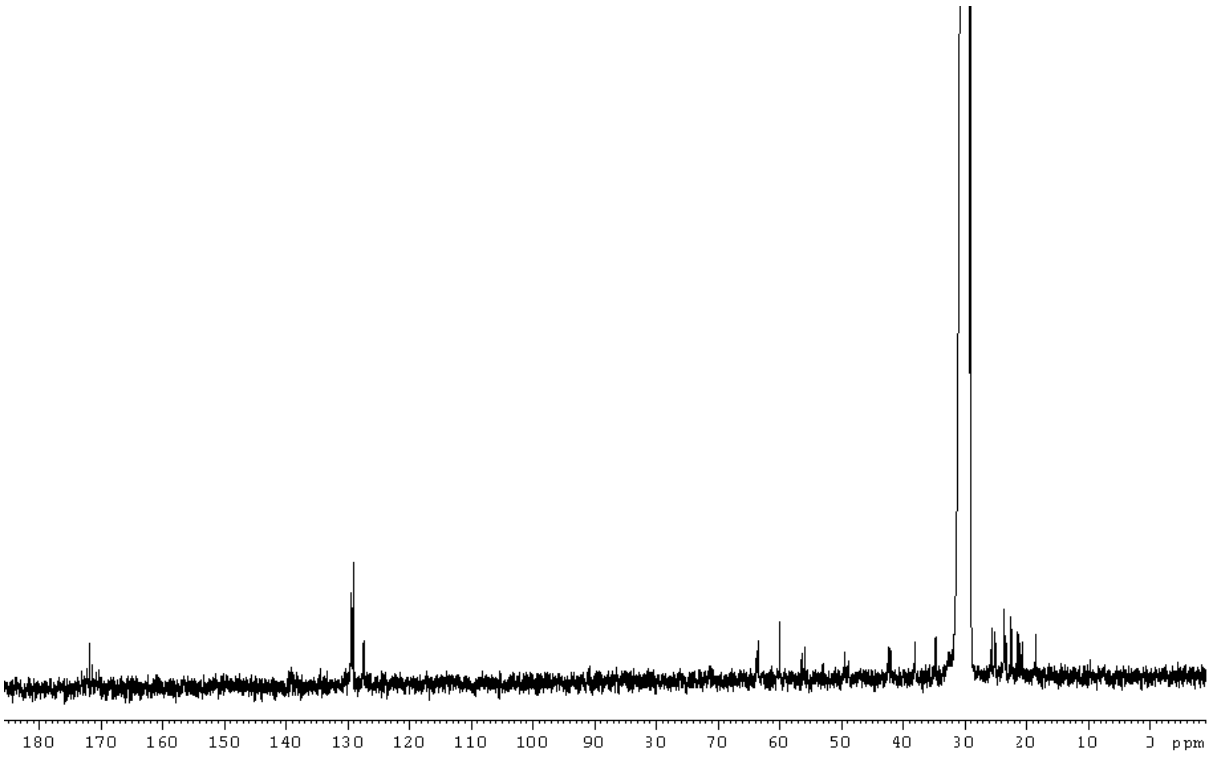

Fig S15. ^{1}H NMR (500 MHz, CD_3COCD_3) spectrum of peptide 7 and 7'.

Peptide 7: (-)-Cyclo-[N-methyl-(L)-3-(3-furyl)-alanyl, (L)-leucyl, N-methyl-(L)-leucyl, (L)-valinyl]

Peptide 7': (-)-Cyclo-[N-methyl-(L)-3-(3-furyl)-alanyl, (L)-valinyl, N-methyl-(L)-leucyl, (L)-leucyl]

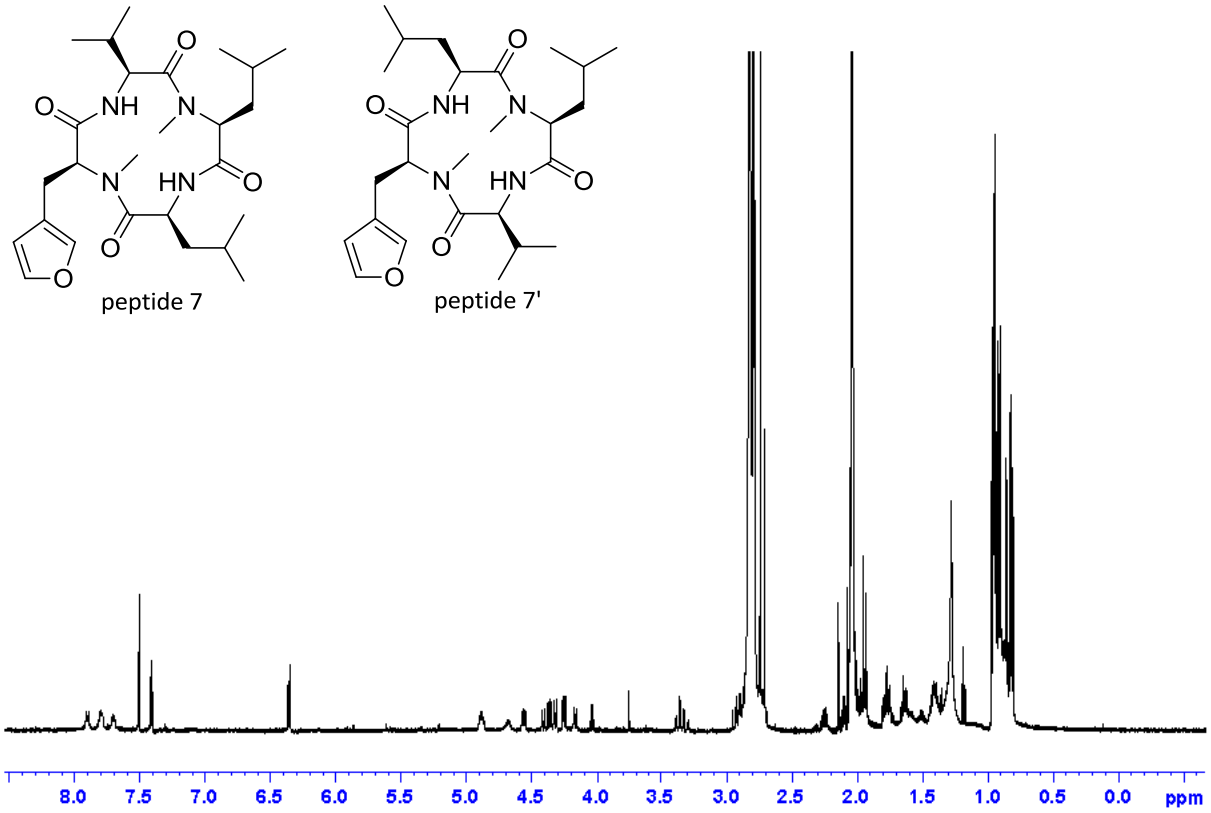

Fig S16. ^{13}C NMR (125 MHz, CD_3COCD_3) spectrum of peptide 7 and 7'.

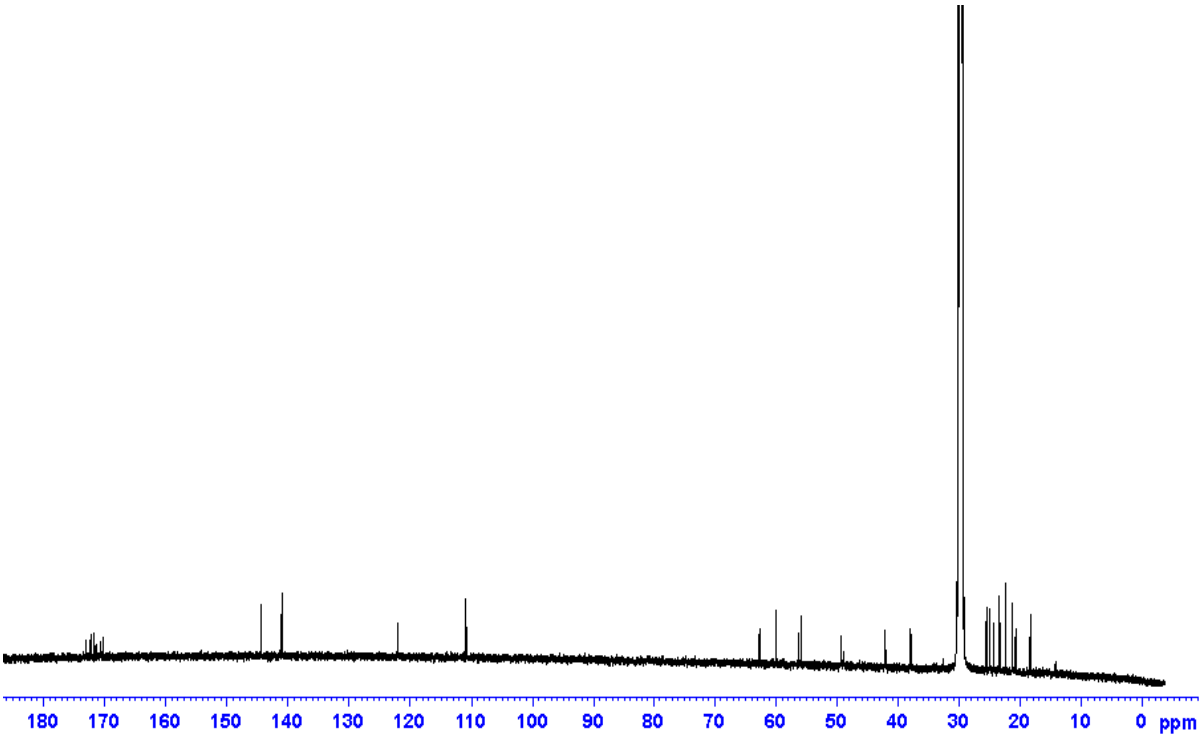

Fig S17. ^{1}H NMR (300 MHz, CD_3COCD_3) spectrum of peptide 8.

(-)-Cyclo-[(L)-leucyl, N-methyl-(L)-phenylalanyl]

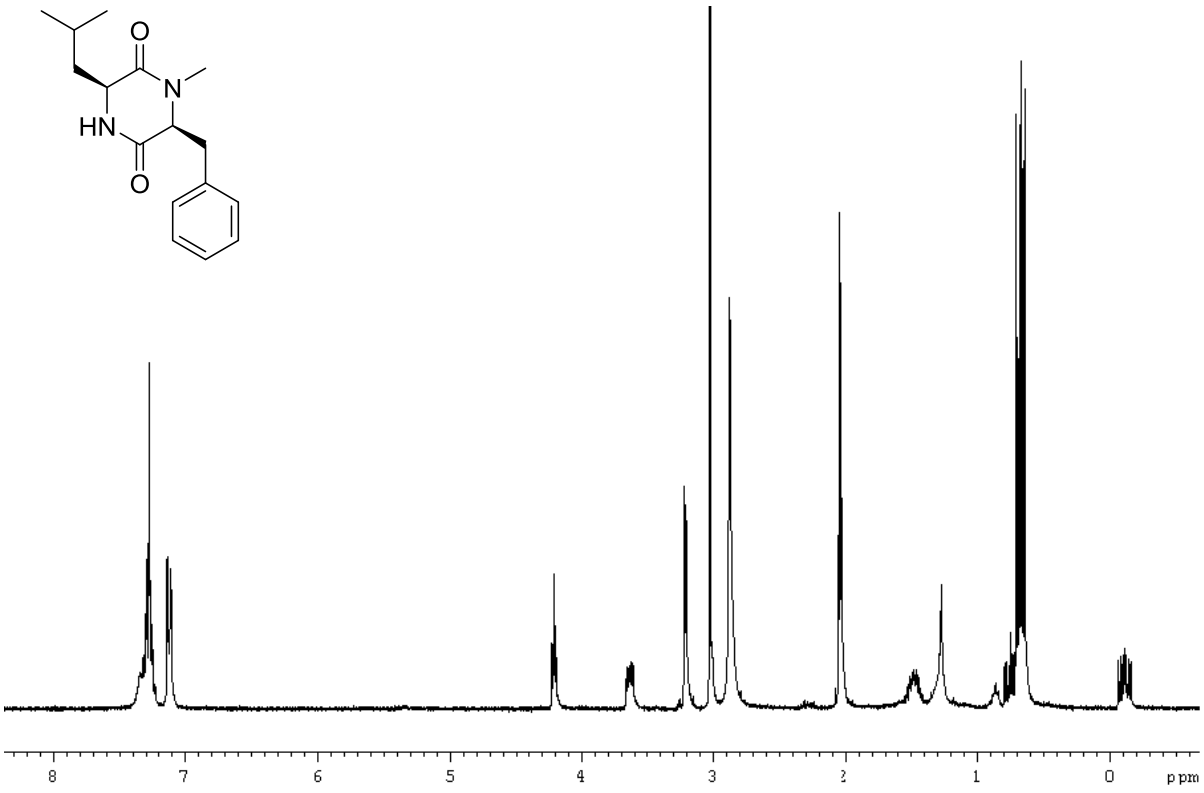

Fig S18. ^{13}C NMR (75 MHz, CD_3COCD_3) spectrum of peptide 8.

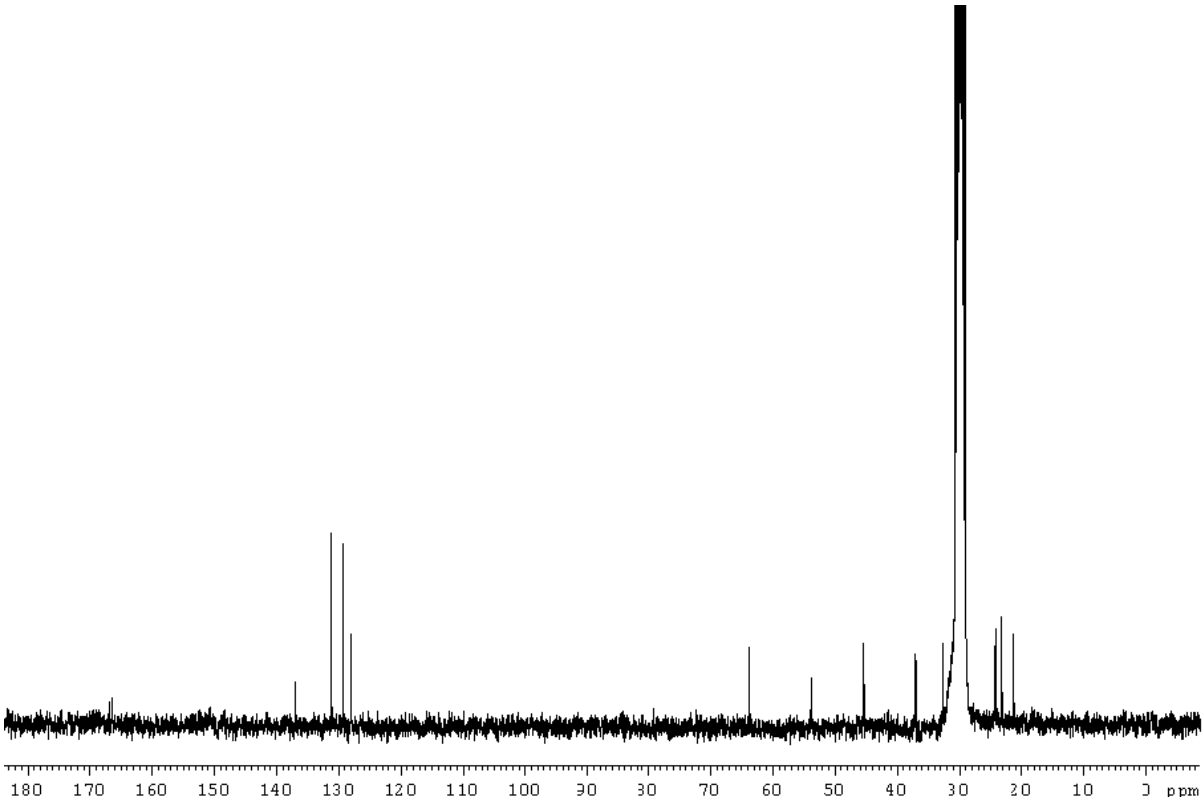

Fig S19. ^{1}H NMR (500 MHz, CD_3COCD_3) spectrum of peptide 9.

(-)-Cyclo-[N-methyl-(L)-leucyl, (L)-phenylalanyl]

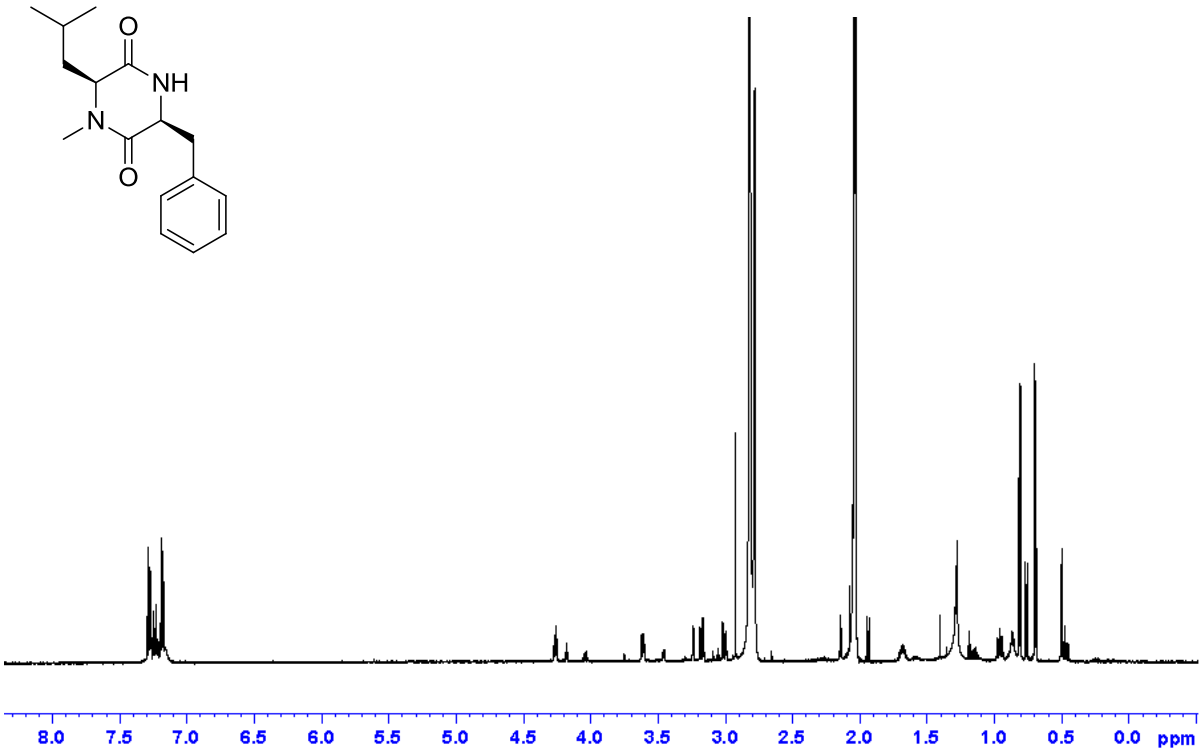

Fig S20. ^{13}C NMR (125 MHz, CD_3COCD_3) spectrum of peptide 9.

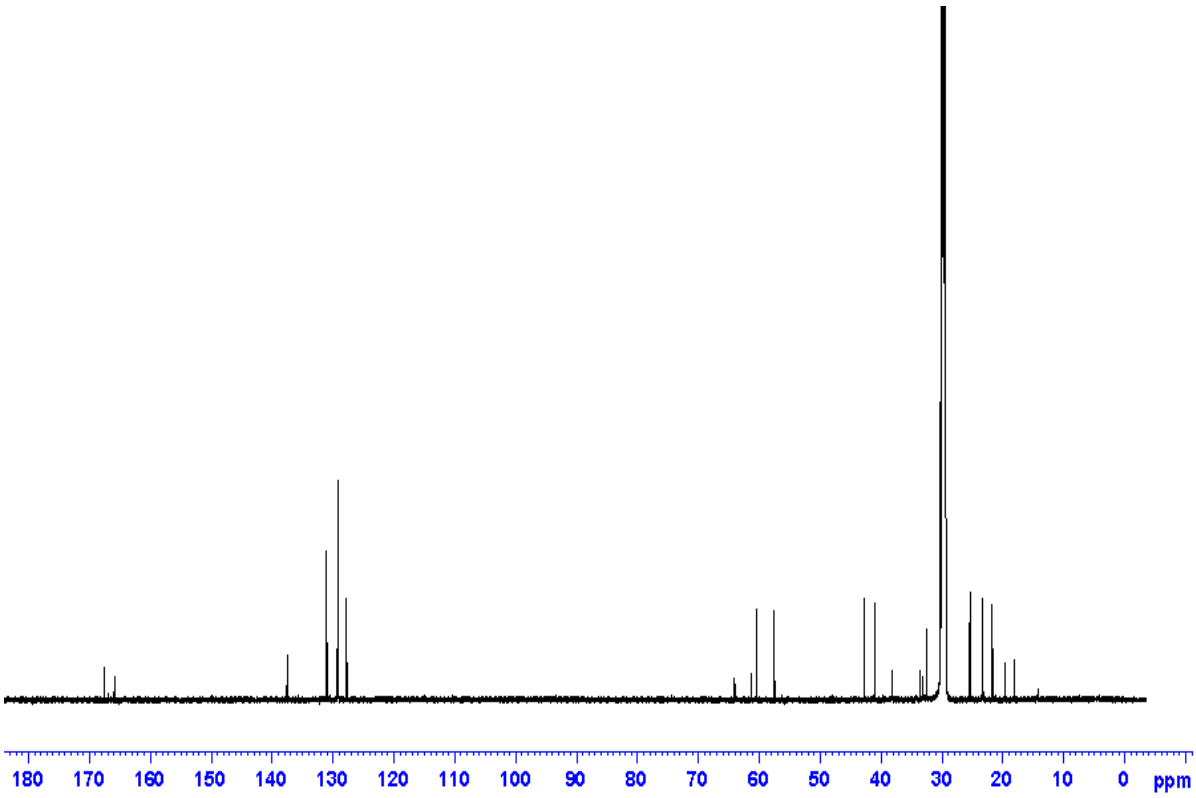

Fig S21. ^{1}H NMR (300 MHz, CD_3COCD_3) spectrum of bisdethiobis(methylthio)-acetylaranotin (BDA).

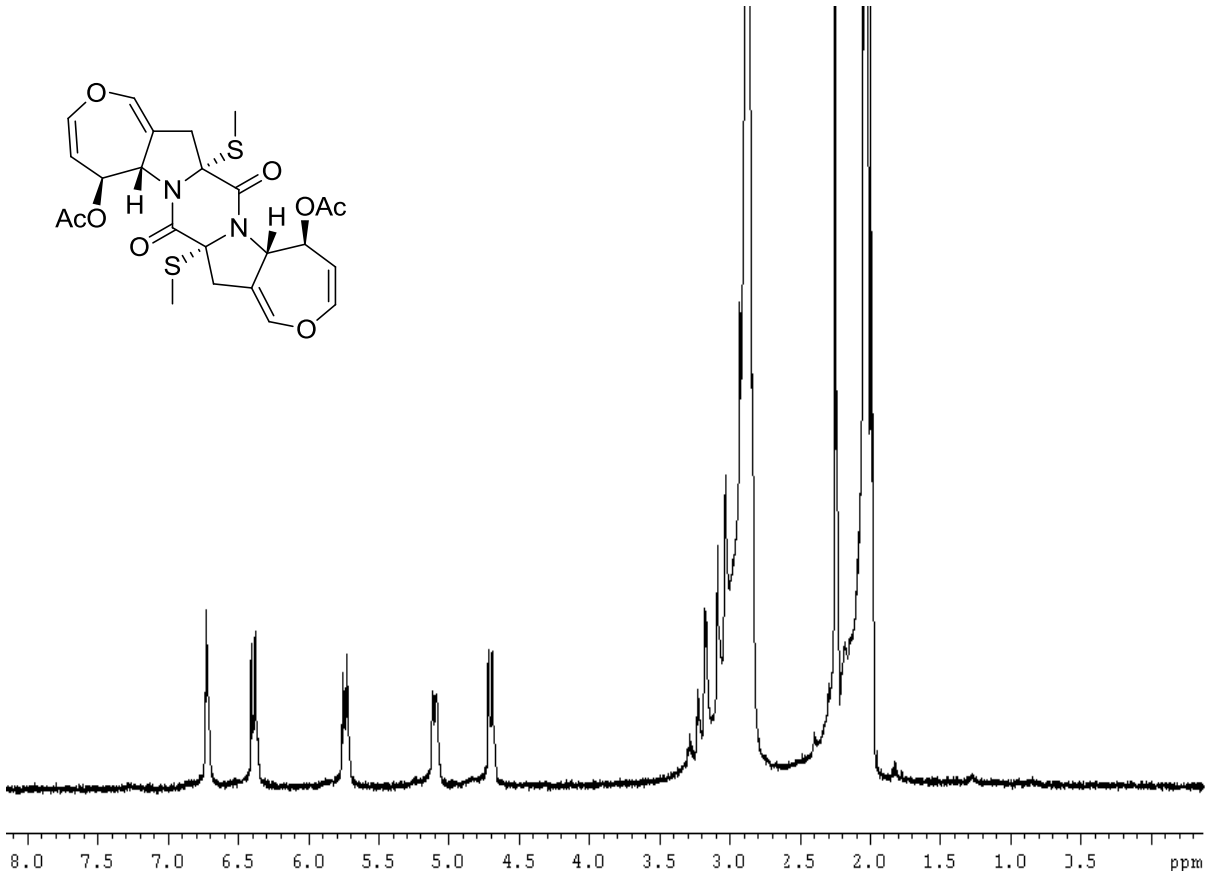

Fig S22. ^{13}C NMR (75 MHz, CD_3COCD_3) spectrum of bisdethiobis(methylthio)-acetylaranotin (BDA).

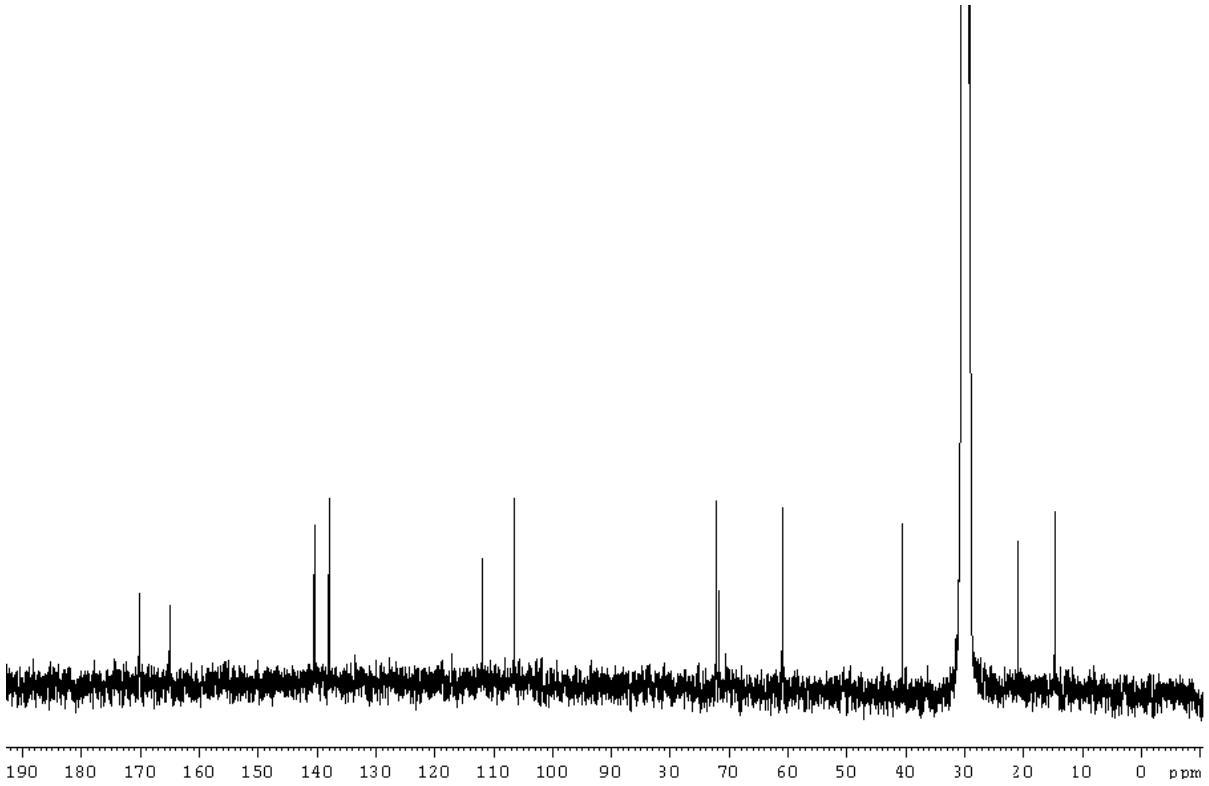

Fig S23. ^{1}H NMR (300 MHz, CD_3COCD_3) spectrum of bisdethiobis(methylthio)-acetylapoaranotin (BDAA).

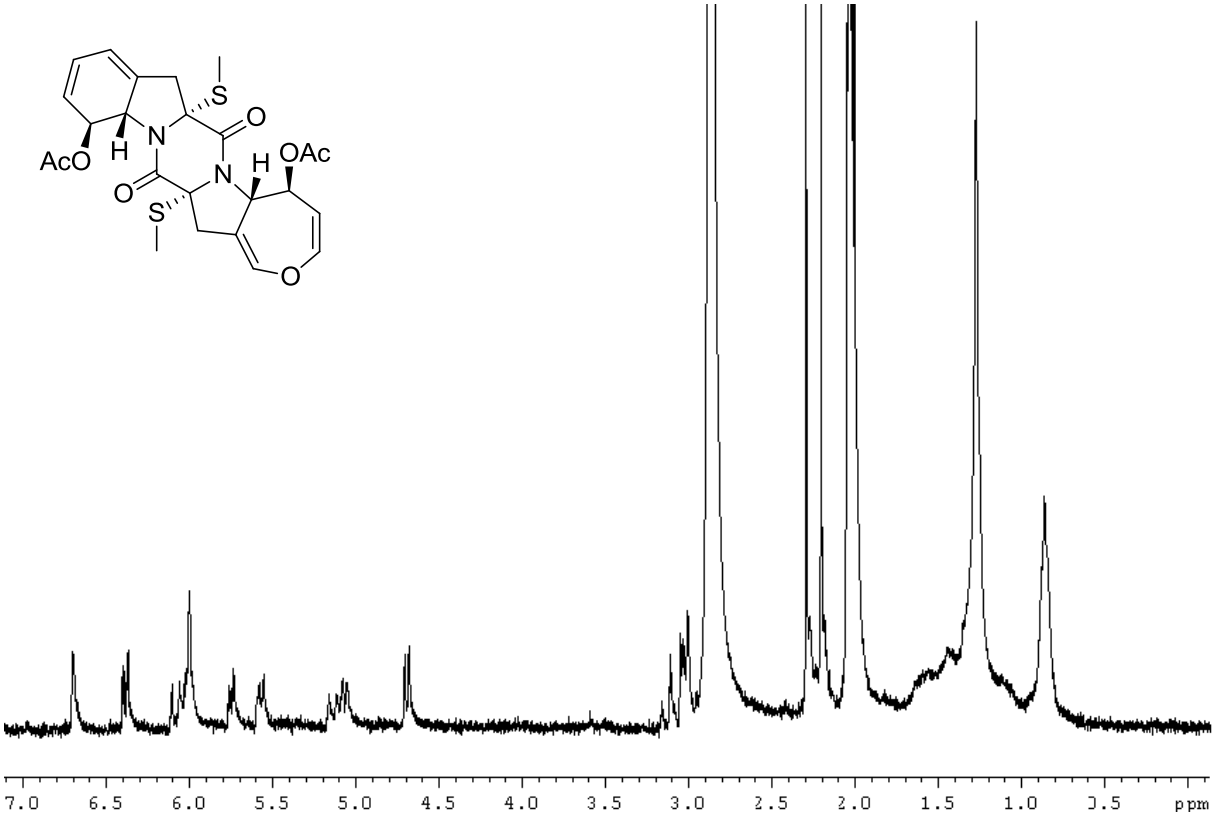

Fig S24. ^{13}C NMR (75 MHz, CD_3COCD_3) spectrum of bisdethiobis(methylthio)-acetylapoaranotin (BDAA).

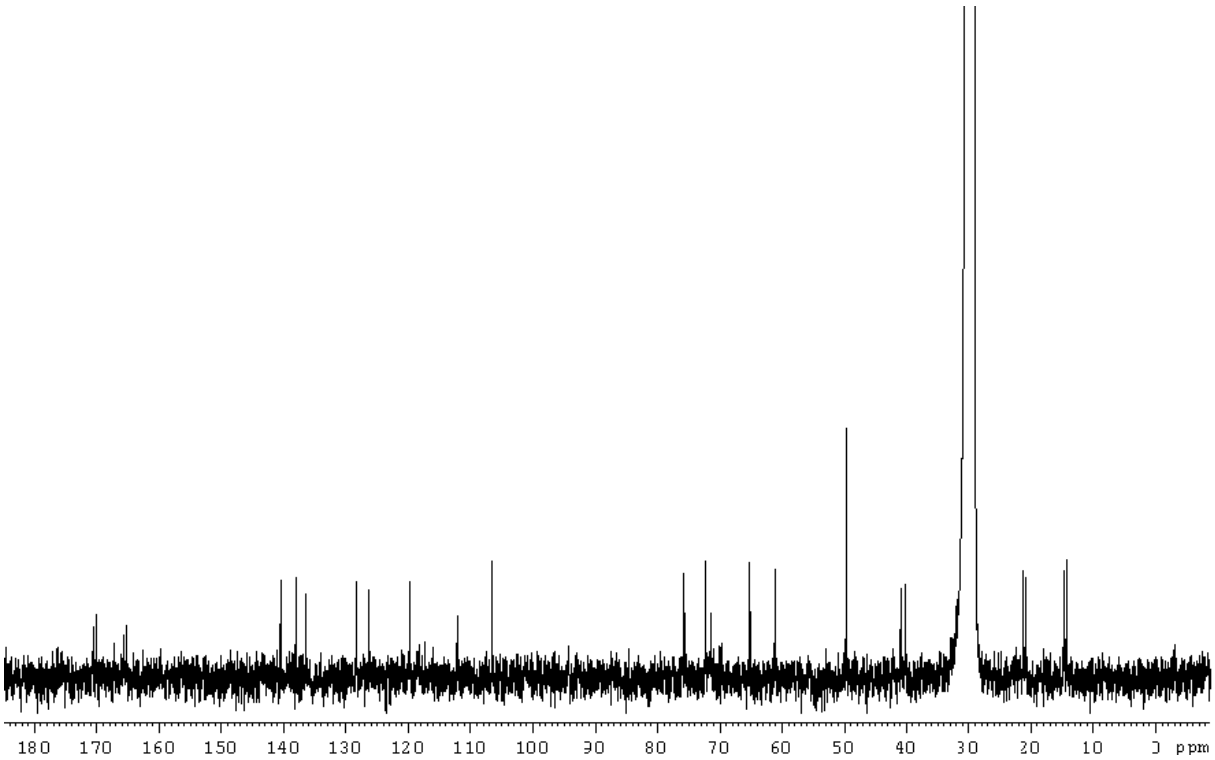

Table S1. 1D NMR spectroscopic data for bisdethiobis(methylthio)-acetylaranotin (BDA) and bisdethiobis(methylthio)-acetylapoaranotin (BDAA).

	BDA		BDAA	
Position	δ_C, mult.[a, b]	δ_H (*J* in Hz)[a]	δ_C, mult.[a, b]	δ_H (*J* in Hz)[a]
1	165.08, qC	-	165.63, qC	-
2	71.70, qC	-	75.53, qC	-
3	40.60, CH_2	3.20, d (15.4) 3.00, d (15.4)	40.17, CH_2	3.11, t (2.2) 3.16, t (2.2)
4	111.93, qC	-	-	-
5	138.04, CH	6.73, t (2.2)	119.75, CH	6.02, m
6	140.52, CH	6.40, dd (8.1, 2.6)	126.29, CH	6.00, m
7	106.55, CH	4.70, dd (8.4, 1.8)	128.30, CH	5.59, m
8	72.22, CH	5.74, dt (8.4, 2.2)	75.90, CH	6.70, m
9	60.97, CH	5.10, d (8.4)	65.21, CH	5.14, d (13.9)
10	170.17, qC	-	170.60, qC	-
11	20.93, CH_3	1.99, s	21.31, CH_3	2.01, s
2-SCH_3	14.69, CH_3	2.25, s	14.35, CH_3	2.20, s
1‘			165.27, qC	-
2‘			71.50, qC	-
3‘			40.96, CH_2	3.11, t (2.2) 3.16, t (2.2)
4‘			112.12, qC	-
5‘			138.07, CH	6.70, d (1.83)
6‘			140.50, CH	6.39, dd (8.1, 2.2)
7‘			106.52, CH	4.69, dd (8.1, 1.8)
8‘			72.30, CH	5.75, dt (8.4, 1.8)
9‘			61.13, CH	5.06, d (8.0)
10‘			170.13, qC	-
11‘			20.96, CH_3	2.00, s
2‘-SCH_3			14.75, CH_3	2.29, s

[a] CD_3COCD_3, 300/75 MHz. [b] Implied multiplicities determined by DEPT.

Fig S25. Key COSY and HMBC correlations of cyclic peptides.

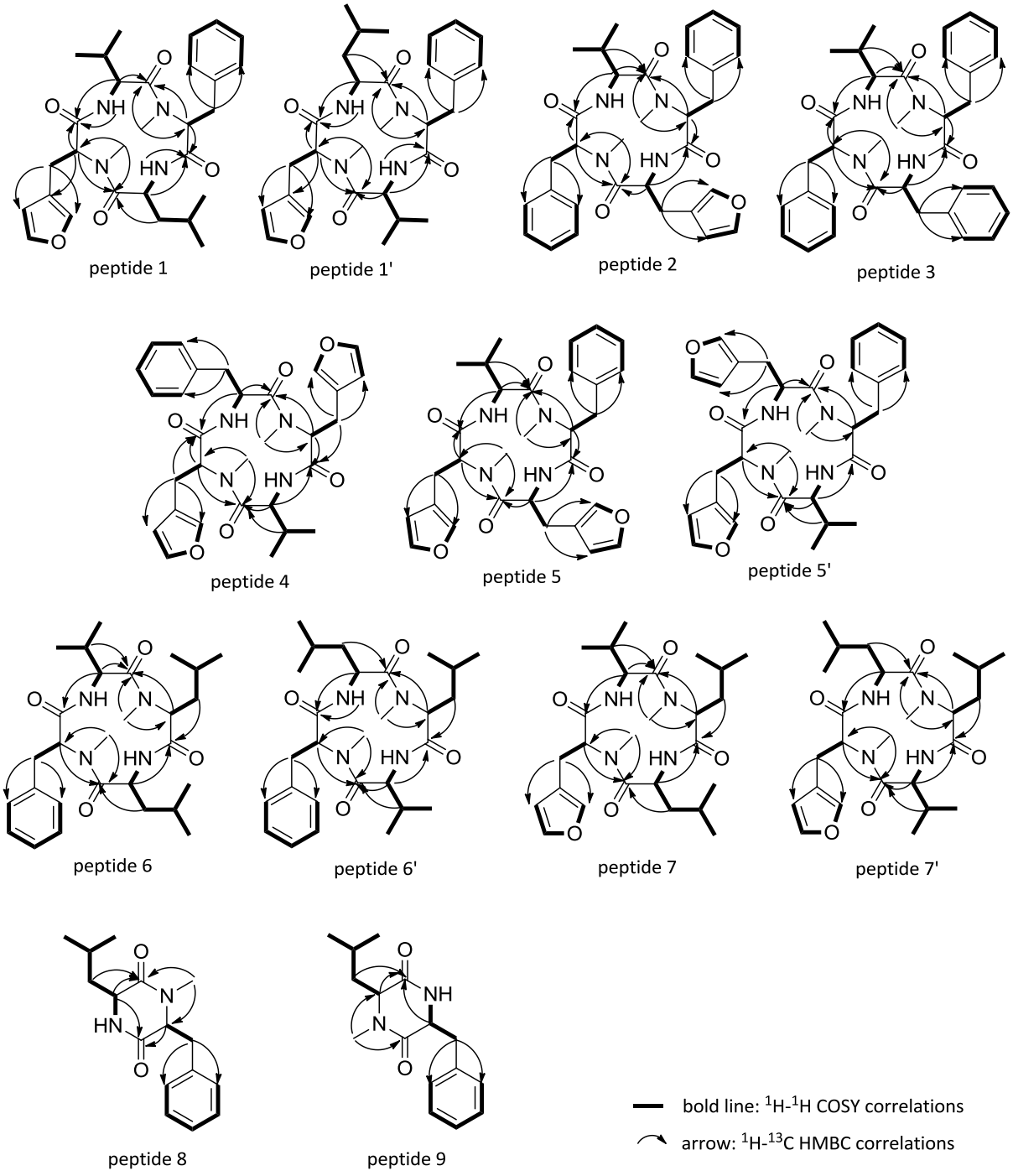

8.3 ^{13}C NMR data of labeled metabolites

Fig S26. ^{13}C NMR (75 MHz, CD_3COCD_3) spectrum of peptide 1 and 1’ after feeding [1-^{13}C]phenylalanine.

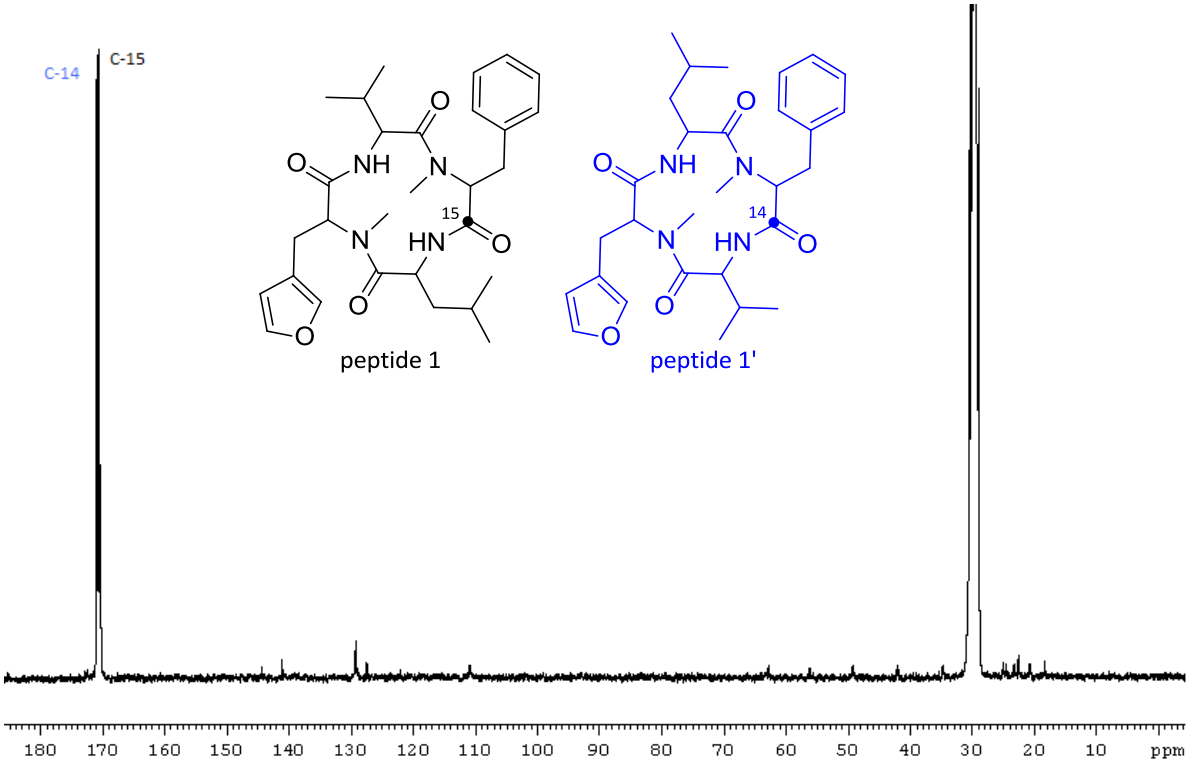

Fig S27. ^{13}C NMR (75 MHz, CD_3COCD_3) spectrum of peptide 3 after feeding [1-^{13}C]phenylalanine.

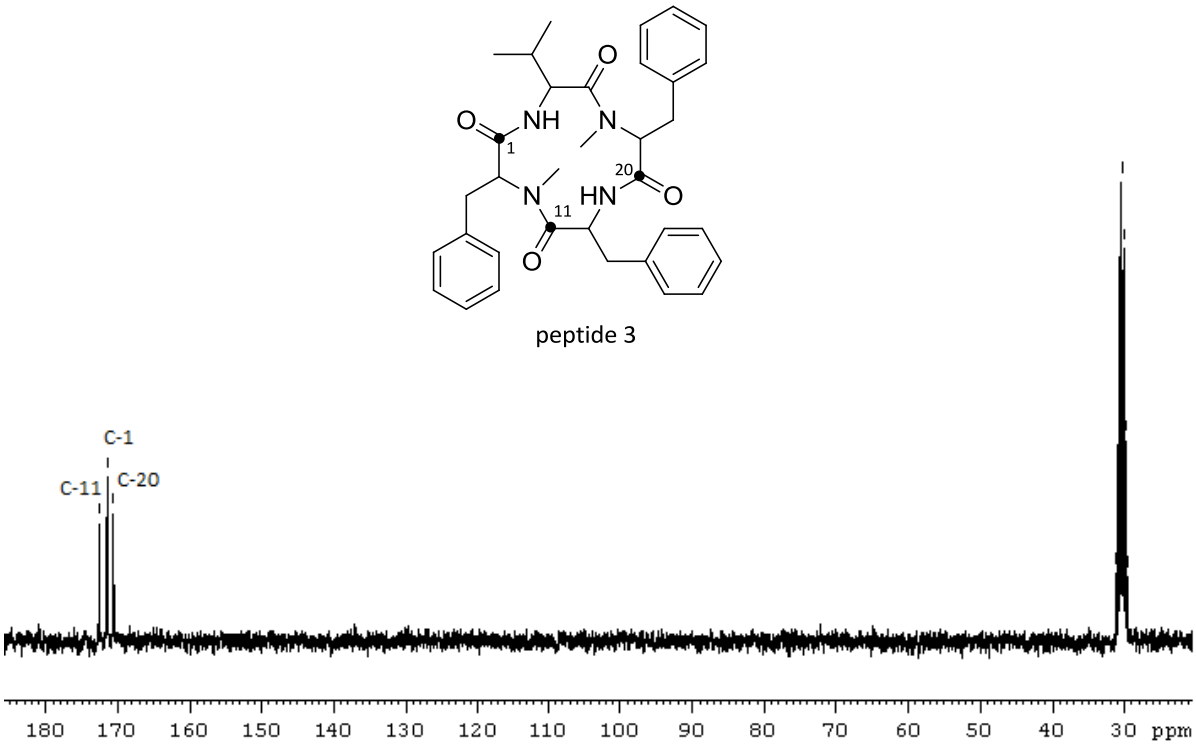

Fig S28. Inverse gated ^{1}H decoupled ^{13}C NMR (75 MHz, CD_3COCD_3) spectrum of peptide 1 and 1' after feeding [U-^{13}C]glycerol.

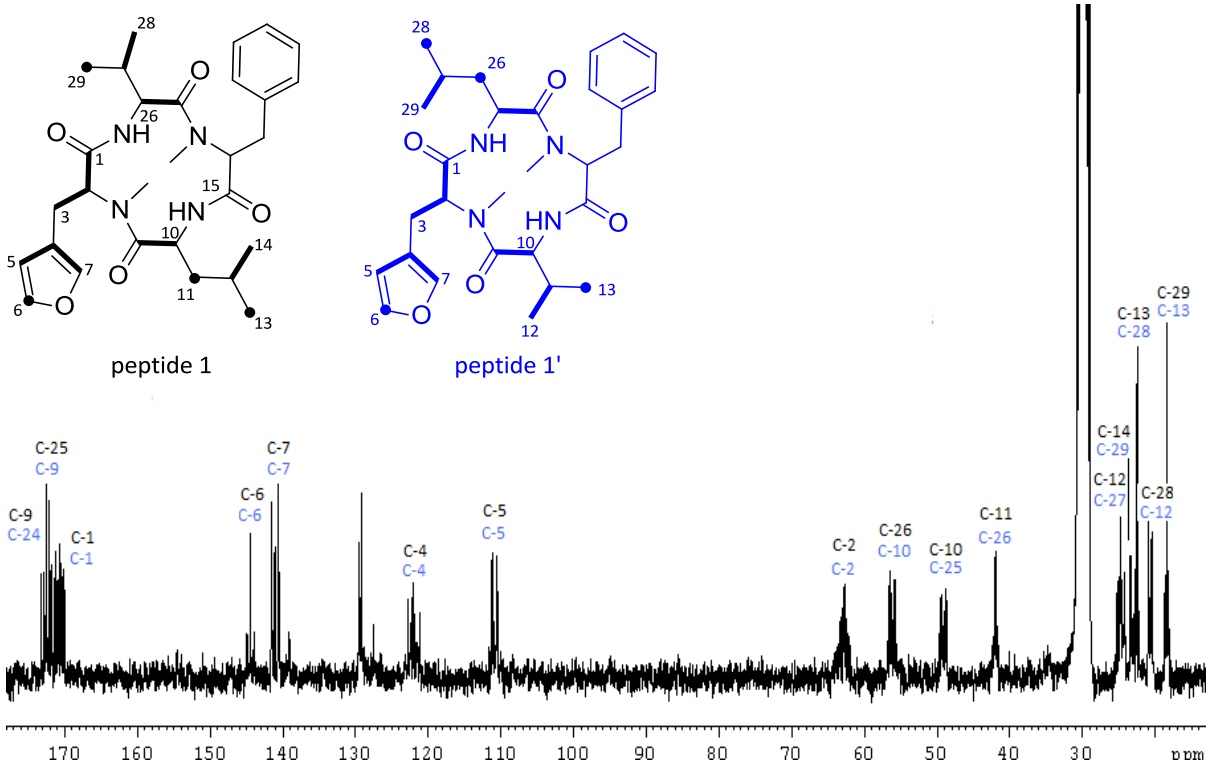

Fig S29. Inverse gated ^{1}H decoupled ^{13}C NMR (75 MHz, CD_3COCD_3) spectrum of peptide 1 and 1' after feeding [1-^{13}C]glucose.

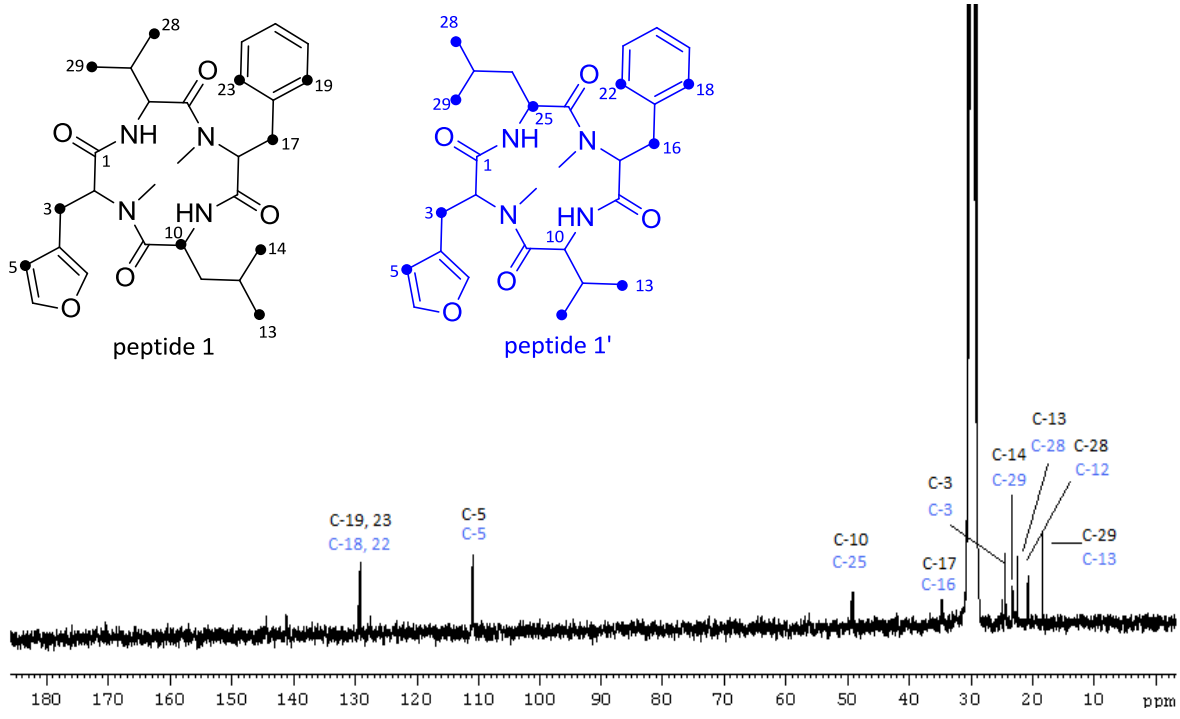

Fig S30. ^{13}C NMR (75 MHz, MeOD) spectrum of peptide 1 and 1’ after feeding [*Me*-^{13}C]methionine.

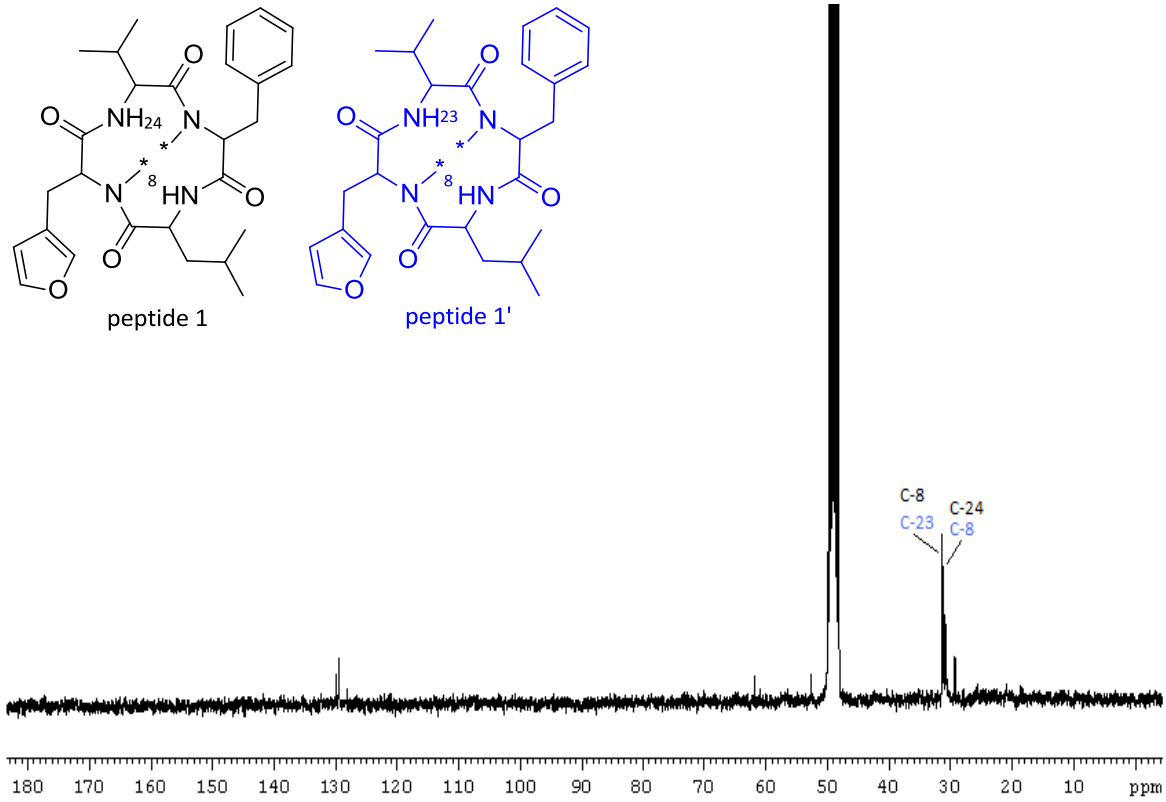

Fig S31. ^{13}C NMR (75 MHz, CD_3COCD_3) spectrum of peptide 1 and 1’ after feeding [1-^{13}C]sodium acetate.

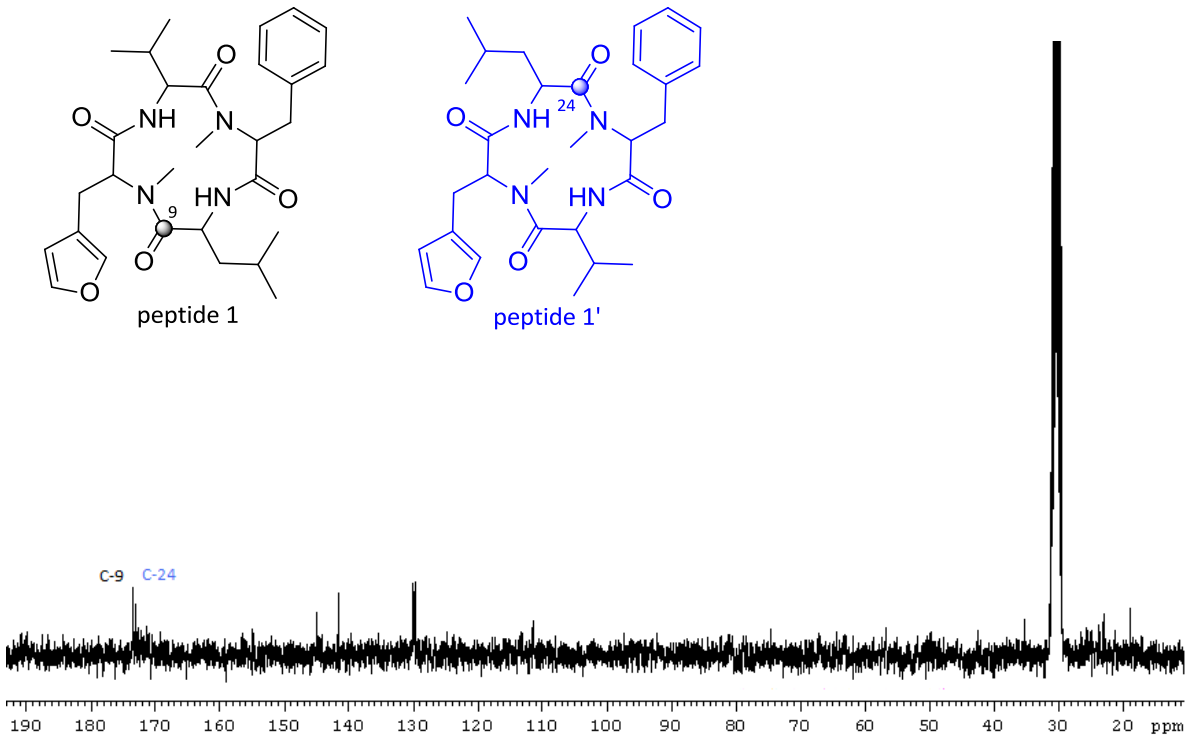

Fig S32. ^{13}C NMR (75 MHz, CD_3COCD_3) spectrum of marilone A after feeding [1-^{13}C]sodium acetate.

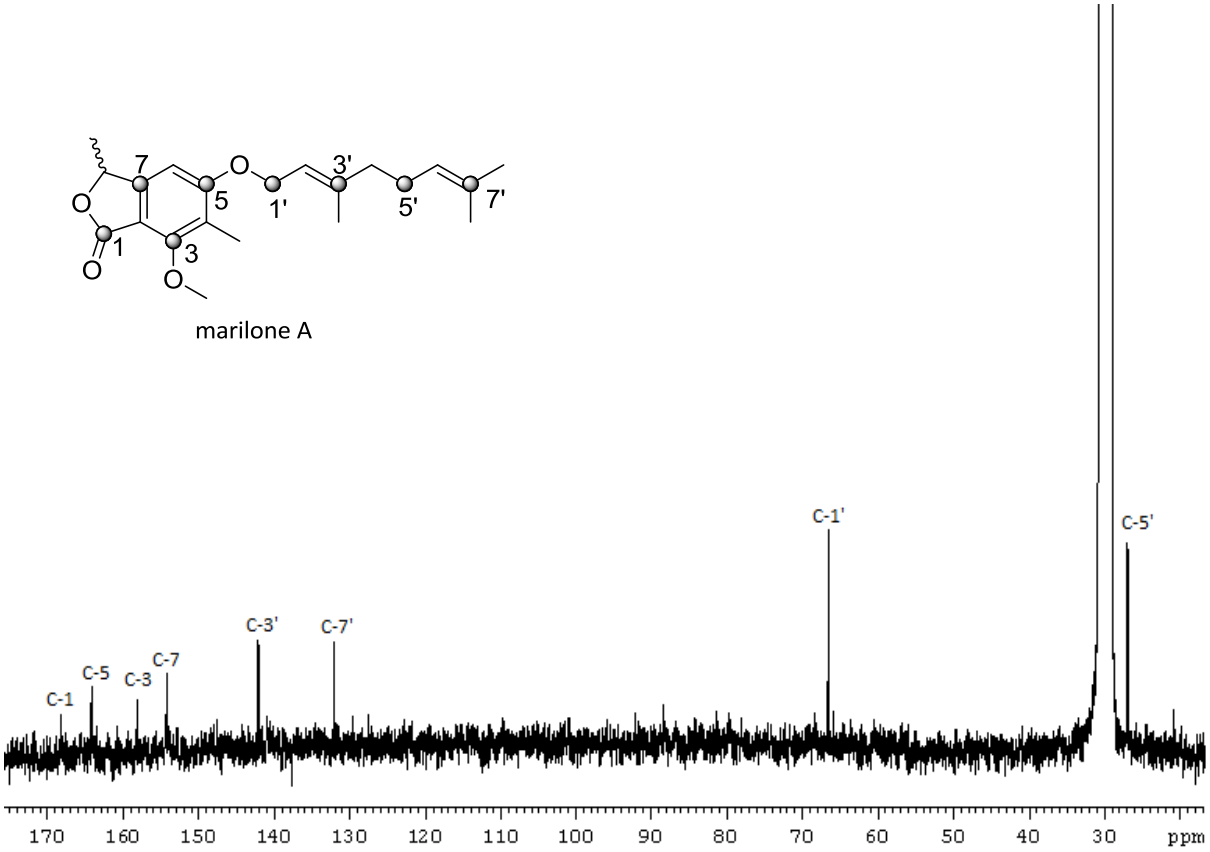

Fig S33. ^{13}C NMR (75 MHz, CD_3COCD_3) spectrum of marilone A (taken from literature).[83]

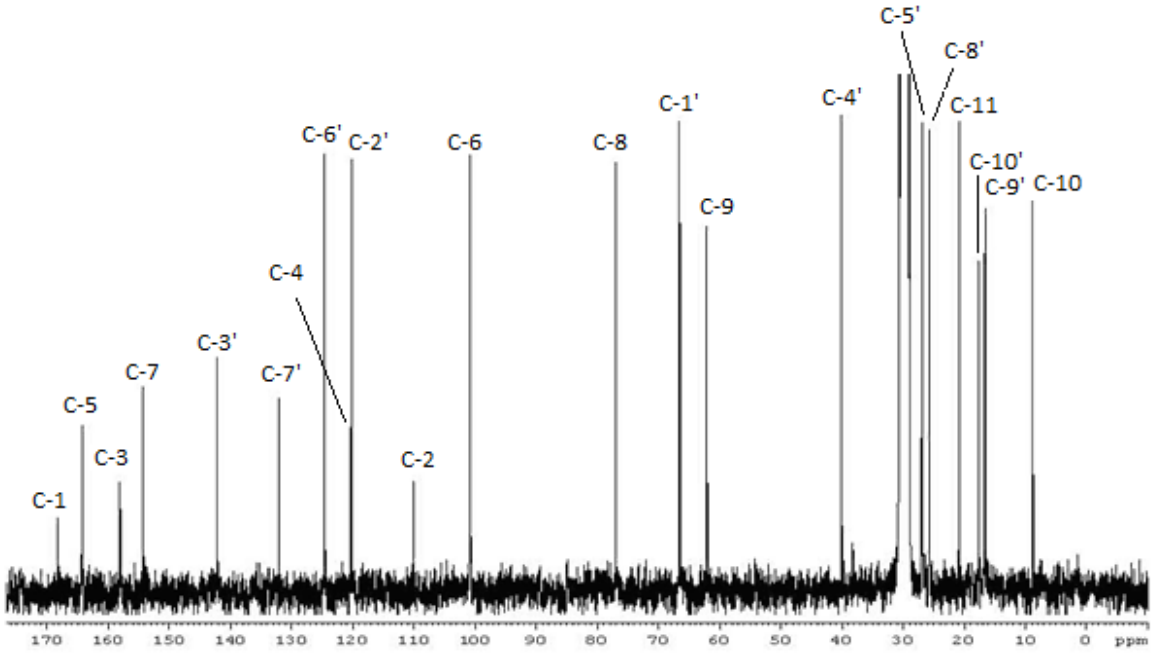

Fig S34. ^{13}C NMR (75 MHz, CD_3COCD_3) spectrum of mariline B after feeding [1-^{13}C]sodium acetate.

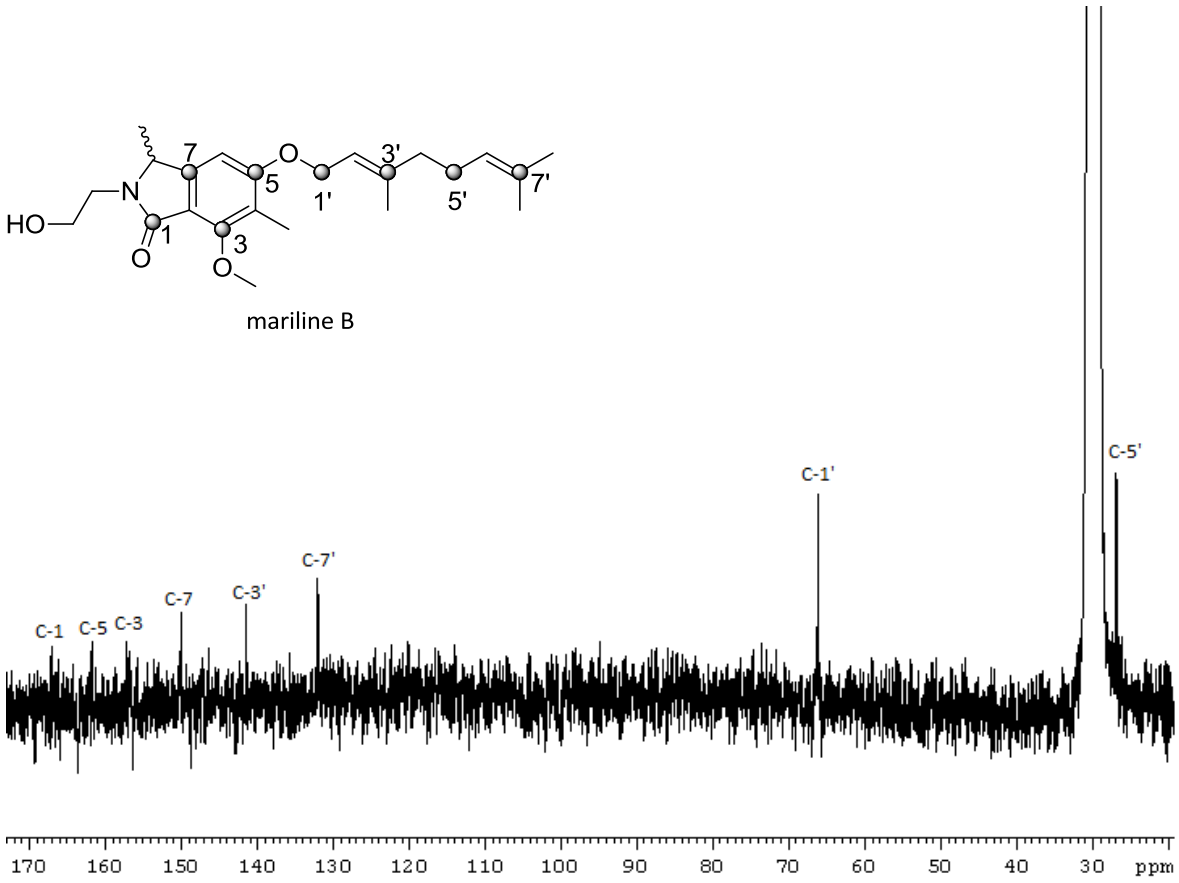

Fig S35. ^{13}C NMR (75 MHz, CD_3COCD_3) spectrum of mariline B (taken from literature).[84]

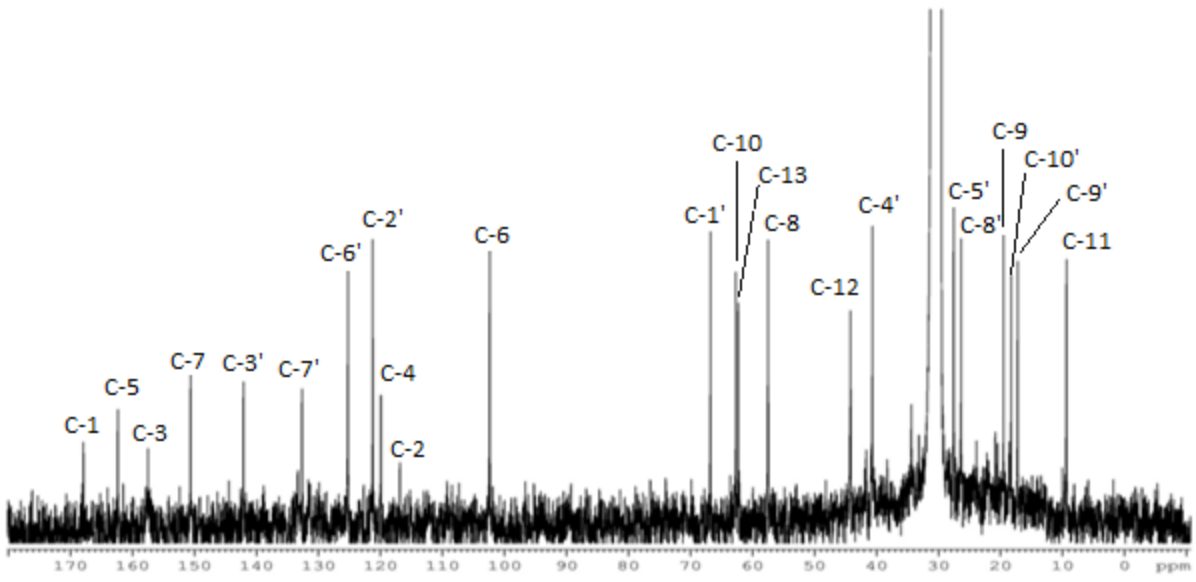

Table S2. ^{13}C-NMR data for [U-^{13}C]glycerol-derived peptide 1 (not including phenylalanine moiety).

C	δc (ppm)	Signal pattern	$J_{(C,C)}$, Hz
1	170.9, qC	dd	$J_{(1,2)}$=53.0 $J_{(1,3)}$=3.0
2	62.8, CH	dd	$J_{(2,1)}$=53.0 $J_{(2,3)}$=38.0
3	24.5, CH_2	dd	$J_{(3,2)}$=38.0 $J_{(3,1)}$=3.0
4	122.0, qC	dd	$J_{(4,5)}$=49.5 $J_{(4,7)}$=73.0
5	110.9, CH	dd	$J_{(5,4)}$=49.5 $J_{(5,7)}$=3.0
6	144.5, CH	s	-
7	141.1, CH	dd	$J_{(7,4)}$=73.0 $J_{(7,5)}$=3.0
9	172.9, qC	d	$J_{(9,10)}$=54.1
10	49.3, CH	d	$J_{(10,9)}$=54.1
11	42.0, CH_2	s	-
12	25.0, CH	d	$J_{(12,14)}$=35.4
13	22.5, CH_3	s	-
14	23.2, CH_3	d	$J_{(14,12)}$=35.4
25	171.8, qC	d	$J_{(25,26)}$=54.1
26	56.2, CH	d	$J_{(26,25)}$=54.1
27	30.0, CH_2	NO	NO
28	20.7, CH_3	d	$J_{(28,27)}$=35.4
29	18.4, CH_3	s	-

dd: doublet of doublet, d: doublet, s: singlet, NO: not observed

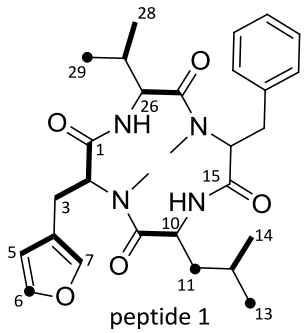

peptide 1

Table S3. ^{13}C-NMR data for [U-^{13}C]glycerol-derived peptide 1’ (not including phenylalanine moiety).

C	δc (ppm)	Signal pattern	$J_{(C,C)}$,Hz
1	170.5, qC	dd	$J_{(1,2)}$=53.0 $J_{(1,3)}$=3.0
2	62.7, CH	dd	$J_{(2,1)}$=53.0 $J_{(2,3)}$=38.0
3	24.5, CH_2	dd	$J_{(3,2)}$=38.0 $J_{(3,1)}$=3.0
4	122.0, qC	dd	$J_{(4,5)}$=49.5 $J_{(4,7)}$=73.0
5	110.9, CH	dd	$J_{(5,4)}$=49.5 $J_{(5,7)}$=3.0
6	144.5, CH	s	-
7	141.1, CH	dd	$J_{(7,4)}$=73.0 $J_{(7,5)}$=3.0
9	172.2, qC	d	$J_{(9,10)}$=54.1
10	56.3, CH	d	$J_{(10,9)}$=54.1
11	30.2, CH	NO	NO
12	20.8, CH_3	d	$J_{(12,11)}$=35.4
13	18.4, CH_3	s	-
24	172.5, qC	d	$J_{(24,25)}$=54.1
25	49.1, CH	d	$J_{(25,24)}$=54.1
26	41.9, CH_2	s	-
27	25.0, CH	d	$J_{(27,29)}$=35.4
28	22.5, CH_3	s	-
29	23.3, CH_3	d	$J_{(29,27)}$=35.4

dd: doublet of doublet, d: doublet, s: singlet, NO: not observed

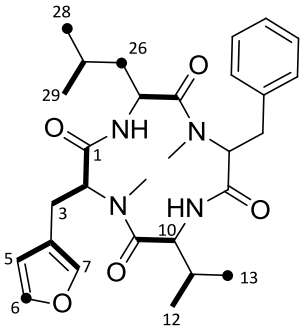

peptide 1'

Table S4. ^{13}C-NMR chemical shifts and ^{13}C enrichments (highlighted boxes) of relevant carbons from incorporation of [1-^{13}C]sodium acetate into marilone A and mariline B.[83,84]

	Marilone A	Mariline B
Position	δ_C, mult.[a,b]	δ_C, mult.[a,b]
1	168.2, qC	167.3, qC
2	110.0, qC	116.3, qC
3	158.0, qC	156.9, qC
4	120.4, qC	119.3, qC
5	164.2, qC	161.7, qC
6	100.8, CH	101.8, CH
7	154.2, qC	150.0, qC
8	77.0, CH	56.9, CH
9	62.1, CH_3	18.9, CH_3
10	8.8, CH_3	62.1, CH_3
11	20.9, CH_3	8.8, CH_3
12	-	43.6, CH_2
13	-	61.7, CH_2
1’	66.5, CH_2	66.2, CH_2
2’	120.1, CH	120.6, CH
3’	142.1, qC	141.5, qC
4’	40.1, CH_2	40.1, CH_2
5’	26.9, CH_2	27.0, CH_2
6’	124.6, CH	124.6, CH
7’	132.1, qC	132.1, qC
8’	25.8, CH_3	25.8, CH_3
9’	16.7, CH_3	16.7, CH_3
10’	17.7, CH_3	17.7, CH_3

[a]Acetone-d_6, 75 MHz. [b]Implied multiplicities determined by DEPT.

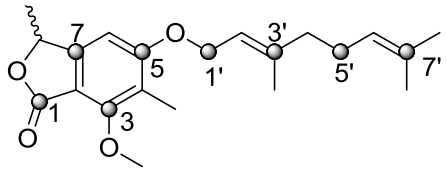

marilone A

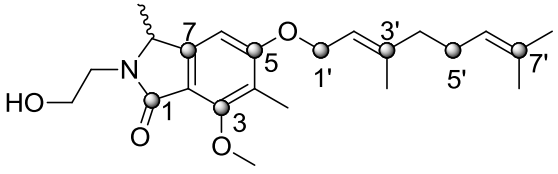

mariline B

8.4 LC-ESIMS data

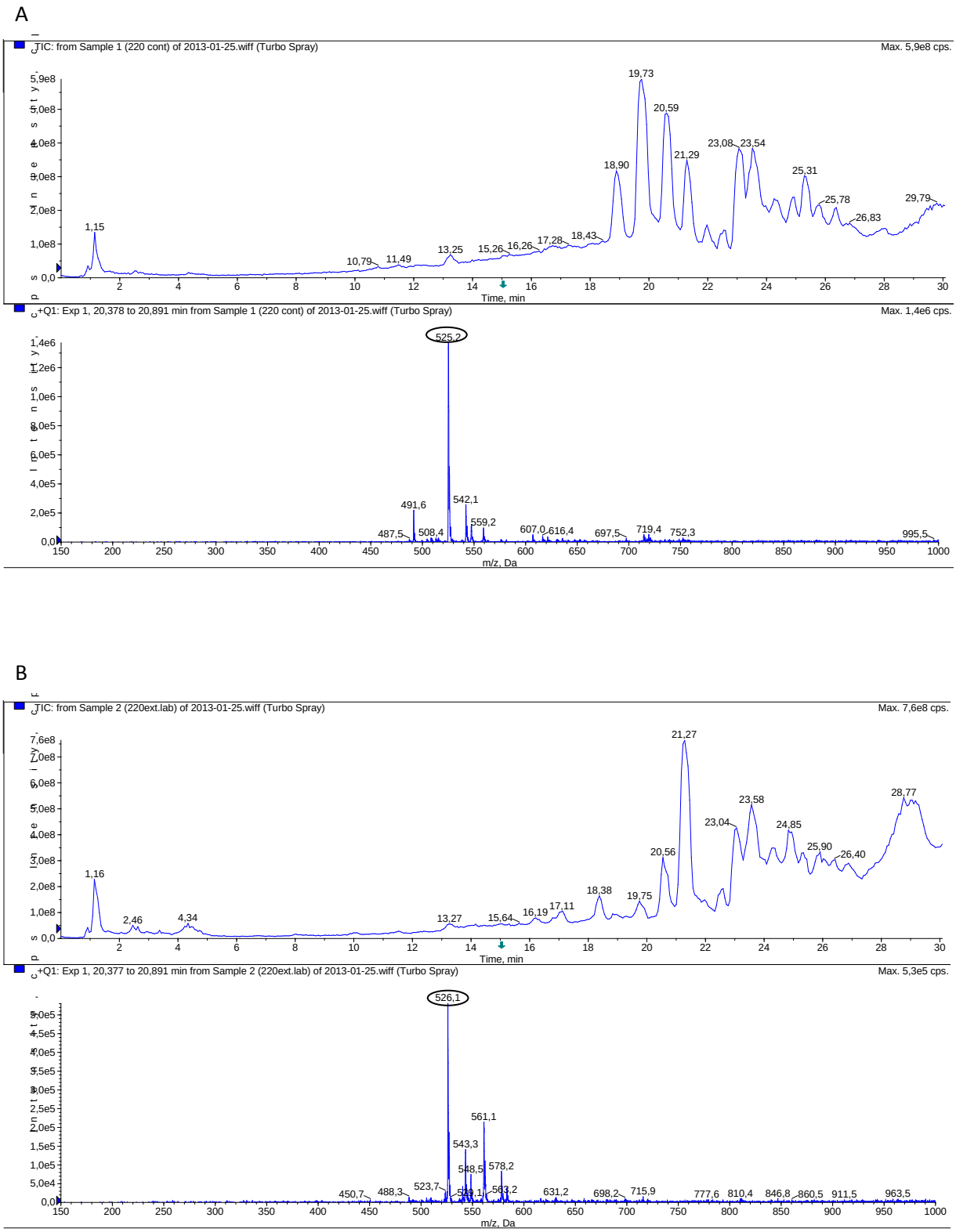

Fig S36. LC-ESIMS spectra of crude extract of *Stachylidium* sp. BMS agar culture (A) control, showing mass peak at *m/z* 525.2 $[M+H]^+$, and supplemented with (B) [1-^{13}C] phenylalanine, showing major isotopic mass peak at *m/z* 526.1 $[M+H+1]^+$.

A

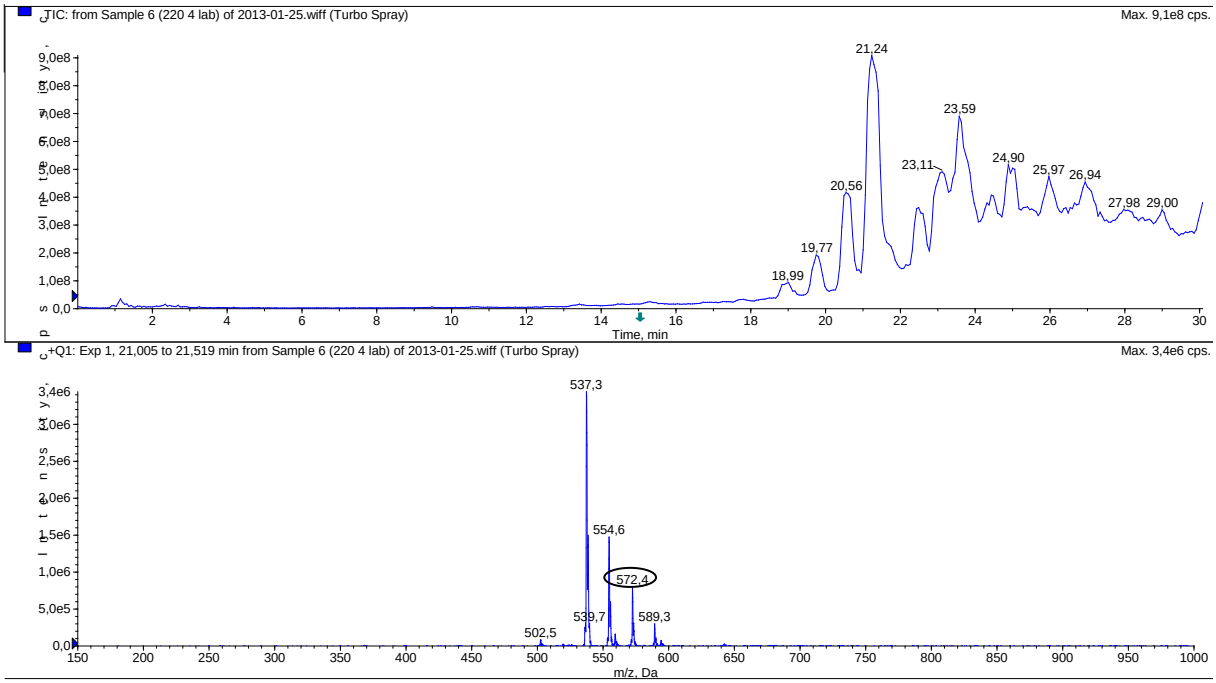

B

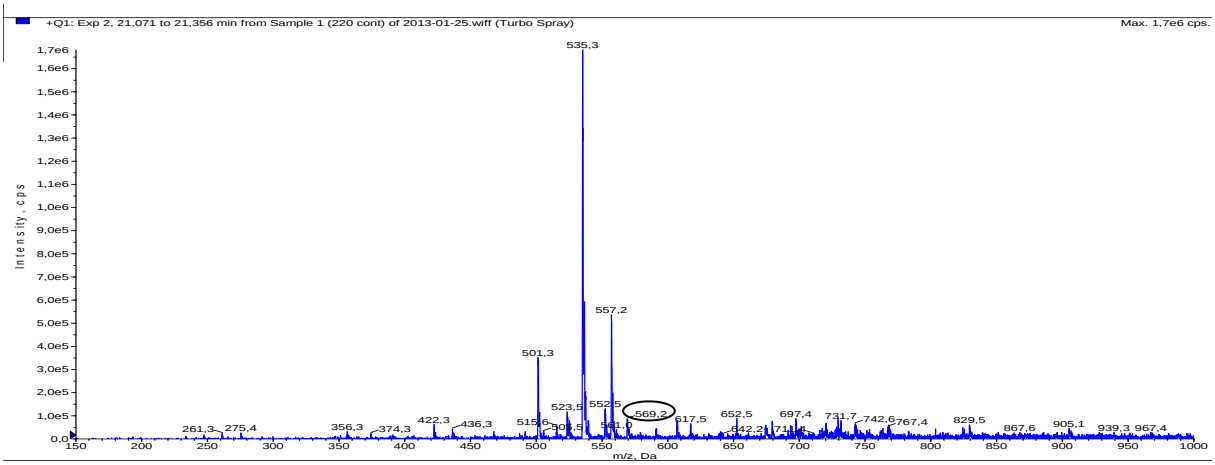

Fig S37. LC-ESIMS spectra of crude extract of *Stachylidium* sp. BMS agar culture (A) supplemented with [1-^{13}C] phenylalanine, showing isotopic mass peak for peptide 3 at *m/z* 572.4 $[M+H+3]^+$ and (B) control, showing mass peak at *m/z* 569.2 $[M+H]^+$ for peptide 3.

A

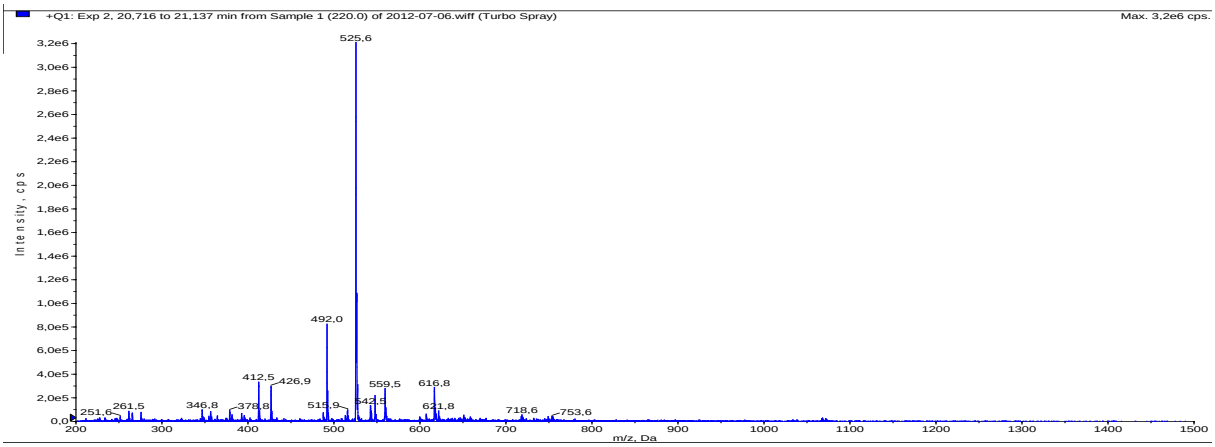
+Q1: Exp 2, 20,716 to 21,137 min from Sample 1 (220.0) of 2012-07-06.wiff (Turbo Spray)
Max. 3,2e6 cps.
Intensity, cps
m/z, Da
525,6
492,0
412,5
426,9
559,5
616,8
251,6
261,5
346,8
378,8
515,9
542,5
621,8
718,6
753,6

B

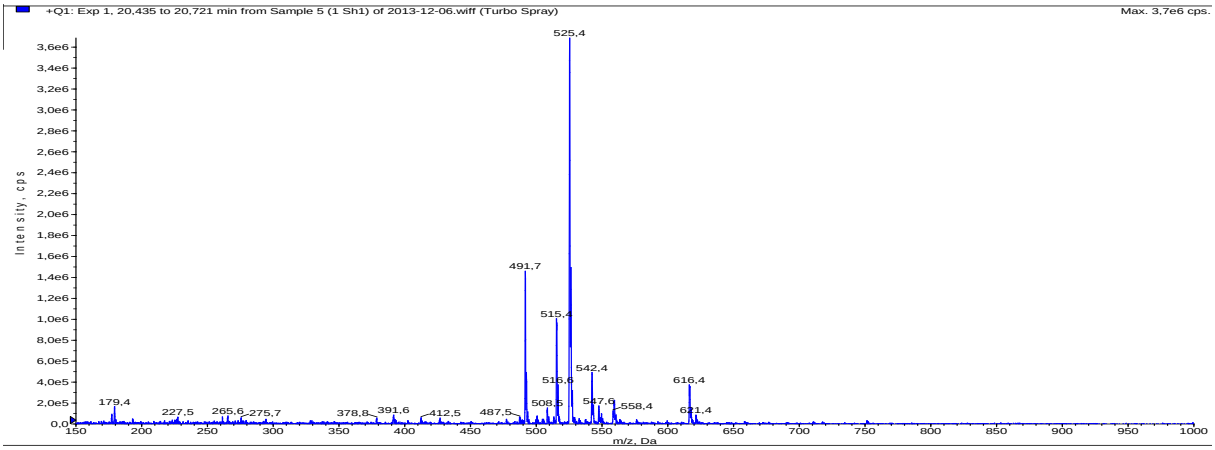
+Q1: Exp 1, 20,435 to 20,721 min from Sample 5 (1 Sh1) of 2013-12-06.wiff (Turbo Spray)
Max. 3,7e6 cps.
Intensity, cps
m/z, Da
525,4
491,7
515,4
542,4
516,6
616,4
179,4
227,5
265,6
275,7
378,8
391,6
412,5
487,5
508,5
547,6
558,4
621,4

C

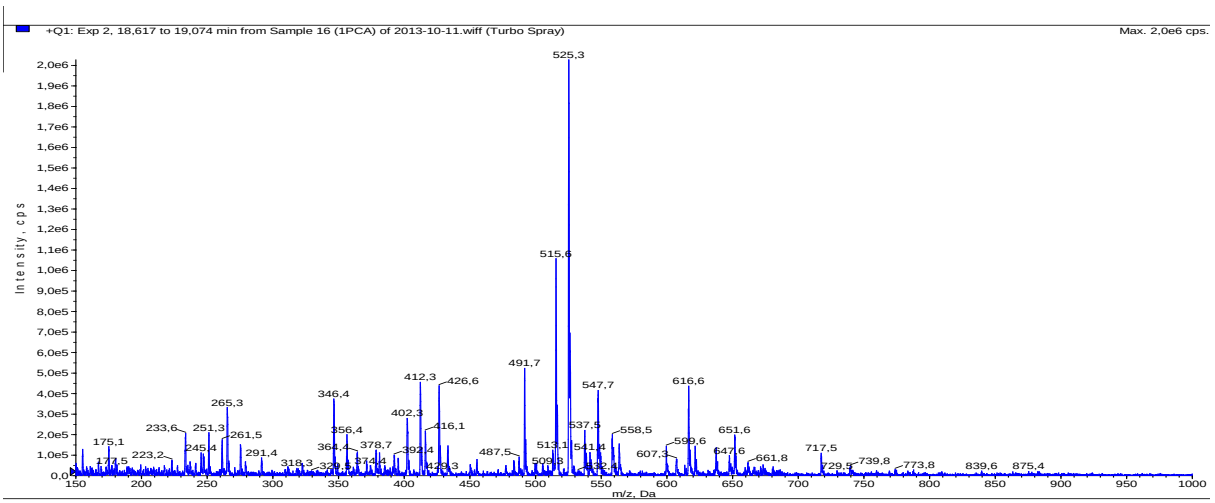
+Q1: Exp 2, 18,617 to 19,074 min from Sample 16 (1PCA) of 2013-10-11.wiff (Turbo Spray)
Max. 2,0e6 cps.
Intensity, cps
m/z, Da
525,3
515,6
491,7
412,3
426,6
547,7
616,6
346,4
265,3
402,3
416,1
537,5
558,5
651,6
233,6
251,3
261,5
356,4
378,7
599,6
175,1
223,2
245,4
291,4
364,4
392,4
487,5
513,1
541,4
607,3
647,6
661,8
717,5
729,5
739,8
773,8
839,6
875,4

D

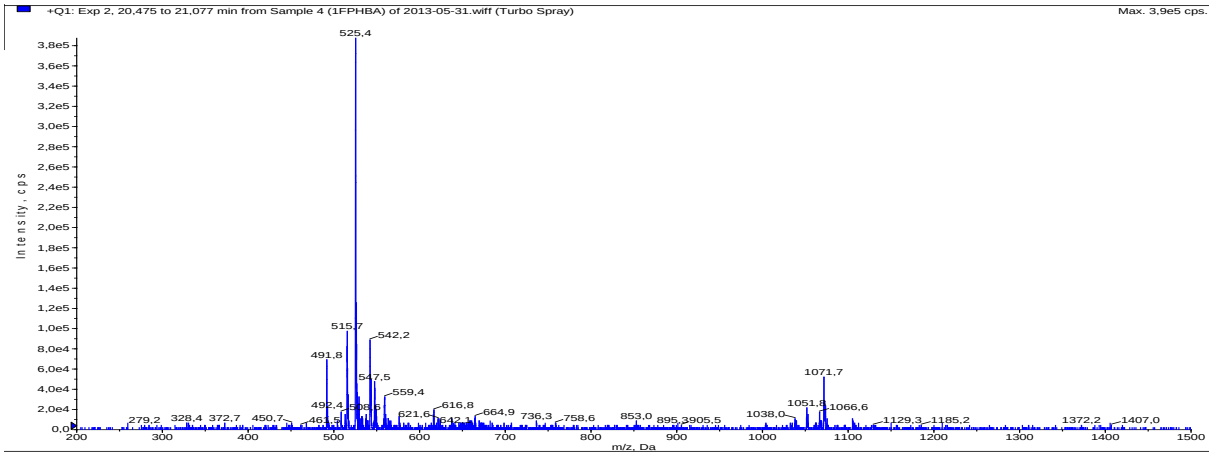

Fig S38. LC-ESIMS spectra of crude extract of *Stachylidium* sp. BMS agar culture (A) control, supplemented with (B) [1,7-^{13}C]shikimic acid, (C) 2-chloro-protocatechuic acid and (D) 2-fluoro-4-hydroxybenzoic acid. No new ions were observed as compared to control.

A

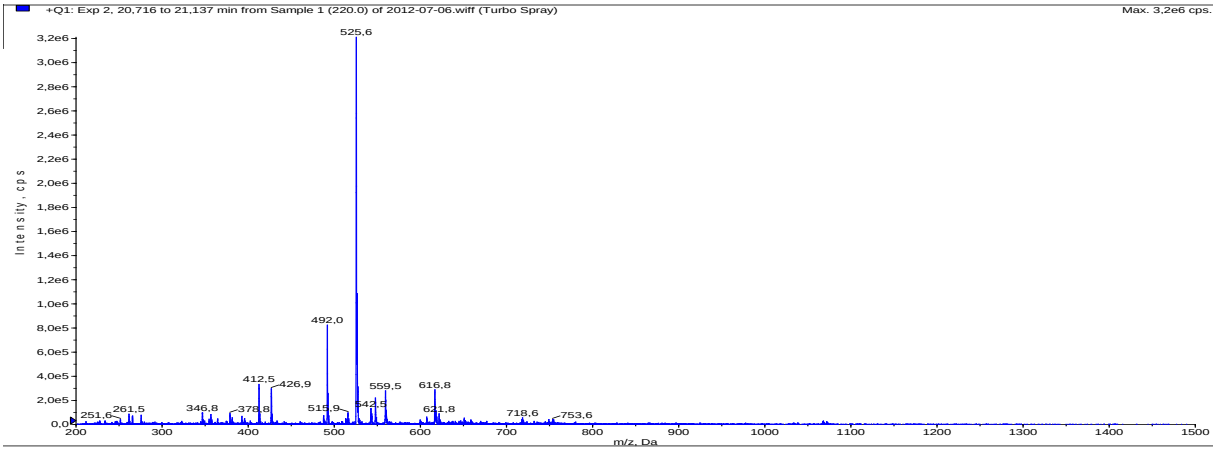
+Q1: Exp 2, 20,716 to 21,137 min from Sample 1 (220.0) of 2012-07-06.wiff (Turbo Spray)
Max. 3,2e6 cps.
Intensity, cps
m/z, Da
525,6
492,0
412,5
426,9
559,5
616,8
251,6
261,5
346,8
378,8
515,9
542,5
621,8
718,6
753,6

B

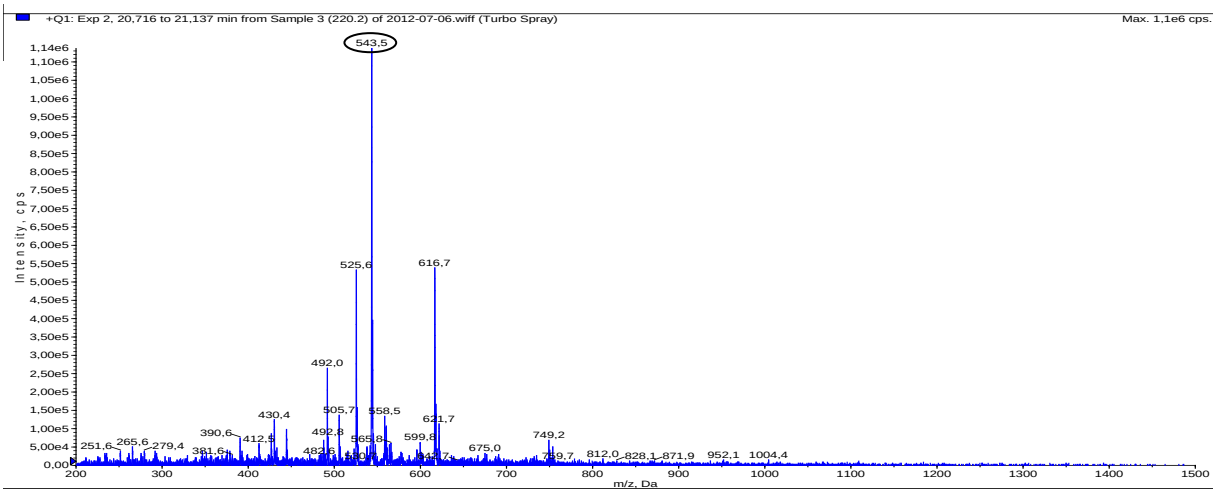
+Q1: Exp 2, 20,716 to 21,137 min from Sample 3 (220.2) of 2012-07-06.wiff (Turbo Spray)
Max. 1,1e6 cps.
Intensity, cps
m/z, Da
543,5
525,6
616,7
492,0
430,4
505,7
558,5
621,7
390,6
412,8
492,8
599,8
749,2
251,6
265,6
279,4
675,0
812,0
828,1
871,9
952,1
1004,4

C

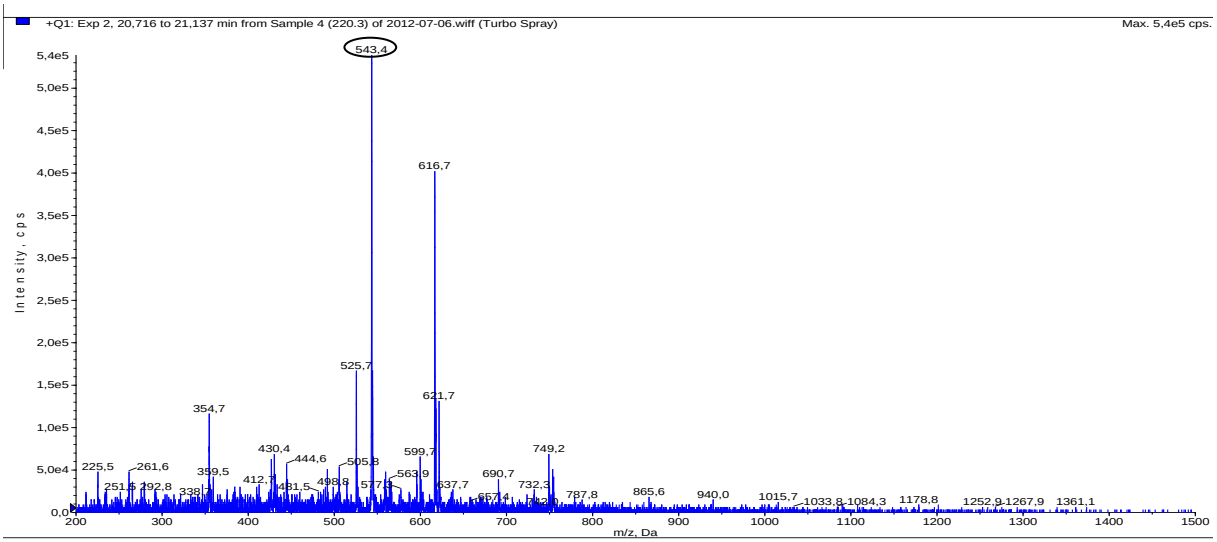
+Q1: Exp 2, 20,716 to 21,137 min from Sample 4 (220.3) of 2012-07-06.wiff (Turbo Spray)
Max. 5,4e5 cps.
Intensity, cps
m/z, Da
543,4
616,7
525,7
621,7
354,7
430,4
444,6
505,8
599,7
749,2
225,5
261,6
359,5
412,7
481,5
498,8
577,5
563,9
637,7
690,7
732,3
787,8
865,6
940,0
1015,7
1033,8
1084,3
1178,8
1252,9
1267,9
1361,1

D

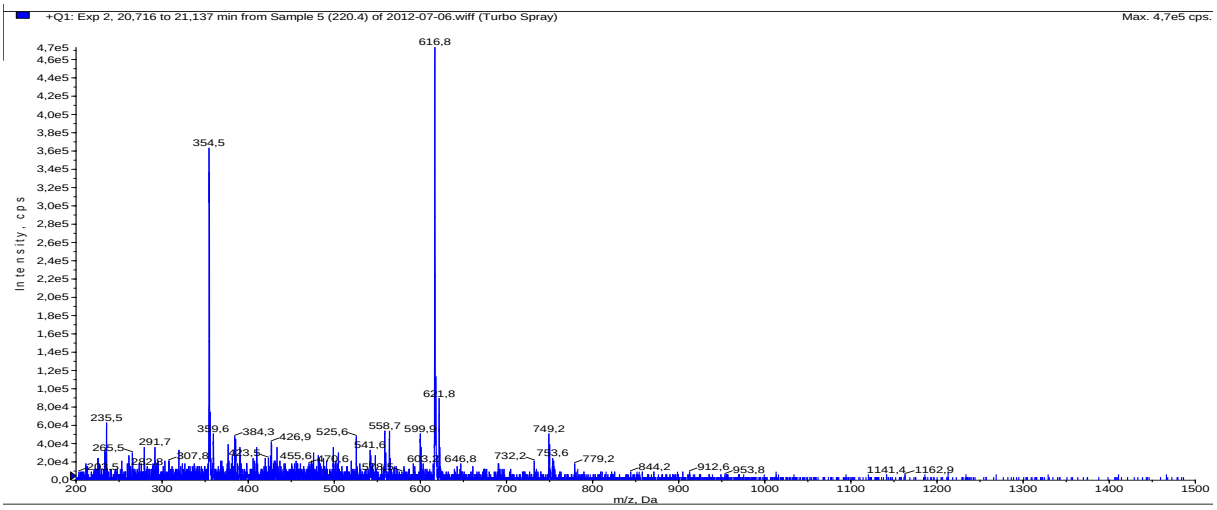

E

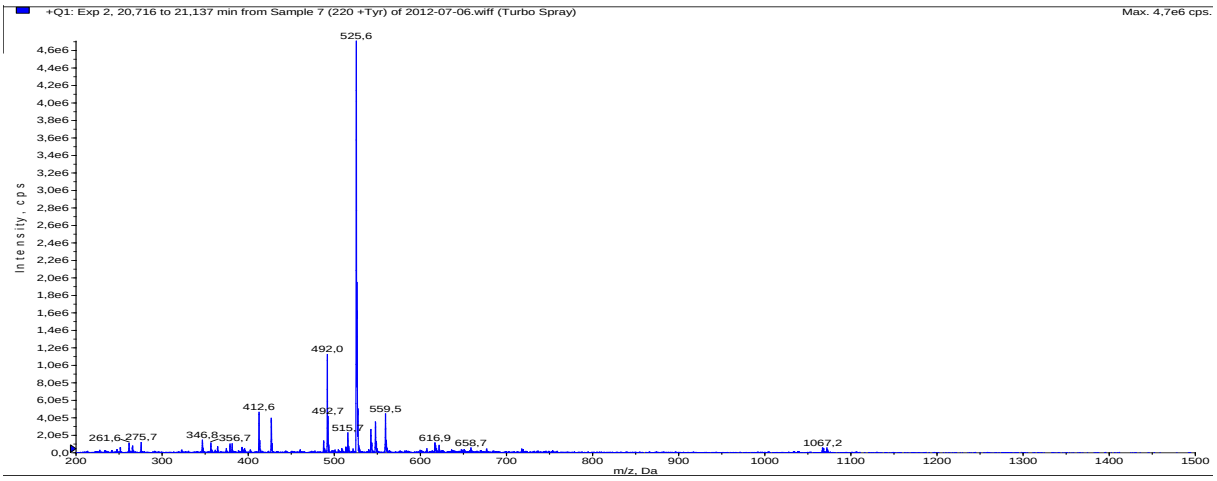

F

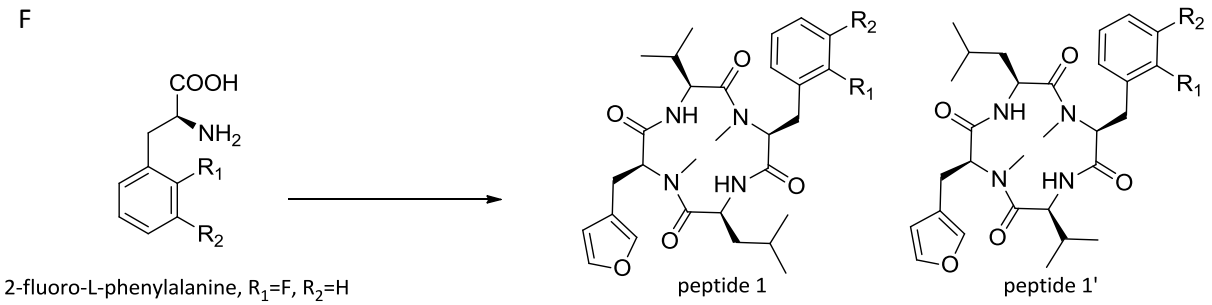

2-fluoro-L-phenylalanine, R_1=F, R_2=H

3-fluoro-L-phenylalanine, R_1=H, R_2=F

$[M+H]^+$ *m/z* 525.6, R_1=H, R_2=H

$[M+H]^+$ *m/z* 543.6, R_1=F, R_2=H

$[M+H]^+$ *m/z* 543.5, R_1=H, R_2=F

Fig S39. LC-ESIMS spectra of crude extract of *Stachylidium* sp. BMS agar culture (A) control, and supplemented with (B) 2-fluoro-L-phenylalanine, (C) 3-fluoro-L-phenylalanine (D) 4-fluoro-L-phenylalanine (E) tyrosine. New ions were observed in (B) and (C) as compared to control culture (A) to which no fluorinated phenylalanine was added. (F) Structure of fluorinated phenylalanine substrates and proposed new products.

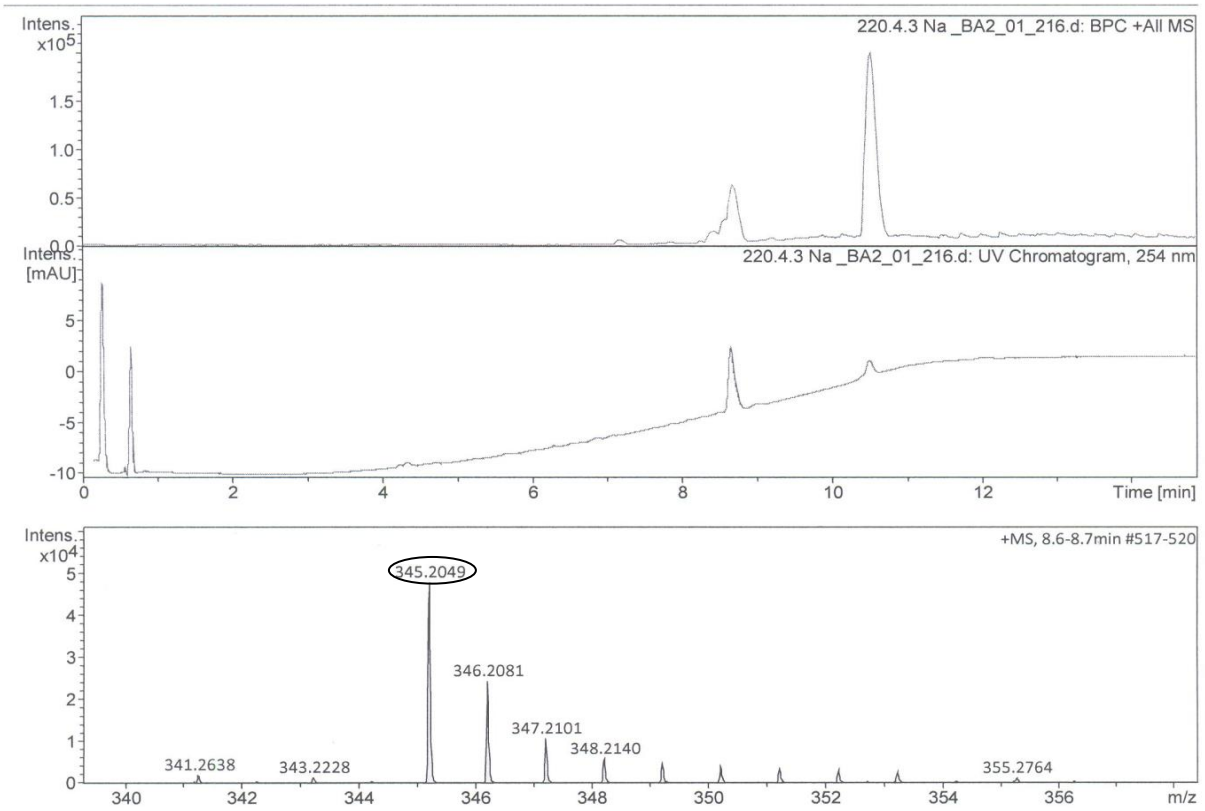

Fig S40. LC-ESIMS spectrum of marilone A isolated from *Stachylidium* sp. BMS agar culture supplemented with [1-^{13}C]sodium acetate, showing major mass peak at *m/z* 345.2049 $[M+H]^+$ and isotopic peaks indicating successful incorporation.

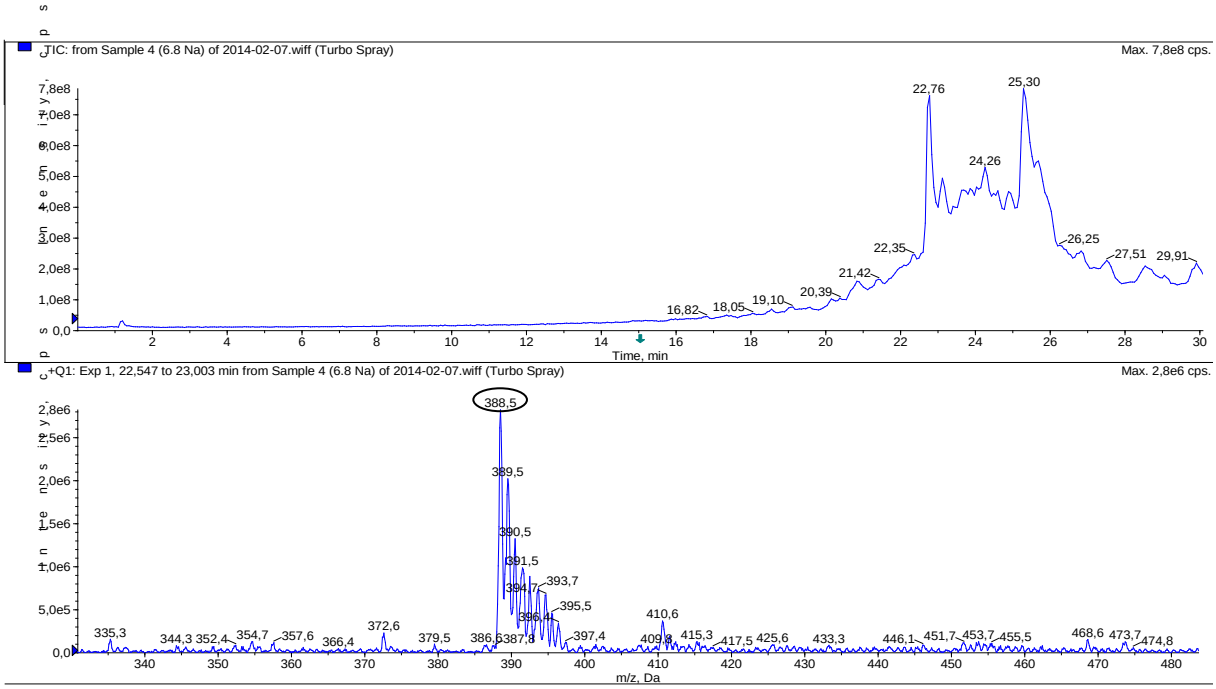

Fig S41. LC-ESIMS spectrum of mariline B isolated from *Stachylidium* sp. BMS agar culture supplemented with [1-^{13}C]sodium acetate, showing major mass peak at *m/z* 388.5 $[M+H]^+$ and isotopic peaks indicating successful incorporation.

A

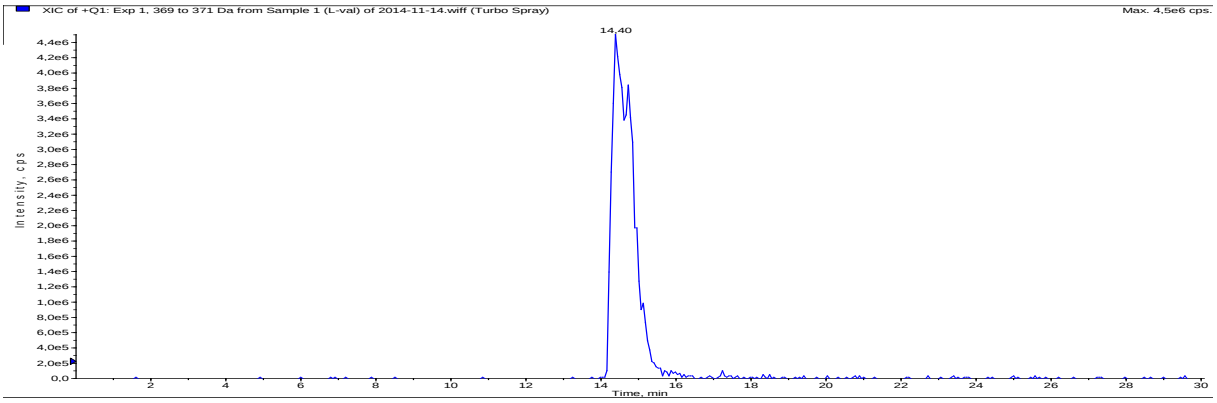

B

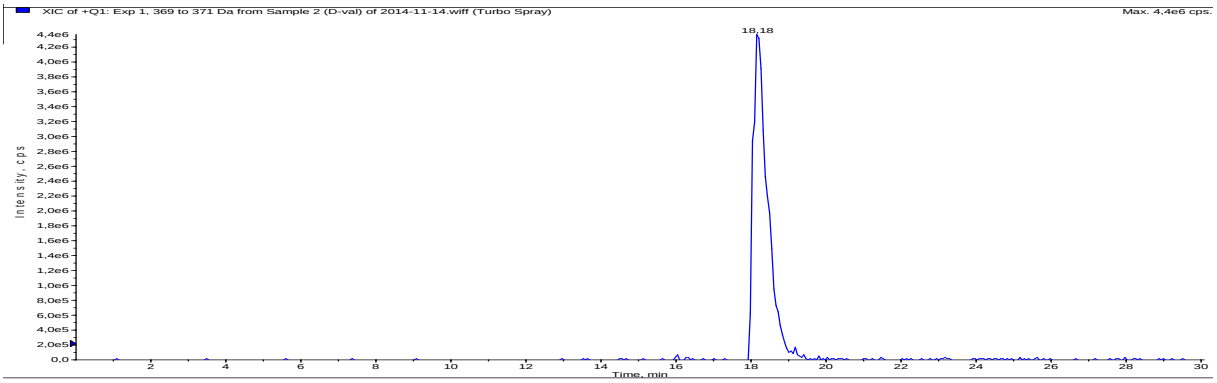

C

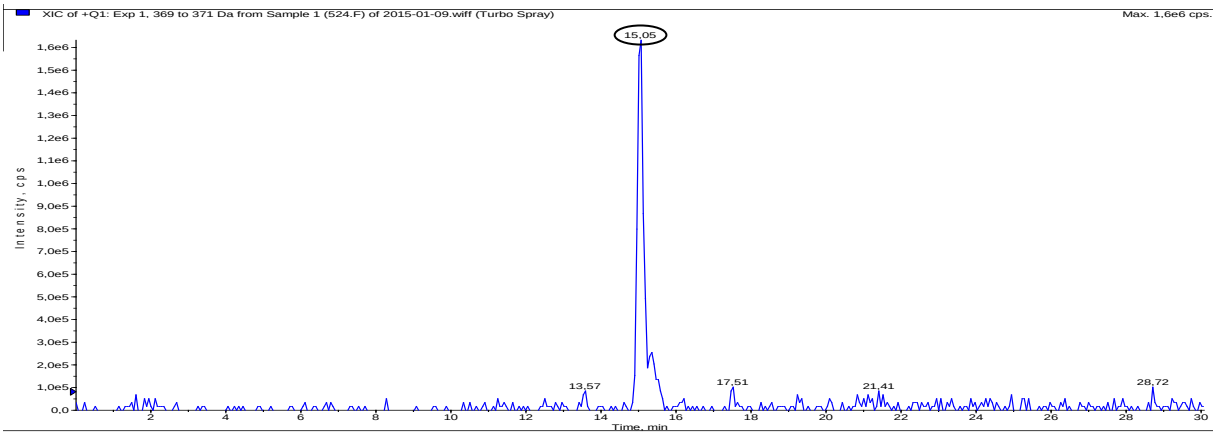

Fig S42. Extracted ion chromatograms (XIC) of a mixture of Marfey's reagent (FDAA) with (A) L-valine, (B) D-valine, and (C) hydrolysed peptide 1, 1' corresponding to molecular mass of L- valine conjugated with Marfey's reagent (FDAA).

A

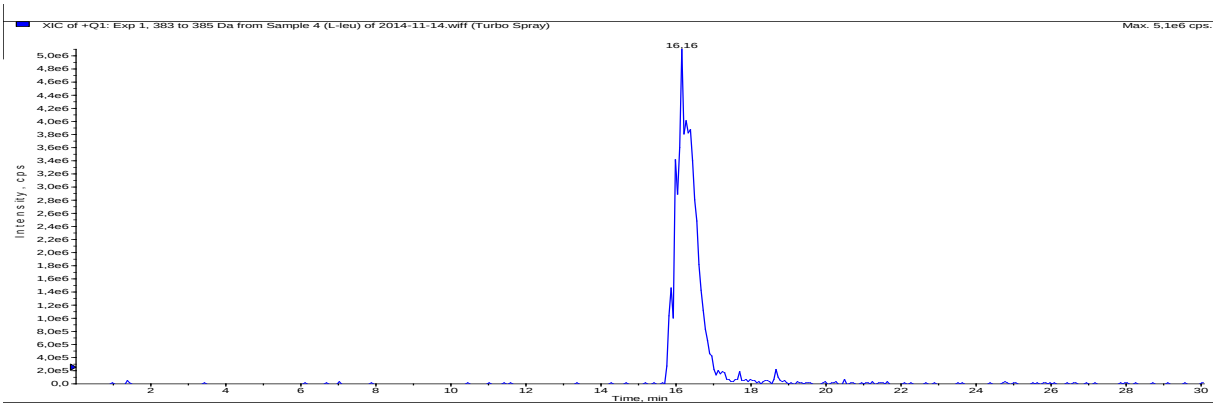

B

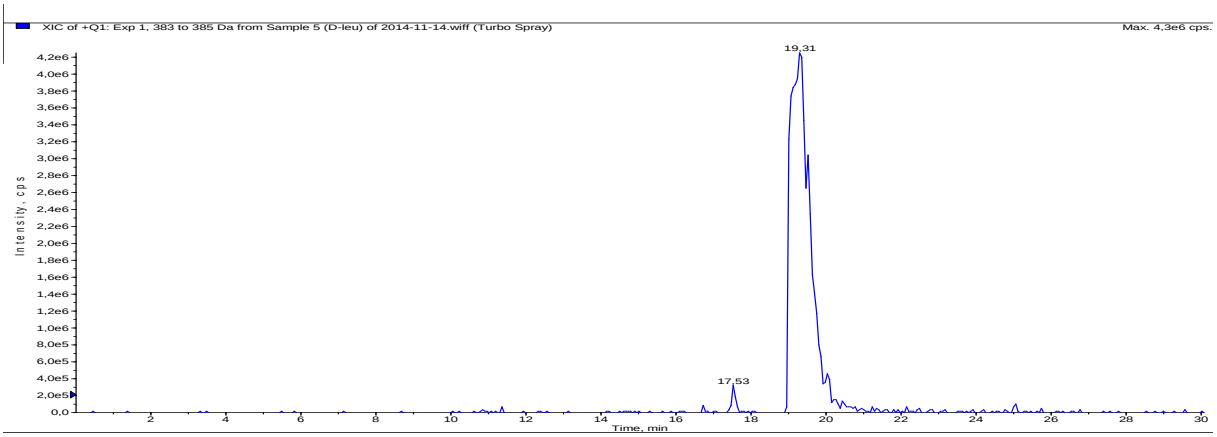

C

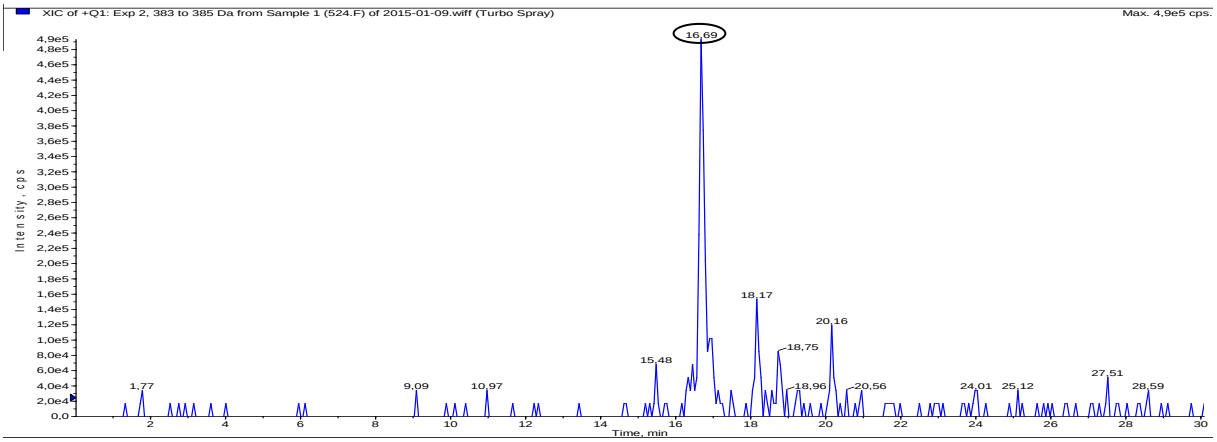

Fig S43. Extracted ion chromatograms (XIC) of a mixture of Marfey's reagent (FDAA) with (A) L-leucine, (B) D-leucine, and (C) hydrolysed peptide 1, 1' corresponding to molecular mass of L-leucine conjugated with Marfey's reagent (FDAA).

A

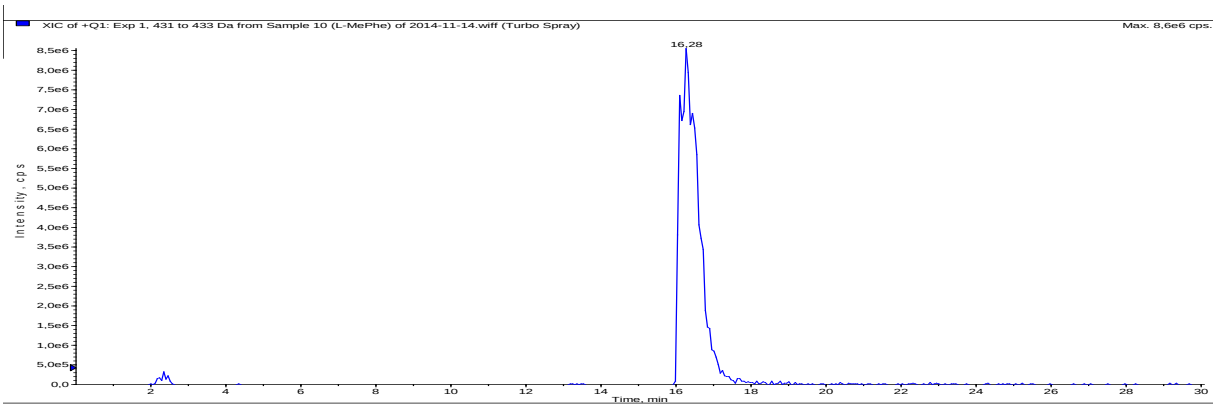

B

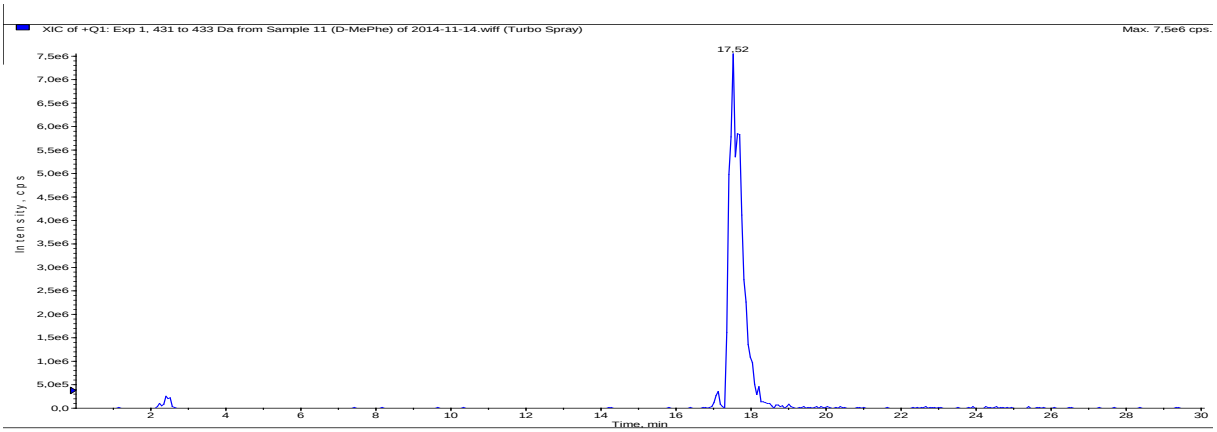

C

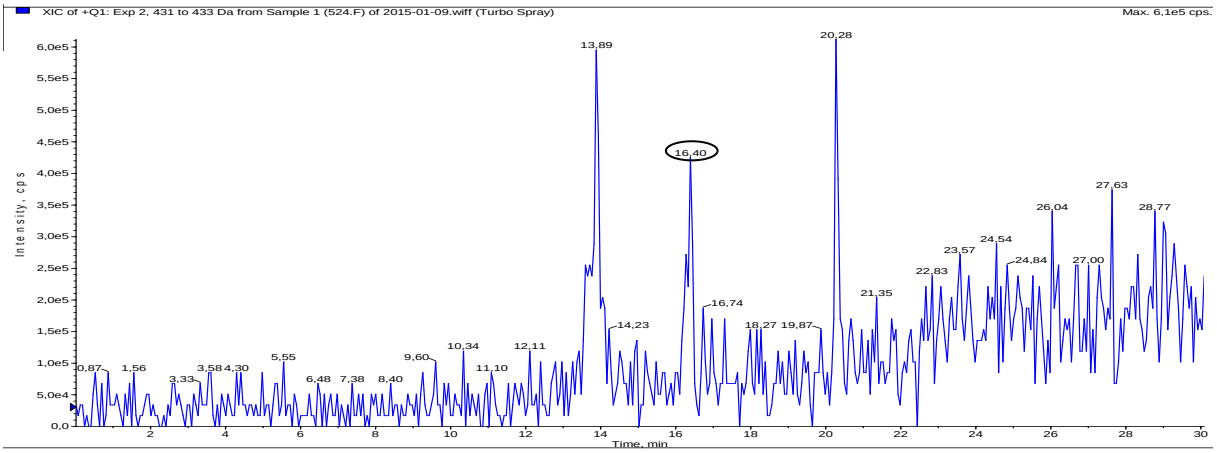

Fig S44. Extracted ion chromatograms (XIC) of a mixture of Marfey's reagent (FDAA) with (A) N-methyl-L-phenylalanine, (B) N-methyl-D-phenylalanine, and (C) hydrolysed peptide 1, 1' corresponding to molecular mass of N-methyl-L-phenylalanine conjugated with Marfey's reagent (FDAA).

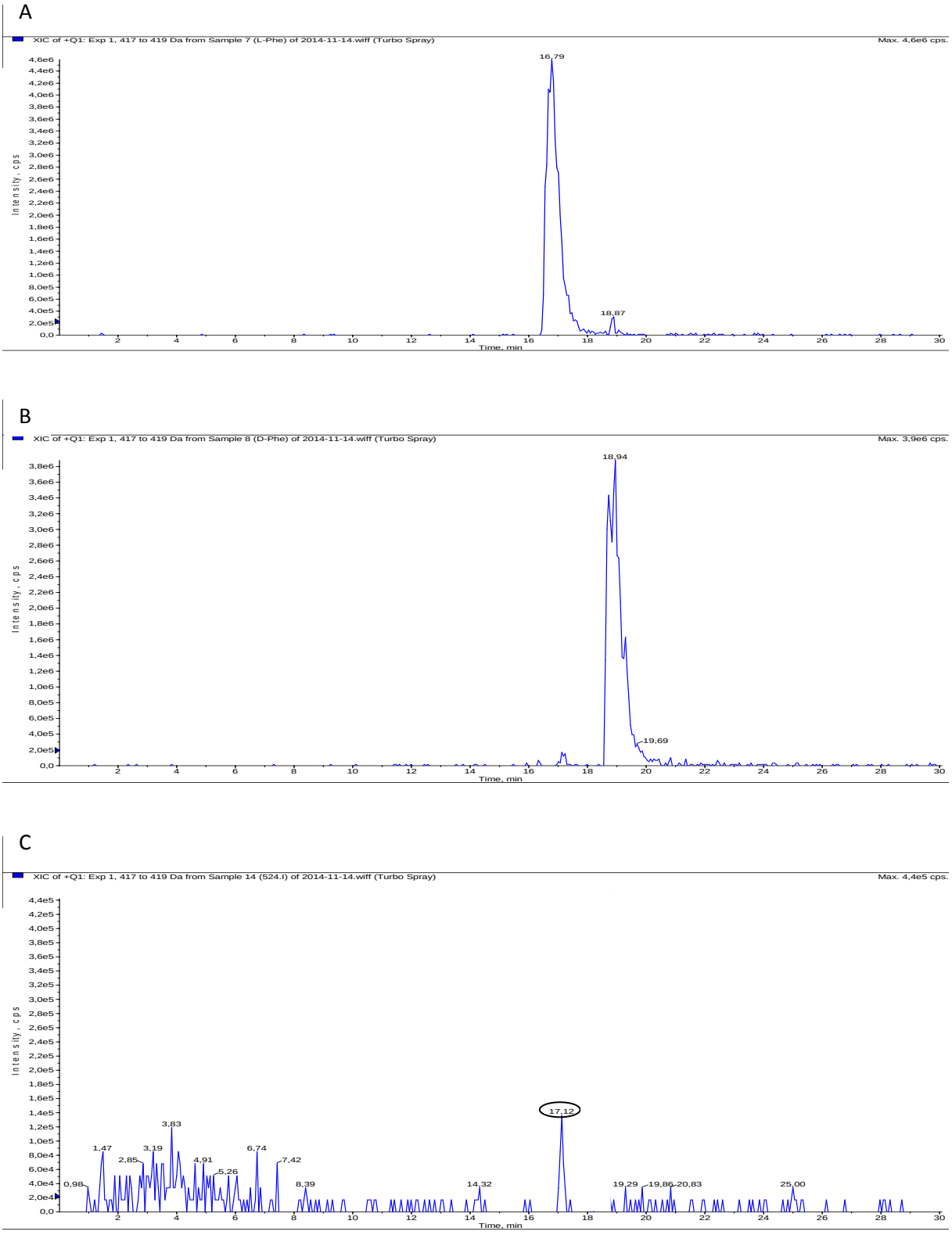

Fig S45. Extracted ion chromatograms (XIC) of a mixture of Marfey's reagent (FDAA) with (A) L-phenylalanine, (B) D-phenylalanine, and (C) hydrolysed peptide 3 corresponding to molecular mass of L-phenylalanine conjugated with Marfey's reagent (FDAA).